Journal of Sensors

AI-Enabled Internet of Everything (IoE) in Next-Generation Wireless Sensor Networks

Lead Guest Editor: Linesh Raja
Guest Editors: Pankaj Dadheech and Vijander Singh

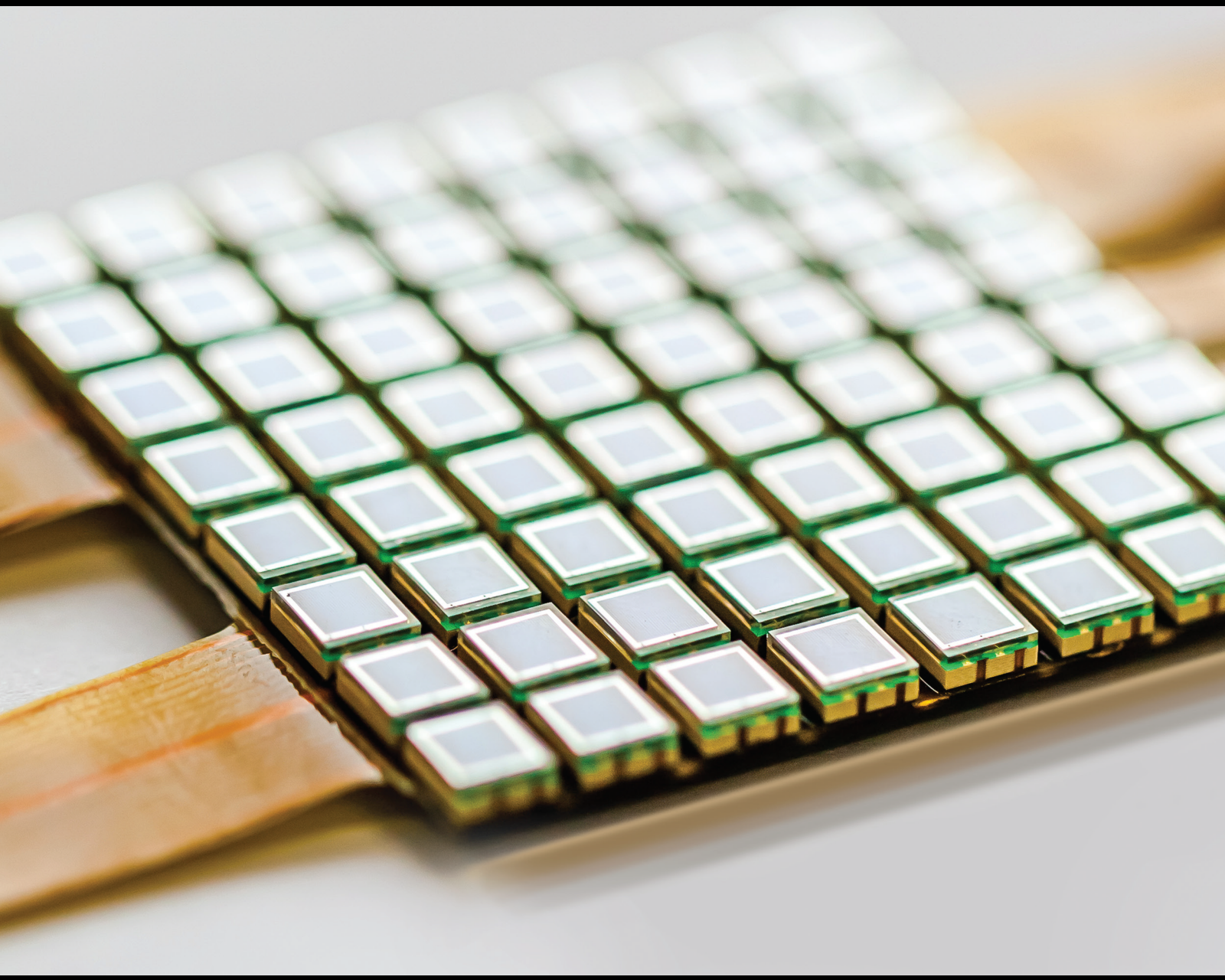

AI-Enabled Internet of Everything (IoE) in Next-Generation Wireless Sensor Networks

Journal of Sensors

AI-Enabled Internet of Everything (IoE) in Next-Generation Wireless Sensor Networks

Lead Guest Editor: Linesh Raja
Guest Editors: Pankaj Dadheech and Vijander Singh

Contents

A Novel AI-Based Approach for Better Segmentation of the Fungal and Bacterial Leaf Diseases of Rice Plant

Yogesh Kumar Rathore, Rekh Ram Janghel, Saroj Kumar Pandey, Ankit Kumar, Kamred Udham Singh, and Mohd Asif Shah

Research Article (12 pages), Article ID 6871085, Volume 2022 (2022)

Hindawi
Journal of Sensors
Volume 2023, Article ID 4343404, 29 pages
https://doi.org/10.1155/2023/4343404

Research Article

Load-Balanced Cluster Head Selection Enhancing Network Lifetime in WSN Using Hybrid Approach for IoT Applications

Ankita Srivastava and Pramod Kumar Mishra

Department of Computer Science, Institute of Science, Banaras Hindu University, Varanasi, India

Correspondence should be addressed to Pramod Kumar Mishra; mishra@bhu.ac.in

Received 22 July 2022; Revised 17 October 2022; Accepted 31 March 2023; Published 9 May 2023

Academic Editor: Akhilesh Pathak

In recent times, the deployment of wireless sensor networks becomes important in revolutionary areas such as smart cities, environmental monitoring, smart transportation, and smart industries. The battery power of sensor nodes is limited due to which their efficient utilization is much necessary as the battery is irreplaceable. Efficient energy utilization is addressed as one of the important issues by many researchers recently in WSN. Clustering is one of the fundamental approaches used for efficient energy utilization in WSNs. The clustering method should be effective for the selection of optimal clusters with efficient energy consumption. Extensive modification in the clustering approaches leads to an increase in the lifetime of sensor nodes which is a unique way for network lifetime enhancement. As the technologies were taken to next the level where multiparameters need to be considered in almost every application in clustering, multiple factors affect the clustering and these factors were conflicting in nature too. Due to the conflicting nature of these factors, it becomes difficult to coordinate among them for optimized clustering. In this paper, we have considered multiattributes and made coordination among these attributes for optimal cluster head selection. We have considered Multi-Attribute Decision-Making (MADM) methods for CH's selection from the available alternatives by making suitable coordination among these attributes, and comparative analysis has been taken in LEACH, LEACH-C, EECS, HEED, HEEC, and DEECET algorithms. The experimental results validate that using MADM approaches, the proposed APRO algorithm proves to be one of the better exhibits for choosing the available CHs.

1. Introduction

Wireless sensor networks are the key step to any new technologies or applications as they can sense and monitor the environment. It collects the data, senses the data, and also makes a decision system for various applications [1, 2]. Sensor nodes have limited battery power and their replacement is not feasible. And it is a still challenge due to which network lifetime depleted and took more energy consumptions. Clustering is a useful approach in wireless sensor networks to increase network lifetime and improve energy efficiency. In clustering as shown in Figure 1, the sensor nodes were grouped into clusters, and from these clusters, CHs were chosen based on some parameters. After CH's selection, the data were transferred to the base station from respective cluster heads [3]. Earlier various algorithms have been presented by researchers which are known to be the basic algorithms for clustering such as LEACH [4, 5], LEACH-C [6], and HEED [7, 8]. In LEACH, the cluster heads were selected based on probabilistic approaches, where CHs have been randomly selected, but later on, more advancement has been made to this approach. But sometimes, the selection of cluster heads was based on the probabilistic method due to which energy consumption increases which leads to overheads. There are various types of methods for the selection of cluster heads as some authors have taken distance from CHs and their residual energy, and some have taken the number of neighbor nodes and residual energy [9–14]. But deciding only on these parameters will not provide optimal CH selection. Thus, the multiattribute needs to be considered [15, 16] for cluster heads. Sensor nodes were the basic in all the emerging fields whether it is IoT [17, 18], digital image processing, cloud computing, or artificial intelligence. Everywhere, sensors were needed for sensing the data and then sending the data

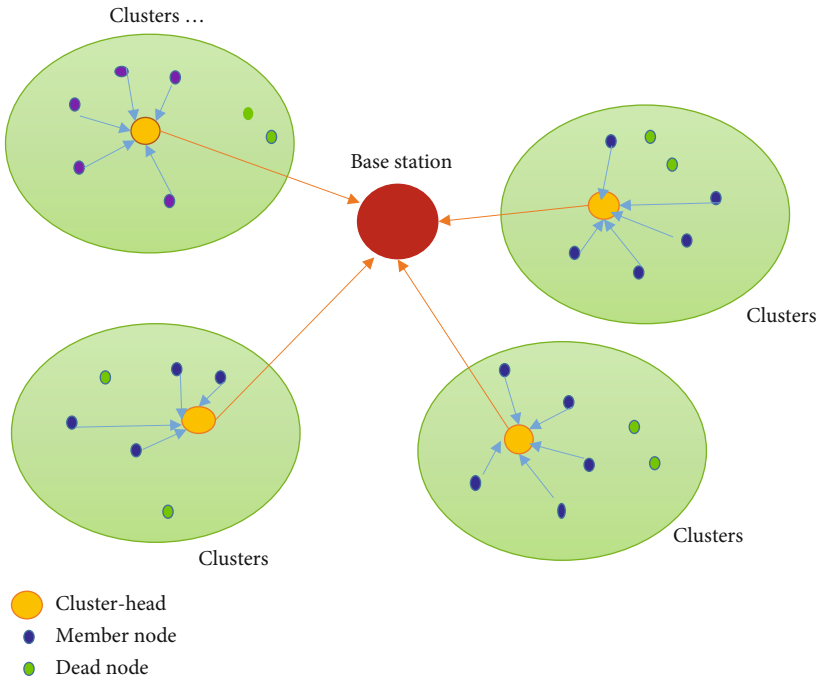

Figure 1: Clustering in WSN.

to the server. In today's era, people were accessing various facilities such as smart home appliances, smart watches, smart TV, smart traffic systems [19], and smart healthcare systems [20] all of these with the help of emerging technologies where sensors play an important role. Considering multiattributes and making coordination among them by Multi-AttributeDecision-Making (MADM) approaches [21, 22] will enhance the network lifetime of the network. Various technologies need optimal node deployment where the performance of applications increases with efficient energy consumption.

In recent technologies, everything is online and sensor nodes were the central part of revolutionary technologies. In a hostile environment, it is believed that energized nodes must be alive for long period but know the fact that their battery is irreplaceable or not feasible to change [23]. This necessity of sensor nodes to be alive for a long time in the network leads to the advent of new alternative approaches for energy-efficient techniques for WSNs for resolving traditional issues such as network lifetime, connectivity, accuracy, latency, distance from the base station, power, and efficient energy consumption; at the same time, these are conflicting in nature too. Thus, these conflicting factors need to be considered in the approach, and proper coordination is needed for making efficient cluster head selection which is the main part of any clustering approach. Various issues and open challenges have been faced by WSNs such as routing, data, topology, coverage, and security, and various clustering approaches have been given to the researchers for resolving these issues [24]. The clustering approach has been used for an efficient energy data process. Some cluster heads (CHs) were chosen from the normal nodes such as in LEACH [25] and HEED [26] and somewhere chosen from the advanced node sometimes known as gateways such as in [27–29], and selected CH is responsible for sending the data back to the base station itself after data aggregation, filtering, or compression. When individual sensor nodes send their data to the base station, energy is not efficiently used. Thus, with the clustering approach, efficient energy utilization is possible, and thus, network lifetime will be enhanced. The cluster head algorithm is used for selecting cluster heads to transmit data to the base station in an efficient way. Some of the CH algorithms are LEACH, LEACH-C, HEED, EECS, and many variants of the LEACH algorithm. In CH selection, the primary goal is to select cluster heads, but for optimal cluster head selection, many factors need to be considered such as energy consumption, connectivity, coverage, load balance, distance to the base station, and distance to neighbor's, but in earlier works, they only focus on one or two attributes, but with time, many updated algorithms were proposed. But in today's scenario, we have to consider multiattributes, and making coordination among them is necessary for finding optimal cluster heads. So, these can be applied to many IoT-based applications and fulfill the current requirement of the users. Optimal cluster head selection [30] leads to efficient energy utilization; therefore, now, researchers were focussing on this, as recently every technology needs sensors for data collection, sensing, and monitoring. Many conflicting attributes play a vital role in efficient energy consumption for data collection, but these attributes were not discovered till now. But there is a need to make coordination among these conflicting attributes which will improve the efficiency of the network. Thus, Multi-AttributeDecision-Making (MADM) is used for making the coordination among the conflicting attributes and selecting the best alternatives among them.

MADM (Multi-Attribute Decision-Making) [31] is an approach applied to solve a problem where the selection of the best alternative can be done from the given alternatives. MADM specifies how we can process the information of the multiple attributes to give the ranking among the given alternatives. In this paper, coordination among the multiple attributes has been done for finding the optimal solution. Sensor nodes were deployed almost in every field according to the applications, but seeing today's user requirement, we need to focus on the multiple attributes which lead to efficient energy which is lacking. We have considered multiconflicting attributes of sensor nodes for the cluster head selection. Results validate that making coordination among conflicting attributes is the better way to choose the cluster heads. In this paper, we have proposed MADM-based method for cluster head selection where network lifetime enhancement and load balance among the sensor nodes were obtained. The principle objective of our proposed work is as follows:

(i) To explore the multi-attribute-based cluster head selection by collaborating with the conflicting attributes. The enhancement of network lifetime and efficient energy consumption was evaluated in terms of FND, CHD, and LND

(ii) To conjoin among conflicting attributes and then to decide the selection of CHs which enhances the network lifetime and efficient energy consumption. The load among the sensor nodes was also balanced with optimal load balancing for sensor nodes

(iii) To evaluate the performance of the network using a multicriteria decision-making approach

The rest of this paper has been arranged as follows: the related work has been discussed in Related Work. The energy model considered for the simulation and parameters used for the experiment have been discussed in Assumption and System Model. The detail of the proposed algorithm and method has been discussed in Evolution Methods for the Selection of CHs Using MADM. Multiattributes taken in this research paper with their detailed description have been discussed in Attributes Considered for the Proposed Work. In Data Set Generation, the generation of data using MATLAB has been discussed. Simulation results and experimentation with case studies have been discussed in Simulation Results, and also, the analysis of the obtained results with their case studies has been discussed. Concluding remarks on the future scope have been discussed in Conclusion and Future Scope.

2. Related Work

Finding an energy-efficient data collection process in WSN is a big challenge. Data collection needs to be optimized as direct data collection will increase the communication heads which leads to less network lifetime. While facing this problem, some of the clustering solutions have been given by researchers [32, 33]. The clustering approach can be defined in several ways such as the CH selection methods (random, deterministic), objective of clustering (coverage, energy, and efficiency), clustering methods (distributed, centralized), or the architecture of the network for doing the communication (multihop, single hop). We can also classify the clustering methods into heuristic and metaheuristic methods. In this paper, we are doing single-hop communication for the wireless network.

LEACH [4] is a classical clustering algorithm that uses the probabilistic method for data collection based on the random number selection of nodes. Many LEACH algorithm variants have been developed for different purposes but have one important objective which is energy conservation. The main objective of the LEACH algorithm is efficient energy consumption by selecting the cluster heads on a rotation-based using a random number. There are several rounds in LEACH where each round is divided into two phases: the set-up phase and the steady phase. The concept used in the LEACH protocol is that it enforces less communication between the sensor node and the base station which increases the network lifetime. LEACH-C [13] is a variant of the LEACH protocol where all the decisions whether it is CH selection, distribution, or cluster formation are taken by the base station. LEACH-DCHS [34] is used for prolonging the network lifetime. Another protocol of LEACH is SLEACH [35] where the energy was harvested from the external source to the sensor node and the concept of solar power can be applied to distribute or centralize clustering. SLEACH [36, 37] is the first protocol that added the concept of security by using the SPIN protocol. This protocol uses the lightweight cryptographic technique in WSNs as this is a challenging task due to limited resources for the sensor nodes. ME-LEACH [38–40] means more energy-efficient LEACH extending the LEACH protocol by minimizing the distance between the sensor nodes and base station. EP-LEACH [41, 42] has improved the lifetime of the LEACH algorithm by using EH-WSN where the sensor nodes have a rechargeable battery that is charged from the environment itself.

HEED is another popular heuristic algorithm based on the single-hop transmission which does not depend upon the density of the sensor network. HEED algorithm considers residual energy and the number of neighboring nodes for selecting the cluster heads. This residual energy of sensor nodes is considered to be the primary attribute for selecting the cluster heads, and the average minimum reachable power works as a tie-breaker between the sensor nodes. The enhanced algorithm of HEED is named DWECH [43] which has the same primary parameter for the selection of cluster heads, but it also takes care of overlapping and unbalanced size when selecting the cluster heads. HEED has a good distribution of cluster heads over the network but has the disadvantage of not covering all nodes in the network. Both HEED and DWECH consume lots of energy due to overhead costs. FLOC [44, 45] is another heuristic algorithm that takes care of sensor nodes not getting overlapped and also creates an almost equal size of clusters such that each has one hop distance to the respective cluster heads. Energy-efficient clustering scheme (EECS) [46] is also another heuristic algorithm that reduces the unbalanced

consumption of energy by considering the three attributes and also considering the respective weight cost factor for the sensor node. EEHC (energy-efficient heterogeneous cluster scheme) [47] provides the election probability weights that are directly related to the residual energy of the sensor node, whereas BEENISH [48] (balanced energy-efficient network-integrated super heterogeneous) protocol is also a clustering algorithm that assigns one of the four energy levels to the sensor node and uses this energy level for selecting the cluster heads. Enhanced developed distributed energy-efficient clustering for heterogeneous network (EDDEEC) [49] classifies nodes as normal nodes and advanced nodes and then changes the probability of becoming cluster heads.

Some of the metaheuristic algorithms were also proposed by the researchers in wireless sensor networks. Among them, the genetic algorithm is one of the most important algorithms used in the clustering approach for sensor networks where it reduces the communication distance of the target [50]. In [51], the authors propose a genetic algorithm-based fuzzy-optimized reclustering scheme to overcome the network lifetime failure, fixed routing path problem, and energy saving for the sensor network for the revolutionary area. The simulation results validate that the proposed algorithm for the network lifetime extension is 3.64-fold by preserving energy efficiency. In [52], the authors proposed a genetic algorithm for the dynamic clustering approach in IoT applications, and the simulation results validate that it has overcome the problem of a dynamic cluster relay node in terms of throughput and standard deviation for the data transmission. In [53], the authors propose the EEWC (energy-efficient weighted clustering) based on a genetic algorithm, and the proposed algorithm modifies the steady-state phase of LEACH and considered three attributes for the optimization which shows that the proposed algorithm is better than ERP, SEP, and IHCR. Some of them also use MADM-based approach for cluster head selection by considering 2 or 3 attributes. In [54], the authors propose an enhanced AHP-TOPSIS-based clustering algorithm for high-quality live video streaming flying in the ad hoc network. The proposed algorithms were simulated on OMNET++. It shows that video quality, UAV energy consumption, and the number of cluster heads needed have been improved when they used two models, namely, random waypoint and paparazzi. In [55], TOPSIS multicriteria decision-making algorithm has been used by OPNET software, and the proposed algorithm proved that it is suitable for clustering and selecting the cluster heads. The data transmission between the nodes has also been used for transmitting the files with improved efficiency of the network and sustainable routing path. In [56], the authors have proposed an ordered clustering based on PROMETHEE and the fuzzy c-mean clustering method. The author has finally proposed OFCM (ordered fuzzy c-mean clustering) for solving the problem of human development indexes, and comparison analysis also validates the efficiency of the OFCM approach.

But these approaches consider two or three factors in clustering which do not guarantee optimal clustering; thus, we need to consider more conflicting factors for achieving the optimal clustering for enhancing network lifetime. Less number of intermediate nodes for data transmission consumes more energy; thus, in [57], the authors suggested using an optimal number of intermediate nodes for the transmission of data enhancing the network lifetime. The authors in [58] have reviewed the renewable energy sources which will help WSN for recharging the battery of sensor nodes. They also discuss issues/challenges and provide future direction for the researcher to work on. In [59], the authors have proposed load-balanced adaptive position update (LAPU) for routing techniques which balances the load among sensor nodes in the selected path. Basically in this approach, the sensor nodes select the two best next hops for the data transmission based on the length queue and mobility of nodes and transmit the data to both selected nodes for balancing the load among sensor nodes. In [60], the authors have proposed a two-tier distributed fuzzy logic-based protocol for efficient data aggregation in multihop wireless sensor networks (TTDFP) for enhancing the network lifetime by combining the efficiency of routing and clustering phases along with two-tier fuzzy logic for tuning the parameters. In [61], a modified CLONal selection algorithm has been proposed for improving the energy efficiency of rule-based fuzzy systems. Here, CLONALG has been modified for constrained approximation problems. In [62], the author proposed hybrid gray wolf optimization (HGWO) for resolving the constrained resource problem in WSNs. These resources can be in any form such as bandwidth and energy consumption.

In [63], the authors have proposed energy-aware clustering and efficient cluster head selection by dividing the network into grids. This cluster head selection was based on only residual energy, distance to the base station, and distance to neighbors. In [64], the authors proposed a low energy clustering hierarchy for mobile sensor networks to not only enhance network lifetime but also reduce packet loss. In [65], the authors proposed a new routing technique for efficient consumption and increased network lifetime by optimal selection of cluster head. But here, cluster head selection is done only based on residual energy and distance to the base station. In [66], fuzzy-based clustering algorithms have been proposed where two types of sensors used, namely, free sensors for communicating to the base station and clustered sensor that sends sensed data to CH and the base station which were based on four parameters. In [67], an extension of the energy prediction with fuzzy logic has been proposed for increasing the network lifetime.

But these factors do not guarantee the optimal solutions in WSNs because many conflicting factors affect the energy consumption such as if it selects cluster heads (CHs) near the base station based on higher residual energy, but it may be possible that some sensor nodes have higher distance from the base station to send the data which consume more energy, which will degrade the efficiency of the sensor networks. We have already seen the problem of resource-constrained in the form of bandwidth and energy consumption which will drastically affect the network lifetime. So we need to focus on cooperating among the conflicting attributes to choose optimal cluster heads which enhance the network lifetime by properly and efficiently utilizing the

resources. Thus, MADM is an emerging approach for applications based on WSNs by considering some important factors too. This paper focuses on the cooperation among the many conflicting attributes and then deciding on optimal cluster heads for efficient energy consumption.

3. Assumption and System Model

In this paper, we have assumed some predetermined values of the parameters and also made some assumptions for our simulation. In the simulation, we have taken an energy model during the data collection process. The considered parameter values and assumption made for simulation purposes have been discussed in this section as follows:

3.1. Assumptions. The following assumptions have been made in our simulation:

(i) Sensor nodes send the data from cluster heads to the base station

(ii) Here, sensor nodes are homogeneous

(iii) Here, the random uniform distribution of sensor nodes has been assumed

(iv) Some gateways were selected as cluster heads and sent the data to the base station

(v) Gateways are approximately six times higher energy than the normal sensor nodes

(vi) The base station knows the location of sensor nodes, gateways, and vice versa

(vii) The base station is considered to be the hefty node having the capability of communicating and computing without having any restriction on energy consumption

(viii) Sensor nodes were having the potential to transmit the data to the fluctuating energy level based on the distance from the sensor nodes

(ix) Sensor nodes are static

3.2. Energy Model. In WSN, most of the sensor nodes sense the data from the environment from their vicinity and send back data to the respective CHs, and CHs send this data to the base station by operating on the data. We need an energy model for transmitting the data, so we have taken the classical energy model for performing the operation mentioned above. The transmitter consumes energy for operating the radio electronics with amplifier power and only the receiver for operating the radio electronics.

In our experiment, we have considered both the free-space channel and multipath model. These models depended on the distance between the transmitter and receiver. Here, appropriate settings have been provided for preventing energy loss and providing power control at the power amplifier, i.e., if the distance for the transmission is less than d_0 which is the threshold distance that a free-space path will be used else a multipath model will be used. Here is an energy model; if l bit packets send at a distance d, then the required energy for the transmission is

$$E_{TRi} = E_{(TR_i-\text{ele})} + E_{(TR_i-mp)},$$

$$E_{TRi} = \begin{cases} l * E_{\text{ele}} + l * \varepsilon_{fs} d^2 & \text{if } d < d_0, \\ l * E_{\text{ele}} + l * \varepsilon_{mp} d^4 & \text{if } d \geq d_0. \end{cases} \quad (1)$$

The energy consumption for receiving the message at the receiver end is given as

$$E_{REi} = E_{(REi-\text{ele})}(l) = lE_{\text{ele}}. \quad (2)$$

Here, E_{ele} is the electronic energy based on some factors such as filtering, signal spreading, modulation, and digital coding. And the amplifier energy is known as $\varepsilon_{fs} d^2$ or $\varepsilon_{mp} d^4$; this is based on the receiver distance and bit error rate. For our experimental analysis, these energy parameters for transmission purpose have been set as follows: $E_{\text{ele}} = 50$ nJ/bit, $\varepsilon_{fs} = 10$ pJ/bit/m, and $\varepsilon_{mp} = 0.0013$ pJ/bit/m. For data aggregation, the energy consumption has been taken as 5 pJ/bit/signal. The optimal number of cluster heads (CHs) can be calculated as

$$k_{\text{opt}} = \frac{\sqrt{n}}{\sqrt{2\pi}} \sqrt{\frac{\varepsilon_{fs}}{\varepsilon_{mp}}} \frac{M}{d^2 \text{ to BS}}. \quad (3)$$

Here, d^2 to BS is known as the distance from cluster heads (CHs) to the base station (BS), $M * M$ is the network deployment area, and n is the number of sensor nodes.

3.3. Parameters and Energy Model for the Simulation. Parameters used in the simulation for energy dissipation have been given in Tables 1 and 2 showing the parameters used for the repeated simulations in our experiment.

4. Attributes Considered for the Proposed Work

Here, we have considered multiattributes for our proposed work, and these are conflicting in nature shown in Figure 2. These attributes have an important impact on cluster head selection. Attributes considered in this paper were given below in the figure. These are conflicting attributes; thus, proper coordination among them is necessary for further use in other applications.

5. Data Set Generation

For the simulation purpose, we have used MATLAB for modeling the WSN. In our simulation, we have generated a random population of 20 for preserving the difference between the 20 alternative populations. The more difference helps us to understand the proposed APRO algorithm in a better way. The population generated in our experiment has been done by using the above equations for every given

Table 1: Parameters used in energy dissipation [4].

Parameters	Value and unit
Initial energy for every gateway	1 J
Initial energy for every node	0.2 J
ε_{fs}	$10 * 10^{-12}$ J
ε_{mp}	$0.0013 * 10^{-2}$ J
E_{TRi}	$50 * 10^{-9}$ J
E_{REi}	$50 * 10^{-9}$ J
EDA	$5 * 10^{-9}$ J
Data package length	4000 bits
Control package length	100 bits

Table 2: Parameters used in the simulation.

Parameters	Value/unit
Coordinates origin	(0,0)
Area	100*100, 200*200, 300*300 m^2
Total number of sensor nodes	100, 150, 200…
Base station coordinates	It is variable
Time for simulation	500, 750, and 1000 rounds
Simulation repeated time	3

alternative. Table 3 shows the brief descriptions about the attributes considered in our proposed work, whereas Table 4 shows the computed values of the attributes for modeled WSN by using the CHs selected for each alternative:

6. Evolution Methods for the Selection of CHs Using MADM

Many methods can be applied to select the best cluster heads (CHs). In this section, we have applied MADM-based methods such as AHP and PROMETHEE for ranking the alternative and selecting the best cluster heads (CHs) among them. Here, each method with its respective results has been discussed.

6.1. AHP (Analytical Hierarchy Process) Method for CH's Selection. Step 1: the first step is to normalize the data set (M_1) by using the following equation; we can denote the matrix by $(M_{1ij})_{mn}$, and the normalized data has been presented in Table 5

There are two types of factors: one is a beneficial factor and the other is a nonbeneficial factor. For the beneficial factor, we have to select the max value of each factor V_j^+ to compute the normalized value to the column i to M and $j = 1, 2, 3 \cdots n$.

$$M_{1ij} = \frac{M_{ij}}{V_j^+}. \tag{4}$$

And for nonbeneficial, the min value for each factor has been calculated V_j^-, where $j = 1, 2, 3 \cdots n$.

$$M_{1ij} = \frac{V_j^-}{M_{1ij}}. \tag{5}$$

The values of the normalized matrix lie between 0 and 1.

Step 2: after this, the relative importance matrix will be generated W_{n*n}

Step 3: geometric mean (GM) of each has been computed by using the following equation, and it is represented in Table 6

$$\mathrm{GM}_i = \prod_{i=1}^{n} W_{ij}, i = 1, 2, \cdots m \text{ and } j = 1, 2, \cdots n. \tag{6}$$

Step 4: in this step, a weighted matrix will be calculated $(M_2)_{n*1}$. Table 7 denotes the weighted matrix of the attributes

$$\mathrm{GM}_i = \frac{\mathrm{GM}_i}{\sum_{i=1}^{n} \mathrm{GM}_i}. \tag{7}$$

And also

$$\sum_{i=1}^{n} M_{2i} = 1. \tag{8}$$

Step 5: check the consistency:

(i) Compute the matrix M_3 and it is represented in Table 8.

$$M_{3n*1} = M_{1n*n} * M_{2n*1}. \tag{9}$$

(ii) Compute the matrix M_4 and it is represented in Table 9.

$$M_{4n*1} = \frac{M_{3n*1}}{M_{2n*1}}. \tag{10}$$

(iii) Compute $\lambda_{\max}$:

$$\lambda_{\max} = \frac{\sum_{i=1}^{n} M_{4i}}{n}. \tag{11}$$

Consistency index (CI) is as follows:

$$\mathrm{CI} = \frac{\lambda_{\max} - n}{n - 1}. \tag{12}$$

(iv) Compute consistency ratio:

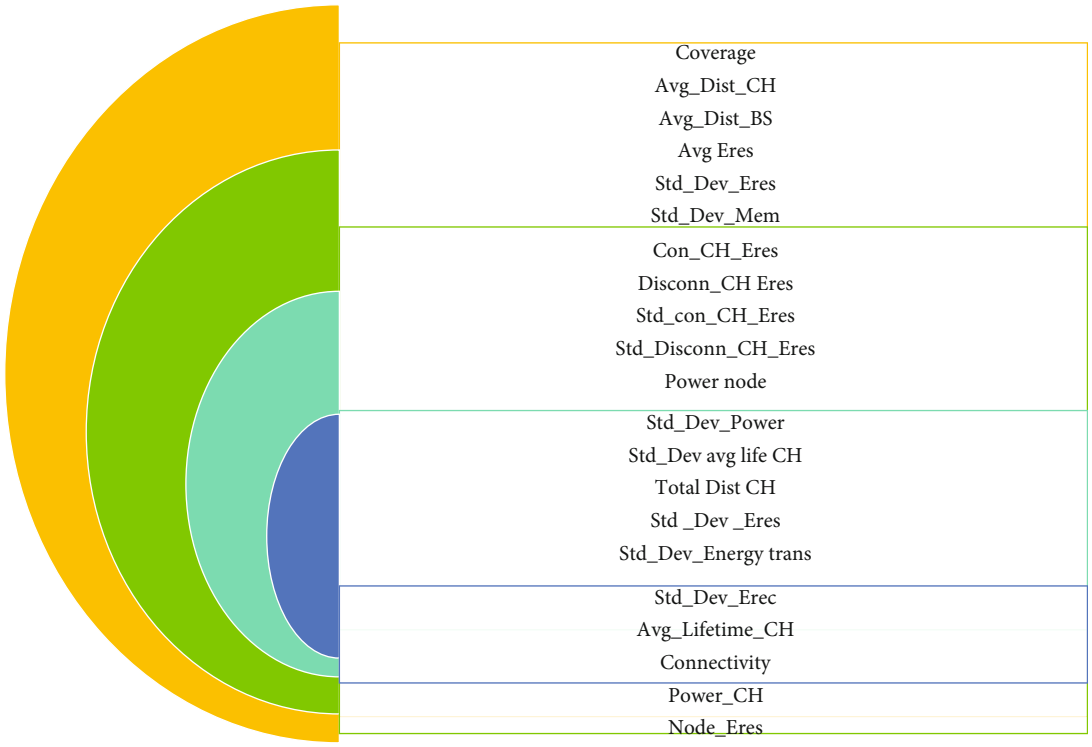

Figure 2: Attributes considered in the proposed work.

Table 3: Description of attributes.

Attributes	Brief description
CH-Cov	Percentage of sensor nodes distance from their respective cluster heads
BS-CH Connectivity	Connectivity of CH to the base station
Avg-CH Life	Average lifetime of cluster heads
Avg-Residual Energy	Average residual energy of sensor nodes
CH-Con-Avg Residual	Average residual energy of connected cluster heads
CH-Dcon-Avg Residual	Average residual energy of disconnected cluster heads
BS-CH Bearing	Load of cluster heads
Std Residual	Standard deviation of residual energy
Avg-BS Life	Lifetime of base station
Std_Avg_Ch_Life	Standard deviation of cluster head lifetime
Maximum_Dis_BS	Maximum distance to the base station
Avg_Dis_CHs	Average distance to cluster heads
Avg_BS_DIS	Average distance to base station
Std_CH_Con_Avg_Residual	Standard deviation residual energy of connected nodes
Std_CH_Dcon_Avg_Residual	Standard deviation residual energy of dis-connected nodes
Std_Residual	Standard deviation of residual energy
Node_Power	Power of sensor nodes
CH_Power	Power of cluster heads
Std_Power	Standard deviation of power
Std_Member Node	Standard deviation of member nodes
Std_Dev_Energy Trans	Standard deviation of energy transmission

Table 4: The computed value of attributes using modelled WSN.

Pop number	AT1	AT2	AT3	AT4	AT5	AT6	AT7	AT8	AT9	AT10	AT11	AT12	AT13	AT14	AT15	AT16	AT17	AT18	AT19	AT20	AT21
p1	100	42.36216	75.48834	0.500632	7.949843	0.00159	134.7252	0.6	0.004733	106.5489	754.8834	0.305308	2.479815	2.526502	0.309211	0.247014	0.002439	0.046685	0.399993	4.21136	4.52*E*-05
p2	97.35	27.64781	73.23843	0.590844	14.97331	0.002995	188.6028	0.6	0.005498	192.4052	732.3843	0.336078	3.838768	2.069676	0.260019	0.414693	0.002443	0.046493	0.399983	4.182947	8.13*E*-05
p3	100	25.85101	75.76089	0.442423	10.25671	0.002051	123.0495	0.6	0.004947	85.245	757.6089	0.21811	2.768477	1.65575	0.21717	0.216411	0.002659	0.047189	0.399931	4.154947	4.46*E*-05
p4	94.89	24.71355	86.05397	0.355837	15.80506	0.003161	148.6975	0.5	0.00563	130.8602	860.5397	0.202941	1.688419	1.869947	0.10286	0.2649	0.002604	0.04819	0.399968	4.125942	0.000156
p5	97.705	71.40099	72.46427	0.502839	13.08434	0.002617	225.0027	0.6	0.005264	292.223	724.6427	0.235293	2.985419	2.04297	0.270038	0.164349	0.002595	0.046899	0.399996	4.098374	7.11*E*-05
p6	99.3575	39.8865	69.20264	0.653394	12.66491	0.002533	504.6872	0.7	0.005214	1006.548	692.0264	0.292498	5.021191	1.512748	0.256218	0.262078	0.002685	0.047165	0.399919	4.070134	6.80*E*-05
p7	99.9825	38.55773	76.93263	0.460625	10.77961	0.002156	135.6407	0.6	0.005008	85.64074	769.3263	0.264736	2.864959	1.741286	0.308765	0.119939	0.002507	0.046546	0.399996	4.042229	4.44*E*-05
p8	100	60.3459	69.39238	0.723671	7.266361	0.001453	188.9398	0.7	0.004691	88.23473	693.9238	0.206317	5.382757	1.853948	0.209852	0.123075	0.00284	0.046266	0.399959	4.014036	4.18*E*-05
p9	94.615	50.66297	89.61767	0.461979	16.75112	0.00335	289.6506	0.5	0.005744	375.1004	896.1767	0.308652	1.713872	2.905919	0.29868	0.342258	0.002385	0.049112	0.399899	3.984999	0.000135
p10	93.7275	60.73158	82.4016	0.490068	10.51665	0.002103	513.9256	0.5	0.00499	1155.767	824.016	0.287279	1.5918	3.308875	0.304253	0.252419	0.00296	0.048933	0.399955	3.956912	0.000168
p11	92.475	31.71374	78.95862	0.621623	15.11952	0.003024	307.3728	0.5	0.005518	361.2157	789.5862	0.304075	3.644347	2.57188	0.232355	0.309969	0.002344	0.048011	0.399995	3.928457	0.000146
p12	100	48.98853	82.83877	0.450328	10.89954	0.00218	145.4711	0.6	0.005015	142.6179	828.3877	0.264371	1.725436	2.777847	0.290212	0.273077	0.002543	0.048357	0.399972	3.901172	3.95*E*-05
p13	99.47	52.21538	78.47428	0.530797	13.69671	0.002739	192.4369	0.5	0.005343	167.3531	784.7428	0.263519	2.338299	2.969674	0.320134	0.243651	0.002682	0.047351	0.399786	3.872966	4.60*E*-05
p14	100	51.50412	66.45519	0.516235	9.497368	0.001899	176.7652	0.5	0.004882	188.4023	664.5519	0.284803	3.011406	2.150942	0.317346	0.277782	0.002857	0.046623	0.399991	3.844796	4.39*E*-05
p15	100	39.63469	66.57997	0.527691	6.60303	0.001321	122.9159	0.9	0.004639	81.29884	665.7997	0.307114	4.910743	0.366162	0.318713	0.220047	0.002605	0.046035	0.399901	3.81673	3.55*E*-05
p16	96.575	60.15173	80.61157	0.314779	15.88081	0.003176	106.993	0.4	0.005639	75.11731	806.1157	0.251882	0.969824	2.177968	0.25899	0.281325	0.002718	0.048352	0.399849	3.787997	8.48*E*-05
p17	95.2825	40.05326	74.22112	0.372444	10.94532	0.002189	94.14851	0.7	0.005014	70.58152	742.2112	0.273516	3.463588	0.260854	0.233701	0.295826	0.00266	0.048688	0.399747	3.759846	0.000148
p18	98.055	49.4015	62.32353	0.566006	9.316652	0.001863	232.1911	0.7	0.004861	288.7712	623.2353	0.259286	4.821899	0.838164	0.144	0.281134	0.002653	0.047326	0.399997	3.731846	6.53*E*-05
p19	99.9975	24.09671	89.33146	0.601859	8.786353	0.001757	157.261	0.4	0.004818	64.62429	893.3146	0.16402	2.569741	3.448852	0.131124	0.199766	0.00269	0.049124	0.399994	3.703793	4.68*E*-05
p20	99.9925	38.17546	84.1947	0.520372	11.61034	0.002322	249.8117	0.4	0.005089	298.3125	841.947	0.275279	1.951679	3.252046	0.227809	0.285932	0.002438	0.048656	52.39001	3.675493	5.55*E*-05

Table 5: Normalization of AHP.

	AT1	AT2	AT3	AT4	AT5	AT6	AT7	AT8	AT9	AT10	AT11	AT12	AT13	AT14	AT15	AT16	AT17	AT18	AT19	AT20	AT21
p1	1	0.668826	0.525605	0.691795	0.830586	0.830586	0.262149	0.666667	0.980169	0.606522	0.825605	0.53723	0.460696	0.732563	0.332655	0.485554	0.961339	0.986084	0.007635	0.872757	0.785712
p2	0.9735	0.871559	0.750968	0.816455	0.440987	0.440987	0.366985	0.666667	0.843684	0.335876	0.850968	0.488042	0.71316	0.600106	0.395588	0.289222	0.959559	0.990143	0.007635	0.878685	0.436559
p3	1	0.932138	0.822635	0.611359	0.643777	0.643777	0.23943	0.666667	0.937641	0.758101	0.822635	0.752007	0.514323	0.480087	0.473641	0.554218	0.88169	0.975543	0.007634	0.884606	0.795808
p4	0.9489	0.97504	0.724238	0.491711	0.417779	0.417779	0.289337	0.555556	0.823902	0.493842	0.724238	0.808216	0.313672	0.542194	1	0.45277	0.900316	0.955289	0.007634	0.890825	0.22781
p5	0.97705	0.337484	0.860059	0.694845	0.504651	0.504651	0.437812	0.666667	0.881299	0.221147	0.860059	0.697091	0.554626	0.592362	0.380911	0.72978	0.90347	0.981571	0.007635	0.896817	0.499472
p6	0.993575	0.604132	0.900595	0.902889	0.521364	0.521364	0.982024	0.777778	0.889678	0.064204	0.900595	0.560758	0.932829	0.438624	0.401456	0.457645	0.873218	0.976037	0.007634	0.90304	0.522045
p7	0.999825	0.624951	0.810105	0.636511	0.612548	0.612548	0.263931	0.666667	0.926362	0.754597	0.810105	0.619563	0.532248	0.504889	0.333136	1	0.935243	0.989022	0.007635	0.909274	0.799448
p8	1	0.39931	0.898132	1	0.908712	0.908712	0.36764	0.777778	0.988977	0.732413	0.898132	0.794992	1	0.537555	0.490156	0.974515	0.82547	0.995004	0.007634	0.91566	0.848795
p9	0.94615	0.475628	0.695438	0.638383	0.394184	0.394184	0.563604	0.555556	0.807539	0.172285	0.695438	0.531409	0.3184	0.842576	0.344384	0.350433	0.983082	0.937347	0.007633	0.922332	0.26318
p10	0.937275	0.396774	0.756339	0.677197	0.627864	0.627864	1	0.555556	0.92963	0.055915	0.756339	0.570945	0.295722	0.959413	0.338075	0.475157	0.79206	0.940772	0.007634	0.928879	0.211809
p11	0.92475	0.759819	0.789319	0.858986	0.436722	0.436722	0.598088	0.555556	0.84068	0.178908	0.789319	0.539407	0.677041	0.745721	0.442687	0.386938	1	0.958845	0.007635	0.935607	0.24375
p12	1	0.491885	0.752347	0.622284	0.605808	0.605808	0.283059	0.666667	0.924957	0.453129	0.752347	0.620417	0.320549	0.805441	0.354432	0.439211	0.921999	0.951975	0.007635	0.942151	0.897991
p13	0.9947	0.461487	0.79419	0.733479	0.482089	0.482089	0.374445	0.555556	0.868149	0.386155	0.79419	0.622424	0.434405	0.861061	0.321304	0.492256	0.874112	0.972207	0.007631	0.949013	0.771043
p14	1	0.46786	0.937828	0.713356	0.695248	0.695248	0.343951	0.555556	0.950187	0.343012	0.937828	0.575909	0.559454	0.623669	0.324128	0.431773	0.820535	0.987389	0.007635	0.955966	0.807924
p15	1	0.60797	0.93607	0.729186	1	1	0.239171	1	1	0.794898	0.93607	0.53407	0.91231	0.106169	0.322737	0.545059	0.899869	1	0.007633	0.962995	1
p16	0.96575	0.400599	0.773134	0.434976	0.415787	0.415787	0.208188	0.444444	0.822586	0.860312	0.773134	0.651179	0.180172	0.631505	0.397161	0.426335	0.862615	0.952084	0.007632	0.9703	0.418816
p17	0.952825	0.601617	0.839701	0.51466	0.603274	0.603274	0.183195	0.777778	0.925139	0.915598	0.839701	0.599674	0.64346	0.075635	0.440137	0.405436	0.881286	0.945516	0.00763	0.977565	0.240169
p18	0.98055	0.487773	1	0.782133	0.708734	0.708734	0.451799	0.777778	0.954344	0.223791	1	0.632584	0.895805	0.243027	0.714308	0.426625	0.883562	0.972728	0.007635	0.9849	0.544049
p19	0.999975	1	0.697666	0.831676	0.75151	0.75151	0.305999	0.444444	0.962899	1	0.697666	1	0.477402	1	0.784453	0.600397	0.871472	0.937121	0.007635	0.992359	0.75918
p20	0.999925	0.631209	0.740231	0.719074	0.56872	0.56872	0.486085	0.444444	0.911574	0.216633	0.740231	0.595833	0.36258	0.942936	0.45152	0.419466	0.961546	0.946137	1	1	0.639372

Table 6: Geometric mean.

AT1	2.296165
AT2	1.785906
AT3	1.530776
AT4	2.296165
AT5	0.255129
AT6	0.255129
AT7	1.275647
AT8	2.296165
AT9	1.275647
AT10	0.255129
AT11	1.275647
AT12	0.255129
AT13	0.255129
AT14	0.765388
AT15	2.296165
AT16	0.255129
AT17	1.785906
AT18	1.785906
AT19	1.785906
AT20	2.296165
AT21	2.296165

Table 7: Weighted matrix.

AT1	0.080357
AT2	0.0625
AT3	0.053571
AT4	0.080357
AT5	0.008929
AT6	0.008929
AT7	0.044643
AT8	0.080357
AT9	0.044643
AT10	0.008929
AT11	0.044643
AT12	0.008929
AT13	0.008929
AT14	0.026786
AT15	0.080357
AT16	0.008929
AT17	0.0625
AT18	0.0625
AT19	0.0625
AT20	0.080357
AT21	0.080357

Table 8: Consistency check.

a3	
AT1	1.6875
AT2	1.3125
AT3	1.125
AT4	1.6875
AT5	0.1875
AT6	0.1875
AT7	0.9375
AT8	1.6875
AT9	0.9375
AT10	0.1875
AT11	0.9375
AT12	0.1875
AT13	0.1875
AT14	0.5625
AT15	1.6875
AT16	0.1875
AT17	1.3125
AT18	1.3125
AT19	1.3125
AT20	1.6875

Table 9: Matrix $M_{4.}$

a4	
AT1	21
AT2	21
AT3	21
AT4	21
AT5	21
AT6	21
AT7	21
AT8	21
AT9	21
AT10	21
AT11	21
AT12	21
AT13	21
AT14	21
AT15	21
AT16	21
AT17	21
AT18	21
AT19	21
AT20	21

$$\mathrm{CR} = \frac{\mathrm{CI}}{\mathrm{RI}}. \tag{13}$$

Here, RI is the random index.

Step 6: calculate the value of P_i by using the SAW method. In our experiment, we used the SAW method for selecting the CH. The value is presented in Table 10

$$P_i = \sum_{j=1}^{n} M_{2i} * M_{1ij}, i = 1, 2, 3\, m. \tag{14}$$

Step 7: in this step, we finally rank the alternative according to the higher value of P_i. And the rank is presented in Table 11

6.2. PROMETHEE Method for CH Selection. Step 1: calculate the denomination matrix for each n attribute and m alternatives $m * m$ matrix. $Q_{j_{m*m}}$. For each attribute, the denomination matrix has been given in Tables 12–34. In Table 35, we have presented the abbreviation of attributes used in the simulation

Step 2: now, the corresponding weights of each attribute are multiplied by each denomination matrix, and the final matrix is calculated by doing the summation of each matrix. And the final denomination matrix is presented in Table 33

$$\left(M_{j_{m*m}}\right) = Q_{j_{m*m}} * w_j, \tag{15}$$

where $w_j = 1$.

$$Q_{m*m} = \sum_{j=1}^{n} \left(M_{j_{m*m}}\right), i = 1, 2, \cdots..m. \tag{16}$$

Step 3: now, compute $\$_i^+$ and $\$_i^-$ by adding rows and columns. This is presented in Table 36

Step 4: compute the net flow by using the following equation as presented in Table 37:

$$\$_i = \$_i^+ - \$_i^-. \tag{17}$$

Step 5: lastly, rank the alternative according to the higher value of $\$_i$, and the rank is given in Table 38

7. Simulation Results

This section evaluates the proposed APRO algorithm against other clustering algorithms under a different scenario. In this, MATLAB is used for the simulation, and we have compared the proposed algorithm by LEACH, LEACH-C, EECS, HEED, HEEC, and DEECET. We have performed the proposed APRO algorithm under different scenarios using three metrics FND, CHD, and Network_Dead. Here, network dead means when 75% of the nodes are dead. A total of five scenarios Table 39–43 have been considered where the simulation area, number of nodes, the initial energy of the sensor nodes, and base station position values are considered different. In all five scenarios, it is shown that the proposed algorithm preserves the energy of sensor nodes and outperforms the other algorithms. Here, we have taken five scenarios by changing the values of the simulation area, the number of nodes, and the base station position, and in all scenarios,

Table 10: SAW method.

P1	0.696925
P2	0.689571
P3	0.711684
P4	0.669327
P5	0.65802
P6	0.726547
P7	0.692058
P8	0.754268
P9	0.616516
P10	0.636602
P11	0.674155
P12	0.685208
P13	0.674693
P14	0.688882
P15	0.753036
P16	0.595946
P17	0.633541
P18	0.730995
P19	0.755554
P20	0.747793
P1	0.696925

Table 11: Rank of the alternatives.

Pop	Rank
1	8
2	10
3	7
4	15
5	16
6	6
7	9
8	2
9	19
10	17
11	14
12	12
13	13
14	11
15	3
16	20
17	18
18	5
19	1
20	4

Table 12: Denomination matrix for AT1.

Pop	1	2	3	4	5	6	7	8	9	10	11	12	13	14	15	16	17	18	19	20
1	0	1	0	1	1	1	1	0	1	1	1	0	1	0	0	1	1	1	1	1
2	0	0	0	1	0	0	0	0	1	1	1	0	0	0	0	1	1	0	0	0
3	0	1	0	1	1	1	1	0	1	1	1	0	1	0	0	1	1	1	1	1
4	0	0	0	0	0	0	0	0	1	1	1	0	0	0	0	0	0	0	0	0
5	0	1	0	1	0	0	0	0	1	1	1	0	0	0	0	1	1	0	0	0
6	0	1	0	1	1	0	0	0	1	1	1	0	0	0	0	1	1	1	0	0
7	0	1	0	1	1	1	0	0	1	1	1	0	1	0	0	1	1	1	0	0
8	0	1	0	1	1	1	1	0	1	1	1	0	1	0	0	1	1	1	1	1
9	0	0	0	0	0	0	0	0	0	1	1	0	0	0	0	0	0	0	0	0
10	0	0	0	0	0	0	0	0	0	0	1	0	0	0	0	0	0	0	0	0
11	0	0	0	0	0	0	0	0	0	0	0	0	0	0	0	0	0	0	0	0
12	0	1	0	1	1	1	1	0	1	1	1	0	1	0	0	1	1	1	1	1
13	0	1	0	1	1	1	0	0	1	1	1	0	0	0	0	1	1	1	0	0
14	0	1	0	1	1	1	1	0	1	1	1	0	1	0	0	1	1	1	1	1
15	0	1	0	1	1	1	1	0	1	1	1	0	1	0	0	1	1	1	1	1
16	0	0	0	1	0	0	0	0	1	1	1	0	0	0	0	0	1	0	0	0
17	0	0	0	1	0	0	0	0	1	1	1	0	0	0	0	0	0	0	0	0
18	0	1	0	1	1	0	0	0	1	1	1	0	0	0	0	1	1	0	0	0
19	0	1	0	1	1	1	1	0	1	1	1	0	1	0	0	1	1	1	0	1
20	0	1	0	1	1	1	1	0	1	1	1	0	1	0	0	1	1	1	0	0

Table 13: Denomination matrix for AT2.

Pop	1	2	3	4	5	6	7	8	9	10	11	12	13	14	15	Pop	1	2	3	4
1	0	0	0	0	1	0	0	1	1	1	0	1	1	1	0	1	0	0	0	0
2	1	0	0	0	1	1	1	1	1	1	1	1	1	1	1	2	1	0	0	0
3	1	1	0	0	1	1	1	1	1	1	1	1	1	1	1	3	1	1	0	0
4	1	1	1	0	1	1	1	1	1	1	1	1	1	1	1	4	1	1	1	0
5	0	0	0	0	0	0	0	0	0	0	0	0	0	0	0	5	0	0	0	0
6	1	0	0	0	1	0	0	1	1	1	0	1	1	1	0	6	1	0	0	0
7	1	0	0	0	1	1	0	1	1	1	0	1	1	1	1	7	1	0	0	0
8	0	0	0	0	1	0	0	0	0	1	0	0	0	0	0	8	0	0	0	0
9	0	0	0	0	1	0	0	1	0	1	0	0	1	1	0	9	0	0	0	0
10	0	0	0	0	1	0	0	0	0	0	0	0	0	0	0	10	0	0	0	0
11	1	0	0	0	1	1	1	1	1	1	0	1	1	1	1	11	1	0	0	0
12	0	0	0	0	1	0	0	1	1	1	0	0	1	1	0	12	0	0	0	0
13	0	0	0	0	1	0	0	1	0	1	0	0	0	0	0	13	0	0	0	0
14	0	0	0	0	1	0	0	1	0	1	0	0	1	0	0	14	0	0	0	0
15	1	0	0	0	1	1	0	1	1	1	0	1	1	1	0	15	1	0	0	0
16	0	0	0	0	1	0	0	1	0	1	0	0	0	0	0	16	0	0	0	0
17	1	0	0	0	1	0	0	1	1	1	0	1	1	1	0	17	1	0	0	0
18	0	0	0	0	1	0	0	1	1	1	0	0	1	1	0	18	0	0	0	0
19	1	1	1	1	1	1	1	1	1	1	1	1	1	1	1	19	1	1	1	1
20	1	0	0	0	1	1	1	1	1	1	0	1	1	1	1	20	1	0	0	0

Table 14: Denomination matrix for AT3.

Pop	1	2	3	4	5	6	7	8	9	10	11	12	13	14	15	16	17	18	19	20
1	0	0	1	1	0	0	1	0	1	1	1	1	1	0	0	1	0	0	1	1
2	1	0	1	1	0	0	1	0	1	1	1	1	1	0	0	1	1	0	1	1
3	0	0	0	1	0	0	1	0	1	1	1	1	1	0	0	1	0	0	1	1
4	0	0	0	0	0	0	0	0	1	0	0	0	0	0	0	0	0	0	1	0
5	1	1	1	1	0	0	1	0	1	1	1	1	1	0	0	1	1	0	1	1
6	1	1	1	1	1	0	1	1	1	1	1	1	1	0	0	1	1	0	1	1
7	0	0	0	1	0	0	0	0	1	1	1	1	1	0	0	1	0	0	1	1
8	1	1	1	1	1	0	1	0	1	1	1	1	1	0	0	1	1	0	1	1
9	0	0	0	0	0	0	0	0	0	0	0	0	0	0	0	0	0	0	0	0
10	0	0	0	1	0	0	0	0	1	0	0	1	0	0	0	0	0	0	1	1
11	0	0	0	1	0	0	0	0	1	1	0	1	0	0	0	1	0	0	1	1
12	0	0	0	1	0	0	0	0	1	0	0	0	0	0	0	0	0	0	1	1
13	0	0	0	1	0	0	0	0	1	1	1	1	0	0	0	1	0	0	1	1
14	1	1	1	1	1	1	1	1	1	1	1	1	1	0	1	1	1	0	1	1
15	1	1	1	1	1	1	1	1	1	1	1	1	1	0	0	1	1	0	1	1
16	0	0	0	1	0	0	0	0	1	1	0	1	0	0	0	0	0	0	1	1
17	1	0	1	1	0	0	1	0	1	1	1	1	1	0	0	1	0	0	1	1
18	1	1	1	1	1	1	1	1	1	1	1	1	1	1	1	1	1	0	1	1
19	0	0	0	0	0	0	0	0	1	0	0	0	0	0	0	0	0	0	0	0
20	0	0	0	1	0	0	0	0	1	0	0	0	0	0	0	0	0	0	1	0

Table 15: Denomination matrix for AT4.

Pop	1	2	3	4	5	6	7	8	9	10	11	12	13	14	15	16	17	18	19	20
1	0	0	1	1	0	0	1	0	1	1	0	1	0	0	0	1	1	0	0	0
2	1	0	1	1	1	0	1	0	1	1	0	1	1	1	1	1	1	1	0	1
3	0	0	0	1	0	0	0	0	0	0	0	0	0	0	0	1	1	0	0	0
4	0	0	0	0	0	0	0	0	0	0	0	0	0	0	0	1	0	0	0	0
5	1	0	1	1	0	0	1	0	1	1	0	1	0	0	0	1	1	0	0	0
6	1	1	1	1	1	0	1	0	1	1	1	1	1	1	1	1	1	1	1	1
7	0	0	1	1	0	0	0	0	0	0	0	1	0	0	0	1	1	0	0	0
8	1	1	1	1	1	1	1	0	1	1	1	1	1	1	1	1	1	1	1	1
9	0	0	1	1	0	0	1	0	0	0	0	1	0	0	0	1	1	0	0	0
10	0	0	1	1	0	0	1	0	1	0	0	1	0	0	0	1	1	0	0	0
11	1	1	1	1	1	0	1	0	1	1	0	1	1	1	1	1	1	1	1	1
12	0	0	1	1	0	0	0	0	0	0	0	0	0	0	0	1	1	0	0	0
13	1	0	1	1	1	0	1	0	1	1	0	1	0	1	1	1	1	0	0	1
14	1	0	1	1	1	0	1	0	1	1	0	1	0	0	0	1	1	0	0	0
15	1	0	1	1	1	0	1	0	1	1	0	1	0	1	0	1	1	0	0	1
16	0	0	0	0	0	0	0	0	0	0	0	0	0	0	0	0	0	0	0	0
17	0	0	0	1	0	0	0	0	0	0	0	0	0	0	0	1	0	0	0	0
18	1	0	1	1	1	0	1	0	1	1	0	1	1	1	1	1	1	0	0	1
19	1	1	1	1	1	0	1	0	1	1	0	1	1	1	1	1	1	1	0	1
20	1	0	1	1	1	0	1	0	1	1	0	1	0	1	0	1	1	0	0	0

Table 16: Denomination matrix for AT5.

Pop	1	2	3	4	5	6	7	8	9	10	11	12	13	14	15	16	17	18	19	20
1	0	1	1	1	1	1	1	0	1	1	1	1	1	1	0	1	1	1	1	1
2	0	0	0	1	0	0	0	0	1	0	1	0	0	0	0	1	0	0	0	0
3	0	1	0	1	1	1	1	0	1	1	1	1	1	0	0	1	1	0	0	1
4	0	0	0	0	0	0	0	0	1	0	0	0	0	0	0	1	0	0	0	0
5	0	1	0	1	0	0	0	0	1	0	1	0	1	0	0	1	0	0	0	0
6	0	1	0	1	1	0	0	0	1	0	1	0	1	0	0	1	0	0	0	0
7	0	1	0	1	1	1	0	0	1	0	1	1	1	0	0	1	1	0	0	1
8	1	1	1	1	1	1	1	0	1	1	1	1	1	1	0	1	1	1	1	1
9	0	0	0	0	0	0	0	0	0	0	0	0	0	0	0	0	0	0	0	0
10	0	1	0	1	1	1	1	0	1	0	1	1	1	0	0	1	1	0	0	1
11	0	0	0	1	0	0	0	0	1	0	0	0	0	0	0	1	0	0	0	0
12	0	1	0	1	1	1	0	0	1	0	1	0	1	0	0	1	1	0	0	1
13	0	1	0	1	0	0	0	0	1	0	1	0	0	0	0	1	0	0	0	0
14	0	1	1	1	1	1	1	0	1	1	1	1	1	0	0	1	1	0	0	1
15	1	1	1	1	1	1	1	1	1	1	1	1	1	1	0	1	1	1	1	1
16	0	0	0	0	0	0	0	0	1	0	0	0	0	0	0	0	0	0	0	0
17	0	1	0	1	1	1	0	0	1	0	1	0	1	0	0	1	0	0	0	1
18	0	1	1	1	1	1	1	0	1	1	1	1	1	1	0	1	1	0	0	1
19	0	1	1	1	1	1	1	0	1	1	1	1	1	1	0	1	1	1	0	1
20	0	1	0	1	1	1	0	0	1	0	1	0	1	0	0	1	0	0	0	0

Table 17: Denomination matrix for AT6.

Pop	1	2	3	4	5	6	7	8	9	10	11	12	13	14	15	16	17	18	19	20
1	0	1	1	1	1	1	1	0	1	1	1	1	1	1	0	1	1	1	1	1
2	0	0	0	1	0	0	0	0	1	0	1	0	0	0	0	1	0	0	0	0
3	0	1	0	1	1	1	1	0	1	1	1	1	1	0	0	1	1	0	0	1
4	0	0	0	0	0	0	0	0	1	0	0	0	0	0	0	1	0	0	0	0
5	0	1	0	1	0	0	0	0	1	0	1	0	1	0	0	1	0	0	0	0
6	0	1	0	1	1	0	0	0	1	0	1	0	1	0	0	1	0	0	0	0
7	0	1	0	1	1	1	0	0	1	0	1	1	1	0	0	1	1	0	0	1
8	1	1	1	1	1	1	1	0	1	1	1	1	1	1	0	1	1	1	1	1
9	0	0	0	0	0	0	0	0	0	0	0	0	0	0	0	0	0	0	0	0
10	0	1	0	1	1	1	1	0	1	0	1	1	1	0	0	1	1	0	0	1
11	0	0	0	1	0	0	0	0	1	0	0	0	0	0	0	1	0	0	0	0
12	0	1	0	1	1	1	0	0	1	0	1	0	1	0	0	1	1	0	0	1
13	0	1	0	1	0	0	0	0	1	0	1	0	0	0	0	1	0	0	0	0
14	0	1	1	1	1	1	1	0	1	1	1	1	1	0	0	1	1	0	0	1
15	1	1	1	1	1	1	1	1	1	1	1	1	1	1	0	1	1	1	1	1
16	0	0	0	0	0	0	0	0	1	0	0	0	0	0	0	0	0	0	0	0
17	0	1	0	1	1	1	0	0	1	0	1	0	1	0	0	1	0	0	0	1
18	0	1	1	1	1	1	1	0	1	1	1	1	1	1	0	1	1	0	0	1
19	0	1	1	1	1	1	1	0	1	1	1	1	1	1	0	1	1	1	0	1
20	0	1	0	1	1	1	0	0	1	0	1	0	1	0	0	1	0	0	0	0

Table 18: Denomination matrix for AT7.

Pop	1	2	3	4	5	6	7	8	9	10	11	12	13	14	15	16	17	18	19	20
1	0	0	1	0	0	0	0	0	0	0	0	0	0	0	1	1	1	0	0	0
2	1	0	1	1	0	0	1	0	0	0	0	1	0	1	1	1	1	0	1	0
3	0	0	0	0	0	0	0	0	0	0	0	0	0	0	1	1	1	0	0	0
4	1	0	1	0	0	0	1	0	0	0	0	1	0	0	1	1	1	0	0	0
5	1	1	1	1	0	0	1	1	0	0	0	1	1	1	1	1	1	0	1	0
6	1	1	1	1	1	0	1	1	1	0	1	1	1	1	1	1	1	1	1	1
7	1	0	1	0	0	0	0	0	0	0	0	0	0	0	1	1	1	0	0	0
8	1	1	1	1	0	0	1	0	0	0	0	1	0	1	1	1	1	0	1	0
9	1	1	1	1	1	0	1	1	0	0	0	1	1	1	1	1	1	1	1	1
10	1	1	1	1	1	1	1	1	1	0	1	1	1	1	1	1	1	1	1	1
11	1	1	1	1	1	0	1	1	1	0	0	1	1	1	1	1	1	1	1	1
12	1	0	1	0	0	0	1	0	0	0	0	0	0	0	1	1	1	0	0	0
13	1	1	1	1	0	0	1	1	0	0	0	1	0	1	1	1	1	0	1	0
14	1	0	1	1	0	0	1	0	0	0	0	1	0	0	1	1	1	0	1	0
15	0	0	0	0	0	0	0	0	0	0	0	0	0	0	0	1	1	0	0	0
16	0	0	0	0	0	0	0	0	0	0	0	0	0	0	0	0	1	0	0	0
17	0	0	0	0	0	0	0	0	0	0	0	0	0	0	0	0	0	0	0	0
18	1	1	1	1	1	0	1	1	0	0	0	1	1	1	1	1	1	0	1	0
19	1	0	1	1	0	0	1	0	0	0	0	1	0	0	1	1	1	0	0	0
20	1	1	1	1	1	0	1	1	0	0	0	1	1	1	1	1	1	1	1	0

Table 19: Denomination matrix for AT8.

Pop	1	2	3	4	5	6	7	8	9	10	11	12	13	14	15	16	17	18	19	20
1	0	0	0	1	0	0	0	0	1	1	1	0	1	1	0	1	0	0	1	1
2	0	0	0	1	0	0	0	0	1	1	1	0	1	1	0	1	0	0	1	1
3	0	0	0	1	0	0	0	0	1	1	1	0	1	1	0	1	0	0	1	1
4	0	0	0	0	0	0	0	0	0	0	0	0	0	0	0	1	0	0	1	1
5	0	0	0	1	0	0	0	0	1	1	1	0	1	1	0	1	0	0	1	1
6	1	1	1	1	1	0	1	0	1	1	1	1	1	1	0	1	0	0	1	1
7	0	0	0	1	0	0	0	0	1	1	1	0	1	1	0	1	0	0	1	1
8	1	1	1	1	1	0	1	0	1	1	1	1	1	1	0	1	0	0	1	1
9	0	0	0	0	0	0	0	0	0	0	0	0	0	0	0	1	0	0	1	1
10	0	0	0	0	0	0	0	0	0	0	0	0	0	0	0	1	0	0	1	1
11	0	0	0	0	0	0	0	0	0	0	0	0	0	0	0	1	0	0	1	1
12	0	0	0	1	0	0	0	0	1	1	1	0	1	1	0	1	0	0	1	1
13	0	0	0	0	0	0	0	0	0	0	0	0	0	0	0	1	0	0	1	1
14	0	0	0	0	0	0	0	0	0	0	0	0	0	0	0	1	0	0	1	1
15	1	1	1	1	1	1	1	1	1	1	1	1	1	1	0	1	1	1	1	1
16	0	0	0	0	0	0	0	0	0	0	0	0	0	0	0	0	0	0	0	0
17	1	1	1	1	1	0	1	0	1	1	1	1	1	1	0	1	0	0	1	1
18	1	1	1	1	1	0	1	0	1	1	1	1	1	1	0	1	0	0	1	1
19	0	0	0	0	0	0	0	0	0	0	0	0	0	0	0	0	0	0	0	0
20	0	0	0	0	0	0	0	0	0	0	0	0	0	0	0	0	0	0	0	0

Table 20: Denomination matrix for AT9.

Pop	1	2	3	4	5	6	7	8	9	10	11	12	13	14	15	16	17	18	19	20
1	0	1	1	1	1	1	1	0	1	1	1	1	1	1	0	1	1	1	1	1
2	0	0	0	1	0	0	0	0	1	0	1	0	0	0	0	1	0	0	0	0
3	0	1	0	1	1	1	1	0	1	1	1	1	1	0	0	1	1	0	0	1
4	0	0	0	0	0	0	0	0	1	0	0	0	0	0	0	1	0	0	0	0
5	0	1	0	1	0	0	0	0	1	0	1	0	1	0	0	1	0	0	0	0
6	0	1	0	1	1	0	0	0	1	0	1	0	1	0	0	1	0	0	0	0
7	0	1	0	1	1	1	0	0	1	0	1	1	1	0	0	1	1	0	0	1
8	1	1	1	1	1	1	1	0	1	1	1	1	1	1	0	1	1	1	1	1
9	0	0	0	0	0	0	0	0	0	0	0	0	0	0	0	0	0	0	0	0
10	0	1	0	1	1	1	1	0	1	0	1	1	1	0	0	1	1	0	0	1
11	0	0	0	1	0	0	0	0	1	0	0	0	0	0	0	1	0	0	0	0
12	0	1	0	1	1	1	0	0	1	0	1	0	1	0	0	1	0	0	0	1
13	0	1	0	1	0	0	0	0	1	0	1	0	0	0	0	1	0	0	0	0
14	0	1	1	1	1	1	1	0	1	1	1	1	1	0	0	1	1	0	0	1
15	1	1	1	1	1	1	1	1	1	1	1	1	1	1	0	1	1	1	1	1
16	0	0	0	0	0	0	0	0	1	0	0	0	0	0	0	0	0	0	0	0
17	0	1	0	1	1	1	0	0	1	0	1	1	1	0	0	1	0	0	0	1
18	0	1	1	1	1	1	1	0	1	1	1	1	1	1	0	1	1	0	0	1
19	0	1	1	1	1	1	1	0	1	1	1	1	1	1	0	1	1	1	0	1
20	0	1	0	1	1	1	0	0	1	0	1	0	1	0	0	1	0	0	0	0

Table 21: Denomination matrix for AT10.

Pop	1	2	3	4	5	6	7	8	9	10	11	12	13	14	15	16	17	18	19	20
1	0	1	0	1	1	1	0	0	1	1	1	1	1	1	0	0	0	1	0	1
2	0	0	0	0	1	1	0	0	1	1	1	0	0	0	0	0	0	1	0	1
3	1	1	0	1	1	1	1	1	1	1	1	1	1	1	0	0	0	1	0	1
4	0	1	0	0	1	1	0	0	1	1	1	1	1	1	0	0	0	1	0	1
5	0	0	0	0	0	1	0	0	1	1	1	0	0	0	0	0	0	0	0	1
6	0	0	0	0	0	0	0	0	0	1	0	0	0	0	0	0	0	0	0	0
7	1	1	0	1	1	1	0	1	1	1	1	1	1	1	0	0	0	1	0	1
8	1	1	0	1	1	1	0	0	1	1	1	1	1	1	0	0	0	1	0	1
9	0	0	0	0	0	1	0	0	0	1	0	0	0	0	0	0	0	0	0	0
10	0	0	0	0	0	0	0	0	0	0	0	0	0	0	0	0	0	0	0	0
11	0	0	0	0	0	1	0	0	1	1	0	0	0	0	0	0	0	0	0	0
12	0	1	0	0	1	1	0	0	1	1	1	0	1	1	0	0	0	1	0	1
13	0	1	0	0	1	1	0	0	1	1	1	0	0	1	0	0	0	1	0	1
14	0	1	0	0	1	1	0	0	1	1	1	0	0	0	0	0	0	1	0	1
15	1	1	1	1	1	1	1	1	1	1	1	1	1	1	0	0	0	1	0	1
16	1	1	1	1	1	1	1	1	1	1	1	1	1	1	1	0	0	1	0	1
17	1	1	1	1	1	1	1	1	1	1	1	1	1	1	1	1	0	1	0	1
18	0	0	0	0	1	1	0	0	1	1	1	0	0	0	0	0	0	0	0	1
19	1	1	1	1	1	1	1	1	1	1	1	1	1	1	1	1	1	1	0	1
20	0	0	0	0	0	1	0	0	1	1	1	0	0	0	0	0	0	0	0	0

Table 22: Denomination matrix for AT11.

Pop	1	2	3	4	5	6	7	8	9	10	11	12	13	14	15	16	17	18	19	20
1	0	0	1	1	0	0	1	0	1	1	1	1	1	0	0	1	0	0	1	1
2	1	0	1	1	0	0	1	0	1	1	1	1	1	0	0	1	1	0	1	1
3	0	0	0	1	0	0	1	0	1	1	1	1	1	0	0	1	0	0	1	1
4	0	0	0	0	0	0	0	0	1	0	0	0	0	0	0	0	0	0	1	0
5	1	1	1	1	0	0	1	0	1	1	1	1	1	0	0	1	1	0	1	1
6	1	1	1	1	1	0	1	1	1	1	1	1	1	0	0	1	1	0	1	1
7	0	0	0	1	0	0	0	0	1	1	1	1	1	0	0	1	0	0	1	1
8	1	1	1	1	1	0	1	0	1	1	1	1	1	0	0	1	1	0	1	1
9	0	0	0	0	0	0	0	0	0	0	0	0	0	0	0	0	0	0	0	0
10	0	0	0	1	0	0	0	0	1	0	0	1	0	0	0	0	0	0	1	1
11	0	0	0	1	0	0	0	0	1	1	0	1	0	0	0	1	0	0	1	1
12	0	0	0	1	0	0	0	0	1	0	0	0	0	0	0	0	0	0	1	1
13	0	0	0	1	0	0	0	0	1	1	1	1	0	0	0	1	0	0	1	1
14	1	1	1	1	1	1	1	1	1	1	1	1	1	0	1	1	1	0	1	1
15	1	1	1	1	1	1	1	1	1	1	1	1	1	0	0	1	1	0	1	1
16	0	0	0	1	0	0	0	0	1	1	0	1	0	0	0	0	0	0	1	1
17	1	0	1	1	0	0	1	0	1	1	1	1	1	0	0	1	0	0	1	1
18	1	1	1	1	1	1	1	1	1	1	1	1	1	1	1	1	1	0	1	1
19	0	0	0	0	0	0	0	0	1	0	0	0	0	0	0	0	0	0	0	0
20	0	0	0	1	0	0	0	0	1	0	0	0	0	0	0	0	0	0	1	0

Table 23: Denomination matrix for AT12.

Pop	1	2	3	4	5	6	7	8	9	10	11	12	13	14	15	16	17	18	19	20
1	0	1	1	1	1	1	1	0	1	1	1	1	1	1	0	1	1	1	1	1
2	0	0	0	1	0	0	0	0	1	0	1	0	0	0	0	1	0	0	0	0
3	0	1	0	1	1	1	1	0	1	1	1	1	1	0	0	1	1	0	0	1
4	0	0	0	0	0	0	0	0	1	0	0	0	0	0	0	1	0	0	0	0
5	0	1	0	1	0	0	0	0	1	0	1	0	1	0	0	1	0	0	0	0
6	0	1	0	1	1	0	0	0	1	0	1	0	1	0	0	1	0	0	0	0
7	0	1	0	1	1	1	0	0	1	0	1	1	1	0	0	1	1	0	0	1
8	1	1	1	1	1	1	1	0	1	1	1	1	1	1	0	1	1	1	1	1
9	0	0	0	0	0	0	0	0	0	0	0	0	0	0	0	0	0	0	0	0
10	0	1	0	1	1	1	1	0	1	0	1	1	1	0	0	1	1	0	0	1
11	0	0	0	1	0	0	0	0	1	0	0	0	0	0	0	1	0	0	0	0
12	0	1	0	1	1	1	0	0	1	0	1	0	1	0	0	1	1	0	0	1
13	0	1	0	1	0	0	0	0	1	0	1	0	0	0	0	1	0	0	0	0
14	0	1	1	1	1	1	1	0	1	1	1	1	1	0	0	1	1	0	0	1
15	1	1	1	1	1	1	1	1	1	1	1	1	1	1	0	1	1	1	1	1
16	0	0	0	0	0	0	0	0	1	0	0	0	0	0	0	0	0	0	0	0
17	0	1	0	1	1	1	0	0	1	0	1	0	1	0	0	1	0	0	0	1
18	0	1	1	1	1	1	1	0	1	1	1	1	1	1	0	1	1	0	0	1
19	0	1	1	1	1	1	1	0	1	1	1	1	1	1	0	1	1	1	0	1
20	0	1	0	1	1	1	0	0	1	0	1	0	1	0	0	1	0	0	0	0

Table 24: Denomination matrix for AT13.

Pop	1	2	3	4	5	6	7	8	9	10	11	12	13	14	15	16	17	18	19	20
1	0	0	0	1	0	0	0	0	1	1	0	1	1	0	0	1	0	0	0	1
2	1	0	1	1	1	0	1	0	1	1	1	1	1	1	0	1	1	0	1	1
3	1	0	0	1	0	0	0	0	1	1	0	1	1	0	0	1	0	0	1	1
4	0	0	0	0	0	0	0	0	0	1	0	0	0	0	0	1	0	0	0	0
5	1	0	1	1	0	0	1	0	1	1	0	1	1	0	0	1	0	0	1	1
6	1	1	1	1	1	0	1	0	1	1	1	1	1	1	1	1	1	1	1	1
7	1	0	1	1	0	0	0	0	1	1	0	1	1	0	0	1	0	0	1	1
8	1	1	1	1	1	1	1	0	1	1	1	1	1	1	1	1	1	1	1	1
9	0	0	0	1	0	0	0	0	0	1	0	0	0	0	0	1	0	0	0	0
10	0	0	0	0	0	0	0	0	0	0	0	0	0	0	0	1	0	0	0	0
11	1	0	1	1	1	0	1	0	1	1	0	1	1	1	0	1	1	0	1	1
12	0	0	0	1	0	0	0	0	1	1	0	0	0	0	0	1	0	0	0	0
13	0	0	0	1	0	0	0	0	1	1	0	1	0	0	0	1	0	0	0	1
14	1	0	1	1	1	0	1	0	1	1	0	1	1	0	0	1	0	0	1	1
15	1	1	1	1	1	0	1	0	1	1	1	1	1	1	0	1	1	1	1	1
16	0	0	0	0	0	0	0	0	0	0	0	0	0	0	0	0	0	0	0	0
17	1	0	1	1	1	0	1	0	1	1	0	1	1	1	0	1	0	0	1	1
18	1	1	1	1	1	0	1	0	1	1	1	1	1	1	0	1	1	0	1	1
19	1	0	0	1	0	0	0	0	1	1	0	1	1	0	0	1	0	0	0	1
20	0	0	0	1	0	0	0	0	1	1	0	1	0	0	0	1	0	0	0	0

Table 25: Denomination matrix for AT14.

Pop	1	2	3	4	5	6	7	8	9	10	11	12	13	14	15	16	17	18	19	20
1	0	1	1	1	1	1	1	1	0	0	0	0	0	1	1	1	1	1	0	0
2	0	0	1	1	1	1	1	1	0	0	0	0	0	0	1	0	1	1	0	0
3	0	0	0	0	0	1	0	0	0	0	0	0	0	0	1	0	1	1	0	0
4	0	0	1	0	0	1	1	1	0	0	0	0	0	0	1	0	1	1	0	0
5	0	0	1	1	0	1	1	1	0	0	0	0	0	0	1	0	1	1	0	0
6	0	0	0	0	0	0	0	0	0	0	0	0	0	0	1	0	1	1	0	0
7	0	0	1	0	0	1	0	0	0	0	0	0	0	0	1	0	1	1	0	0
8	0	0	1	0	0	1	1	0	0	0	0	0	0	0	1	0	1	1	0	0
9	1	1	1	1	1	1	1	1	0	0	1	1	0	1	1	1	1	1	0	0
10	1	1	1	1	1	1	1	1	1	0	1	1	1	1	1	1	1	1	0	1
11	1	1	1	1	1	1	1	1	0	0	0	0	0	1	1	1	1	1	0	0
12	1	1	1	1	1	1	1	1	0	0	1	0	0	1	1	1	1	1	0	0
13	1	1	1	1	1	1	1	1	1	0	1	1	0	1	1	1	1	1	0	0
14	0	1	1	1	1	1	1	1	0	0	0	0	0	0	1	0	1	1	0	0
15	0	0	0	0	0	0	0	0	0	0	0	0	0	0	0	0	1	0	0	0
16	0	1	1	1	1	1	1	1	0	0	0	0	0	1	1	0	1	1	0	0
17	0	0	0	0	0	0	0	0	0	0	0	0	0	0	0	0	0	0	0	0
18	0	0	0	0	0	0	0	0	0	0	0	0	0	0	1	0	1	0	0	0
19	1	1	1	1	1	1	1	1	1	1	1	1	1	1	1	1	1	1	0	1
20	1	1	1	1	1	1	1	1	1	0	1	1	1	1	1	1	1	1	0	0

Table 26: Denomination matrix for AT15.

Pop	1	2	3	4	5	6	7	8	9	10	11	12	13	14	15	16	17	18	19	20
1	0	0	0	0	0	0	0	0	0	0	0	0	1	1	1	0	0	0	0	0
2	1	0	0	0	1	0	1	0	1	1	0	1	1	1	1	0	0	0	0	0
3	1	1	0	0	1	1	1	0	1	1	1	1	1	1	1	1	1	0	0	1
4	1	1	1	0	1	1	1	1	1	1	1	1	1	1	1	1	1	1	1	1
5	1	0	0	0	0	0	1	0	1	1	0	1	1	1	1	0	0	0	0	0
6	1	1	0	0	1	0	1	0	1	1	0	1	1	1	1	1	0	0	0	0
7	1	0	0	0	0	0	0	0	0	0	0	0	1	1	1	0	0	0	0	0
8	1	1	1	0	1	1	1	0	1	1	1	1	1	1	1	1	1	0	0	1
9	1	0	0	0	0	0	1	0	0	1	0	0	1	1	1	0	0	0	0	0
10	1	0	0	0	0	0	1	0	0	0	0	0	1	1	1	0	0	0	0	0
11	1	1	0	0	1	1	1	0	1	1	0	1	1	1	1	1	1	0	0	0
12	1	0	0	0	0	0	1	0	1	1	0	0	1	1	1	0	0	0	0	0
13	0	0	0	0	0	0	0	0	0	0	0	0	0	0	0	0	0	0	0	0
14	0	0	0	0	0	0	0	0	0	0	0	0	1	0	1	0	0	0	0	0
15	0	0	0	0	0	0	0	0	0	0	0	0	1	0	0	0	0	0	0	0
16	1	1	0	0	1	0	1	0	1	1	0	1	1	1	1	0	0	0	0	0
17	1	1	0	0	1	1	1	0	1	1	0	1	1	1	1	1	0	0	0	0
18	1	1	1	0	1	1	1	1	1	1	1	1	1	1	1	1	1	0	0	1
19	1	1	1	0	1	1	1	1	1	1	1	1	1	1	1	1	1	1	0	1
20	1	1	0	0	1	1	1	0	1	1	1	1	1	1	1	1	1	0	0	0

Table 27: Denomination matrix for AT16.

Pop	1	2	3	4	5	6	7	8	9	10	11	12	13	14	15	16	17	18	19	20
1	0	1	0	1	0	1	0	0	1	1	1	1	0	1	0	1	1	1	0	1
2	0	0	0	0	0	0	0	0	0	0	0	0	0	0	0	0	0	0	0	0
3	1	1	0	1	0	1	0	0	1	1	1	1	1	1	1	1	1	1	0	1
4	0	1	0	0	0	0	0	0	1	0	1	1	0	1	0	1	1	1	0	1
5	1	1	1	1	0	1	0	0	1	1	1	1	1	1	1	1	1	1	1	1
6	0	1	0	1	0	0	0	0	1	0	1	1	0	1	0	1	1	1	0	1
7	1	1	1	1	1	1	0	1	1	1	1	1	1	1	1	1	1	1	1	1
8	1	1	1	1	1	1	0	0	1	1	1	1	1	1	1	1	1	1	1	1
9	0	1	0	0	0	0	0	0	0	0	0	0	0	0	0	0	0	0	0	0
10	0	1	0	1	0	1	0	0	1	0	1	1	0	1	0	1	1	1	0	1
11	0	1	0	0	0	0	0	0	1	0	0	0	0	0	0	0	0	0	0	0
12	0	1	0	0	0	0	0	0	1	0	1	0	0	1	0	1	1	1	0	1
13	1	1	0	1	0	1	0	0	1	1	1	1	0	1	0	1	1	1	0	1
14	0	1	0	0	0	0	0	0	1	0	1	0	0	0	0	1	1	1	0	1
15	1	1	0	1	0	1	0	0	1	1	1	1	1	1	0	1	1	1	0	1
16	0	1	0	0	0	0	0	0	1	0	1	0	0	0	0	0	1	0	0	1
17	0	1	0	0	0	0	0	0	1	0	1	0	0	0	0	0	0	0	0	0
18	0	1	0	0	0	0	0	0	1	0	1	0	0	0	0	1	1	0	0	1
19	1	1	1	1	0	1	0	0	1	1	1	1	1	1	1	1	1	1	0	1
20	0	1	0	0	0	0	0	0	1	0	1	0	0	0	0	0	1	0	0	0

Table 28: Denomination matrix for AT17.

Pop	1	2	3	4	5	6	7	8	9	10	11	12	13	14	15	16	17	18	19	20
1	0	1	1	1	1	1	1	1	0	1	0	1	1	1	1	1	1	1	1	0
2	0	0	1	1	1	1	1	1	0	1	0	1	1	1	1	1	1	1	1	0
3	0	0	0	0	0	1	0	1	0	1	0	0	1	1	0	1	1	0	1	0
4	0	0	1	0	0	1	0	1	0	1	0	0	1	1	1	1	1	1	1	0
5	0	0	1	1	0	1	0	1	0	1	0	0	1	1	1	1	1	1	1	0
6	0	0	0	0	0	0	0	1	0	1	0	0	0	1	0	1	0	0	1	0
7	0	0	1	1	1	1	0	1	0	1	0	1	1	1	1	1	1	1	1	0
8	0	0	0	0	0	0	0	0	0	1	0	0	0	1	0	0	0	0	0	0
9	1	1	1	1	1	1	1	1	0	1	0	1	1	1	1	1	1	1	1	1
10	0	0	0	0	0	0	0	0	0	0	0	0	0	0	0	0	0	0	0	0
11	1	1	1	1	1	1	1	1	1	1	0	1	1	1	1	1	1	1	1	1
12	0	0	1	1	1	1	0	1	0	1	0	0	1	1	1	1	1	1	1	0
13	0	0	0	0	0	1	0	1	0	1	0	0	0	1	0	1	0	0	1	0
14	0	0	0	0	0	0	0	0	0	1	0	0	0	0	0	0	0	0	0	0
15	0	0	1	0	0	1	0	1	0	1	0	0	1	1	0	1	1	1	1	0
16	0	0	0	0	0	0	0	1	0	1	0	0	0	1	0	0	0	0	0	0
17	0	0	0	0	0	1	0	1	0	1	0	0	1	1	0	1	0	0	1	0
18	0	0	1	0	0	1	0	1	0	1	0	0	1	1	0	1	1	0	1	0
19	0	0	0	0	0	0	0	1	0	1	0	0	0	1	0	1	0	0	0	0
20	1	1	1	1	1	1	1	1	0	1	0	1	1	1	1	1	1	1	1	0

Table 29: Denomination matrix for AT18.

Pop	1	2	3	4	5	6	7	8	9	10	11	12	13	14	15	16	17	18	19	20
1	0	0	1	1	1	1	0	0	1	1	1	1	1	0	0	1	1	1	1	1
2	1	0	1	1	1	1	1	0	1	1	1	1	1	1	0	1	1	1	1	1
3	0	0	0	1	0	0	0	0	1	1	1	1	1	0	0	1	1	1	1	1
4	0	0	0	0	0	0	0	0	1	1	0	1	0	0	0	1	1	0	1	1
5	0	0	1	1	0	1	0	0	1	1	1	1	1	0	0	1	1	1	1	1
6	0	0	1	1	0	0	0	0	1	1	1	1	1	0	0	1	1	1	1	1
7	1	0	1	1	1	1	0	0	1	1	1	1	1	1	0	1	1	1	1	1
8	1	1	1	1	1	1	1	0	1	1	1	1	1	1	0	1	1	1	1	1
9	0	0	0	0	0	0	0	0	0	0	0	0	0	0	0	0	0	0	1	0
10	0	0	0	0	0	0	0	0	1	0	0	0	0	0	0	0	0	0	1	0
11	0	0	0	1	0	0	0	0	1	1	0	1	0	0	0	1	1	0	1	1
12	0	0	0	0	0	0	0	0	1	1	0	0	0	0	0	0	1	0	1	1
13	0	0	0	1	0	0	0	0	1	1	1	1	0	0	0	1	1	0	1	1
14	1	0	1	1	1	1	0	0	1	1	1	1	1	0	0	1	1	1	1	1
15	1	1	1	1	1	1	1	1	1	1	1	1	1	1	0	1	1	1	1	1
16	0	0	0	0	0	0	0	0	1	1	0	1	0	0	0	0	1	0	1	1
17	0	0	0	0	0	0	0	0	1	1	0	0	0	0	0	0	0	0	1	0
18	0	0	0	1	0	0	0	0	1	1	1	1	1	0	0	1	1	0	1	1
19	0	0	0	0	0	0	0	0	0	0	0	0	0	0	0	0	0	0	0	0
20	0	0	0	0	0	0	0	0	1	1	0	0	0	0	0	0	1	0	1	0

Table 30: Denomination matrix for AT19.

Pop	1	2	3	4	5	6	7	8	9	10	11	12	13	14	15	16	17	18	19	20
1	0	1	1	1	0	1	0	1	1	1	0	1	1	1	1	1	1	0	0	0
2	0	0	1	1	0	1	0	1	1	1	0	1	1	0	1	1	1	0	0	0
3	0	0	0	0	0	1	0	0	1	0	0	0	1	0	1	1	1	0	0	0
4	0	0	1	0	0	1	0	1	1	1	0	0	1	0	1	1	1	0	0	0
5	1	1	1	1	0	1	1	1	1	1	1	1	1	1	1	1	1	0	1	0
6	0	0	0	0	0	0	0	0	1	0	0	0	1	0	1	1	1	0	0	0
7	1	1	1	1	0	1	0	1	1	1	1	1	1	1	1	1	1	0	1	0
8	0	0	1	0	0	1	0	0	1	1	0	0	1	0	1	1	1	0	0	0
9	0	0	0	0	0	0	0	0	0	0	0	0	1	0	0	1	1	0	0	0
10	0	0	1	0	0	1	0	0	1	0	0	0	1	0	1	1	1	0	0	0
11	1	1	1	1	0	1	0	1	1	1	0	1	1	1	1	1	1	0	1	0
12	0	0	1	1	0	1	0	1	1	1	0	0	1	0	1	1	1	0	0	0
13	0	0	0	0	0	0	0	0	0	0	0	0	0	0	0	0	1	0	0	0
14	0	1	1	1	0	1	0	1	1	1	0	1	1	0	1	1	1	0	0	0
15	0	0	0	0	0	0	0	0	1	0	0	0	1	0	0	1	1	0	0	0
16	0	0	0	0	0	0	0	0	0	0	0	0	1	0	0	0	1	0	0	0
17	0	0	0	0	0	0	0	0	0	0	0	0	0	0	0	0	0	0	0	0
18	1	1	1	1	1	1	1	1	1	1	1	1	1	1	1	1	1	0	1	0
19	1	1	1	1	0	1	0	1	1	1	0	1	1	1	1	1	1	0	0	0
20	1	1	1	1	1	1	1	1	1	1	1	1	1	1	1	1	1	1	1	0

Table 31: Denomination matrix for AT20.

Pop	1	2	3	4	5	6	7	8	9	10	11	12	13	14	15	16	17	18	19	20
1	0	0	0	0	0	0	0	0	0	0	0	0	0	0	0	0	0	0	0	0
2	1	0	0	0	0	0	0	0	0	0	0	0	0	0	0	0	0	0	0	0
3	1	1	0	0	0	0	0	0	0	0	0	0	0	0	0	0	0	0	0	0
4	1	1	1	0	0	0	0	0	0	0	0	0	0	0	0	0	0	0	0	0
5	1	1	1	1	0	0	0	0	0	0	0	0	0	0	0	0	0	0	0	0
6	1	1	1	1	1	0	0	0	0	0	0	0	0	0	0	0	0	0	0	0
7	1	1	1	1	1	1	0	0	0	0	0	0	0	0	0	0	0	0	0	0
8	1	1	1	1	1	1	1	0	0	0	0	0	0	0	0	0	0	0	0	0
9	1	1	1	1	1	1	1	1	0	0	0	0	0	0	0	0	0	0	0	0
10	1	1	1	1	1	1	1	1	1	0	0	0	0	0	0	0	0	0	0	0
11	1	1	1	1	1	1	1	1	1	1	0	0	0	0	0	0	0	0	0	0
12	1	1	1	1	1	1	1	1	1	1	1	0	0	0	0	0	0	0	0	0
13	1	1	1	1	1	1	1	1	1	1	1	1	0	0	0	0	0	0	0	0
14	1	1	1	1	1	1	1	1	1	1	1	1	1	0	0	0	0	0	0	0
15	1	1	1	1	1	1	1	1	1	1	1	1	1	1	0	0	0	0	0	0
16	1	1	1	1	1	1	1	1	1	1	1	1	1	1	1	0	0	0	0	0
17	1	1	1	1	1	1	1	1	1	1	1	1	1	1	1	1	0	0	0	0
18	1	1	1	1	1	1	1	1	1	1	1	1	1	1	1	1	1	0	0	0
19	1	1	1	1	1	1	1	1	1	1	1	1	1	1	1	1	1	1	0	0
20	1	1	1	1	1	1	1	1	1	1	1	1	1	1	1	1	1	1	1	0

Table 32: Denomination matrix for AT21.

Pop	1	2	3	4	5	6	7	8	9	10	11	12	13	14	15	16	17	18	19	20
1	0	1	0	1	1	1	0	0	1	1	1	0	1	0	0	1	1	1	1	1
2	0	0	0	1	0	0	0	0	1	1	1	0	0	0	0	1	1	0	0	0
3	1	1	0	1	1	1	0	0	1	1	1	0	1	0	0	1	1	1	1	1
4	0	0	0	0	0	0	0	0	0	1	0	0	0	0	0	0	0	0	0	0
5	0	1	0	1	0	0	0	0	1	1	1	0	0	0	0	1	1	0	0	0
6	0	1	0	1	1	0	0	0	1	1	1	0	0	0	0	1	1	0	0	0
7	1	1	1	1	1	1	0	0	1	1	1	0	1	0	0	1	1	1	1	1
8	1	1	1	1	1	1	1	0	1	1	1	0	1	1	0	1	1	1	1	1
9	0	0	0	1	0	0	0	0	0	1	1	0	0	0	0	0	1	0	0	0
10	0	0	0	0	0	0	0	0	0	0	0	0	0	0	0	0	0	0	0	0
11	0	0	0	1	0	0	0	0	0	1	0	0	0	0	0	0	1	0	0	0
12	1	1	1	1	1	1	1	1	1	1	1	0	1	1	0	1	1	1	1	1
13	0	1	0	1	1	1	0	0	1	1	1	0	0	0	0	1	1	1	1	1
14	1	1	1	1	1	1	1	0	1	1	1	0	1	0	0	1	1	1	1	1
15	1	1	1	1	1	1	1	1	1	1	1	1	1	1	0	1	1	1	1	1
16	0	0	0	1	0	0	0	0	1	1	1	0	0	0	0	0	1	0	0	0
17	0	0	0	1	0	0	0	0	0	1	0	0	0	0	0	0	0	0	0	0
18	0	1	0	1	1	1	0	0	1	1	1	0	0	0	0	1	1	0	0	0
19	0	1	0	1	1	1	0	0	1	1	1	0	0	0	0	1	1	1	0	1
20	0	1	0	1	1	1	0	0	1	1	1	0	0	0	0	1	1	1	0	0

Table 33: Final denomination matrix.

Pop	1	2	3	4	5	6	7	8	9	10
1	0	0.196429	0.3125	0.455357	0.241071	0.1875	0.348214	0.089286	0.5	0.491071
2	0.375	0	0.258929	0.482143	0.267857	0.098214	0.401786	0.089286	0.5625	0.5
3	0.178571	0.3125	0	0.428571	0.303571	0.339286	0.401786	0.071429	0.5	0.5
4	0.196429	0.169643	0.223214	0	0.160714	0.1875	0.223214	0.178571	0.410714	0.25
5	0.330357	0.303571	0.267857	0.491071	0	0.053571	0.348214	0.071429	0.517857	0.455357
6	0.464286	0.553571	0.3125	0.464286	0.598214	0	0.392857	0.205357	0.616071	0.5
7	0.223214	0.169643	0.169643	0.428571	0.223214	0.258929	0	0.080357	0.419643	0.357143
8	0.482143	0.5625	0.5	0.473214	0.580357	0.366071	0.571429	0	0.517857	0.580357
9	0.151786	0.089286	0.151786	0.160714	0.133929	0.035714	0.232143	0.133929	0	0.241071
10	0.160714	0.151786	0.151786	0.321429	0.196429	0.151786	0.294643	0.071429	0.330357	0
11	0.3125	0.25	0.160714	0.321429	0.303571	0.178571	0.303571	0.133929	0.464286	0.339286
12	0.160714	0.196429	0.151786	0.4375	0.241071	0.1875	0.241071	0.089286	0.5	0.330357
13	0.169643	0.241071	0.151786	0.410714	0.258929	0.133929	0.160714	0.133929	0.383929	0.357143
14	0.241071	0.294643	0.321429	0.401786	0.428571	0.285714	0.401786	0.1875	0.357143	0.410714
15	0.410714	0.357143	0.339286	0.428571	0.482143	0.401786	0.419643	0.3125	0.5	0.491071
16	0.098214	0.133929	0.035714	0.214286	0.178571	0.044643	0.125	0.098214	0.348214	0.339286
17	0.348214	0.25	0.196429	0.419643	0.303571	0.160714	0.276786	0.071429	0.5	0.428571
18	0.401786	0.473214	0.455357	0.455357	0.607143	0.258929	0.464286	0.285714	0.580357	0.571429
19	0.330357	0.419643	0.383929	0.392857	0.410714	0.339286	0.455357	0.1875	0.526786	0.428571
20	0.303571	0.3125	0.151786	0.401786	0.4375	0.330357	0.375	0.133929	0.526786	0.330357

Table 34: Final denomination matrix.

	11	12	13	14	15	16	17	18	19	20
1	0.339286	0.330357	0.482143	0.330357	0.160714	0.553571	0.303571	0.25	0.321429	0.348214
2	0.401786	0.375	0.410714	0.357143	0.294643	0.517857	0.401786	0.178571	0.232143	0.339286
3	0.491071	0.339286	0.5	0.25	0.232143	0.616071	0.455357	0.196429	0.267857	0.5
4	0.25	0.214286	0.160714	0.169643	0.223214	0.4375	0.232143	0.196429	0.258929	0.25
5	0.348214	0.330357	0.392857	0.223214	0.169643	0.473214	0.348214	0.044643	0.241071	0.214286
6	0.473214	0.464286	0.517857	0.366071	0.25	0.607143	0.410714	0.3125	0.3125	0.321429
7	0.348214	0.330357	0.491071	0.25	0.232143	0.526786	0.375	0.1875	0.196429	0.276786
8	0.517857	0.482143	0.517857	0.383929	0.258929	0.553571	0.5	0.285714	0.464286	0.517857
9	0.107143	0.151786	0.1875	0.214286	0.151786	0.303571	0.151786	0.071429	0.125	0.125
10	0.232143	0.321429	0.214286	0.160714	0.160714	0.3125	0.223214	0.080357	0.223214	0.321429
11	0	0.375	0.276786	0.303571	0.303571	0.544643	0.303571	0.214286	0.3125	0.375
12	0.276786	0	0.375	0.276786	0.160714	0.455357	0.267857	0.1875	0.258929	0.348214
13	0.294643	0.276786	0	0.178571	0.160714	0.553571	0.25	0.125	0.223214	0.294643
14	0.267857	0.294643	0.392857	0	0.258929	0.526786	0.401786	0.125	0.3125	0.348214
15	0.348214	0.410714	0.491071	0.3125	0	0.526786	0.553571	0.3125	0.330357	0.428571
16	0.107143	0.196429	0.098214	0.125	0.125	0	0.169643	0.044643	0.098214	0.125
17	0.348214	0.383929	0.401786	0.25	0.098214	0.482143	0	0.071429	0.1875	0.267857
18	0.4375	0.464286	0.526786	0.526786	0.339286	0.607143	0.5	0	0.232143	0.4375
19	0.339286	0.392857	0.428571	0.339286	0.321429	0.473214	0.464286	0.419643	0	0.428571
20	0.276786	0.303571	0.357143	0.303571	0.223214	0.446429	0.383929	0.214286	0.142857	0

Table 35: Abbreviations of attribute.

Attributes used	Abbreviations
CH-Cov	AT1
BS-CH Connectivity	AT2
Avg-CH Life	AT3
Avg-Residual Energy	AT4
CH-Con-Avg Residual	AT5
CH-Dcon-Avg Residual	AT6
BS-CH Bearing	AT7
Std Residual	AT8
Avg-BS Life	AT9
Std_Avg_Ch_Life	AT10
Maximum_Dis_BS	AT11
Avg_Dis_CHs	AT12
Avg_BS_DIS	AT13
Std_CH_Con_Avg_Residual	AT14
Std_CH_Dcon_Avg_Residual	AT15
Std_Residual	AT16
Node_Power	AT17
CH_Power	AT18
Std_Power	AT19
Std_Member Node	AT20
Std_Dev_Energy Trans	AT21

Table 36: Vec Pos and Vec Neg.

	Vec Pos	Vec Neg
1	6.241071	5.339286
2	6.544643	5.4375
3	6.883929	4.696429
4	4.392857	7.589286
5	5.625	6.357143
6	8.142857	4
7	5.544643	6.4375
8	9.116071	2.625
9	2.919643	9.0625
10	4.080357	7.901786
11	5.776786	6.205357
12	5.142857	6.4375
13	4.758929	7.223214
14	6.258929	5.321429
15	7.857143	4.125
16	2.705357	9.517857
17	5.446429	6.696429
18	8.625	3.517857
19	7.482143	4.741071
20	5.955357	6.267857

our proposed algorithm (Table 44) performs better than LEACH, LEACH-C, EECS, HEED, HEEC, and DEECET. The performance has been measured in terms of the first node dead, the cluster head dead, and the last node dead. We measured network lifetime in terms of dead nodes, as network lifetime means how much time a network sustains.

Table 37: Net flow.

Alternatives	Net flow
1	0.901786
2	1.107143
3	2.1875
4	-3.19643
5	-0.73214
6	4.142857
7	-0.89286
8	6.491071
9	-6.14286
10	-3.82143
11	-0.42857
12	-1.29464
13	-2.46429
14	0.9375
15	3.732143
16	-6.8125
17	-1.25
18	5.107143
19	2.741071
20	-0.3125

Table 38: Rank of the PROMETHEE.

Pop	Rank
1	8
2	18
3	6
4	15
5	19
6	3
7	2
8	14
9	1
10	20
11	11
12	5
13	7
14	17
15	12
16	13
17	4
18	10
19	9
20	16

The proposed APRO method is a hybrid approach of AHP and PROMETHEE, and the time complexity of the algorithm is $o(mn^2)$ and $O(mnlogn)$, respectively, and the overall proposed APRO hybrid algorithmic complexity is $O(mnlogn)$.

Table 39: First scenario.

Parameter	Values
Area of deployment	200*200
Sensor nodes	150
Base station position	(100, 100)
Initial node power	.2 J

Table 40: Second scenario.

Parameter	Values
Area of deployment	250*250
Sensor nodes	150
Base station position	(100, 100)
Initial node power	.2 J

Table 41: Third scenario.

Parameter	Values
Area of deployment	300*300
Sensor nodes	200
Base station position	(100, 150)
Initial node power	.2 J

Table 42: Fourth scenario.

Parameter	Values
Area of deployment	400*400
Sensor nodes	250
Base station position	(150, 200)
Initial node power	.2 J

Table 43: Fifth scenario.

Parameter	Values
Area of deployment	500*500
Sensor nodes	1000
Base station position	(250, 250)
Initial node power	.2 J

Table 44: Abbreviations used for comparison of our proposed algorithms.

Abbreviations used for algorithms	Name of the algorithms
C1	APRO (proposed algorithm)
C2	LEACH
C3	LEACH-C
C4	EECS
C5	HEED
C6	HEEC
C7	DEECET

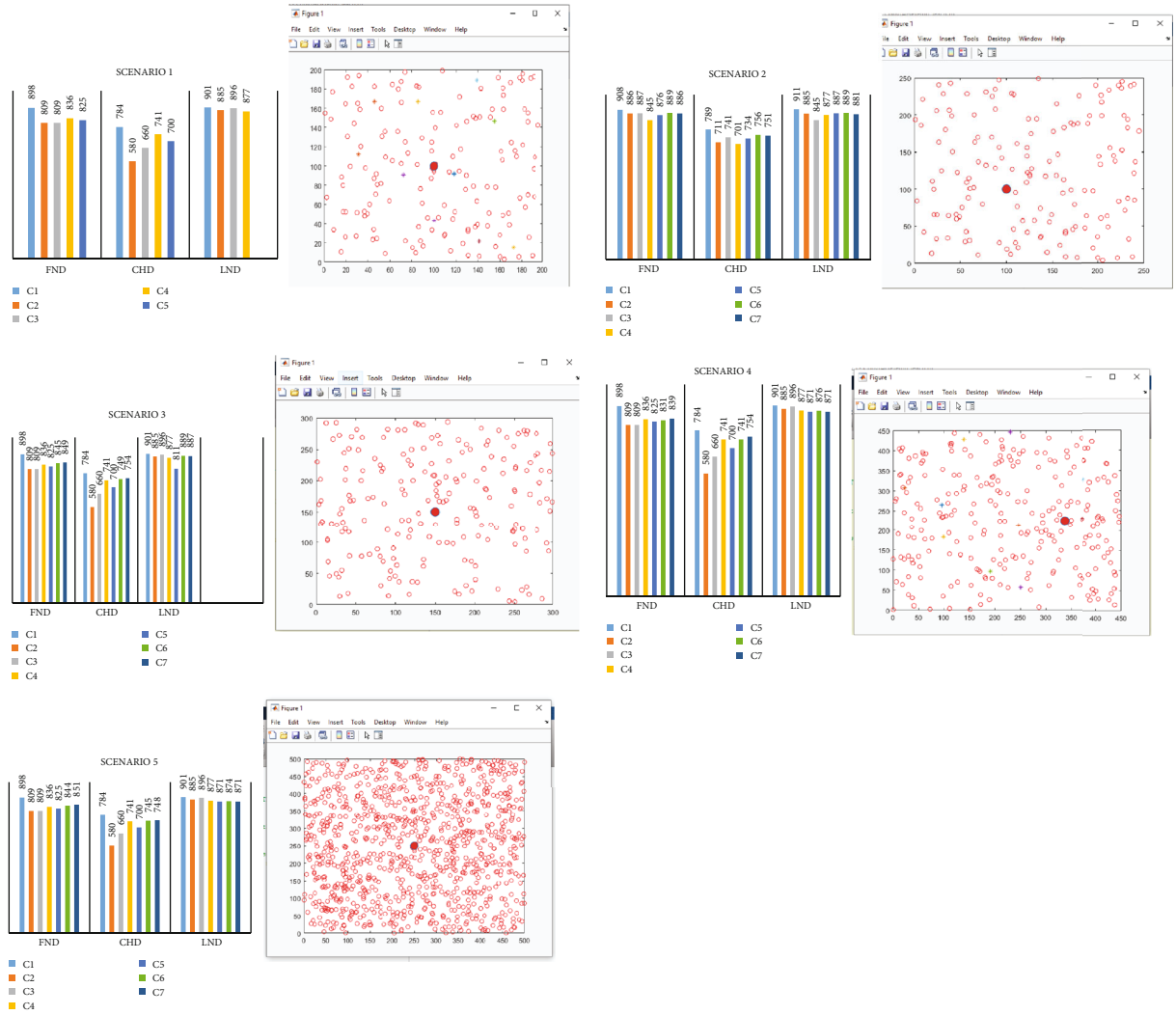

Figure 3: Performance of the experimental results.

The confidence interval of the proposed approach is 99% which can be calculated as

$$\text{Confidence Interval} = 20.6 \pm 0.219(\pm 1.1\%)[20.381 - 20.819],$$

$$\text{C.I} = \bar{x} \pm Z \times \frac{s}{\sqrt{n}} = 20.6 \pm 2.5758 \times \frac{1.2}{\sqrt{200}} 20.6 \pm 0.219. \tag{18}$$

Figure 3 shows that in all the scenario whether we change the simulation area, increase the number of sensor nodes, or change the base station position, the proposed APRO algorithm performs better than other algorithms. In the figure, we have also shown the simulated area with sensor nodes in each scenario so that we can better understand the scenarios. In our proposed APRO algorithm, applying multiattributes for cluster head selection shows that network lifetime has been increased with efficient energy consumption. Also considering every aspect of sensor nodes, load balance between nodes and thus efficient energy consumption helps in increasing the network lifetime.

7.1. Statistical Analysis. Here, Table 45 represents the statistical significance of analyzing the performance of the network. If we choose the alternative based on maximum residual, maximum coverage, and maximum connectivity, then the 1st alternative is for maximum coverage, the 3rd for maximum connectivity, and the 11th for maximum residual energy. Although the rank of the best alternatives has been given the solution by our proposed algorithm, these alternatives are 8th, 18th, and 11th (PROM ranking) and 8th, 10th, and 14th (AHP ranking). If we choose alternative 1st based on maximum coverage, then it will show that sensor nodes are near to the base station and they will consume less energy, but it will not guarantee that distance from CH to the base station is less and CHs are having higher residual energy for the data transmission. The chosen alternative shows that the solution is not optimal as it consumes more energy for data transmission which lowers network lifetime as other attributes were not optimal. The rank given to this alternative by PROMETHHE and AHP is 8th.

If we choose 3rd alternative based on maximum connectivity, then it will assure that CH is near the base station but

Table 45: Statistical significance of the attributes.

	AHP	PROMETHEE	Max residual	Max CN	Max COV
Ch-Cov	97.674	100	89.117	92.341	100
Bs-Ch Connectivity	.6138	.6138	.5816	.8954	.6389
Avg-Ch Life	2631.6713	2754.4364	2612.6781	2234.15167	2314.7827
Avg-Residual Energy	.6453	.6453	.69874	.5887	.6193
Ch-Con-Avg Residual	.3986	3.9876	3.2581	4.6897	3.7862
Ch-Dcon-Avg Residual	1.5637	1.5627	.56379	3.5788	2.6737
Bs-Ch Bearing	98.8967	98.9899	93.6578	91.2567	92.5364
Std Residual	2.6897	2.8967	2.3552	2.1547	2.4567
Avg-Bs Life	148.8753	169.6475	145.6742	154.7836	158.5362
Std_Avg_Ch_Life	167.3899	189.3748	156.7411	141.4748	190.3832
Maximum_Dis_Bs	575.2891	517.3849	784.3628	628.3718	616.3783
Avg_Dis_Chs	56.1123	56.4783	99.4738	78.4949	72.3949
Avg_BS_DIS	61.3849	56.3839	89.9401	78.4839	81.4788
Std_Ch_Con_Avg_Residual	.26178	.26894	.31473	.27671	.2134
Std_CH_Dcon_Avg_Residual	.2084	.2568	.3897	.2897	.2979
Std_Residual	.00156	.00167	.00238	.01383	.01898
Node_Power	.002146	.002146	.01278	.01238	.01287
Ch_Power	.00247	.00247	.00357	.003897	.00387
Std_Power	.004678	.004768	.005678	.005987	.006178
Std_Member Node	.28971	.28917	.36887	.34572	.37826
Std_Dev_Energy Trans	.00237	.00267	.01837	.01987	.02397

not guarantee higher residual energy. The sensor nodes other than the CH will be far away from the base station. As normal sensor nodes were at a higher distance, they require higher residual energy for data transmission. In this case, the network lifetime and residual energy will be lower. The rank given by the proposed algorithm is 6^{th} and 7^{th}, respectively. If we choose the 8^{th} alternative based on higher maximum residual energy, then it will give higher residual energy to sensor nodes. But sensor nodes were not equally distributed and sensor nodes' loads were also not balanced which causes a lower network lifetime. The rank given by our proposed APRO algorithm to this alternative is 11^{th} and 14^{th}. The other attribute values prove that the above results were not optimal; thus, we can say that with many limitations, the solutions were not optimal. Thus, we have to consider other attributes for CH's selection for data transmission. Such selected CHs should have a maximum lifetime with evenly distributed sensor nodes and have efficient energy consumption. The proposed algorithm provides optimal CH selection where all attributes have their optimal values and the simulation results were evaluated in terms of FND, CHD, and LND.

8. Conclusion and Future Scope

The proposed APRO algorithm provides a load-balanced and increased network lifetime for the selection of cluster heads by considering the twenty-one attributes. All the attributes were considered and synchronized among them for the data collection process. The selected cluster heads (CHs) have a balanced load among the sensor nodes with optimal energy consumption for the data transmission to the base station. The results validate the outcome of our proposed algorithm which verify consume optimal energy consumption for data transmissions. Results show that the considered 21 attributes play an important role in efficient energy consumption and increased network lifetime. As far as energy consumption is considered to be the most important factor in sensor networks, thus sensor nodes consume less energy and also balance the load among the sensor nodes. So, our proposed algorithm favored the data transmission and collection for a longer time in the network. Also, we have taken some scenarios in which we have changed the number of sensor nodes, deployment area, and base station position, where we can see that our proposed algorithm performs well compared to other algorithms. This shows that our proposed algorithm is scalable to small or large deployment areas and applications. We conclude that our proposed algorithm performs better than the other algorithms and our results validate as well.

In the future automatic weight, an assignment can be done using the fuzzy logic approach in place of relative weight. Automatic weight assignment can be done for enhancing the performance of the network. Further, we can move to the multihop transmission of data.

Data Availability

Data will be made available after making reasonable request from the author.

Conflicts of Interest

There is no conflict of interest among the authors.

Authors' Contributions

The authors have given consent for the publication.

Acknowledgments

The first author is thankful for the UGC-BHU-NET fellowship. The corresponding author is grateful for IoE grant of the Banaras Hindu University.

References

[1] I. F. Akyildiz, W. Su, Y. Sankarasubramaniam, and E. Cayirci, "Wireless sensor networks: a survey," *Computer Networks*, vol. 38, no. 4, pp. 393–422, 2002.

[2] A. Shahraki, A. Taherkordi, Ø. Haugen, and F. Eliassen, "Clustering objectives in wireless sensor networks: a survey and research direction analysis," *Computer Networks*, vol. 180, article 107376, 2020.

[3] A. A. Abbasi and M. Younis, "A survey on clustering algorithms for wireless sensor networks," *Computer Communications*, vol. 30, no. 14-15, pp. 2826–2841, 2007.

[4] W. B. Heinzelman, A. P. Chandrakasan, and H. Balakrishnan, "An application-specific protocol architecture for wireless microsensor networks," *IEEE Transactions on Wireless Communications*, vol. 1, no. 4, pp. 660–670, 2002.

[5] T. M. Behera, U. C. Samal, and S. K. Mohapatra, "Energy-efficient modified LEACH protocol for IoT application," *IET Wireless Sensor Systems*, vol. 8, no. 5, pp. 223–228, 2018.

[6] S. Shi, X. Liu, and X. Gu, "An energy-efficiency optimized LEACH-C for wireless sensor networks," in *7th International Conference on Communications and Networking in China*, pp. 487–492, Kunming, China, 2012.

[7] O. Younis and S. Fahmy, "HEED: a hybrid, energy-efficient, distributed clustering approach for ad hoc sensor networks," *IEEE Transactions on Mobile Computing*, vol. 3, no. 4, pp. 366–379, 2004.

[8] Z. Ullah, "A survey on hybrid, energy efficient and distributed (HEED) based energy efficient clustering protocols for wireless sensor networks," *Wireless Personal Communications*, vol. 112, no. 4, pp. 2685–2713, 2020.

[9] S. Bharany, S. Sharma, S. Badotra et al., "Energy-efficient clustering scheme for flying ad-hoc networks using an optimized LEACH protocol," *Energies*, vol. 14, no. 19, p. 6016, 2021.

[10] M. N. Khan and M. Jamil, "Performance improvement in lifetime and throughput of LEACH protocol," *Indian Journal of Science and Technology*, vol. 9, no. 21, pp. 1–6, 2016.

[11] H. Liang, S. Yang, L. Li, and J. Gao, "Research on routing optimization of WSNs based on improved LEACH protocol," *EURASIP Journal on Wireless Communications and Networking*, vol. 2019, no. 1, Article ID 194, 2019.

[12] S. Tyagi and N. Kumar, "A systematic review on clustering and routing techniques based upon LEACH protocol for wireless sensor networks," *Journal of Network and Computer Applications*, vol. 36, no. 2, pp. 623–645, 2013.

[13] S. E. Khediri, N. Nasri, A. Wei, and A. Kachouri, "A new approach for clustering in wireless sensors networks based on LEACH," *Procedia Computer Science*, vol. 32, pp. 1180–1185, 2014.

[14] M. A. Al Sibahee, S. Lu, M. Z. Masoud, Z. A. Hussien, M. A. Hussain, and Z. A. Abduljabbar, "LEACH-T: LEACH clustering protocol based on three layers," in *2016 International Conference on Network and Information Systems for Computers (ICNISC)*, pp. 36–40, Wuhan, China, 2016.

[15] P. Rajpoot and P. Dwivedi, "Multiple parameter based energy balanced and optimized clustering for WSN to enhance the lifetime using MADM approaches," *Wireless Personal Communications*, vol. 106, no. 2, pp. 829–877, 2019.

[16] D. Kalaimani, Z. Zah, and S. Vashist, "Energy-efficient density-based fuzzy C-means clustering in WSN for smart grids," *Australian Journal of Multi-Disciplinary Engineering*, vol. 17, no. 1, pp. 23–38, 2021.

[17] S. Ketu and P. K. Mishra, "Internet of healthcare things: a contemporary survey," *Journal of Network and Computer Applications*, vol. 192, article 103179, 2021.

[18] S. Ketu and P. K. Mishra, "Cloud, fog and mist computing in IoT: an indication of emerging opportunities," *IETE Technical Review*, vol. 39, no. 3, pp. 713–724, 2022.

[19] S. Dhingra, R. B. Madda, R. Patan, P. Jiao, K. Barri, and A. H. Alavi, "Internet of things-based fog and cloud computing technology for smart traffic monitoring," *Internet of Things*, vol. 14, article 100175, 2021.

[20] S. Ketu and P. K. Mishra, "Empirical analysis of machine learning algorithms on imbalance electrocardiogram based arrhythmia dataset for heart disease detection," *Arabian Journal for Science and Engineering*, vol. 47, no. 2, pp. 1447–1469, 2022.

[21] S. Singh and A. H. Ganie, "Applications of picture fuzzy similarity measures in pattern recognition, clustering, and MADM," *Expert Systems with Applications*, vol. 168, article 114264, 2021.

[22] P. Rajpoot and P. Dwivedi, "MADM based optimal nodes deployment for WSN with optimal coverage and connectivity," *IOP Conference Series: Materials Science and Engineering*, vol. 1020, no. 1, article 012003, 2021.

[23] P. Rawat and S. Chauhan, "Clustering protocols in wireless sensor network: a survey, classification, issues, and future directions," *Computer Science Review*, vol. 40, article 100396, 2021.

[24] A. Srivastava and P. K. Mishra, "A survey on WSN issues with its heuristics and meta-heuristics solutions," *Wireless Personal Communications*, vol. 121, no. 1, pp. 745–814, 2021.

[25] I. Daanoune, B. Abdennaceur, and A. Ballouk, "A comprehensive survey on LEACH-based clustering routing protocols in wireless sensor networks," *Ad Hoc Networks*, vol. 114, article 102409, 2021.

[26] S. T. Sheriba and D. H. Rajesh, "Energy-efficient clustering protocol for WSN based on improved black widow optimization and fuzzy logic," *Telecommunication Systems*, vol. 77, no. 1, pp. 213–230, 2021.

[27] Y. M. Raghavendra and U. B. Mahadevaswamy, "Energy efficient intra cluster gateway optimal placement in wireless sensor network," *Wireless Personal Communications*, vol. 119, no. 2, pp. 1009–1028, 2021.

[28] S. Madhu, R. K. Prasad, P. Ramotra, D. R. Edla, and A. Lipare, "A location-less energy efficient algorithm for load balanced clustering in wireless sensor networks," *Wireless Personal Communications*, vol. 122, no. 2, pp. 1967–1985, 2022.

[29] R. K. Prasad, S. Madhu, P. Ramotra, and D. R. Edla, "Firework inspired load balancing approach for wireless sensor networks," *Wireless Networks*, vol. 27, no. 6, pp. 4111–4122, 2021.

[30] S. M. Bozorgi and A. M. Bidgoli, "HEEC: a hybrid unequal energy efficient clustering for wireless sensor networks," *Wireless Networks*, vol. 25, no. 8, pp. 4751–4772, 2019.

[31] A. Srivastava and P. K. Mishra, "Multi-attributes based energy efficient clustering for enhancing network lifetime in WSN's," *Peer-to-Peer Networking and Applications*, vol. 15, no. 6, pp. 2670–2693, 2022.

[32] A. Shahraki, A. Taherkordi, Ø. Haugen, and F. Eliassen, "A survey and future directions on clustering: from WSNs to IoT and modern networking paradigms," *IEEE Transactions on Network and Service Management*, vol. 18, no. 2, pp. 2242–2274, 2021.

[33] A. A. H. Hassan, W. M. Shah, A. H. H. Habeb, M. F. I. Othman, and M. N. Al-Mhiqani, "An improved energy-efficient clustering protocol to prolong the lifetime of the WSN-based IoT," *IEEE Access*, vol. 8, pp. 200500–200517, 2020.

[34] Y. Liu, J. Gao, Y. Jia, and L. Zhu, "A cluster maintenance algorithm based on LEACH-DCHS protoclol," in *2008 International Conference on Networking, Architecture, and Storage*, pp. 165-166, Chongqing, China, 2008.

[35] M. El_Saadawy and E. Shaaba, "Enhancing S-LEACH security for wireless sensor networks," in *2012 IEEE International Conference on Electro/Information Technology*, pp. 1–6, Indianapolis, IN, USA, 2012.

[36] A. F. Marhoon and M. H. Awaad, "Reduce energy consumption by improving the LEACH protocol," *International Journal of Computer Science and Mobile Computing*, vol. 3, no. 1, pp. 1–9, 2014.

[37] A. Tripathi, N. Yadav, and R. Dadhich, "Optimization of clustering in SPIN-C and LEACH for data centric wireless sensor networks," *Proceedings of Fourth International Conference on Soft Computing for Problem Solving*, 2015, pp. 197–205, Springer, New Delhi, 2015.

[38] A. Das and P. N. Astya, "A relative survey of various LEACH based routing protocols in wireless sensor networks," in *2017 International Conference on Computing, Communication and Automation (ICCCA)*, pp. 630–636, Greater Noida, India, 2017.

[39] S. K. Singh, P. Kumar, and J. P. Singh, "A survey on successors of LEACH protocol," *IEEE Access*, vol. 5, pp. 4298–4328, 2017.

[40] M. Abdurohman, Y. Supriadi, and F. Z. Fahmi, "A modified E-LEACH routing protocol for improving the lifetime of a wireless sensor network," *Journal of Information Processing Systems*, vol. 16, no. 4, pp. 845–858, 2020.

[41] M. Xiao, X. Zhang, and Y. Dong, "An effective routing protocol for energy harvesting wireless sensor networks," in *2013 IEEE Wireless Communications and Networking Conference (WCNC)*, pp. 2080–2084, Shanghai, China, 2013.

[42] W. He, "Energy-saving algorithm and simulation of wireless sensor networks based on clustering routing protocol," *IEEE Access*, vol. 7, pp. 172505–172514, 2019.

[43] X. Zhao and N. Wang, "An unequal layered clustering approach for large scale wireless sensor networks," in *2010 2nd International Conference on Future Computer and Communication*, pp. V1-750–V1-756, Wuhan, China, 2010.

[44] M. Demirbas, A. Arora, V. Mittal, and V. Kulathumani, "Design and analysis of a fast local clustering service for wireless sensor networks," in *First International Conference on Broadband Networks*, pp. 700–709, San Jose, CA, USA, 2004.

[45] N. Aslam, W. Phillips, W. Robertson, and S. Sivakumar, "A multi-criterion optimization technique for energy efficient cluster formation in wireless sensor networks," *Information Fusion*, vol. 12, no. 3, pp. 202–212, 2011.

[46] M. Ye, C. Li, G. Chen, and J. Wu, "EECS: an energy efficient clustering scheme in wireless sensor networks," in *PCCC 2005. 24th IEEE International Performance, Computing, and Communications Conference, 2005.*, pp. 535–540, Phoenix, AZ, USA, 2005.

[47] D. Kumar, T. C. Aseri, and R. Patel, "EEHC: energy efficient heterogeneous clustered scheme for wireless sensor networks," *Computer Communications*, vol. 32, no. 4, pp. 662–667, 2009.

[48] T. N. Qureshi, N. Javaid, A. H. Khan, A. Iqbal, E. Akhtar, and M. Ishfaq, "BEENISH: balanced energy efficient network integrated super heterogeneous protocol for wireless sensor networks," *Procedia Computer Science*, vol. 19, pp. 920–925, 2013.

[49] N. Javaid, T. N. Qureshi, A. H. Khan, A. Iqbal, E. Akhtar, and M. Ishfaq, "EDDEEC: enhanced developed distributed energy-efficient clustering for heterogeneous wireless sensor networks," *Procedia computer science*, vol. 19, pp. 914–919, 2013.

[50] S. Jinlei, L. Wei, T. Chuanyu, W. Tianru, J. Tao, and T. Yong, "A novel active equalization method for series-connected battery packs based on clustering analysis with genetic algorithm," *IEEE Transactions on Power Electronics*, vol. 36, no. 7, pp. 7853–7865, 2021.

[51] M. K. Shahzad, S. M. Islam, M. Hossain, M. Abdullah-Al-Wadud, A. Alamri, and M. Hussain, "GAFOR: genetic algorithm based fuzzy optimized re-clustering in wireless sensor networks," *Mathematics*, vol. 9, no. 1, p. 43, 2021.

[52] S. Rani, S. H. Ahmed, and R. Rastogi, "Dynamic clustering approach based on wireless sensor networks genetic algorithm for IoT applications," *Wireless Networks*, vol. 26, no. 4, pp. 2307–2316, 2020.

[53] P. Raju, Y. Subash, and K. Rishabh, "EEWC: energy-efficient weighted clustering method based on genetic algorithm for HWSNs," *Complex & Intelligent Systems*, vol. 6, no. 2, pp. 391–400, 2020.

[54] E. Khanmohammadi, B. Barekatain, and A. A. Quintana, "An enhanced AHP-TOPSIS-based clustering algorithm for high-quality live video streaming in flying ad hoc networks," *The Journal of Supercomputing*, vol. 77, no. 9, pp. 10664–10698, 2021.

[55] A. Shelebaf and S. Tabatabaei, "A novel method for clustering in WSNs via TOPSIS multi-criteria decision-making algorithm," *Wireless Personal Communications*, vol. 112, no. 2, pp. 985–1001, 2020.

[56] C. Bai, R. Zhang, L. Qian, L. Liu, and Y. Wu, "An ordered clustering algorithm based on fuzzy c-means and PROMETHEE," *International Journal of Machine Learning and Cybernetics*, vol. 10, no. 6, pp. 1423–1436, 2019.

[57] H. Li, Y. Liu, W. Chen, W. Jia, B. Li, and J. Xiong, "COCA: constructing optimal clustering architecture to maximize sensor network lifetime," *Computer Communications*, vol. 36, no. 3, pp. 256–268, 2013.

[58] D. K. Sah and T. Amgoth, "Renewable energy harvesting schemes in wireless sensor networks: a survey," *Information Fusion*, vol. 63, pp. 223–247, 2020.

[59] S. Venkatraman and S. K. Sarvepalli, "Load balance technique with adaptive position updates (LAPU) for geographic routing

in MANETs," *EURASIP Journal on Wireless Communications and Networking*, vol. 2018, no. 1, Article ID 73, 2018.

[60] S. A. Sert, A. Alchihabi, and A. Yazici, "A two-tier distributed fuzzy logic based protocol for efficient data aggregation in multihop wireless sensor networks," *IEEE Transactions on Fuzzy Systems*, vol. 26, no. 6, pp. 3615–3629, 2018.

[61] S. A. Sert and A. Yazici, "Increasing energy efficiency of rule-based fuzzy clustering algorithms using CLONALG-M for wireless sensor networks," *Applied Soft Computing*, vol. 109, article 107510, 2021.

[62] S. A. Sert, "A novel hybrid grey wolf optimization methodology for resource constrained networks," in *2022 30th Signal Processing and Communications Applications Conference (SIU)*, pp. 1–4, Safranbolu, Turkey, 2022.

[63] E. I. Nezha, N. Abdellah, and E. A. Hassan, "Energy-aware clustering and efficient cluster head selection," *International Journal on Smart Sensing and Intelligent Systems*, vol. 14, no. 1, pp. 1–15, 2021.

[64] J. S. Lee and C. L. Teng, "An enhanced hierarchical clustering approach for mobile sensor networks using fuzzy inference systems," *IEEE Internet of Things Journal*, vol. 4, no. 4, pp. 1095–1103, 2017.

[65] N. El Idrissi, A. Najid, and H. El Alami, "New routing technique to enhance energy efficiency and maximize lifetime of the network in WSNs," *International Journal of Wireless Networks and Broadband Technologies*, vol. 9, no. 2, pp. 81–93, 2020.

[66] H. El Alami and A. Najid, "A new fuzzy clustering algorithm to enhance lifetime of wireless sensor networks," in *International Afro-European Conference for Industrial Advancement*, pp. 68–76, Springer, Cham, 2018.

[67] J. S. Lee and W. L. Cheng, "Fuzzy-logic-based clustering approach for wireless sensor networks using energy predication," *IEEE Sensors Journal*, vol. 12, no. 9, pp. 2891–2897, 2012.

Hindawi
Journal of Sensors
Volume 2023, Article ID 6807212, 13 pages
https://doi.org/10.1155/2023/6807212

Research Article

New Foundation Treatment Technology Using Cement Soil Composite Tubular Piles Supported by Optical Fiber Sensing Technology

Fan Sun

College of Civil Engineering and Architecture, Zhejiang University, Hangzhou, 310058 Zhejiang, China

Correspondence should be addressed to Fan Sun; 11512027@zju.edu.cn

Received 18 July 2022; Revised 19 September 2022; Accepted 29 September 2022; Published 8 May 2023

Academic Editor: Linesh Raja

The purpose is to optimize the foundation's treatment process and improve the foundation's construction effect to better apply the cement soil composite tubular piles. This exploration is to study the cement composite tubular piles. First, the principle and application of optical fiber sensing technology are discussed. Then, the application design and conditions of the cement composite tubular pile are discussed. Finally, a new foundation treatment technology supported by optical fiber sensing technology is proposed and comprehensively evaluated based on the application of cement soil composite tubular piles. The research results show that: (1) the new foundation treatment technology reflects the optimization of the optical fiber sensing technology for the foundation treatment. Moreover, it is further optimized through the application of cement soil composite tubular piles. (2) When subjected to the same load, the longer the core pile is, the smaller the cement soil composite pile's settlement is. When the inner core pile is 20 m ~24 m long, the settlement of the cement soil composite pile is small. When the length of the inner core pipe pile is 16 m ~20 m, the settlement range of cement soil composite pile becomes larger. (3) With the increase of friction coefficient, the settlement distance of cement soil composite tubular pile will decrease. The above data show that compared with the traditional foundation treatment technology, the new foundation treatment technology designed based on the application of composite tubular piles, supported by optical fiber sensing technology, can well solve the foundation construction problems, avoid pavement settlement, cracking, and other phenomena, and ensure the overall safety of the road. This exploration fully reflects the advantages of the new technology of foundation treatment and ensures the quality of road engineering. It provides a reference for the development of foundation treatment technology of construction projects and contributes to the development of the construction industry.

1. Introduction

Currently, the scale of infrastructure construction in China is increasingly large, super large, super heavy, and super high-rise buildings are springing up on the land of the motherland. Buildings have higher and higher requirements for the foundation's bearing capacity and deformation control. However, most of the underground soil layers of sites that can be adopted for construction in cities are complex, and construction teams need to carry out construction on complex soil layers with large changes in stiffness and flexibility [1]. Hence, in modern project engineering, the speculative proportion of foundation and the engineering quantity of foundation construction are considerable and are increasingly higher. The quality of the foundation can even determine the construction quality of buildings [2]. Accidents that cause dangerous situations in buildings due to problems in the foundation occur frequently. The foundation is a hidden project. Once a problem arises, the personnel, materials, and funds to repair the foundation are huge. With the increasing development of the construction industry, in addition to providing sufficient safety, the current construction scheme also needs to be highly economical and have a short construction period. In this way, the construction party can construct to serve society as soon as possible [3]. Since entering the 21st century, the domestic economy has

entered a period of rapid development. High-rise, super high-rise buildings, and heavy structures have been continuously built, and pile foundation projects have also been developed rapidly. Various new pile types, processes, and technologies are emerging, and some new fields have emerged, showing a new development trend. Pile foundations are developing towards large-diameter long piles, micro piles, high-strength piles, and composite piles. Given the development direction of pile foundation, combined with the characteristics of the east coast of China and the alluvial plain strata of rivers and lakes, Shandong Academy of Building Sciences has developed a composite pile technology, namely cement soil composite tubular pile technology, which is suitable for soft soil areas. The cement soil composite tubular pile is composed of the cement soil pile formed by the high-pressure jet mixing method and the concentrically implanted prestressed high-strength concrete tubular pile. It has the characteristics of large diameter, long pile, high bearing capacity, high-cost performance, and high construction efficiency. As a new technology, the bearing mechanism of cement soil composite tubular pile is obviously different from that of an ordinary pile, and the mechanical performance of the composite pile is also greatly different from that of the existing core inserted pile technology. In order to make the resistance of the soil around the pile and the strength of the pile material reach the limit state at the same time, meet the theoretical optimal matching relationship, and give full play to the technical advantages of the cement soil composite tubular pile, it is essential to research the bearing mechanism of the cement soil composite tubular pile. Based on the field test and numerical simulation test, this exploration studies the vertical compressive bearing mechanism of cement soil composite tubular pile, and obtains the influence rules of cement soil pile diameter, tubular pile diameter, cement soil pile length, tubular pile length, cement soil strength, stratum conditions, and other factors on the vertical compressive bearing mechanism of cement soil composite tubular pile.

Recently, the rising optical fiber sensing technology has attracted more and more researchers' attention. The characteristics such as durability, small volume, strong anti-electromagnetic interference ability, and portability make the optical cable easy to lay and install, good matching with the measurement target, and small stress impact on the measured target. It can carry out signal transmission. Good use of optical fiber sensing technology can realize real-time, remote and all-weather measurements of various structures in civil engineering [4]. The distributed optical fiber sensing technology based on Brillouin Optical Time Domain Reflectometry (BOTDR) has the characteristics of long monitoring distance, fast signal transmission, and high accuracy. According to these characteristics, it can be adopted for remote real-time monitoring of each item in the project to ensure its smooth progress [5]. In some developed countries, the application of optical fiber in civil engineering has been studied for decades. For example, Japan, Switzerland, France, and the United States have made crucial inventions and innovations in this technology. These studies have laid a good foundation for future projects' health monitoring and safety early warning [6]. The common distributed optical fiber sensing technology can be divided into the following two categories: interferometric distributed optical fiber sensing technology and scattering distributed optical fiber sensing technology. Among them, the distributed optical fiber sensing technology based on the interference principle appears earlier. It includes the distributed optical fiber sensing technology based on Michelson optical fiber interferometer, based on Mach-Zehnder optical fiber interferometer, based on Sagnac optical fiber interferometer, and based on composite structure interferometer. Distributed optical fiber sensing technology based on the scattering principle appears late, including distributed optical fiber sensing technology based on Raman scattering, distributed optical fiber sensing technology based on Brillouin scattering and distributed optical fiber sensing technology based on Rayleigh scattering.

A new foundation treatment technology supported by optical fiber sensing technology is proposed. It is to use optical fiber sensing technology to realize automatic monitoring of foundation settlement. Then, the stress characteristics and working mechanism of cement soil composite tubular piles are studied. The influence of the bearing capacity of cement soil composite tubular piles on settlement is researched. Next, the deformation and settlement law of the foundation based on cement soil composite tubular piles are obtained to study the reasonable method of foundation treatment and reduce the uneven settlement of the pavement and pavement damage. This exploration provides a reference for the development of foundation treatment technology of construction engineering and contributes to the development of the construction industry.

2. Methods

2.1. Optical Fiber Sensing Technology. Distributed optical fiber sensing technology based on Optical Time Domain Reflection (OTDR) includes Rayleigh OTDR and BOTDR [7]. The advantage of distributed optical fiber sensing technology is that it can simultaneously measure the continuously distributed temporal and spatial information on the optical fiber path without making multiple-point sensors. It overcomes the defect that the traditional point sensor is difficult to monitor the measured object continuously in an all-round way. Moreover, it has good performance that traditional sensors do not have, such as less energy loss and data transmission of multiple signals [8]. OTDR measurement technology is to receive the pulse signal of light in the optical fiber, and then transmit the pulse signal of light in the optical fiber. When the pulse signal of light encounters the nature of the optical fiber itself, the interface, the bending of the optical fiber, the optical fiber connecting other devices, or other similar events, the pulse signal of light will produce reflected light and scattered light. Part of the reflected light and scattered light will return to the pulse signal port of the emitted light along the same path [9]. According to the time difference t between the pulse signal of the emitted light and the pulse signal of the received light, OTDR can

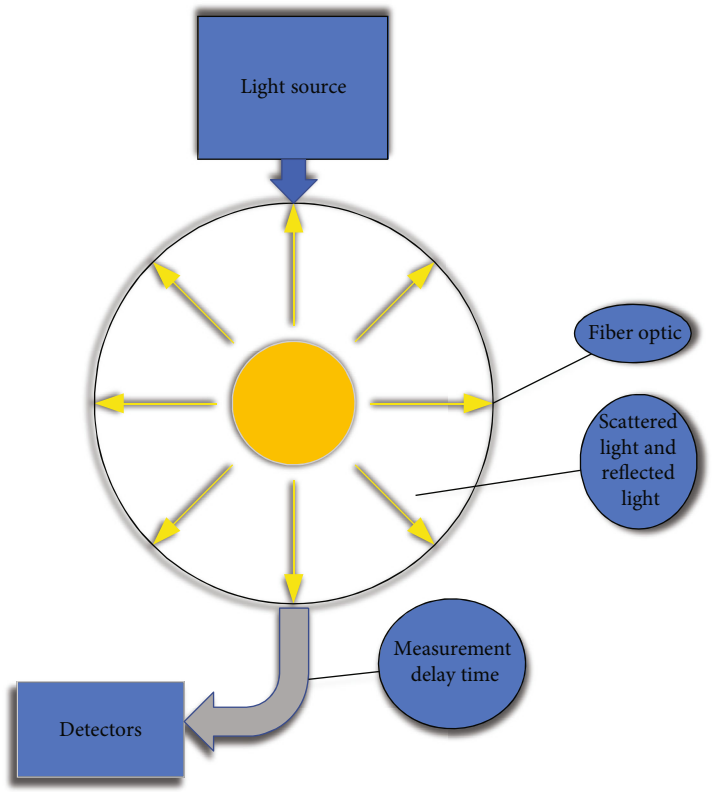

Figure 1: The schematic diagram of OTDR technology.

calculate the distance d between the above measurement point and OTDR through:

$$d = \frac{ct}{2n}. \quad (1)$$

c is the propagation speed of light in the optical fiber; n is the refractive index of the optical fiber itself [10].

Figure 1 displays the principle of OTDR technology.

OTDR technology can continuously display the loss distance of optical pulse and the changes of scattered light and refracted light on the whole optical fiber line, without any damage to the optical fiber during measurement.

Optical fiber sensing technology is widely adopted in structural engineering detection. For example, reinforced concrete is a widely used material at present. Embedding optical fiber materials directly in concrete structures or pasting them on the surface is the main application form of optical fiber, which can detect thermal stress and curing, deflection, bending, stress, and strain. The concrete will generate a temperature gradient due to hydration during solidification. If the cooling process is uneven, the thermal stress will cause cracks in the structure. The use of optical fiber sensors embedded in concrete can monitor its internal temperature changes, thus controlling the cooling rate. Hence, the optical fiber sensing technology will have a significant application prospect in the foundation treatment.

2.2. Fiber and Brillouin Scattering. The silicon material of optical fiber is a kind of electrostrictive material. When the high-power pump light propagates in the fiber, its refractive index will increase, resulting in the electrostriction effect, which causes most of the transmitted light to be converted into the backscattered light, resulting in stimulated Brillouin scattering. The specific process is as follows: when the pump light propagates in the optical fiber, its self-issued Brillouin scattering light propagates in the opposite direction of the pump light. When the intensity of the pump light increases, the intensity of the self-issued Brillouin scattering increases. When it increases to a certain extent, the backward transmitted Stokes light and the pump light will interfere, producing strong interference fringes, which greatly increases the local refractive index of the fiber. In this way, a sound wave will be generated due to the electrostriction effect. The sound wave generation will stimulate more Brillouin scattering light, and the generated scattering light will strengthen the sound wave. Such interaction produces strong scattering, which is called stimulated Brillouin scattering. Compared with light waves, the energy of sound waves is negligible. Hence, without considering the acoustic wave, the process of stimulated Brillouin scattering can be summarized as the process of energy transfer from higher frequency pump light to lower frequency Stokes light. In this way, stimulated Brillouin scattering can be regarded as a process of optical gain for Stokes light propagating in electrostrictive materials in the presence of pump light. In stimulated Brillouin scattering, although the anti-Stokes and Stokes light exist theoretically, they are generally only Stokes light.

2.3. Basic Principles of BOTDR. BOTDR is a technology that uses the relationship between Brillouin scattering frequency

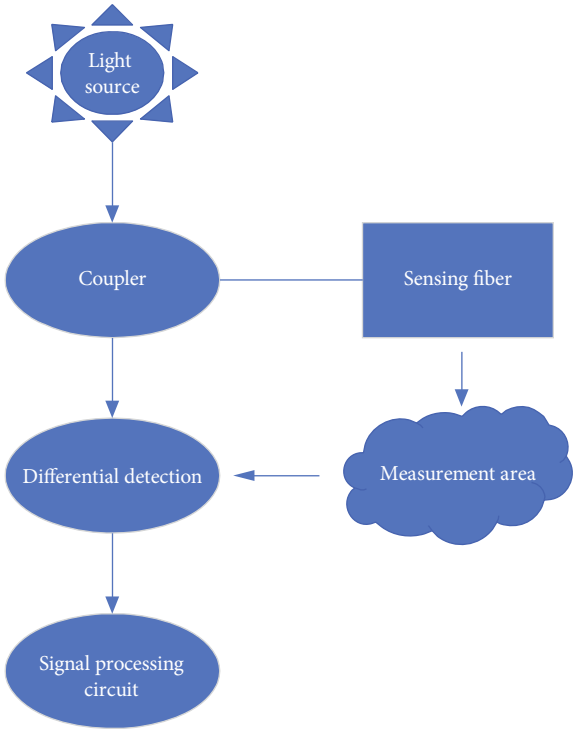

Figure 2: Basic block diagram of distributed optical fiber sensing system based on BOTDR.

shift in optical fiber, the temperature of optical fiber and the strain of optical fiber to realize measurement [11]. The distributed optical fiber sensor based on BOTDR is a measurement sensor for stress change and temperature change combined with OTDR measurement technology and Brillouin scattering. Figure 2 presents the principle:

The detector receives Brillouin scattering light, which will have a frequency shift relative to the pulse signal of the incident light [12]. When the temperature of the optical fiber changes and strains occur, the refractive index n of the optical fiber core and the propagation speed v of light in the optical fiber will change accordingly, resulting in the change of Brillouin frequency shift [13]. Since Brillouin frequency shifts are linearly related to fiber temperature and strain, it is only necessary to measure the change of Brillouin frequency shift to obtain the change of temperature and generated stress and strain. Measuring the return time of scattered light can determine the position of the corresponding point.

In fact, in the distributed optical fiber sensor system based on BOTDR, the output continuous light of the laser is modulated into pulse light and shoots into the sensing fiber to generate Brillouin Stokes and anti-Stokes light with frequency shifts up and down. A filter is adopted to filter out the scattered light signal of one of the frequencies detected by the photodetector. Through signal processing, the Brillouin gain spectra at different positions are fitted by Lorentz to obtain the Brillouin frequency shift curve along the fiber. According to the corresponding relationship between Brillouin frequency shift and temperature and stress, the change of external temperature and stress can be deduced. BOTDR technology can realize both distributed temperature sensing and stress sensing. However, due to the limited incident light power of BOTDR, the natural attenuation of optical fiber makes the sensing signal weak and difficult to detect, and shortens sensing distance.

Figures 3 and 4 show the relationship between the frequency shift change of Brillouin scattered light and strain and temperature in BOTDR measurement technology:

Figures 3 and 4 reveal that if the temperature change of the working environment where the optical fiber is located is less than 4°C, the influence of temperature on Brillouin frequency shift is ignored. When the stress change of the optical fiber is 0, the change of temperature is positively and linearly related to the change of Brillouin frequency shift, that is:

$$\nu_B(T) = \nu_B(T_0) + \frac{d\nu_B(T)}{dT}\Delta T. \tag{2}$$

T_0 is the initial temperature, T is the temperature at the time of measurement, and $\triangle T$ is the temperature change [14].

Moreover, Figure 3 shows that the relationship between Brillouin frequency shift and fiber temperature and fiber strain is [15]:

$$\nu_B(\varepsilon, T) = \nu_B(0, T_0) + \frac{\partial \nu_B(\varepsilon, T)}{\partial \varepsilon} + \frac{\partial \nu_B(\varepsilon, T)}{\partial T}. \tag{3}$$

$\nu_B(\varepsilon, T)$ is the Brillouin frequency shift change when the fiber strain is ε and the temperature is T. $\nu_B(0, T)$ is the Brillouin frequency shift when the fiber strain is 0 and the temperature is T_0. T_0 is the initial temperature, and T is the temperature at the measurement time. ε is strain. $\partial \nu_B(\varepsilon, T)/\partial \varepsilon$ is the relevant variation parameter between Brillouin frequency shift and strain, about 493 MHz. $\partial \nu_B(\varepsilon, T)/\partial T$ is the variation parameter between Brillouin frequency shift and temperature. The variation parameters between fiber temperature and fiber strain are compared. It is found that the stress change of light has a greater influence on the Brillouin frequency shift of light.

2.4. Structural Characteristics of Cement Soil Composite Tubular Piles. The cement soil composite tubular pile is composed of a core pile and a cement soil mixing pile. The prestressed high-strength tubular pile, cast-in-place pile, and structural steel are mainly used as the stiffening core. Cement soil mixing piles can be formed by deep mixing, powder spraying, or high-pressure rotary spraying [16]. Cement soil composite tubular pile can be divided into the short core pile, equal core pile, and long core pile according to the core pile length. They are divided into equal section piles (square, circular, annular lamp, pyramid, or combined type) and nonequal section piles (wedge and cone) according to the geometry of core piles. Among them, constant section tubular piles are more common. According to whether the peripheral surface of the core pile is regular, it can be divided into the smooth type and ribbed type [17], as shown in Figure 5:

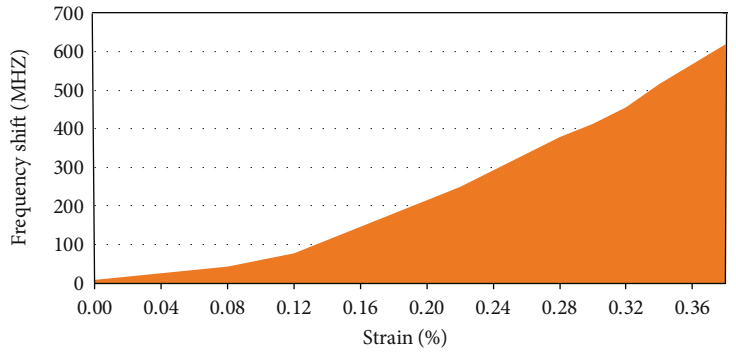

Figure 3: Relationship between Brillouin frequency shift and strain.

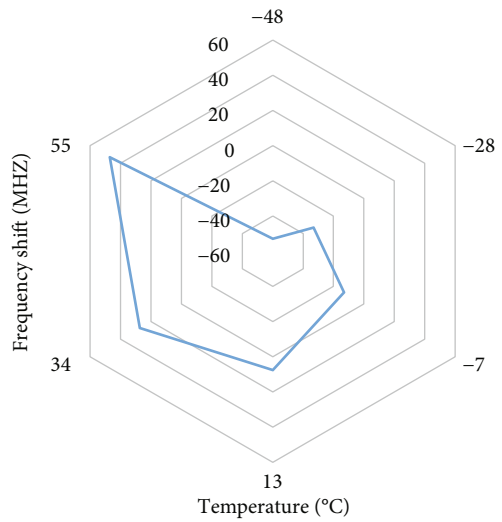

Figure 4: Relationship between Brillouin frequency shift and temperature.

2.5. Calculation of Bearing Capacity of Composite Pile. National regulations and standards: the bearing capacity of a single pile of cement soil composite pile is composed of the frictional resistance Q_{su} on the side of the composite pile and the frictional resistance Q_{pu} on the cross-section of the cement soil composite pile. When the interaction between the end face resistance and the side resistance is ignored, the bearing capacity of a single pile is [18]:

$$Q_u = Q_{su} + Q_{pu} = \sum U_i L_i q_{sui} + A_p q_{pu}. \quad (4)$$

U_i refers to the perimeter of the composite pile of the soil layer i around the pile, and L_i is the corresponding thickness of the i-th layer of soil around the pile. q_{sui} is the ultimate side friction resistance of the i-th layer of soil. q_{pu} is the end face resistance of layer i soil to the pile end.

For the loose rigid composite pile, it is generally considered that its failure surface is located in the inner and outer core sections, so its vertical resist compression bearing capacity can be estimated through Equations (5) and (6). For rigid-flexible composite pile and multielement composite pile, according to the form of failure, it can be calculated through equations (5)–(8) [19];

Long core pile:

$$R_a = u^c q_{sa}^c l^c + u^c \sum q_{sja}^c l_j + q_{pa}^c A_p^c. \quad (5)$$

Short core pile and equal core pile:

$$Ra = u^c q_{sa}^c l^c + q_{pa}^c A_p^c. \quad (6)$$

The failure surface of the side of the rigid composite pile is at the section of the composite pile core and the soil around the pile. The equations for estimating the resist compression bearing capacity of composite piles are Equation (7) and Equation (8) [20]:

Long core pile:

$$R_a = u \sum \varepsilon_{si} q_{sia} l_i + u^c \sum q_{sja} l_j + q_{pa}^c A_p^c. \quad (7)$$

Short core pile and equal core pile:

$$R_a = u \sum \xi_{si} q_{sia} l_i + \alpha \xi_p q_{pa} A_p. \quad (8)$$

R_a is the characteristic value of vertical resist compressive bearing capacity of cement soil composite pile. u^c and u are the perimeter of the inner core pile and composite section pile of cement soil composite pile, respectively. l^C is the length of the composite section of the cement soil composite pile, and l_j is the thickness of the j-th soil layer of the length of the noncomposite section. A_P^c and A_p are the area of the inner core section of the cement soil composite pile and the area of the composite section pile, respectively. q_{sa}^c is the friction resistance of the inner core side of the composite section of cement soil composite pile.

q_{sja}^c refers to the side friction of the j-th layer of the inner core of the noncomposite section of the cement soil composite pile. q_{sia} is the side friction resistance of the i-th layer of the outer core of the cement soil composite pile. q_{pa}^c and q_{pa} are the end resistance of the inner core pile end of the cement soil composite pile and the pressure of the end of

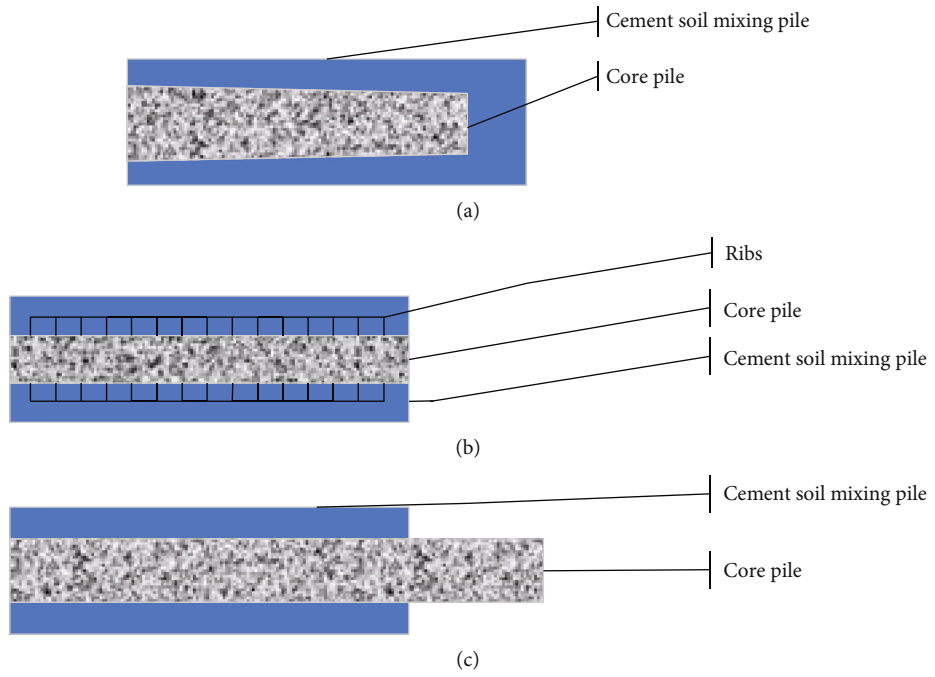

Figure 5: Types of cement soil composite tubular pile (a) short-core pile; (b) equal-core pile; (c) long-core pile.

the cement soil composite pile, respectively. There is a great relationship between the vertical bearing capacity of composite piles and the failure forms of composite piles. The failure forms of composite piles have four primary cases [21]: compression failure occurs at the upper part of tubular piles, relative sliding failure occurs at the side of cement soil piles, large sliding failure occurs between cement soil piles and tubular piles, and failure occurs when foreign matters penetrate the pile ends. Currently, the calculation equation involving long core composite piles is as follows [22].

$$R_{a1} = \xi u_p \sum_{0}^{L} q_{sia} L_i + \alpha q_p A_p + u_c \sum_{L}^{l} q_c^{sia} L_i + q_{pa}^c A_c, \quad (9)$$

$$R_{a2} = \psi_c A_c f_{ck}^c + \eta f_{cu} A_p, \quad (10)$$

$$R_{a3} = \zeta_c \eta f_{cu} A_{cf} + u_c \sum_{L}^{l} q_c^{sia} L_i + q_{pa}^c A_c, \quad (11)$$

$$R_{a3} = \xi u_p \sum_{0}^{L} q_{sia} L_i + \alpha q_{pa} A_p + \Psi A_c f_{ck}^c. \quad (12)$$

Equation (9) is to assume damage to the outer surface of cement soil. Equation (10) is to assume failure due to insufficient compressive bearing capacity of the pile body. Equation (11) is to assume failure of the inner and outer cores of cement soil. Equation (12) is to assume that the failure location is in the concrete of the noncomposite section.

2.6. New Foundation Treatment Technology Supported by Optical Fiber Sensing Technology. This exploration summarizes the worldwide research on the road problems, such as pavement subsidence and cracking in road engineering. It conducts theoretical analysis and research on engineering practice and indoor tests. The research contents are as follows:

(1) The optical fiber sensing technology is studied. The sensing parameters of temperature change and strain of optical fibers are studied by marking the temperature change and strain of optical fibers. The sensitivity of sensing fiber is compared, the factors affecting the sensitivity of optical fiber sensing are studied, and the reliability of the optical fiber sensing system is tested. Based on the principle of BOTDR, the measurement scheme of BOTDR with deformation and failure of the subgrade is designed

(2) With a road project in Hangzhou as the simulation object, a 20 : 1 road model is established indoors. According to the designed measurement scheme, the optical fiber is embedded in the road model to verify the possibility of optical fiber measuring soil and gravel settlement, and to verify the synchronous deformation ability of optical fiber and road. The measurement results of the sensing fiber are compared with that of the dial indicator, and the reliability and accuracy of the sensing fiber measuring the subgrade deformation failure are analyzed

(3) The stress of each segment of the tubular pile of cement soil composite pile under load is studied. For the bored precast pile, when making the reinforcement cage, it is essential to place the measuring stress gauge at the appropriate position and export it

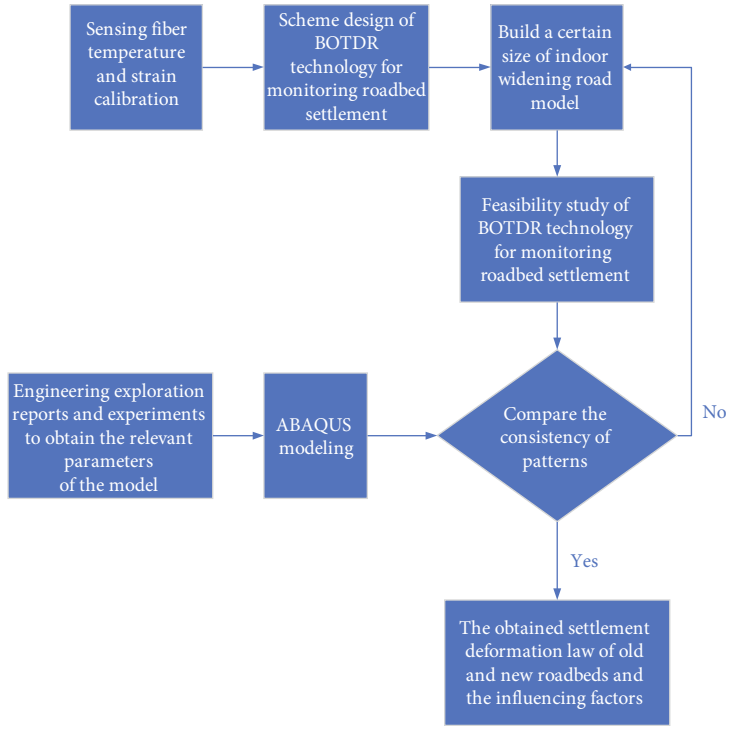

Figure 6: Technology roadmap.

along with the longitudinal reinforcement. In order to measure the axial force of the tubular pile during the tubular pile's manufacturing process, it is necessary to weld and fix the stress meter of the measuring reinforcement on the steel bar of the tubular pile

(4) In the indoor research, the dangerous simulated subgrade section is selected, and the sensing fiber and corresponding monitoring equipment are arranged to detect the settlement difference of the subgrade and the deformation and settlement of the cement soil composite tubular pile. The measured data are collected at regular intervals, and the subgrade settlement deformation measured by the sensing optical cable and the stress-strain data of the cement soil composite tubular pile are analyzed. The reliability of sensing optical cable monitoring subgrade deformation to prevent road collapse and deformation is analyzed

Based on summarizing and investigating the research on the differential settlement of new and old subgrade and worldwide BOTDR monitoring, this exploration mainly adopts the technical route of combining indoor test research, numerical analysis and comparison, engineering practice, and other means. Figure 6 displays the technical route.

Figure 6 reveals that the implementation steps of the new foundation treatment method proposed based on optical fiber sensing technology are as follows. The first step is to calibrate the optical fiber sensing temperature and strain. The second step is to use BOTDR technology to construct a monitoring scheme for subgrade settlement. The third step

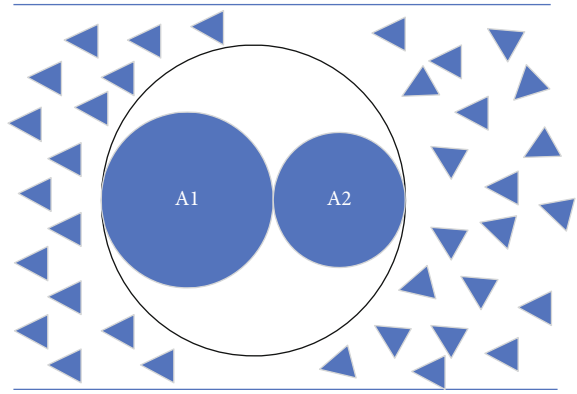

Figure 7: Schematic diagram of implantable fixed optical fiber laying.

Table 1: Parameters of measurement system.

Technical indicators	Parameters
Working temperature	5-40°C
Power supply	150-240 VAC/50-60 Hz
Sensing fiber	Standard single mode fiber
Spatial resolution	≤1.2 m
Measurement range of Brillouin frequency shift	10GHz-13GHz
Resolution of Brillouin frequency shift measurement	≤0.1 MHz

Table 2: Optical fiber information.

Fiber type	Length (m)	Diameter (mm)	Surface material	Strain sensing coefficient/(MHZ/%)	Temperature sensing coefficient/(MHZ/°C)
A1	100	3.00	Polyurethane	498	2.96
A2	100	0.8	Nylon	505	2.99

is to build a certain size indoor widening road model. The fourth step is to analyze the feasibility of the subgrade settlement monitoring method based on BOTDR technology. The fifth step is to obtain the settlement deformation law of the indoor widened road by using BOTDR technology. The sixth step is to get the model parameters according to the actual investigation. The seventh step is to use ABAQUS to model. Finally, by comparing and analyzing whether the settlement law is consistent, the deformation law of new and old subgrade settlements is obtained.

2.7. Synchronous Deformation of Optical Fiber and Subgrade. When the optical fiber is applied in subgrade engineering, optical fiber is implanted into subgrade filler. The protection of sensing fiber should be considered when using implantable methods. The sensing fiber can be directly filled into the loose soil. When the medium contains crushed stone or hard materials, these crushed stones or hard materials will cut the optical fiber and make it invalid, and the optical fiber cannot accurately reflect the subgrade condition. Hence, the surrounding medium must be treated when the implantable optical fiber is adopted in the crushed stone or hard material subgrade. Figure 7 is the schematic diagram of implantable fixed optical fiber laying:

2.8. Temperature Compensation. The temperature compensation of optical fiber has direct and indirect methods. The indirect method first measures the surrounding temperature environment, marks the temperature parameters of the optical fiber, and uses the conversion equation between temperature and Brillouin frequency shift to calculate the temperature value that needs to be compensated. The direct method is to keep the stress around the optical fiber stable, and the optical fiber is in a loose state. The temperature compensation is conducted by testing the tension state of the optical fiber through the analytical instrument. When arranging the optical fiber measurement line, an unstressed loose optical fiber needs to be arranged to compensate for the temperature of the whole optical fiber laying line. The Brillouin frequencies of the two sensing fibers are compared to obtain the optical fiber deformation frequency's change value. The indirect method first needs to mark the sensor, and then needs a thermometer to measure the temperature, and then convert it through various equations. In this way, the error is relatively large. When the measured area is relatively large, more thermometers need to be arranged, which is cumbersome to operate and inconvenient to mark the sensor. Hence, the indirect method is rarely used in engineering practice. When the onsite temperature change is less than 4°C, the influence of temperature on the frequency shift change can be ignored.

Table 3: Relationship between temperature and Brillouin frequency.

Temperature/°C	A1- Brillouin frequency/GHz	A2- Brillouin frequency/GHz
25	10.81668	10.82941
35	10.83838	10.84176
45	10.87717	10.85941
55	10.89034	10.88412
65	10.9	10.90588

2.9. Experimental Preparation. In order to verify the effect of the measurement system based on BOTDR technology, the system operation environment is first designed, then, the monitoring time of the system is set to obtain effective data, and finally the data are saved and processed. Table 1 displays the parameters of the measurement system based on BOTDR technology.

Table 1 suggests that when using BOTDR technology to measure various variables of optical fiber, high temperature may cause damage to the experimental equipment, thus affecting the measurement results. Therefore, the operating temperature is set at 5-40°C. The power supply voltage should not be too high, and it can be controlled near 200 V, so the voltage range of the power supply given in the experiment is 150-240 V. In the experiment, its numerical value is controlled within 1.2 m to avoid excessive resolution of optical fiber. Moreover, in order to make the Brillouin frequency shift measurement more effective, the Brillouin frequency shift measurement range and Brillouin frequency shift measurement resolution are set at 10GHz-13GHz and 0.1 MHz, respectively, in the experiment.

The sensitivity of optical fiber is studied. Table 2 presents the optical fiber information used in this test:

3. Results and Analysis

3.1. Indoor Temperature Mark of the Sensing Fiber. First, the known standard quantity is inputted into the sensor to be marked through experiments, and the sensor's output is detected to obtain the correlation error between the input and output of the sensor. Table 3 and Figure 8 show the change of external temperature measured by other instruments and Brillouin light frequency measured by the system:

The influence coefficients of the temperature of A1 and A2 sensing optical fibers on Brillouin frequency shift are 2.96 MHz/°C and 2.99 MHz/°C, respectively. The coefficients of the two optical fibers are basically the same. The analysis of optical fibers shows that the coefficients of A1 and A2

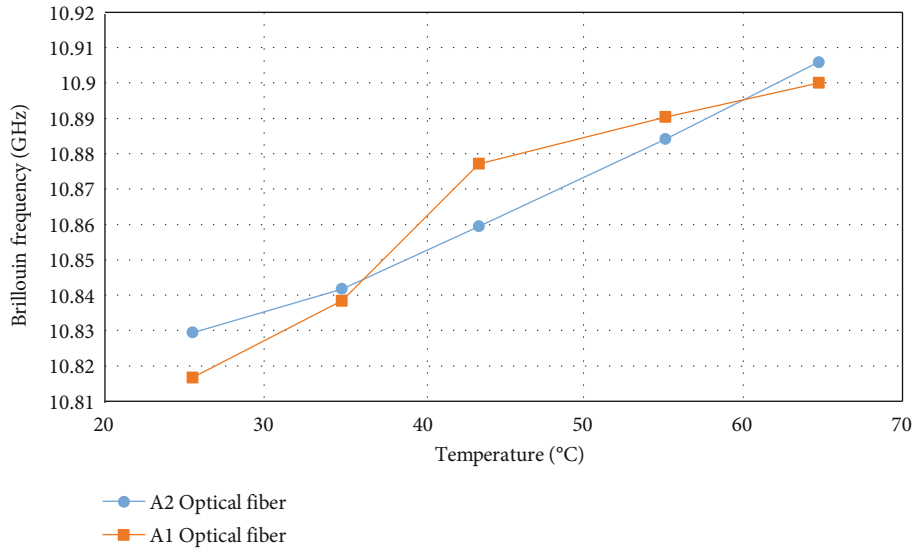

Figure 8: Relationship between temperature and Brillouin frequency.

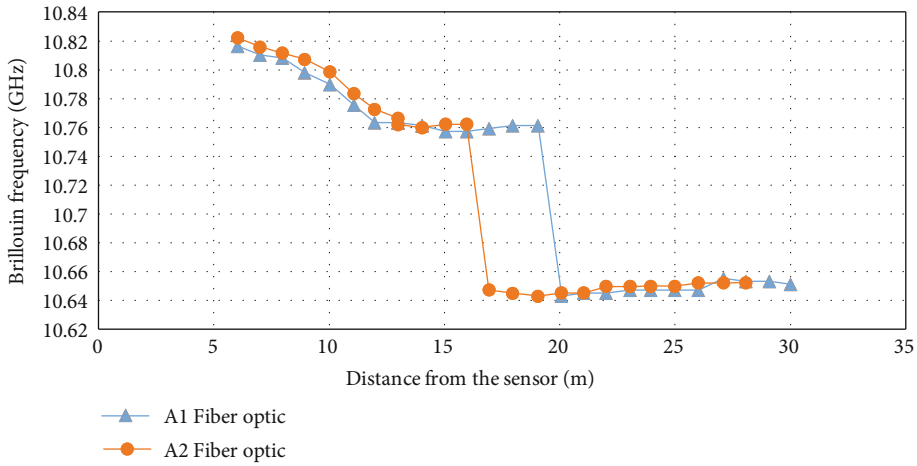

Figure 9: Monitoring results of sensing fiber on subgrade.

single-mode fibers are almost the same due to uniform heating in a constant temperature water bath. However, this does not mean that A1 and A2 sensing fibers have the same temperature sensitivity. The experimental diagram suggests that A2 fiber has a better correlation than A1 fiber, and A2 has better temperature sensitivity than A1 fiber. The diameter of A2 fiber is relatively small, so the range of acceptable temperature change is relatively large.

3.2. Feasibility Analysis of Sensing Optical Cable Project. In September 2020, the sensing fiber was placed on the monitoring section's subgrade base, the subgrade filler was backfilled, and then the mechanical compaction was conducted. In December 2020, the subgrade construction was completed, and the initial monitoring was conducted. Figure 9 displays some monitoring results:

Figure 9 suggests that the measurement functions of A1 and A2 sensing optical cables are in the normal state, and the system operates well without any abnormality. Thereby, BOTDR technology can monitor the settlement deformation of the subgrade.

3.3. Load Analysis of Cement Soil Composite Pile. The variable parameter analysis of the cement soil composite tubular pile studied in the test is conducted. For the length of the cement soil composite tubular pile, the lengths of 16 m, 18 m, 20 m, and 22 m are, respectively, taken for simulation analysis, and compared with the composite pile with the length of 24 m. Then, the composite tubular pile load with different lengths under the same vertical load is obtained. The vertical load is 5000 kN. Figure 10 displays the deformation of vertical piles with different inner core lengths:

Figure 10 suggests that the settlement effects of cement soil composite piles with different core piles under the same load are different, which indicates that the settlement degree of cement soil composite piles may be related to the core pile

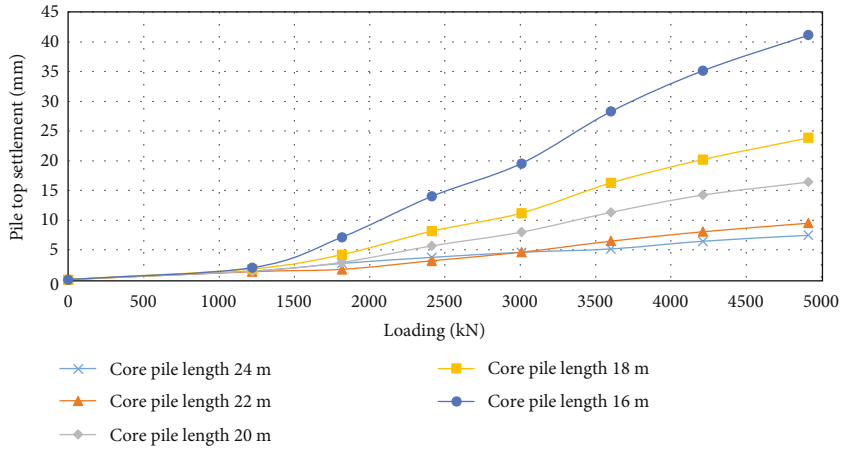

Figure 10: Deformation of vertical piles with different inner core lengths.

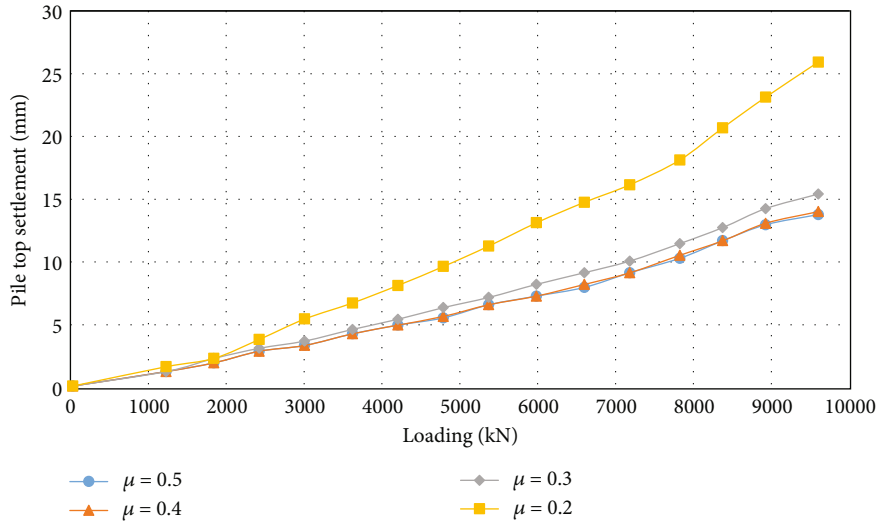

Figure 11: Influence of different friction coefficients on settlement of tubular piles.

size of composite piles. After further analysis, the relationship between the pile top settlement of the cement soil composite pile and the length of the inner core pile can be obtained. It suggests that when subjected to the same load, the longer the core pile is, the smaller the cement soil composite pile's settlement is. When the inner core pile is 20 m ~24 m long, the settlement amplitude of the cement soil composite pile is small. When the length of the inner core tubular pile is 16 m ~20 m, the settlement range of the cement soil composite pile becomes larger.

In the manufacturing process of cement soil composite tubular pile, the friction between cement soil composite tubular pile and the surrounding soil layer will be different due to the different material composition, material ratio, and manufacturing process of cement soil mixing pile. Usually, the tubular pile made by the dry method will have a large shear effect on the surrounding soil layer during the construction process to split the surrounding soil layer, and absorb the water of some surrounding soil layers, increasing the shear strength of the surrounding soil layer. On the contrary, the composite tubular pile made through the wet method increases the water content of the surrounding soil layer during the construction process, and the strength of the soil layer around the composite tubular pile will be reduced. Different soil layers will produce different friction coefficients μ for tubular piles. Figure 11 displays the influence of different friction coefficients on the settlement of tubular piles:

Figure 11 suggests that the settlement degree of the same cement soil composite pile under different friction coefficients is different. It shows that the settlement of the cement soil composite pile may be related to the friction coefficient between the pile and the soil. After further analysis, the influence of different friction coefficients on tubular pile settlement can be known. With the increase of friction coefficient, the settlement distance of tubular piles will decrease.

3.4. Relationship between Road Settlement and Cement Soil Composite Tubular Pile Settlement. Figure 12 displays the road settlement and cement soil composite tubular pile settlement:

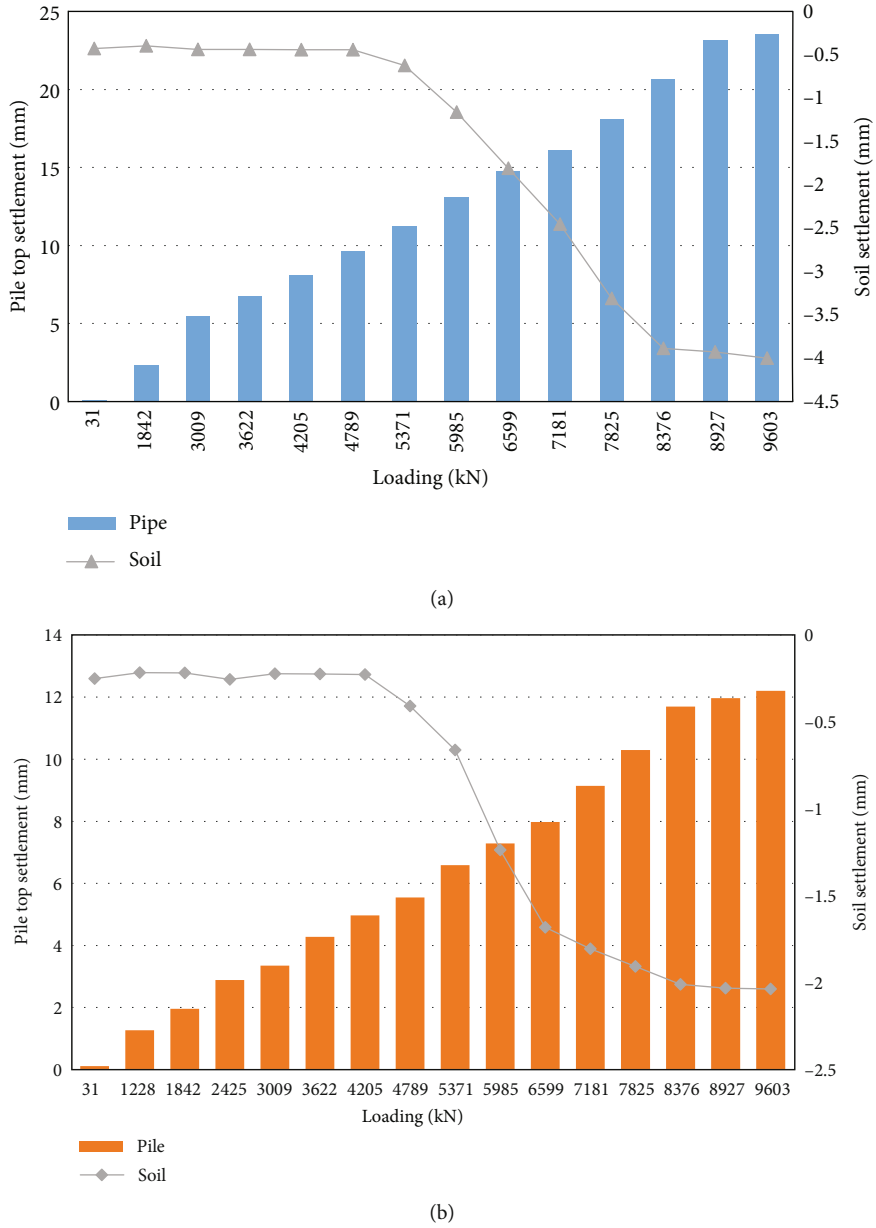

Figure 12: Road settlement and cement soil composite tubular pile settlement (a) $\mu = 0.2 \sim 0.4$; (b) $\mu = 0.4 \sim 0.5$.

Figure 12(a) reveals that when the friction coefficient μ between piles and soil is $0.2 \sim 0.4$, the pavement begins to settle under a load of 4789 kN. When the load increases to 8927 kN, the pavement settlement tends to be stable. The measured settlement of cement soil composite tubular pile is 14 mm, the settlement of pavement is 4 mm, and the settlement ratio of pavement and cement soil composite tubular pile is 28.57%. It can be considered that when the friction coefficient changes in this interval, it greatly impacts the settlement of composite piles. Figure 12(b) reveals that when μ is $0.4 \sim 0.5$, the pavement begins to settle when it is loaded with 4789 kN. When the load increases to 8376 kN, the pavement settlement tends to be stable. The measured settlement of cement tubular piles is 7 mm, the pavement settlement is 1.6 mm, and the settlement ratio of pavement to cement soil composite tubular pile is reduced by 22.86%. With the increase of pile top load, the friction between cement soil composite tubular pile and surrounding soil layer will also increase. After reaching a certain limit, this friction will remain unchanged. With the increase of the friction coefficient, the pile top load will cause the settlement of the surrounding soil layer, and the influence range of the surrounding soil layer settlement will gradually increase. However, the settlement of cement soil composite tubular piles will gradually decrease.

4. Conclusion

In recent years, optical fiber sensing technology has been widely used in foundation treatment, and has achieved good results. This exploration aims to integrate BOTDR technology with optical fiber sensing technology to achieve a better

foundation treatment effect. Hence, a new foundation treatment technology supported by optical fiber sensing technology is proposed based on the application of cement soil composite tubular pile, and its comprehensive evaluation is conducted. It is found that the application of sensing fiber to monitor the settlement of soil and gravel is feasible, and the synchronous deformation ability of the sensing fiber and subgrade is relatively good. By measuring the influence parameters of the temperature of A1 and A2 sensing fibers on Brillouin frequency shift, it is found that the diameter, sheath thickness, and type of sensing fibers impact the temperature sensing coefficient and strain sensing coefficient. The settlement of composite piles decreases with the increase of tubular pile length. When the friction coefficient μ between the pile-soil interface changes between $0.2 \sim 0.4$, the settlement of composite piles varies widely. When μ changes between $0.4 \sim 0.5$, the variation range of composite pile settlement is small. The relationship between the settlement of cement soil composite tubular pile and subgrade settlement is measured under different friction coefficients between pile and soil interface. With the load increase, the settlement of cement soil composite tubular pile in the pile-soil layer with a small friction coefficient is greater than that of the tubular pile in the pile-soil layer with a large friction coefficient. Moreover, the friction coefficient's inconsistency also affects the pavement settlement. The pavement settlement with a large friction coefficient between pile and soil interface is also smaller than that of pavement with a small friction coefficient. The purpose is to further optimize the optical fiber sensing technology by using BOTDR technology to better apply it to the foundation treatment work, and obtain a higher quality foundation treatment effect.

Due to the limited time, the monitoring time for the foundation settlement deformation law and the cement soil composite tubular pile's settlement law is relatively short. Hence, the complete monitoring data of sensing optical cables and conventional monitoring instruments in the project cannot be obtained. Long-term observation will be conducted in future research to verify the accuracy of the application of sensing optical cables in civil engineering.

Data Availability

The data used to support the findings of this study are available from the corresponding author upon request.

Conflicts of Interest

The author declares that there are no known competing financial interests.

Acknowledgments

This work was supported by the Key Project of Natural Science Foundation of Zhejiang Province (grant no. LXZ22E080001) and National Natural Science Foundation of China (grant nos. 52178358 and 52108349).

References

[1] X. Wang, X. Cao, H. Xu et al., "Research on the properties of peat soil and foundation treatment technology," *E3S Web of Conferences*, vol. 272, article 02019, 2021.

[2] L. Shao, Q. Wang, G. Qin, and R. Liu, "Elementary discussion on construction technology of foundation treatment for water conservancy and hydropower projects," *Smart Construction Research*, vol. 2, no. 3, 2018.

[3] X. C. Lao and X. F. Zhang, "Reinforcement scheme and construction technology for leakage treatment sof deep well foundation pit," *Guabfzhou Architecture*, vol. 49, no. 3, p. 33, 2021.

[4] J. Li, D. Zheng, L. Wu, and F. Wang, "Application of visualization modeling technology in the determination of reinforcement range of deep soft soil foundation," *Environmental Earth Sciences*, vol. 81, no. 7, pp. 1–13, 2022.

[5] N. Lalam, W. P. Ng, X. Dai, Q. Wu, and Y. Q. Fu, "Performance improvement of Brillouin ring laser based BOTDR system employing a wavelength diversity technique," *Journal of Lightwave Technology*, vol. 36, no. 4, pp. 1084–1090, 2018.

[6] D. Tosi, E. Schena, C. Molardi, and S. Korganbayev, "Fiber optic sensors for sub-centimeter spatially resolved measurements: review and biomedical applications," *Optical Fiber Technology*, vol. 43, pp. 6–19, 2018.

[7] H. D. Bhatta, L. Costa, A. Garcia-Ruiz et al., "Dynamic measurements of 1000 microstrains using chirped-pulse phase-sensitive optical time-domain reflectometry," *Journal of Lightwave Technology*, vol. 37, no. 18, pp. 4888–4895, 2019.

[8] G. Bashan, H. H. Diamandi, Y. London, E. Preter, and A. Zadok, "Optomechanical time-domain reflectometry," *Nature Communications*, vol. 9, no. 1, pp. 1–9, 2018.

[9] A. Aitkulov and D. Tosi, "Optical fiber sensor based on plastic optical fiber and smartphone for measurement of the breathing rate," *IEEE Sensors Journal*, vol. 19, no. 9, pp. 3282–3287, 2019.

[10] M. Shanafield, E. W. Banks, J. W. Arkwright, and M. B. Hausner, "Fiber-optic sensing for environmental applications: where we have come from and what is possible," *Water Resources Research*, vol. 54, no. 11, pp. 8552–8557, 2018.

[11] F. L. Barkov, Y. A. Konstantinov, and A. I. Krivosheev, "A novel method of spectra processing for brillouin optical time domain reflectometry," *Fibers*, vol. 8, no. 9, p. 60, 2020.

[12] A. Zafeiropoulou, A. Masoudi, A. Zdagkas, L. Cooper, and G. Brambilla, "Curvature sensing with a D-shaped multicore fibre and Brillouin optical time-domain reflectometry," *Optics Express*, vol. 28, no. 2, pp. 1291–1299, 2020.

[13] T. Horiguchi, Y. Masui, and M. S. D. Zan, "Analysis of phase-shift pulse brillouin optical time-domain reflectometry," *Sensors*, vol. 19, no. 7, p. 1497, 2019.

[14] S. K. Almoosa, A. E. Hamzah, M. S. D. Zan, M. F. Ibrahim, N. Arsad, and M. M. Elgaud, "Improving the Brillouin frequency shift measurement resolution in the Brillouin optical time domain reflectometry (BOTDR) fiber sensor by artificial neural network (ANN)," *Optical Fiber Technology*, vol. 70, p. 102860, 2022.

[15] T. Oda, A. Nakamura, Y. Koshikiya, and N. Honda, "Brillouin optical time domain reflectometry for estimating loss and crosstalk at the splice point in few-mode fibers," *Optical Fiber Technology*, vol. 68, article 102741, 2022.

[16] S. Yang, M. Zhang, X. Bai, X. Liu, and C. Zheng, "Experiment investigation on stress characteristics of grouting microsteel

pipe piles with cement-soil wall," *Advances in Materials Science and Engineering*, vol. 2020, Article ID 9704589, 10 pages, 2020.

[17] X. Lu, M. Song, and P. Wang, "Numerical simulation of the composite foundation of cement soil mixing piles using FLAC3D," *Cluster Computing*, vol. 22, no. S4, pp. 7965–7974, 2019.

[18] Y. Wu, K. Zhang, L. Fu, J. Liu, and J. He, "Performance of cement–soil pile composite foundation with lateral constraint," *Arabian Journal for Science and Engineering*, vol. 44, no. 5, pp. 4693–4702, 2019.

[19] R. Liu and C. Liang, "Study of the bearing capacity at the variable cross-section of a riser-surface casing composite pile," *China Ocean Engineering*, vol. 35, no. 2, pp. 262–271, 2021.

[20] X. Wang, Y. Que, K. Wang et al., "Modeling test and numerical simulation of vertical bearing performance for rigid-flexible composite pouch piles with expanded bottom (RFCPPEB)," *Symmetry*, vol. 14, no. 1, p. 107, 2022.

[21] N. B. Umravia and C. H. Solanki, "Comparative study of existing cement fly ash gravel pile and encased stone column composite foundation," *IOP Conference Series: Materials Science and Engineering*, vol. 1197, no. 1, article 012002, 2021.

[22] C. Phutthananon, P. Jongpradist, and P. Jamsawang, "Influence of cap size and strength on settlements of TDM-piled embankments over soft ground," *Marine Georesources & Geotechnology*, vol. 38, no. 6, pp. 686–705, 2020.

Hindawi
Journal of Sensors
Volume 2023, Article ID 6326423, 19 pages
https://doi.org/10.1155/2023/6326423

Research Article

Offering a Demand-Based Charging Method Using the GBO Algorithm and Fuzzy Logic in the WRSN for Wireless Power Transfer by UAV

Payman Habibi,[1] Goran Hassanifard,[1] Abdulbaghi Ghaderzadeh,[2] and Arez Nosratpour[1]

[1]*Department of Electrical Engineering, Sanandaj Branch, Islamic Azad University, Sanandaj, Iran*
[2]*Department of Computer Engineering, Sanandaj Branch, Islamic Azad University, Sanandaj, Iran*

Correspondence should be addressed to Goran Hassanifard; hassanifardgoran@gmail.com

Received 11 August 2022; Revised 2 December 2022; Accepted 5 April 2023; Published 2 May 2023

Academic Editor: Giovanni Pau

An extremely high number of geographically dispersed, energy-limited sensor nodes make up wireless sensor networks. One of the critical difficulties with these networks is their network lifetime. Wirelessly charging the sensors continuously is one technique to lengthen the network's lifespan. In order to compensate for the sensor nodes' energy through a wireless medium, a mobile charger (MC) is employed in wireless sensor networks (WRSN). Designing a charging scheme that best extends the network's lifetime in such a situation is difficult. In this paper, a demand-based charging method using unmanned aerial vehicles (UAVs) is provided for wireless rechargeable sensor networks. In this regard, first, sensors are grouped according to their geographic position using the K-means clustering technique. Then, with the aid of a fuzzy logic system, these clusters are ranked in order of priority based on the parameters of the average percentage of battery life left in the sensor nodes' batteries, the number of sensors, and critical sensors that must be charged, and the distance between each cluster's center and the MC charging station. It then displays the positions of the UAV to choose the crucial sensor nodes using a routing algorithm based on the shortest and most vital path in each cluster. Notably, the gradient-based optimization (GBO) algorithm has been applied in this work for intracluster routing. A case study for a wireless rechargeable sensor network has been carried out in MATLAB to assess the performance of the suggested design. The outcomes of the simulation show that the suggested technique was successful in extending the network's lifetime. Based on the simulation results, compared to the genetic algorithm, the proposed algorithm has been able to reduce total energy consumption, total distance during the tour, and total travel delay by 26%, 17.2%, and 25.4%, respectively.

1. Introduction

Wireless sensor networks (WSNs) consist of many energy-limited sensors and several sink nodes, where the sensor nodes can sense events such as temperature, humidity, and the content of atmospheric pollutants. These functional scenarios require WSN to work consistently. These application scenarios require the WSN to operate continuously. In particular, the performance of a WSN is limited by the battery capacity [1–3]. To augment the lifetime of a WSN as much as possible, many researchers have proposed various approaches. The existing reports can be divided into three categories, namely, energy conservation [4], energy harvesting [5], and wireless energy transfer (WET) [6].

Limited lifetime remains a key factor affecting large-scale deployment of WSNs. In general, there are two types of methods to solve the problem. The first method is a

resource-saving method that uses an optimization method to improve the efficiency of the WSN. The energy-saving scheme increases the lifetime of the sensor nodes by reducing the energy consumption per unit of time or workload. While the energy of sensor nodes is still limited, this method cannot fundamentally solve the problem. The second method is wireless energy transfer (WET). The main idea is to charge sensor nodes with the use of a magnetic resonance coupling, and the WET can provide a stable energy source with a controlled charge power. With the help of the promising WET method, researchers have proposed a new concept of wireless rechargeable sensor networks (WRSNs) [7–9]. In WRSNs, sensor nodes can be charged by wireless charging equipment (WCE). Hence, the WCE charging schedule becomes a prominent issue in WRSNs. To date, various perspectives on charge scheduling have been investigated, including route planning and system performance optimization [10].

In WRSNs, since multihop data routing is usually used to send data from sensor nodes to the base station, the nodes that are closer to the base station usually consume more energy than others, resulting in unbalanced energy consumption patterns (for instance, the energy hole phenomenon [11]). Hence, a rational charging scheduling scheme that also takes both effectiveness and fairness should still be designed to meet the purpose of ensuring the lifetime of global sensor nodes in WRSN. Additionally, due to the limited charging capacity of WCVs in WRSNs, several imperative elements in charging planning must be considered, including the number, movement speed, charging power, charging range, charging path, and charging period of WCVs in each charging cycle and period. Moreover, the joint optimization of charging scheduling and network protocols of WSNs will certainly minimize charging costs and progress connectivity, coverage, and lifetime of WRSNs [12–14].

In the overall framework of the wireless rechargeable sensor network, there are maintenance stations, base stations (BS), one or more agents or mobile charging vehicles (MCVs) on the ground or in the air, and a large number of rechargeable sensors (Figure 1). In this study, UAV is used as MCV. The maintenance station can meet the charging demand. The base station collects and aggregates the sensor data from the sensors and usually has no energy limitations. After deploying the sensors, the location of each sensor can be determined. A set of sensors with random battery capacity is distributed in a certain range. Sensors are categorized into several clusters based on their position and residual energy. The sensor collects data and transmits it to the cluster heads. When the power is less than the threshold, each sensor sends a real charge request to the MCV. The request delivery time is assumed to be insignificant compared to the moving time of the mobile charging vehicle (MCV) [5].

In this work, two issues of energy efficiency and transmission speed are considered for charging planning. Based on the needs of wireless sensor networks to continue working and increase their lifespan, the contributions of this article are stated as follows:

(i) Considering the reduction of energy losses for charging sensor nodes, we seek to provide the shortest path to reach all sensor nodes

(ii) With the help of tracking the nodes in urgent need of charging, priority is provided to choose the route

(iii) With the approach of segmenting different areas, the risk of WSN nodes death is reduced

(iv) By using UAV to charge nodes and also the GBO algorithm in this article, the time delay of charging at sensitive nodes is reduced

In the current investigation, we mainly study UAV routing and charging strategy in WRSN. Section 2 briefly reviews the literature. We introduce the concepts related to our work in Section 3. In Section 4, the routing strategy is proposed in detail. Simulations and analysis are presented in Section 5. Ultimately, Section 6 concludes and offers suggestions for further work.

2. Related Work

Charging problems in wireless rechargeable sensor networks and the Internet of Things are common exploration challenges. Utilizing wireless energy transmission technology, we are capable of transferring electric power from wireless charging equipment (WCE) to sensor networks and also providing a new model for increasing the network lifetime. The current investigation usually uses a periodic and deterministic charging process, but the limited energy and impact of nondeterministic factors such as topological changes and sensor failures can be ignored, making them unsuitable for real networks. In [15], the goal is to minimize the number of dead sensors, while the maximum use of WCE energy is given by considering its limited energy. In this effort, the swarm reinforcement learning (SRL) method is first presented to attain the independent planning ability of WCE. Furthermore, to solve the inadequate search problem in the existing SRL algorithm, this algorithm has been improved with the help of the firefly algorithm, and a new charging algorithm, called swarm reinforcement learning based on firefly algorithm (SRL-FA), is proposed for demand charging architecture. Article [16] manifests a demand-based charging strategy (DBCS) in WRSN. Moreover, in the mentioned study, charging scheduling is developed in four ways: clustering method, selection of charging sensors, charging route, and schedule. At first, a multipoint improved K-means clustering algorithm is proposed to balance energy consumption that can be grouped based on location, residual energy, and past contribution. Secondly, to select charging sensors based on demand, a dynamic selection algorithm for charging nodes (DSACN) is planned. Third, simulated annealing based on performance and efficiency (SABPE) is designed to optimize the charging path for a mobile charging vehicle and reduce charging time. Eventually, in order to augment the efficiency of MCV, DBCS was suggested.

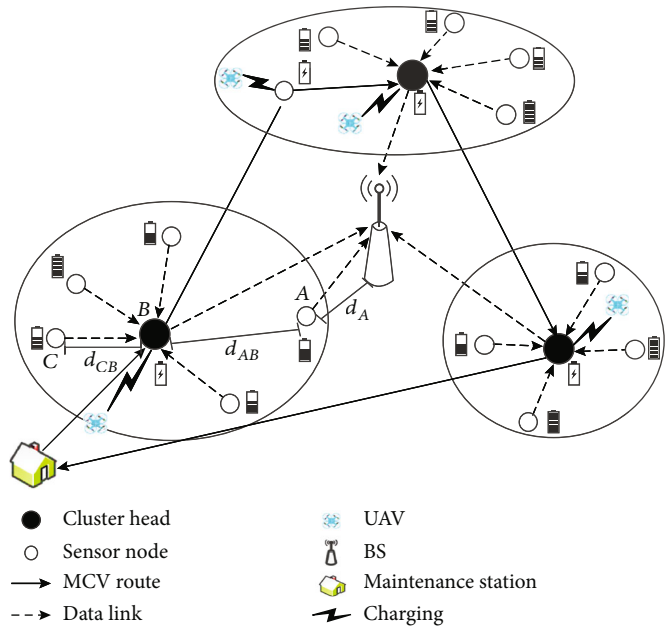

Figure 1: Framework of WRSN [5].

In [17], a new criterion is presented which is called the charging reward. This novel criterion will assist to measure the quality of sensor charging and then monitor how mobile charger planning is designed to fill the sensor supply so that the total charging rewards collected by the mobile charger in the charging are maximized. It is worthy to note that the total charging reward collected is subject to the energy capacity limit of the mobile charger and the charging time windows of all sensors. Owing to the problem's complexity, the deep reinforcement learning technique is utilized to achieve the moving path for the moving charger.

In [18], a dynamic charging scheme (DCS) in WRSN based on the actor-critic reinforcement learning (ACRL) algorithm is proposed. In ACRL, gated recurrent units (GRU) are presented to record the relationships of charging actions in time order. Using an actor-network or agent with a GRU layer, one can choose a desired or nearly optimal sensor from the candidate sensor as the next target of charging and speed up the model training. Meanwhile, the length of the tour and the number of dead sensors are considered as the reward signal. The actor and critic networks are updated with the function of R and V error criteria.

To attain stable and reliable energy supplements through wireless charging, it is imperative to optimize the path of mobile phone chargers. Hence, the objective of article [19] is to provide a charging strategy and scheduling algorithm for directional wireless power transmission in WRSN. First, to regulate the priority of charging requests, the degree of charging demand is well defined. Thereafter, to avoid node energy losses, the charger orientation angle selection algorithm is considered according to the charging priority. Lastly, it formulates the directional charger deployment problem into a discrete unit disk-covering problem and suggests a trajectory planning scheme based on an improved genetic algorithm to optimize energy charging efficiency.

In the case of wireless sensor networks charging and the Internet of Things, it is anticipated that the mobile energy of wireless charging equipment (WCE) has adequate energy to recharge the trip and that the amount of energy discharge per sensor is identical. However, these hypotheses are not realistic. Actually, the energy of the WCE tour is restricted by the energy capacity of the WCE, and the energy consumption of different sensors is unbalanced. In the paper [20], periodic charging scheduling is proposed for mobile WCE with limited travel energy. In this circumstance, the connection time ratio is optimized and maximized. Then this periodic charging schedule guarantees that the energy of the sensors in the WRSN varies periodically and that the sensors do not die continuously. To alleviate this problem, a hybrid particle swarm optimization genetic algorithm (HPSOGA) is suggested for solving NP-hard problems.

In [21], an effective algorithm has been proposed to improve the lifetime of mobile wireless networks. It controls the communication between users and the sensor sink by solving a simple convex optimization problem. In the current study, the systemic performance of this algorithm was evaluated by bearing in mind that (1) energy storage devices of sensors are subject to recharging through radiative wireless power transfer events, (2) sensor mobility patterns by random waypoints, Gauss-Markov random and reference group models are considered, (3) a propagation path loss prediction model depending on the distance between two sensors, energy consumption, and the amount of charge delivered to the sensors, and (4) recharge which is done through omnidirectional and directional radiation patterns. Importantly, many of the previous works are not capable of utilizing the full benefits of WMC because it starts to recharge the sensor when its energy level reaches the threshold, resulting in an increasing WMC idle time. Moreover, although there has been an upsurge of interest in using

WMC, the restriction of network lifetime was observed. However, the optimal sharing of WMC energy between sensors can guarantee permanent network performance. Therefore, the suggestion of an efficient method that jointly solves these challenges is required. In [22], the Fair Energy Division Scheme (FEDS) is presented, which will undertake the permanent network operation with optimization of energy sharing at the beginning of each cycle.

In [23], a charging scheduling algorithm for directional wireless power transfer in WRSNs is proposed. Firstly, the charging demand degree is distincted to regulate the priority of charging requests. Then, to circumvent the occurrence of the node's energy being drained, the charger's orientation angle selection algorithm based on charging priority is designed. Finally, it is formulated that the problem of directional charger deployment is a discrete unit disk cover problem and proposed a moving path planning scheme based on an improved genetic algorithm to optimize the energy charging efficiency. Simulation results illustrate the benefit of our proposed scheme over the benchmark.

In [24], the WCV charging strategy in WRSN is studied due to the significance of different sensor nodes in the transmission of data and rough energy consumption. According to the importance of the sensor node, which is accompanied by the distance to the base station, we divide the sensor nodes into two types: sensor nodes in the inner ring and sensor nodes in the outer ring. Therefore, a new charging model is suggested to adopt various charging strategies for different sensor nodes. In order to become more efficient, the sensor nodes of the WCV sensor put one into an inner circle and then charged several sensor nodes simultaneously in the outer loop. A new measure called normal dead time is presented for approximating network lifetime. Maximizing network lifetime is modeled as minimizing the normal amount of dead time, and an efficient algorithm is presented to minimize the amount of normal dead time by searching for optimal charging time sequences. Then, by resetting the charging time of the sensor nodes, the minimum travel cost algorithm minimizes the WCV travel distance and ensures the network lifetime. A cluster head node with more battery capacity was organized to charge other sensor nodes within a limited distance. An algorithm for cluster head node energy predistribution is presented.

Up to date, a great number of optimization methods for obtaining the charging path with the objective of minimizing the charging cost have been well documented. However, autonomous charging path planning for MC in a switchable network is not considered. Article [11] emphasizes on the charging path for MC because MC is stopped at each sensor node until the sensor node is fully charged. In the present exploration, reinforcement learning (RL) is stated to charge route planning for MC in WRSN. To enhance MC independence, a new charging strategy for RL-based WRSNs (CSRL) is proposed according to the effects of changing the energy and location of sensor nodes. In [25], the operation of wireless sensor networks on the basis of WPT wireless energy transfer using a mobile charging vehicle (MCV) provides a periodic strategy for the permanent operation of the network. The goal is to diminish the total energy consumption of the system and maintain network performance at all times. In this context, according to the analysis of total energy consumption, it proposes an energy-efficient renewable scheme (ERSVC) to achieve energy savings. In [26], using the traditional MTSP model for reference, the minimum energy consumption path and battery capacity planning model under multiple chargers are established. Then, the creative balance factor is designed and applied. In the next steps, an improved genetic algorithm based on the degree of balance is planned.

The article [27] surveys the problem of the minimum battery capacity essential for the normal operation of each sensor when determining the charging path of the mobile charger. Then, the parameters of the wireless rechargeable sensor network are studied. In these circumstances, the objective is to minimize the battery capacity required by each sensor and ensure the continuous operation of the wireless rechargeable sensor network with minimal sensor energy consumption. To minimize the battery capacity of each sensor, a linear programming model is considered. Also, the Lingo method is used to solve the model.

Article [28] establishes a new scheduling scheme for on-demand charging in WRSNs. First, it provides an efficient network partitioning method for MCS to balance their workload equally. Thereafter, fuzzy logic was employed to determine the MCS charging schedule. Besides, it forms an expression to regulate the charging threshold for nodes that varies depending on their energy consumption.

Paper [29] focuses on the on-demand wireless rechargeable sensor networks (WRSNs) to consent for continuing and sustainable monitoring and provide application-based services matching goals, circumstances, and the environment within smart metropolises. This work proposes a calibration fuzzy-metaheuristic clustering routing scheme (CFMCRS) for on-demand WRSNs. The proposed CFMCRS assistances from resource-saving and energy supplementary techniques in addition to using metaheuristic and fuzzy logic methods to achieve roles and energy distribution in nodes and across the network. It also uses a multiobjective function to standardize the network with the nearest-job-next with preemption (NJNP) charging scheduler to meet WRSN requirements in smart cities. Based on simulation results, this strategy can delay the WRSN's lifetime.

A wireless rechargeable sensor network (WRSN) assisted by unmanned aerial vehicles (UAV) is a promising application in providing a stable power supply to rechargeable sensor nodes (SN). Creating a path for the UAV to traverse all SNs with the cheapest hacking cost for energy consumption is an important issue in UAV-assisted WRSN. Based on the studies in this section, although some exact algorithms and heuristic methods have been proposed, they cannot achieve an excellent result for large-scale networks in a tolerable time and respond well to energy constraints. In this paper, we examine the problem of UAV trajectory optimization from a new perspective that the designed trajectory should maximize the UAV's energy utilization efficiency. The energy efficiency problem is decomposed into integer programming and nonconvex optimization problems using the maximum energy of the UAV. To solve the problem of UAV charging position,

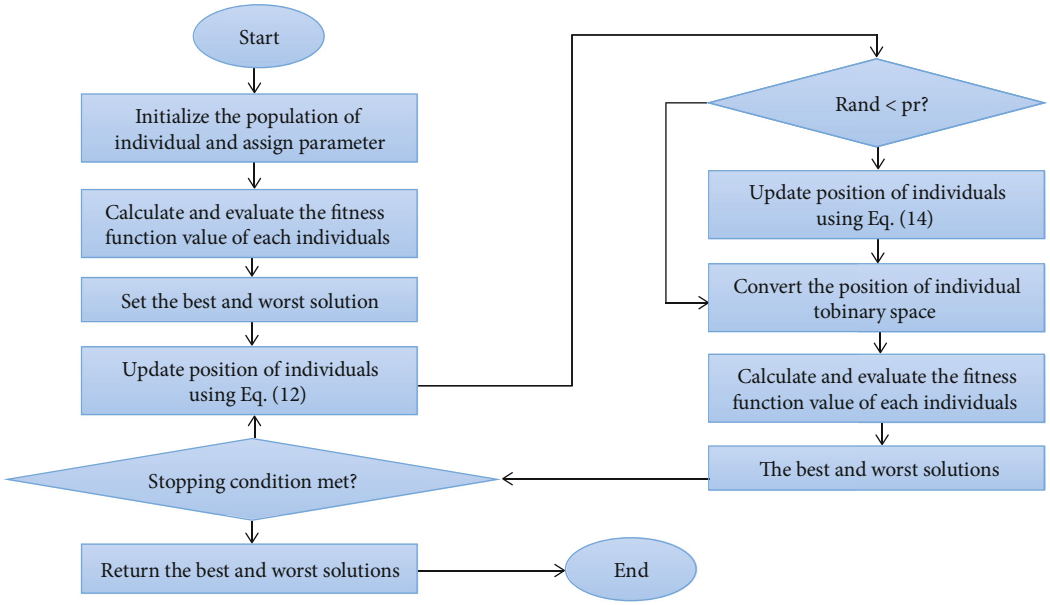

Figure 2: Flowchart of GBO algorithm [32].

we speed up the performance of the GBO algorithm by limiting the search direction, initial search position, and search space. For this problem, large systems are divided into smaller networks with the help of K-means clustering, and a route search is done for each cluster.

3. Basic Concepts

3.1. Gradient-Based Optimizer (GBO). The metaheuristic algorithm was first presented by Ahmadian Far et al. in 2020 to solve optimization problems related to engineering applications. Exploration and exploitation are the two main steps in metaheuristic algorithms that aim to improve the convergence speed and/or local optimal avoidance of the algorithm when searching for a target/situation. GBO is managed to make an appropriate trade-off between exploration and exploitation using two main operators: the gradient search rule (GSR) and the local escape operator (LEO). A simple introduction to this algorithm is explained as follows.

3.1.1. Gradient Search Rule (GSR). First, GBO suggests the first GSR function, which helps GBO to consider random behavior in the optimization process to facilitate the exploration and avoidance of local optimal. Directional motion (DM) is added to the GSR, which is used to perform a suitable local search process to facilitate the convergence speed of the GBO algorithm. Based on GSR and DM, the following equation is used to update the current vector position ($X^m{}_n$) [30, 31].

$$X1_n^m = x_n^m - \text{randn} \times \rho_1 \times \frac{2\Delta x \times x_n^m}{x_{\text{worst}} - x_{\text{best}} + \varepsilon} + \text{rand} \times \rho_2 \times (x_{\text{best}} - x_n^m), \quad (1)$$

$$\rho_1 = x \times \text{rand} \times \alpha - \alpha, \quad (2)$$

$$\alpha = \left|\beta \times \sin\left(\frac{3\pi}{2} + \sin\left(\beta \times \frac{3\pi}{2}\right)\right)\right|, \quad (3)$$

$$\beta = \beta_{\min} + (\beta_{\max} + \beta_{\min}) \times \left(1 - \left(\frac{m}{M}\right)^3\right)^2, \quad (4)$$

where $\beta_{\min}$ and $\beta_{\max}$ are 0.2 and 1.2, respectively, m is the number of iterations, and M is the total number of iterations. Moreover, randn is a normally distributed random number, and randn is a small number in the range [0, 0.1]. ρ_2 can be calculated using the following relationship:

$$\rho_2 = 2 \times \text{rand} \times \alpha - \alpha, \quad (5)$$

$$\Delta x = \text{rand}\,(1 : N) \times |\text{step}|, \quad (6)$$

$$\text{step} = \frac{(x_{\text{best}} - x_{r1}^m) + \delta}{2}, \quad (7)$$

$$\delta = 2 \times \text{rand} \times \left(\left|\frac{x_{r1}^m + x_{r2}^m + x_{r3}^m + x_{r4}^m}{4} - x_n^m\right|\right), \quad (8)$$

where rand $(1 : N)$ is an N-dimensional random number, $r1$, $r2$, $r3$, and $r4$, which are completely opposite to each other, are different integers randomly selected from $[1, N]$, step is a step size determined by the x_{best} and $x^m{}_{r1}$. By replacing the position of the best vector (x_{best}) with the current vector ($X^m{}_n$) for Equation (1), the new vector ($X2^m{}_n$) can be generated as follows:

$$X2_n^m = x_{\text{best}} - \text{randn} \times \rho_1 \times \frac{2\Delta x \times x_n^m}{yp_n^m - yq_n^m + \varepsilon} + \text{rand} + \rho_2 \times (x_{r1}^m - x_{r2}^m), \quad (9)$$

$$yp_n = \text{rand} \times \left(\frac{[z_{n+1} + x_n]}{2} + \text{rand} \times \Delta x\right), \quad (10)$$

$$yq_n = \text{rand} \times \left(\frac{[z_{n+1} + x_n]}{2} - \text{rand} \times \Delta x \right). \tag{11}$$

Based on the positions $X2^m{}_n$ and $X1^m{}_n$ of the current position ($X^m{}_n$), the new solution in the next iteration ($X^{m+1}{}_n$) can be defined as follows:

$$x_n^{m+1} = r_a \times (r_b \times X1_n^m + (1 - r_a) \times X2_n^m) + (1 - r_a) \times X3_n^m, \tag{12}$$

$$X3_n^m = X_n^m - \rho_1 \times (X2_n^m - X1_n^m). \tag{13}$$

3.1.2. Local Escaping Operator (LEO). LEO is the second operator introduced by GBO. LEO is introduced to make GBO still effective in dealing with complex high-dimensional problems. LEO is defined using several solutions, including the best position (x_{best}), solutions $X2^m{}_n$ and $X1^m{}_n$, two random solutions $X^m{}_{r2}$ and $X^m{}_{r1}$, and a new randomly generated solution ($X^m{}_k$). The $X^m{}_{\text{LEO}}$ solution is generated by the following scheme:

$$\begin{gathered}
\text{if rand} < pr \\
\text{if rand} < 0.5 \\
X_{\text{LEO}}^m = \frac{X_n^{m+1} + f_1 \times (u_1 \times x_{best} - u_2 \times x_k^m) + f_2 \times \rho_1 \times (u_3 \times (X2_n^m - X1_n^m) + u_2 \times (x_{r1}^m - x_{r2}^m))}{2} \\
X_n^{m+1} = X_{\text{LEO}}^m \\
\text{else} \\
X_{\text{LEO}}^m = \frac{X_{best} + f_1 \times (u_1 \times x_{best} - u_2 \times x_k^m) + f_2 \times \rho_1 \times (u_3 \times (X2_n^m - X1_n^m) + u_2 \times (x_{r1}^m - x_{r2}^m))}{2} \\
X_n^{m+1} = X_{\text{LEO}}^m \\
\text{End} \\
\text{End},
\end{gathered} \tag{14}$$

where f_1 is a random number in the interval [-1,1]. f_2 is a random number from a normal distribution with mean 0 and standard deviation 1, pr is the probability, and u_1, u_2, and u_3 are three random numbers defined as follows:

$$\begin{aligned}
u_1 &= L_1 \times 2 \times \text{rand} + (1 - L_1), \\
u_2 &= L_1 \times \text{rand} + (1 - L_1), \\
u_3 &= L_1 \times \text{rand} + (1 - L_1),
\end{aligned} \tag{15}$$

where L_1 is a binary parameter with a value of 0 or 1. Figure 2 shows the flowchart of the GBO algorithm.

3.2. K-Means Clustering. In fact, K-means clustering is a vector quantization method originally derived from signal processing and is popular for clustering analysis in data mining. K-means clustering is aimed at decomposing n observations into k clusters, where each observation belongs to the cluster with the closest mean, this mean is used as a sample.

Given a set of observations $(x_1, x_2, x_3, \cdots, x_n)$ where each observation is a d-dimensional real vector. K-means clustering is aimed at partitioning n observations into $K \le N$ set $S = \{s_1, s_2, s_3, \cdots, s_k\}$ so that the sum of squared differences from the mean (i.e., variance) for each cluster is minimized. Its exact mathematical definition is as follows:

$$\arg_s^{\min} \sum_{i=1}^{k} \sum_{x \in Si} \|x - \mu_i\|^2 = \arg_s^{\min} \sum_{i=1}^{k} |S_i| \text{Var}(S_i)^{\cdot}, \tag{16}$$

where μ_i is the mean of the points in S_i. This is equivalent to minimizing the two-squared deviations of points in the same cluster:

$$\sum_{\text{Cluster } Ci} \sum_{\text{Dimension } d} \sum_{x,y \in Ci} (x_d - y_d)^2. \tag{17}$$

Since the total variance is constant, it can be concluded from the law of total variance that this equation is equal to maximizing the square of the deviations between the points of different clusters (BCSS) [33–35].

3.3. Fuzzy Logic Technique. Fuzzy image processing can be defined as a set of all methods that are able to understand, display, and process images, parts, and features as fuzzy sets. Fuzzy image processing has three fundamental steps: image fuzzification, modification of membership values, and if needed, image defuzzification. The fuzzification step is attributed to the coding of image data. Besides, defuzzification is the decoding of the results. These stages make us the opportunity to process images with fuzzy techniques.

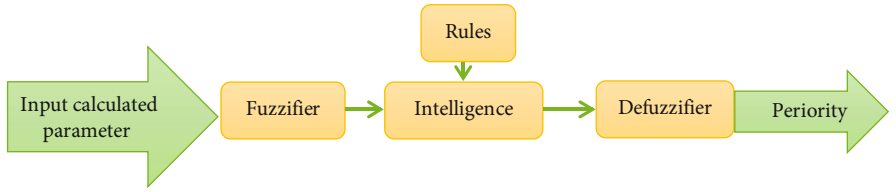

Figure 3: Steps involved in fuzzy image processing [11].

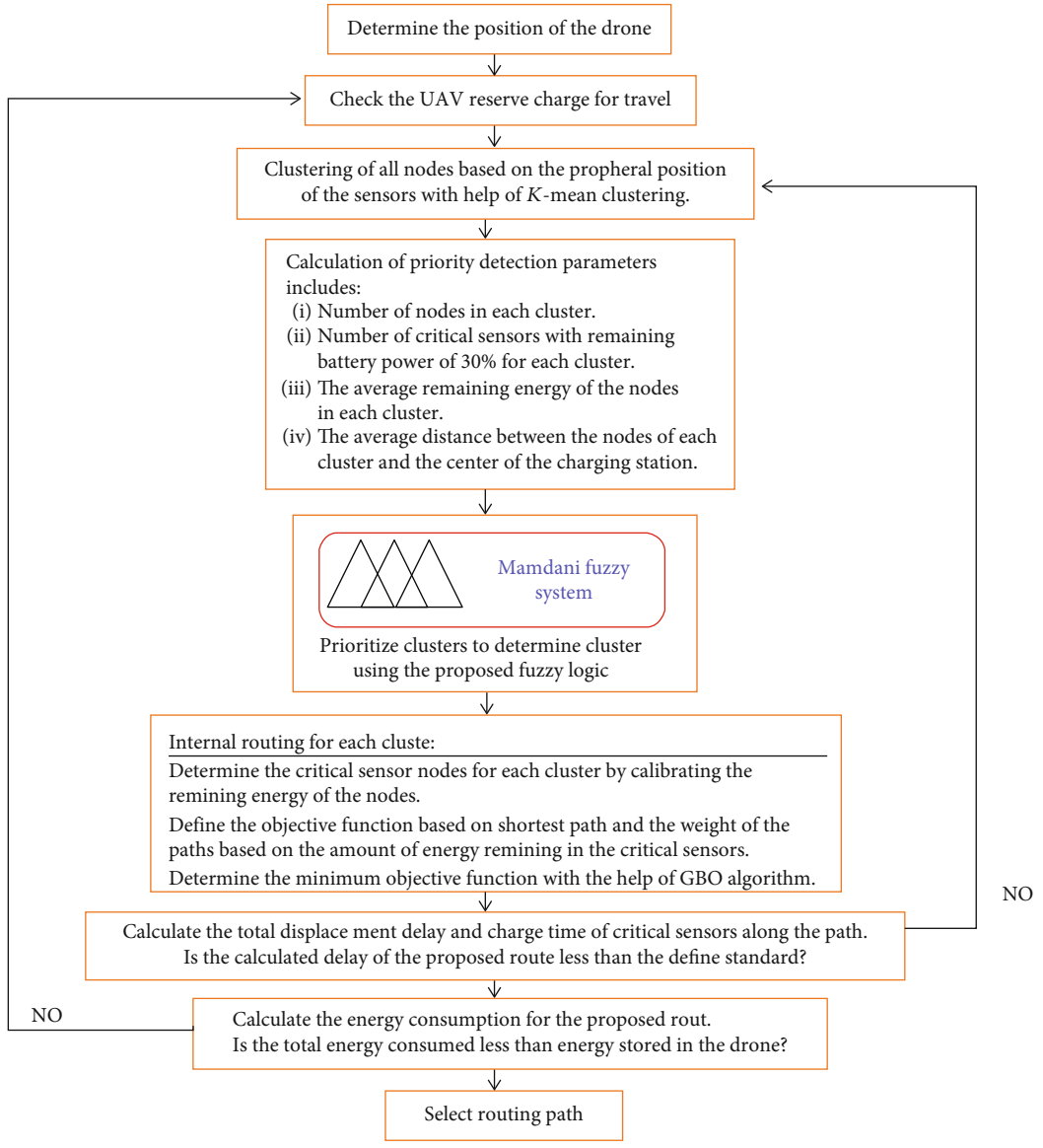

Figure 4: Flowchart of proposed plan strategy.

Hence, the coding of image data (fuzzification) and decoding of the results (defuzzification) are the most significant stages that provide us with the ability to handle the image with techniques as shown in Figure 3 [11, 36].

The most effective element of fuzzy image processing is that it can be observed in the middle stage, i.e., by modifying the membership values that can be considered as intelligent, since these steps make the difference between the approach and the other. Fuzzy logic is characterized by a wide variety of membership functions which include triangular, trapezoidal, Gaussian, and bell membership functions. Each of them has a distinctive influence. The use of appropriate membership by fuzzy system inference increases the effectiveness of the method. This method assumes the adjacent points of pixels and then divides them into classes using the membership function [37, 38].

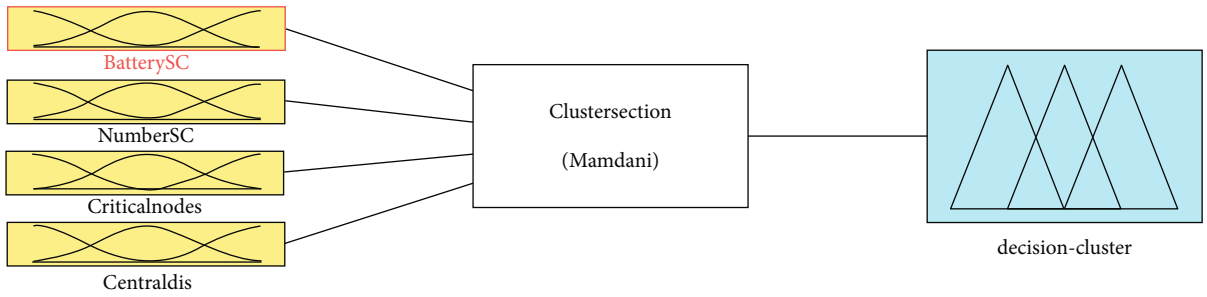

(a)

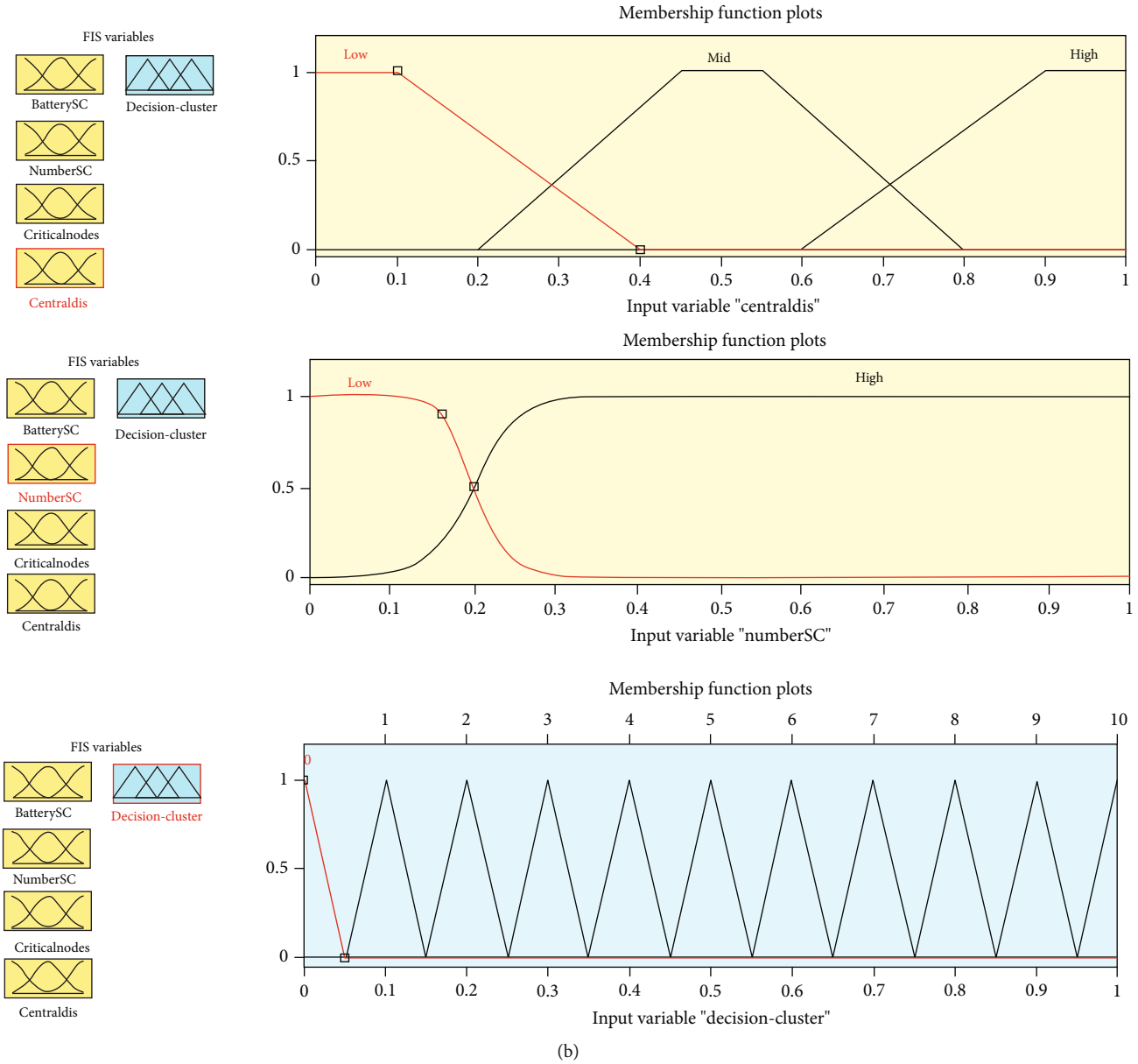

(b)

Figure 5: Continued.

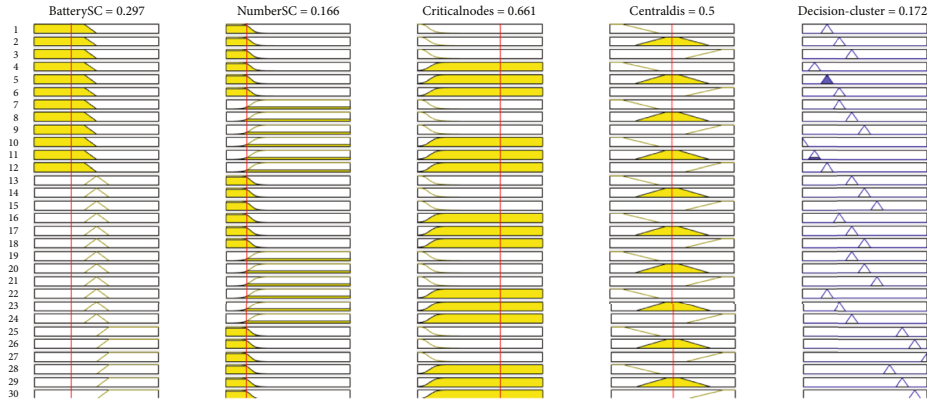

(c)

Figure 5: (a) The proposed fuzzy system, (b) input and output membership function, and (c) an example of implementing fuzzy rules.

The image that can be used in fuzzy logic technology must be transformed into a gray level and then converted to a membership function (fuzzification step), where its value can be readily adjusted by fuzzy technology. This could either be called a fuzzy clustering, a fuzzy rule-based approach, or a fuzzy integration approach. To realize the uncertainty in the data, fuzzy image processing is required. Many of the benefits of image processing based on fuzzy logic are expressed as follows:

(a) Fuzzy techniques are considered as dominant tools for displaying and processing an image

(b) It provides us the opportunity to handle and manage obscurity with efficiency

(c) The conception of fuzzy logic is not complicated

(d) Fuzzy logic offers a huge flexibility

(e) Fuzzy logic is operative even if the data is inaccurate

It is worthy to note that fuzzy logic works better than others because everything suffers from imprecision, whereas fuzzy logic makes its understanding by considering structure.

In several image-processing applications, to handle various types of complexities such as object recognition and scene analysis, it is recommended to utilize human logic according to if-then rules which can be accessible by fuzzy set theory and fuzzy logic. In contrast, many reasons like randomness, ambiguity, and vagueness make uncertainty in image processing results and data. Furthermore, those uncertainties have a negative impact on image processing progress that leads to many complications [39–41].

4. Proposed Work

Based on the studies conducted in different fields for charging sensors in WRSN, the use of mobile charger brings different problems for planning and scheduling in critical nodes that require emergency charging. The target subject is the moving path of the charger vehicle. In this article, we use a UAV aerial transmission system so that we can reduce the path well for different urban and moving environments such as trees and buildings. We can also create direct routes between sensor locations for reliable routing. Compared to other mobile chargers, UAVs consume less energy between movement paths. It will also be able to be placed at the closest distance from the sensor for wireless energy transfer. Therefore, in this work, we consider the moving position of the UAV near the sensor nodes for charging. This work reduces the power and power losses to transfer energy from the UAV to the destination to its lowest value. Another noteworthy point about the use of UAVs is the constant speed of the UAV during the route between the nodes, which makes the route and energy consumption more accurate and simple. Figure 4 shows the flowchart of the proposed strategy for UAV movement and sensor charging. The following steps are explained.

4.1. Determining the Position of the UAV. In this case, the position at the origin of the coordinates is usually taken into account, and the subsequent positions along the route are determined, of course, we also define the location of the UAV charging station at the origin so that the UAV returns to the hangar and recharges in each period of travel. In these circumstances, it can be prepared for the next courses.

4.2. Checking the Charge Level of the UAV Storage for Travel. In this case, checking the stored power inside the battery happens every period to reach an optimal approach for recharging the UAV at the charging station.

4.3. Clustering of All Nodes Based on the Environmental Position of Sensors with the Help of K-Means Clustering. In this section, based on the number of clusters introduced in this article, which is equal to 5, the nodes in close positions are placed in a group or cluster.

4.4. Calculation of Priority Detection Parameters Included

(1) The number of nodes in each cluster

Table 1: Fuzzy rule based on fuzzy prioritization.

Num.	Battery SC	Number SC	Critical nodes	Centraldis	Decision cluster
1	Low	Low	Low	Low	2
2	Low	Low	Low	Mid	3
3	Low	Low	Low	High	4
4	Low	Low	High	Low	1
5	Low	Low	High	Mid	2
6	Low	Low	High	High	3
7	Low	High	Low	Low	3
8	Low	High	Low	Mid	4
9	Low	High	Low	High	5
10	Low	High	High	Low	0
11	Low	High	High	Mid	1
12	Low	High	High	High	2
13	Mid	Low	Low	Low	4
14	Mid	Low	Low	Mid	5
15	Mid	Low	Low	High	6
16	Mid	Low	High	Low	3
17	Mid	Low	High	Mid	4
18	Mid	Low	High	High	5
19	Mid	High	Low	Low	4
20	Mid	High	Low	Mid	5
21	Mid	High	Low	High	6
22	Mid	High	High	Low	2
23	Mid	High	High	Mid	3
24	Mid	High	High	High	4
25	High	Low	Low	Low	8
26	High	Low	Low	Mid	9
27	High	Low	Low	High	10
28	High	Low	High	Low	7
29	High	Low	High	Mid	8
30	High	Low	High	High	9
31	High	High	Low	Low	8
32	High	High	Low	Mid	9
33	High	High	Low	High	10
34	High	High	High	Low	6
35	High	High	High	Mid	7
36	High	High	High	High	8

(2) The number of critical sensors with a remaining battery capacity of 30% for each cluster

(3) The average residual energy of nodes in each cluster

(4) The average distance of the nodes of each cluster with the center of the charging station

These four parameters are normalized on the input of the priority detection fuzzy logic system in the range between 0 and 1. Now, these inputs are sent to the membership functions of the fuzzy system so that prioritization is done based on the defined fuzzy rules.

4.5. Prioritizing the Clusters to Determine the Clusters of the UAV Movement Path with the Help of the Proposed Fuzzy Logic. According to various works in Refs. [31–33] in this article, a fuzzy system is used to select and prioritize clusters. Sorting the output of the fuzzy system calculated for each cluster until all clusters are arranged to prioritize the path selection priority.

4.6. Internal Routing for Each Cluster. In this part, UAV movement routing is performed for each cluster in the order of the determined fuzzy priority.

(i) Determining the critical sensor nodes for each cluster by limiting the residual energy of the nodes

(ii) Defining the objective function based on the shortest path and weighting the paths based on the remaining energy of critical sensors

(iii) Determining the minimum of the objective function with the help of the GBO algorithm

4.7. Investigate the Delay and Energy. For this case, in the final routing, two energy limits and delay must be checked in this strategy. In the model presented in this work, first, the calculation of the total displacement delay and the charging time of the critical sensors along the determined path is done. The relationships governing these calculations are as follows:

Calculation of the remaining working time of the MCV (UAV):

First, we calculate the remaining working time of MCV as follows:

$$\text{duration}_{\text{MCV}} = , \tag{18}$$

where $d_{i-1,i}$ represents the distance between two nodes, $d_{n,0}$ represents the maintenance station, v is the speed of the MCV, and τ_i represents the time the MCV stays near node i. When the remaining working time is greater than the MCV duration, the node ensures that it is always working [42, 43].

4.8. Calculation of the Minimum Remaining Working Time of the Sensor. The minimum remaining working time of the sensor in WRSN is calculated by the following relationship:

$$reT_{\min} = \min\left(\frac{E_i(m)}{P_i(m)}\right) 1 \le i \le n, \tag{19}$$

where $E_i(m)$ is the residual energy of the ith node in the mth cluster and $p_i(m)$ represents the power of the ith node.

Here, the condition of the proposed strategy is that the remaining working time of the UAV is less than the minimum remaining working time of the sensors. With this limitation, the condition of convergence and confirmation of the route determined in this period is approved and goes

```
function dist = tourmeter(x0,y0,Z,net,ROC)
%UNTITLED Summary of this function goes here
%   Detailed explanation goes here
x = net.x;
y = net.y;
dist = sqrt(x0^2+y0^2)+sqrt((x(Z(1))-x0)^2+(y(Z(1))-y0)^2)*2^(ROC(Z(1)));
for i = 2:numel(Z)
    dist = dist + sqrt((x(Z(i))-x(Z(i-1)))^2+(y(Z(i))-y(Z(i-1)))^2)*2^(ROC(Z(i)));
end
end
```

Figure 6

Table 2: Simulation parameters.

Parameters	Values
Node number	100-50
Field size (m^2)	400*400
Location of CS	0,0
Initial energy (J)	50 + rand (N)*10
Battery capacity of UAV	1000 kj
Charging loss rate(ρ)	0.2
Energy threshold for sending a charging request	0.5Emax – 50%
UAV speed (m/s)	3-5-8
UAV charging efficiency (η)	0.5
UAV moving consumption (J/m)	8
UAV charging power (W)	10
UAV recharging duration (min)	10

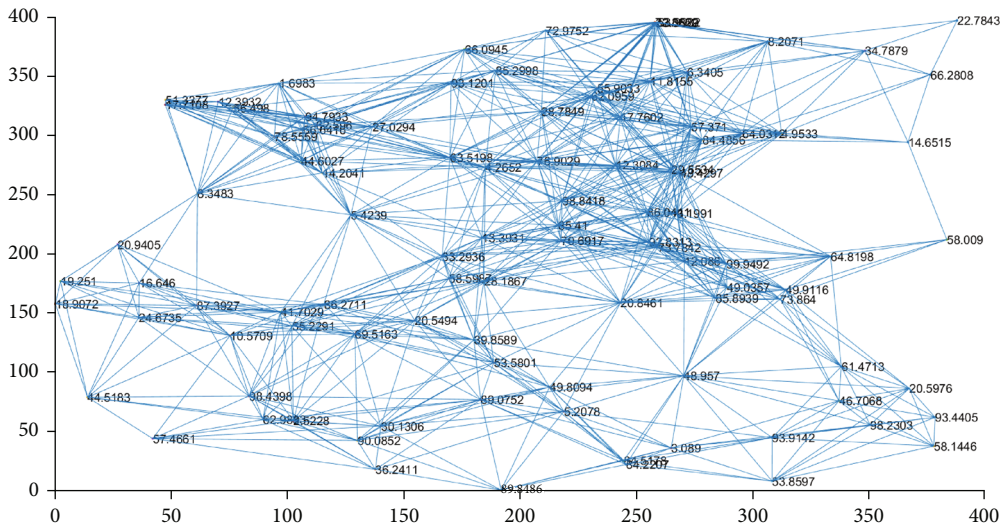

Figure 7: Representation of wireless rechargeable sensor network with 100 nodes.

to the next stage for implementation; otherwise, the proposed strategy should be implemented again to track the new route. By applying this condition to the proposed method, the probability of the death of sensor nodes will reach zero.

After applying the delay condition in the first step, it is time to calculate the energy consumption for the proposed route. In this step, the two problems of energy charging and energy loss by the UAV are calculated according to the length of the path.

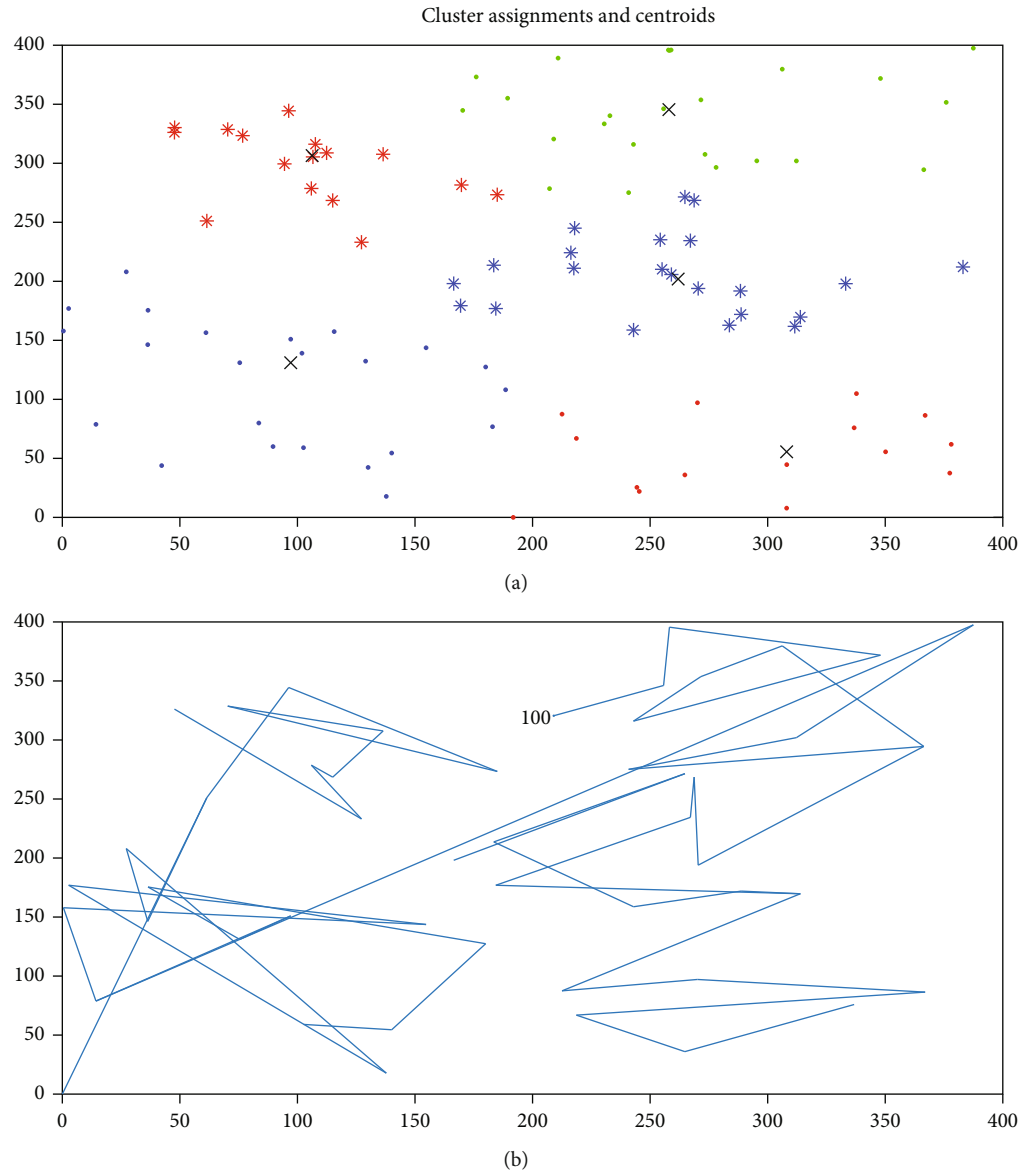

Figure 8: Display routing and clustering results for a network with 100 nodes.

4.9. Energy Charging Model. The energy charge model is defined as the Ferris free space model in (20) [40].

$$P_r(d) = \frac{G_{tx}G_{rx}\eta}{L_p}\left(\frac{\lambda}{4\pi(\mathrm{d}+\delta)}\right)^2 P_{tx}, \tag{20}$$

where G_{tx} is the gain of the source antenna, G_{rx} is the gain of the receiver antenna, η represents the rectifier efficiency, L_p represents the polarization loss, λ is the wavelength, d is the distance of the UAV charge to the sensor node, which is equal to 1 m in this work. δ value is 0.2316 as a parameter to adjust the Ferris free space equation for short-distance transmission, and P_{tx} is the MCV source power. Power consumption for the rest of the UAV can be calculated for each sensor, which is introduced in this article with P_{uav}.

4.10. Energy Consumption Model during UAV Travel. To calculate the energy consumed during the distance traveled by the UAV, due to the same speed of movement, this amount of energy is constant along the path. For modeling, in this regard, the amount of energy consumed is:

$$E_{\mathrm{tour}} = \alpha.L, \tag{21}$$

where L is the total distance traveled during the travel of one charging period. α will be the energy consumption coefficient of MCV along the path, which is assumed to be 0.3 j/m for the UAV in this article.

$$E_{\mathrm{tot}} = E_{\mathrm{tour}} + \sum_{i=1}^{N} P_{\mathrm{UAV}}.T_i + E_r. \tag{22}$$

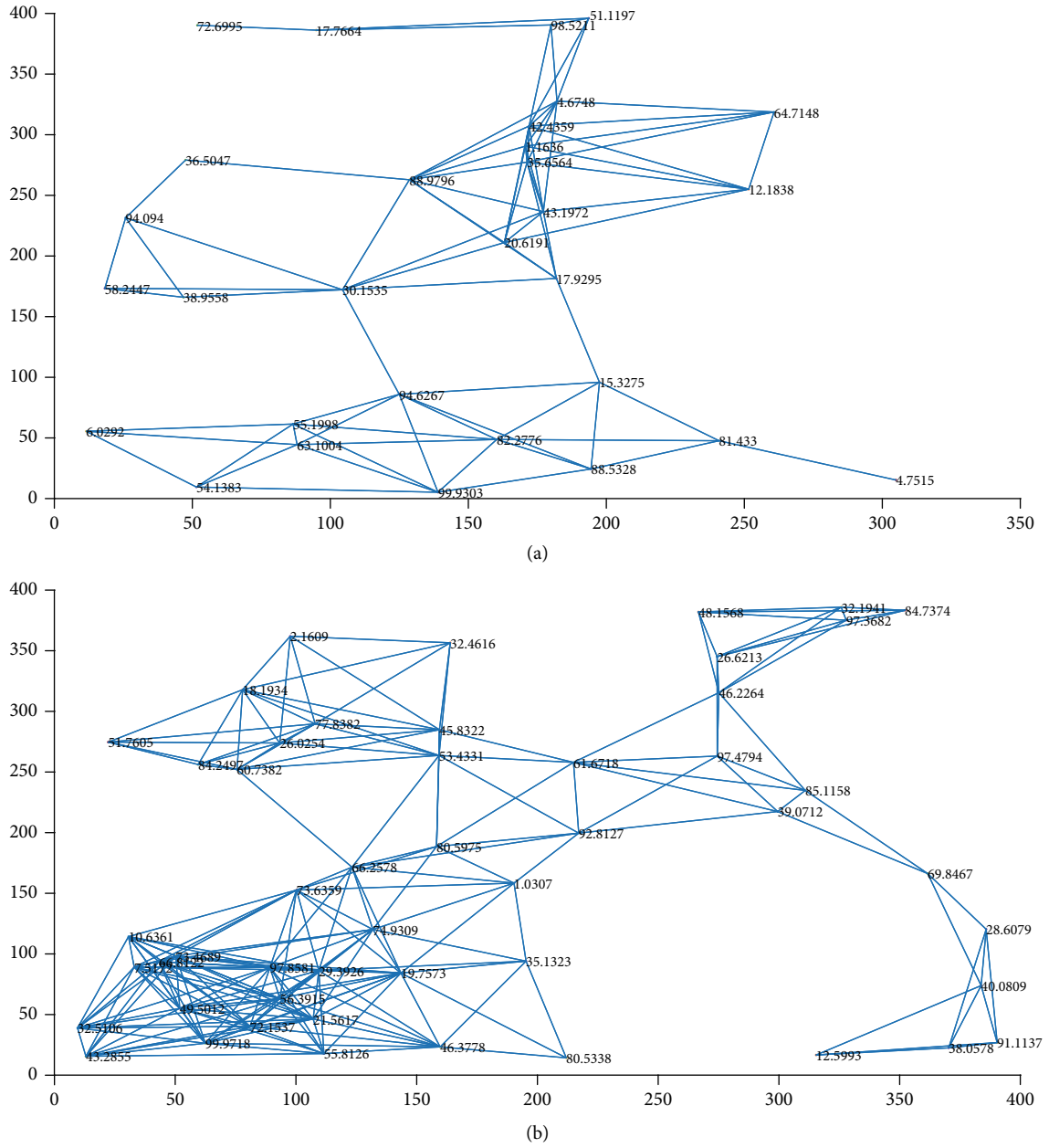

Figure 9: Display of wireless rechargeable sensor network with (a) 30 and (b) 50 nodes.

Based on this, the total amount of energy consumed during the tour of a specific period is calculated as follows:

Where E_r is the energy required to fully charge the sensor node and I_t is the amount of time the charger stays next to sensor node i and is calculated by the following equation:

$$T_i = \frac{E_r}{P_r(1)}. \tag{23}$$

In order to implement the strategy proposed in this article, in the proposed method, the total energy consumption should be less than the periodically charged energy of the UAV, so that the MCV can fully charge both the critical nodes and return to the charging station.

4.11. Proposed Fuzzy Logic System. In this section, the cluster prioritization system is presented with 4 parameters defined in the previous section and fuzzy rules [31, 32]. In this case, we use the parameters of the number of nodes in each cluster and the number of critical nodes with residual power less than 30%, the average energy of the nodes in the cluster, and the distance of each cluster from the maintenance center, which are introduced at the origin of the coordinates, as the input of the fuzzy system (Mamdani type). According to the total number of rechargeable sensor network nodes and the dimensions of the environment, these four parameters should be determined for the interval [0,1] for the input of the fuzzy system. Figure 5 shows the structure and input and output membership functions for the defined fuzzy system. Triangular, trapezoidal, and Gaussian membership

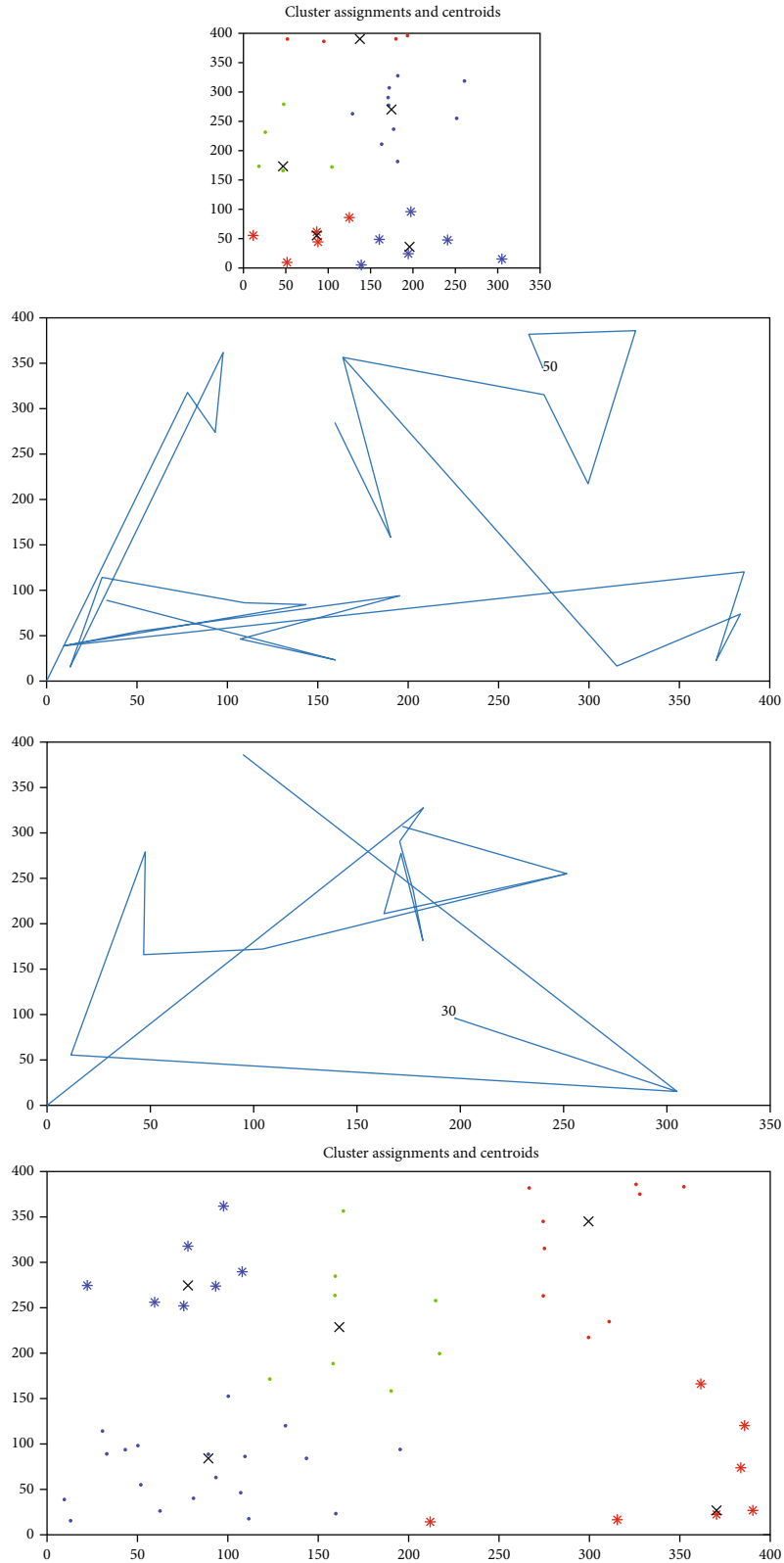

Figure 10: Display routing and clustering results for a network with 50 and 30 nodes.

functions are used in this fuzzy logic. Table 1 also shows the written rules for cluster selection and prioritization. The basis for defining the fuzzy rules for the prioritization system in the clusters will depend on the four input parameters of the fuzzy system, so the lower the average battery charge (battery SC), the lower the priority value of the cluster, that

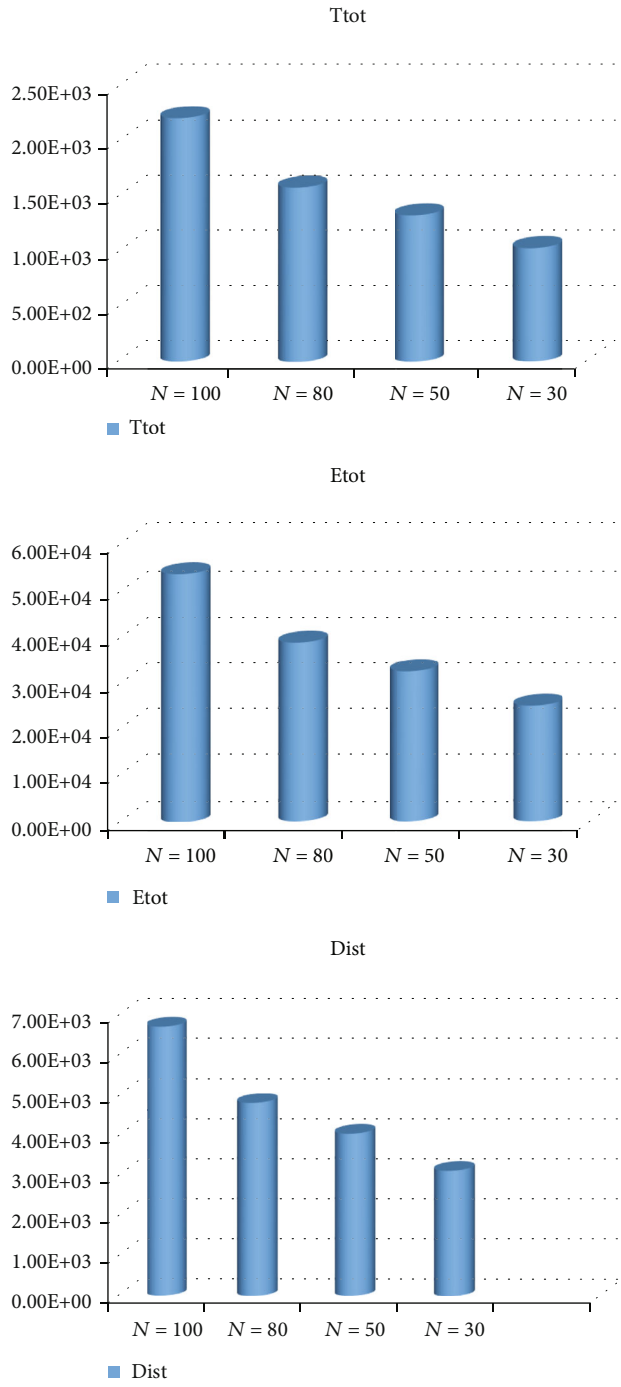

Figure 11: Bar diagram comparing the results for energy consumption and travel distance and time with changing the number of sensor nodes.

is, it is placed in the primary and emergency order for the UAV's path. Also, the lower the number of node members (number SC), the lower the priority value of the cluster, and for the number of critical nodes for the need to charge (critical nodes), the lower priority value is set, and finally, the lower the distance between the center of the nodes and the origin (centraldis), the higher the prioritization (i.e., lower cluster priority value). At this stage, the fuzzification operation is performed for the number of clusters in the WRSN, and the final value is obtained. Then, based on the priority defined in this work and the ascending sorting of the outputs of each cluster, the placement order for the UAV route is introduced. The numbering of the clusters is introduced in order from minimum to maximum based on the fuzzy output of each cluster.

Table 3: Comparison of different algorithms for a network with 100 sensor nodes.

Parameters	GA	GBO
Total energy consumption	$7.30E+04$	$5.40E+04$
Total distance during the tour	$8.10E+03$	$6.70E+03$
Total travel delay	$2.95E+03$	$2.20E+03$
Simulation time(s)	465	334

4.12. Routing with GBO Algorithm. After selecting and prioritizing the clusters, in each cluster, sensitive and critical nodes with less than 30% remaining energy are selected, highlighted, and activated for charging by the UAV. In this step, for each cluster, the fuzzy priority of the UAV route is determined with the help of a gradient-based optimization algorithm for the following proposed objective function. In the first cluster, the initial position of the UAV is selected as the hangar, which is located in the maintenance center at the origin of the coordinates with the positions 0 and 0 introduced, and for the next clusters, the initial position of the location of the last routed node in the previous cluster is introduced. The basis for defining the objective function in each cluster is the path length of the selected nodes and the weighting of each critical sensor node based on the defined function of the following mathematical model:

$$\text{fitnessfunction} = \sum_{k=1}^{n-1} 2^{\text{ROC}(z(k))} \times \sqrt{[x(z(k+1)) - x(z(k))]^2 + [y(z(k+1)) - y(z(k))]^2}, \tag{24}$$

where Z is the number of nodes selected under the algorithm in the cluster and ROC is the relative amount of remaining power of the selected nodes Z which is defined in the range of 0 and 1. Figure 6 shows the MATLAB code of the function:

5. Simulation Results

In this section, extensive simulation experiments are conducted to evaluate the performance of WRSN.

5.1. Model of Study and Simulation. As shown in Table 2, we randomly deploy {100} nodes in a square field of 400 m by 400 m. The coordinates of the maintenance station are at (0, 0), and the UAV is charged there. The information from the nodes, after being received by the individual nodes, is relayed to the center of the station. The sensor node sends a charge request to the station when the remaining energy is below the threshold. In our event-driven simulator,

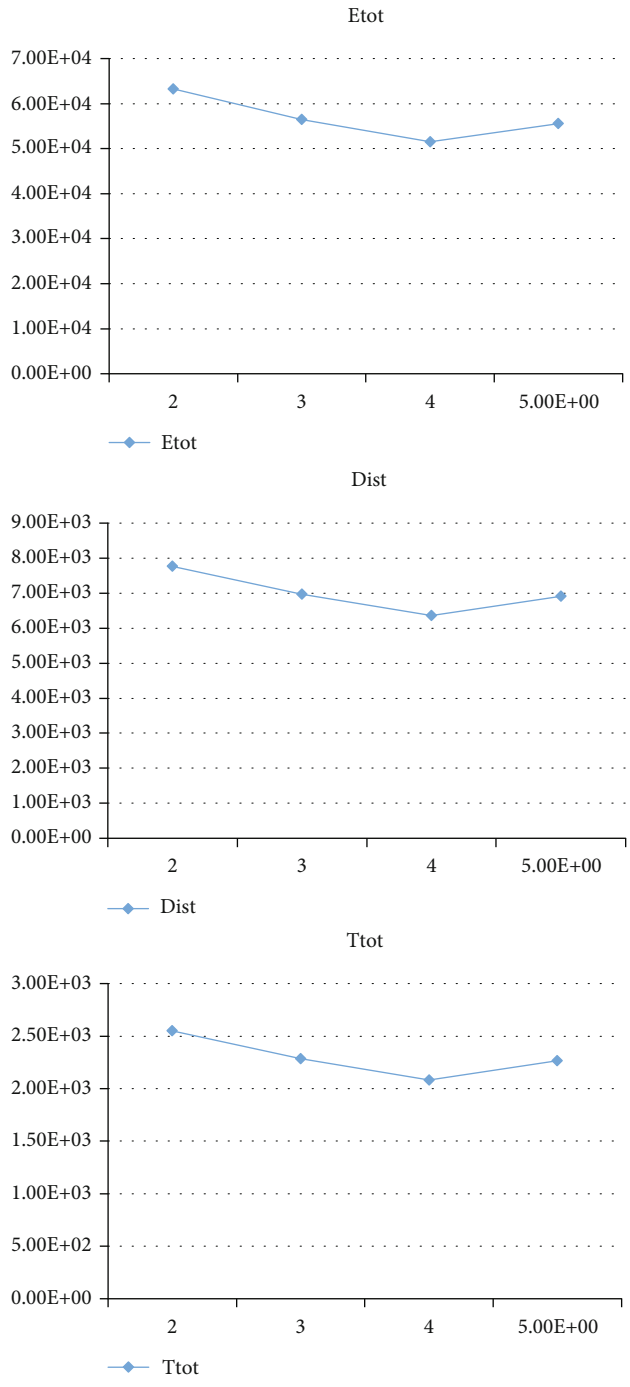

Figure 12: The graph of changes in the number of clusters on the results.

measurement data is simulated as events occur at random times and in random locations. Whenever an event occurs within the range of the sensor node, the node captures the event and sends it to the BS through the constructed route. The mobile charging process is simulated using m-file code in MATLAB 2017b software.

5.2. Showing Results. In this section, the results of a sample system from Figure 7 are shown for the number of 100

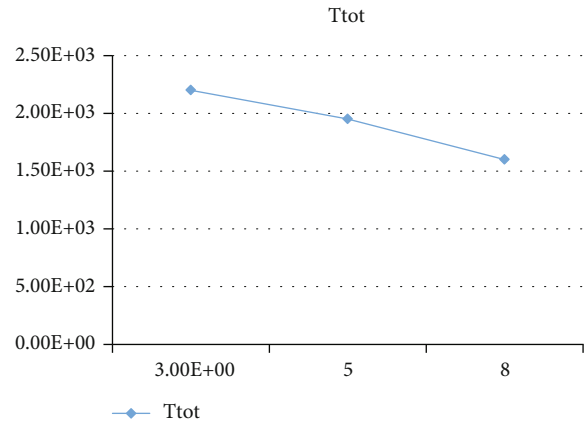

Figure 13: Graph of UAV speed changes on total delay.

rechargeable sensor nodes. According to the figure, the remaining battery capacity of each node is introduced. Nodes with a distance of less than 100 meters will be able to communicate with each other and are connected with a blue line, and communication exchange is more in crowded areas. In this section, the routing results for critical sensors with a charge percentage less than 50% have been discussed using the proposed strategy method of combined fuzzy logic with the GBO algorithm. The basis of wireless energy request from UAV by nodes can be introduced by limiting the residual energy threshold of nodes. By changing this threshold value, the performance of the system can be changed for the charging speed and charging of all nodes and the initial charging of the UAV. Each time the charging strategy is applied, the energy capacity of the batteries is reviewed and quantified in the problem.

Figure 8 shows an example of the system response for the studied network. In this image, the steps for applying the proposed charging techniques are shown. Figure 8(a) shows the results of clustering sensor nodes based on location with the help of the K-means algorithm, and then fuzzy prioritization is performed to select the cluster. The priority order of the clusters is quantified with the help of fuzzy rules, and the clusters with a lower priority value will have a higher chance to be charged early by the UAV.

Figure 8(b) also shows the routing results according to the objective function defined in this article with the help of the GBO algorithm in each cluster. The selection of the routes between the critical nodes is based on the sensitivity of the nodes to reach the charge and minimize the travel distance. Also, Figures 9 and 10 show the simulation results for other examples of the network with 50 and 30 nodes. To evaluate and compare the effectiveness of the suggested design, simulation of other cases is used. The bar graph of the comparison results for networks with different numbers of nodes is shown in Figure 11. As can be seen, by reducing the number of sensors in the network, the amount of energy consumed and the distance and travel time are reduced. In Table 3, three important parameters of energy, time, and length of travel and one parameter of simulating the duration of program execution and decision-making for choosing routes are compared in two genetic algorithms and

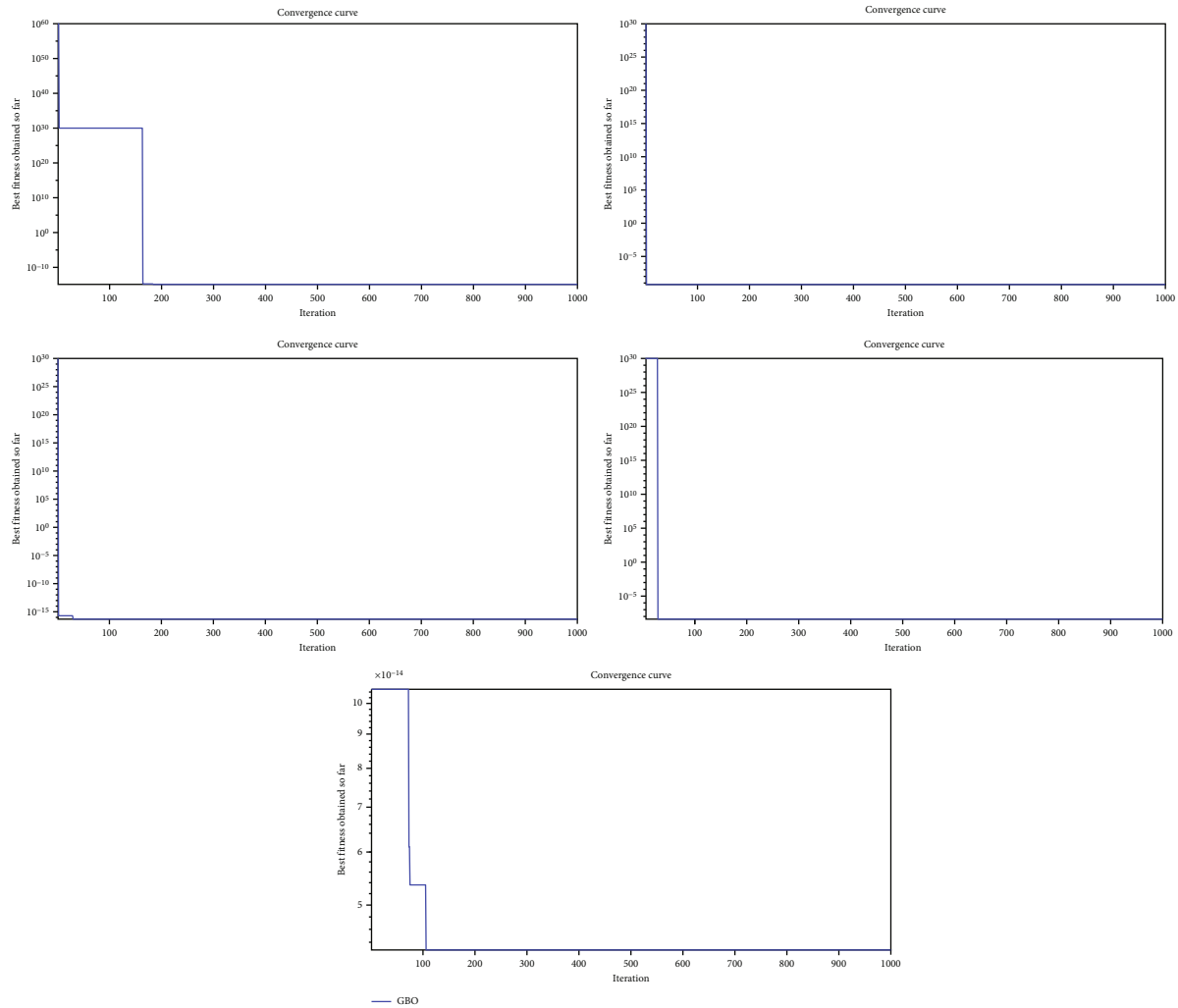

Figure 14: Performance display of the GBO algorithm for each cluster.

GBO, which obtained better answers based on the results of the GBO algorithm. The results discussed in this table are analyzed for a network with 100 nodes.

The important point to analyze the results in this paper is the performance of the proposed technique for changes in the number of clusters and the speed of the UAV. Therefore, in Figure 12, the graph shows the changes in the number of clusters for the system with 100 sensor nodes. According to this figure, by increasing the number of network clusters for charging for the number of 4 clusters, the target parameters including the total flight delay, the distance traveled, and the UAV charging energy will decrease, and then by further increasing these parameters, we have achieved an increase in the target parameters. For clustering with the number of 4 clusters, we have been able to obtain the best response for the charging performance of the sensor network, which provides the best responses in terms of energy consumption, delay, and the length of the UAV's travel path. According to Figure 13, which shows the variation in UAV speed, it reduces the total flight delay during travel and helps to improve the performance of the WRSN charging system. Finally, the performance of the GBO algorithm for 1000 iterations of path tracing for the network with 80 nodes is checked and shown for each cluster in Figure 14. In this figure, it can be seen that all the clusters have reached their global minimum after the period of 300.

6. Conclusion

The current study manifests an on-demand wireless charging algorithm with the help of drones based on fuzzy logic system, and a gradient-based optimization algorithm called fuzzy-GBO is proposed. Using the combined clustering strategy based on fuzzy logic and the GBO routing algorithm, fuzzy-GBO can help the UAV to achieve independent path planning. Moreover, fuzzy-GBO fully considers the operation of the UAV with limited energy and the response to charging requests. Therefore, fuzzy-GBO can improve the performance of UAVs and sensor networks. Subsequently, experiments are conducted to verify the performance of fuzzy-GBO, which is compared with classical on-demand charging algorithms. Remarkably, the simulation results reveal that the fuzzy-GBO is well designed and can effectively increase the lifetime of the networks as well as the

energy utilization of the UAV under the limited energy of the UAV. It is worthy to note that we further analyze how parameters such as the number of sensor nodes, UAV speed, and the number of clusters affect SRL-FA.

In the future, we plan to expand this work by using multiple UAVs and considering the energy consumption dynamics of sensor nodes. Also, the uncertainties of energy consumption and different charging conditions are investigated for each sensor node. It may lead to more cooperation among them to address more practical problems in WRSNs.

Data Availability

The data will be shared only at the request of the esteemed editor for review by the reviewers.

Conflicts of Interest

The authors declare that they have no known competing financial interests or personal relationships that could have appeared to influence the work reported in this paper.

References

[1] D. Yu, J. Kang, and J. Dong, "Service attack improvement in wireless sensor network based on machine learning," *Microprocessors and Microsystems*, vol. 80, article 103637, 2021.

[2] M. M. Ahmed, E. H. Houssein, A. E. Hassanien, A. Taha, and E. Hassanien, "Maximizing lifetime of large-scale wireless sensor networks using multi-objective whale optimization algorithm," *Telecommunication Systems*, vol. 72, no. 2, pp. 243–259, 2019.

[3] D. Dondi, A. Bertacchini, D. Brunelli, L. Larcher, and L. Benini, "Modeling and optimization of a solar energy harvester system for self-powered wireless sensor networks," *IEEE Transactions on Industrial Electronics*, vol. 55, no. 7, pp. 2759–2766, 2008.

[4] A. Shiri and G. K. Khosroshahi, "An FPGA implementation of singular value decomposition," in *2019 27th Iranian Conference on Electrical Engineering (ICEE)*, pp. 416–422, Yazd, Iran, 2019.

[5] L. He, L. Kong, Y. Gu, J. Pan, and T. Zhu, "Evaluating the on-demand mobile charging in wireless sensor networks," *IEEE Transactions on Mobile Computing*, vol. 14, pp. 1861–1875, 2015.

[6] S. Sadeqi, N. Xiros, S. Rouhi, J. Ioup, J. VanZwieten, and C. Sultan, "Wavelet transformation analysis applied to incompressible flow field about a solid cylinder," in *5-6th Thermal and Fluids Engineering Conference (TFEC)*, American Society of Thermal and Fluids Engineers, 2021.

[7] Y. Dong, Y. Wang, S. Li, M. Cui, and H. Wu, "Demand-based charging strategy for wireless rechargeable sensor networks," *ETRI Journal*, vol. 41, no. 3, pp. 326–336, 2019.

[8] M. Trik, A. M. N. G. Molk, F. Ghasemi, and P. Pouryeganeh, "A hybrid selection strategy based on traffic analysis for improving performance in networks on chip," *Journal of Sensors*, vol. 2022, Article ID 3112170, 19 pages, 2022.

[9] F. Abed Azad, S. Ansari Rad, M. R. Hairi Yazdi, M. Tale Masouleh, and A. Kalhor, "Dynamics analysis, offline–online tuning and identification of base inertia parameters for the 3-DOF delta parallel robot under insufficient excitations," *Meccanica*, vol. 57, no. 2, pp. 473–506, 2022.

[10] M. Angurala, M. Bala, and S. S. Bamber, "Implementing MRCRLB technique on modulation schemes in wireless rechargeable sensor networks," *Egyptian Informatics Journal*, vol. 22, no. 4, pp. 473–478, 2021.

[11] G. Kunkel, M. Madani, S. J. White, P. H. Verardi, and A. Tarakanova, "Modeling coronavirus spike protein dynamics: implications for immunogenicity and immune escape," *Biophysical Journal*, vol. 120, no. 24, pp. 5592–5618, 2021.

[12] S. Hosseini and M. B. Khamesee, "Modeling and simulation and imaging of blood flow in the human body," *Nveo-Natural Volatiles & Essential Oils Journal|NVEO*, vol. 8, pp. 13235–13244, 2021.

[13] V. A. Chenarlogh, F. Razzazi, and N. Mohammadyahya, "A multi-view human action recognition system in limited data case using multi-stream CNN," in *2019 5th Iranian Conference on Signal Processing and Intelligent Systems (ICSPIS)*, pp. 1–11, Shahrood, Iran, 2019.

[14] C. R. Bowen and M. H. Arafa, "Energy harvesting technologies for tire pressure monitoring systems," *Advanced Energy Materials*, vol. 5, no. 7, article 1401787, 2015.

[15] A. O. Almagrabi, "Fair energy division scheme to permanentize the network operation for wireless rechargeable sensor networks," *IEEE Access*, vol. 8, pp. 178063–178072, 2020.

[16] A. Golrou, A. Sheikhani, A. M. Nasrabadi, and M. R. Saebipour, "Enhancement of sleep quality and stability using acoustic stimulation during slow wave sleep," *International Clinical Neuroscience Journal*, vol. 5, no. 4, pp. 126–134, 2018.

[17] L. Mo, A. Kritikakou, and S. He, "Energy-aware multiple mobile chargers coordination for wireless rechargeable sensor networks," *IEEE Internet of Things Journal*, vol. 6, no. 5, pp. 8202–8214, 2019.

[18] J. Sun, Y. Zhang, and M. Trik, "PBPHS: a profile-based predictive handover strategy for 5G networks," *Cybernetics and Systems*, vol. 53, no. 5, pp. 1–22, 2022.

[19] S. Pahlavan and V. Ahmadi, "Modeling and analysis of co and counter propagation of picosecond pulses in QD-SOA," *IEEE Journal of Quantum Electronics*, vol. 49, no. 11, pp. 982–989, 2013.

[20] W. Xu, W. Liang, H. Kan, Y. Xu, and X. Zhang, "Minimizing the longest charge delay of multiple mobile chargers for wireless rechargeable sensor networks by charging multiple sensors simultaneously," in *2019 IEEE 39th International Conference on Distributed Computing Systems (ICDCS)*, pp. 881–890, Dallas, TX, USA, 2019.

[21] M. Madani, K. Lin, and A. Tarakanova, "DSResSol: a sequence-based solubility predictor created with dilated squeeze excitation residual networks," *International Journal of Molecular Sciences*, vol. 22, no. 24, p. 13555, 2021.

[22] Z. Chen, X. Chen, D. Zhang, and F. Zeng, "Collaborative mobile charging policy for perpetual operation in large-scale wireless rechargeable sensor networks," *Neurocomputing*, vol. 270, pp. 137–144, 2017.

[23] M. Trik, A. M. Bidgoli, H. Vashani, and S. P. Mozaffari, "A new adaptive selection strategy for reducing latency in networks on chip," *Integration*, vol. 89, pp. 9–24, 2023.

[24] H.-P. Kriegel, E. Schubert, and A. Zimek, "The (black) art of runtime evaluation: are we comparing algorithms or implementations?," *Information Systems*, vol. 52, no. 2, pp. 341–378, 2017.

[25] K. Anindyaguna, N. C. Basjaruddin, and D. Saefudin, "Overtaking assistant system (OAS) with fuzzy logic method using camera sensor," in *2016 2nd international conference of industrial, mechanical, electrical, and chemical engineering (ICIMECE)*, pp. 89–94, Yogyakarta, Indonesia, 2016.

[26] S. Hosseini and M. B. Khamesee, "Design and control of a magnetically driven capsule-robot for endoscopy and drug delivery," in *2009 IEEE Toronto International Conference Science and Technology for Humanity (TIC-STH)*, pp. 697–702, Toronto, ON, Canada, 2009.

[27] Z. Feng and B. Zhang, "Fuzzy clustering image segmentation based on particle swarm optimization," *TELKOMNIKA (Telecommunication Computing Electronics and Control)*, vol. 13, no. 1, pp. 128–136, 2015.

[28] S. Radhoush, M. Bahramipanah, H. Nehrir, and Z. Shahooei, "A review on state estimation techniques in active distribution networks: existing practices and their challenges," *Sustainability*, vol. 14, no. 5, p. 2520, 2022.

[29] T. Zou, S. Lin, Q. Feng, and Y. Chen, "Energy-efficient control with harvesting predictions for solar-powered wireless sensor networks," *Sensors*, vol. 16, no. 1, p. 53, 2016.

[30] F. Fanian and M. K. Rafsanjani, "CFMCRS: calibration fuzzy-metaheuristic clustering routing scheme simultaneous in on-demand WRSNs for sustainable smart city," *Expert Systems with Applications*, vol. 211, article 118619, 2023.

[31] H. El Alami and A. Najid, "A new fuzzy clustering algorithm to enhance lifetime of wireless sensor networks," in *International Afro-European Conference for Industrial Advancement*, pp. 68–76, Springer, Cham, 2016.

[32] J.-S. Lee and C.-L. Teng, "An enhanced hierarchical clustering approach for mobile sensor networks using fuzzy inference systems," *IEEE Internet of Things Journal*, vol. 4, no. 4, pp. 1095–1103, 2017.

[33] N. El Idrissi, A. Najid, and H. El Alami, "New routing technique to enhance energy efficiency and maximize lifetime of the network in WSNs," *International Journal of Wireless Networks and Broadband Technologies (IJWNBT)*, vol. 9, no. 2, pp. 81–93, 2020.

[34] A. Ramtin, V. Hakami, and M. Dehghan, "A self-stabilizing clustering algorithm with fault-containment feature for wireless sensor networks," in *7'th International Symposium on Telecommunications (IST'2014)*, pp. 735–739, Tehran, Iran, 2014.

[35] B. HassanVandi, R. Kurdi, and M. Trik, "Applying a modified triple modular redundancy mechanism to enhance the reliability in software-defined network," *International Journal of Electrical and Computer Sciences (IJECS)*, vol. 3, no. 1, pp. 10–16, 2021.

[36] A. Chapnevis, I. Güvenç, and E. Bulut, "Traffic shifting based resource optimization in aggregated IoT communication," in *2020 IEEE 45th Conference on Local Computer Networks (LCN)*, pp. 233–243, Sydney, NSW, Australia, 2020.

[37] M. Trik, S. P. Mozaffari, and A. M. Bidgoli, "Providing an adaptive routing along with a hybrid selection strategy to increase efficiency in NoC-based neuromorphic systems," *Computational Intelligence and Neuroscience*, vol. 2021, Article ID 8338903, 8 pages, 2021.

[38] A. Rezaee, O. A. Sheikhabad, and L. Beygi, "Quality of transmission-aware control plane performance analysis for elastic optical networks," *Computer Networks*, vol. 187, article 107755, 2021.

[39] H. Mozaffari, A. Houmansadr, and A. Venkataramani, "Blocking-resilient Communications in Information-Centric Networks using router redirection," in *2019 IEEE Globecom Workshops (GC Wkshps)*, pp. 1–6, Waikoloa, HI, USA, 2019.

[40] P. Rafiee and G. Mirjalily, "Distributed network coding-aware routing protocol incorporating fuzzy-logic-based forwarders in wireless ad hoc networks," *Journal of Network and Systems Management*, vol. 28, no. 4, pp. 1279–1315, 2020.

[41] M. Trik, S. Pour Mozafari, and A. M. Bidgoli, "An adaptive routing strategy to reduce energy consumption in network on chip," *Journal of Advances in Computer Research*, vol. 12, no. 3, pp. 13–26, 2021.

[42] B. Yaghooti, K. Safavigerdini, R. Hajiloo, and H. Salarieh, "Stabilizing unstable periodic orbit of unknown fractional-order systems via adaptive delayed feedback control," 2022, https://arxiv.org/abs/2208.06783.

[43] J. Akhavan and S. Manoochehri, "Sensory data fusion using machine learning methods for in-situ defect registration in additive manufacturing: a review," in *2022 IEEE International IOT, Electronics and Mechatronics Conference (IEMTRONICS)*, pp. 1–10, Toronto, ON, Canada, 2022.

Hindawi
Journal of Sensors
Volume 2023, Article ID 3507600, 11 pages
https://doi.org/10.1155/2023/3507600

Research Article

Cluster Head Selection for the Internet of Things Using a Sandpiper Optimization Algorithm (SOA)

S. Sankar[1], **Somula Ramasubbareddy**[2], **Rajesh Kumar Dhanaraj**[3], **Balamurugan Balusamy**[4], **Punit Gupta**[5], **Wubshet Ibrahim**[6] and **Rohit Verma**[7]

[1]*Department of Computer Science Engineering, Sona College of Technology, Salem, 636005 Tamil Nadu, India*
[2]*Department of Information Technology, VNR Vignana Jyothi Institute of Engineering & Technology, India*
[3]*School of Computing Science and Engineering, Galgotias University, India*
[4]*Shiv Nadar University, Delhi-National Capital Region (NCR), India*
[5]*School of Computer Science, University College Dublin, Ireland*
[6]*Department of Mathematics, Ambo University, Ambo, Ethiopia*
[7]*School of Computing, National College of Ireland, Ireland*

Correspondence should be addressed to Punit Gupta; punit.gupta@ucd.ie

Received 29 October 2022; Revised 7 December 2022; Accepted 5 April 2023; Published 25 April 2023

Academic Editor: V. Singh

In recent years, our life has become broader and faster by adapting to the Internet of Things (IoT). In IoT, the devices distributed globally that are connected to the Internet improve productivity in various sectors. The network plays an important role for transferring data to the sink node by collecting from all other nodes in IoT. The IoT requires energy saving since it is connected to resource-constrained devices. Energy preservation is a difficult challenge to improve network lifetime in IoT. Clustering is one of the key techniques to extend the network's life. In that, cluster head selection is one of the promising techniques to extend the lifespan of the IoT network. Many researchers proposed various cluster head (CH) selection techniques in IoT. However, inappropriate CH selection quickly degrades a network battery and creates an energy-hole problem in the network. This paper proposes a novel sandpiper optimization algorithm (SOA) to select CH among the networks. Later, the cluster is formed by using the Euclidean distance. The proposed SOA's accomplishments are compared to fitness value-based improved grey wolf optimization (FIGWO), particle swarm optimization (PSO), artificial bee colony-SD (ABC-SD), and improved artificial bee colony (IABC). The proposed SOA extends the network lifespan by 3-18% and increases the throughput by 6-10%. Thus, the proposed SOA increases the network lifetime and throughput and decreases the energy consumption among the nodes in the network.

1. Introduction

The Internet of Things (IoT) is a new research field that has drawn researchers from academia and industry. The IoT is a new network paradigm that changed the traditional human lifestyle to sophisticated life. Kevin Ashton coined the term IoT in 1999 [1–3]. The IoT is a network of things that are linked to the Internet and that communicate with one another by exchanging information. The IoT applications are smart home, smart farming, smart grid, smart healthcare, smart transportation, smart cities, etc. [4–6].

Wireless sensor networks (WSN) contain an interconnected sensors that can exchange information wirelessly about the environment. With recent technological developments, small sensors and actuators with minimal cost and power consumption are now accessible. Each sensor node is made up of modules for sensing, data processing, and data transfer [7–9]. The WSN applications are personal health monitoring, environment monitoring, etc. Some applications require a large number of nodes. As a result, maintaining a high number of nodes requires efficient, scalable algorithms. The WSN may change the

network structure dynamically due to its external causes or system designers. Therefore, it may suffer the routing process, delay, localization, etc. Hence, WSN requires redesigning a network to improve the overall network performance [10–12].

The WSN concepts can use various applications in real time. The network's nodes are powered by batteries. The energy consumed by wireless communication is proportional to the transmission distance; thus, nodes located in various places spend different amounts of energy [13, 14]. Thus, the network nodes maintain the uneven energy distribution. Routing is significant in the exchange of data between participants and sinks in WSN-based IoT. The routing problem suffers from the overall network lifetime. So, various routing protocols are proposed to improve network performance. The routing protocols are categorized based on network structure, node participation, and mode of functioning and clustering protocols [15, 16].

Clustering is one of the best choices for transmitting the data in WSN-based IoT due to its energy-saving capability. Clustering provides the data aggregation facility to reduce the redundant data transmission between cluster members (CMs) and sink in the network [17, 18]. In clustering protocol, the cluster head (CH) plays a significant role to choose the suitable CM among various other CMs. Numerous researchers proposed various CH selection strategies for finding the good CH in a network. However, optimization is the optimal strategy for determining the CH in a network.

The optimization algorithm is an iterative procedure that can repeatedly execute until it finds the best solution. Numerous researchers have developed a variety of optimization algorithms in the recent years, including ant colony optimization (ACO) [19], particle swarm optimization (PSO) [20], genetic algorithm (GA) [21], grey wolf optimization (GWO) [22], salp swarm algorithm (SSA) [23], krill herd (KH) optimization algorithm [24], and bat algorithm (BA) [25]. Nevertheless, many optimization methods require considerable convergence time during the CH selection process. Thus, the node's battery is depleting quickly after certain network rounds. In order to solve these issues, this paper suggests SOA to increase the network's life. Thus, the proposed SOA extends the network lifetime and throughput.

The primary contribution of this work is as follows:

(i) Design and development of SOA-CHS with the purpose of selecting the optimal CH in addition to extending the network's life and enhancing throughput

(ii) An extensive analysis was conducted with various optimization algorithms with respect to the proposed SOA-CHS algorithm to extend the network's lifespan

(iii) The simulation is run numerous times in order to evaluate the performance of the proposed SOA algorithm, and the sink node is placed in the center of the network region in order to examine its overall performance

(iv) To efficiently compute the fitness function, this paper makes use of the Euclidean distance, and the best sandpiper serves as CH throughout the given network round

The remainder of the paper is divided into the following sections: Section 2 outlines the related work on CH selection algorithms using optimization algorithms. Section 3 describes the proposed CH selection, which is based on the SOA algorithm. Section 4 elaborates on the results and discussion. Section 5 summarizes the paper and mentions future work.

2. Related Work

Wang et al. [26] suggested an improved artificial bee colony (IABC) algorithm to pick CH in IoT. In CH selection, the IABC algorithm considered the parameters, namely, CH energy, CH density, and CH location. The cluster is constructed using a fuzzy C-means algorithm. The CH is chosen using an IABC algorithm. In addition, the polling control mechanism is used to maintain the busy or idle states for intracluster communication. The IABC algorithm is compared to the PSO, ABC-SD, LACH-C, and FIGWO algorithms in terms of efficacy. Thus, it increased the lifespan of the network by 5-8%, respectively. However, the CH is far away from the sink; it consumes more energy than other nodes during the communication.

Alazab et al. [27] proposed a fitness averaged rider optimization algorithm (FA-ROA) for CH selection in IoT. The primary goal of this work is to decrease latency and extend the life of the network. The fitness function is computed utilising factors such as delay, energy, and distance. The proposed FA-ROA provides two sets of solutions. The first set is obtained by taking the average of the bypass rider values and follower rider values. The second set is based on the qualities of the riders who are attempting to overtake and attack. FA-ROA is being evaluated in comparison to ROA, SAWOA, WOA, MFO, and GFO to determine its effectiveness. As a result, the network's lifetime has been extended. However, it consumes more energy by considering the factors, namely, temperature, load, and data traffic. Also, it takes more time to converge during the CH selection. FA-ROA has improved the overall mean performance of alive nodes to 22.13% compared with existing optimization methods.

Bakshi et al. [28] adopted the glow-worm swarm optimization (GWSO) method for determining the CH in the Internet of Things. It provides the adaptive CH selection using the GWSO algorithm. Many existing algorithms form a cluster from the fixed nodes in the network. It is ineffective when there are a large number of dead nodes in the network. In the proposed clustering approach, the nodes are not fixed, and it changes the nodes in the cluster which is dynamic. Thus, it increases the lifespan of the network by 8-12%, respectively. Some nodes perished after a specific run owing to the cluster's dynamic nature.

Sankar et al. [29] proposed an efficient cluster-based routing protocol in IoT. It entails the selection of CHs as well as cluster formation. The sailfish algorithm is employed to pick the CH. The cluster is generated using the Euclidean distance. The SOA's effectiveness is evaluated in comparison to the EPSOCT, HCCHE, and IAB-COCT. The proposed SOA provides superior performance by means of network lifespan and throughput. In contrast to other algorithms, it has difficulties when it comes to trying to increase the number of rounds in the network, and it also takes significantly longer than other algorithms to converge when doing the CH selection process. The proposed SOA method improves network lifespan by 5-10% and decreases latency by 10-20%.

Zhang and Wang [30] proposed an energy-aware bioinspired algorithm in IoT to prolong the network's lifespan. This paper presented the PSO-WZ, which is adopted from the particle swarm optimization (PSO) algorithm. The CH is selected using PSO-WZ. Later, the division rule is used to form the cluster around the CH in the network. The simulation is conducted using MATLAB. The efficacy of the proposed PSO-WZ is compared to LEACH and PSO-C. The proposed PSO-WZ outperforms both LEACH and PSO-C by means of network lifetime and throughput. As a result, the network's lifetime has been improved by 5-10%. However, this type of algorithm is suitable for specific applications in WSN and IoT.

Khot and Naik [31] proposed particle-water wave optimization for CH selection in WSN. This paper presented the particle water wave optimization (PWWO) algorithm, which combines the PSO and water wave optimization (WWO) algorithms. The CH was selected using the PSO algorithm. The fitness value is computed using the parameters, namely, energy, trust, consistency factor, delay, and maintainability factor. After the CH selection, the path is established between CH and sink using the PWWO algorithm. The efficacy of the PWWO algorithm is compared to DICMLA and P-SMO. The proposed PWWO is provided superior performance by means of energy balancing index, network coverage, alive nodes, and left-out energy with values 0.9246, 99.9%, 144, and 0.666 J. As a result, the network's life span is extended. However, the fitness measure takes more time to compute the CH selection.

Shyjith et al. [32] proposed a dynamic CH selection in WSN to enhance the lifespan of the network. The selection of dynamic CH is a pivotal role in WSN to improve the network performances. This paper proposed rider-cat swarm optimization (RCSO) to pick the right CH in the WSN. The RSCO has setup, transmission, and measurement stages. The CH is elected using the RSCO algorithm. The threshold and CH selection are done on the basis of network parameters, namely, distance, delay, and energy. The data transmission stage ensures to exchange the data between CH and sink. Finally, during the measurement phase, the remaining energy of each node in the network is updated on a periodic basis. The proposed RCSO algorithm is compared to similar algorithms. The proposed algorithm improved the overall network performances such as throughput, alive nodes, and maximum provided energy with values 74.715%, 18, and 0.0351 J. During the CH selection process in the network, it takes some time for the network to converge.

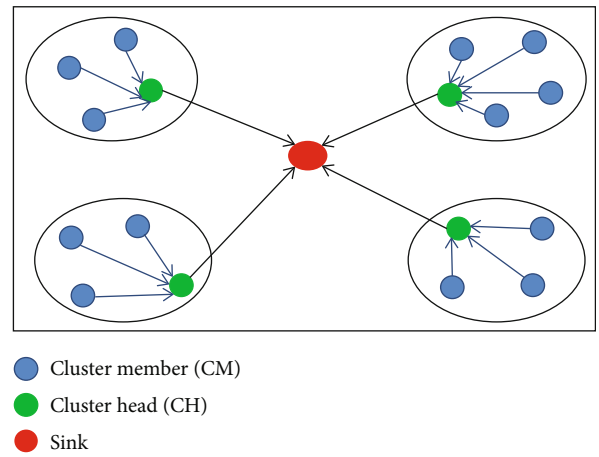

Figure 1: SOA network model.

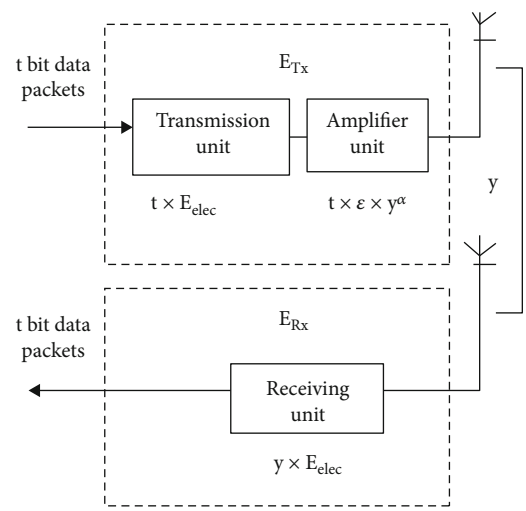

Figure 2: SOA energy model.

After conducting a review of related work, it was discovered that many optimization approaches for CH selection in WSN-based IoT have been presented. It is observed that the following limitations are as follows: (i) it takes more convergence time. (ii) It takes time to compute the fitness function. To solve these limitations, this paper proposes SOA-based CH selection to increase the network's lifespan.

3. System Model

3.1. Network Model. The network contains "*N*" nodes deployed randomly in monitoring areas. All the nodes are static and cannot move from one place to another after the deployment, and no intervention happens once the network is created. Each node in the network has a unique ID and is homogeneous with other nodes in terms of initial energy, processing, and communicational energies. The sink is located at the center of the network. The CH node is a focusing element in the network that affects the communication among sensor nodes. The CH selection algorithm runs in

Input: Network population is set of nodes "N".
Output: Best Sandpipers location act as CH.
1: while (true)
2: Initialize search agent S_p and movement of sandpiper S_m.
//migration phase.
3: Compute S_p and S_m for collision avoidance using Equations (4) and (5).
4: Compute best position of sandpiper using Equation (6).
5: Updating position of the best sandpiper using Equation (8).
// Attacking phase.
6: Create spiral behavior to attack the prey using Equation (9)-Equation (12).
7: Compute the fitness function Equation (16).
8: if sandpiper reaches its best search agent in the network then.
9: Best sandpipers act as CH
10: else.
11: Go to step 1
12: return CH.

Algorithm 1: CH selection using SOA.

the sink. The sink selects the optimal CH in the network nodes using SOA. Later, the clusters form on the basis of the Euclidean distance. The CH gathers the data and transfers the aggregated data to the sink. Figure 1 shows the SOA network model.

3.2. Energy Model. Figure 2 shows the SOA energy model which is followed by the standard WSN energy model [33]. The SOA follows the channel model according to the distance "y" between the transmitter "s" and receiver "r."

The amount of energy is consumed by "t" bits of data between transmitter "s" and receiver "r," and it is given in the following equation:

$$E_{\mathrm{TX}}(t, y) = tE_{\mathrm{elec}} + m\varepsilon \mathrm{y}(\mathrm{s}, \mathrm{r})^{\alpha} = \begin{cases} tE_{\mathrm{elec}} + t\varepsilon_{\mathrm{ft}} \mathrm{y}(\mathrm{s}, \mathrm{r})^2 \text{ where } \mathrm{y}(\mathrm{s}, \mathrm{r}) < \mathrm{y}_0 \\ tE_{\mathrm{elec}} + t\varepsilon_{\mathrm{mp}} \mathrm{y}(\mathrm{s}, \mathrm{r})^4 \text{ where } \mathrm{y}(\mathrm{s}, \mathrm{r}) \geq \mathrm{y}_0 \end{cases}, \quad (1)$$

where $t\varepsilon_{\mathrm{fr}}\mathrm{y}(\mathrm{s}, \mathrm{r})^2$ or $t\varepsilon_{\mathrm{mp}}\mathrm{y}(\mathrm{s}, \mathrm{r})^4$ is the energy consumption of the amplifier unit.

The threshold value y_0 is calculated in the following equation:

$$y_0 = \sqrt{\frac{\varepsilon_{\mathrm{ft}}}{\varepsilon_{\mathrm{mp}}}}, \quad (2)$$

where $\varepsilon_{\mathrm{ft}}$ is free space fading amplifier energy and $\varepsilon_{\mathrm{mp}}$ is multipath fading amplifier energy.

The receiver spends the amount of energy for receiving "y" bits from r to s, and its calculation is given in the following equation:

$$E_{\mathrm{RX}}(y) = yE_{\mathrm{elec}}, \quad (3)$$

where E_{elec} is the cost of circuit energy when transmitting or receiving one bit of data and y is the number of transmitted bits.

Table 1: Simulation setting and value.

Parameter	Value
Network area	$100 \times 100\mathrm{m}^2$
Sink location	(50, 50)
Number of sensor nodes	100, 200, and 300
Percentage of CH	5%
Control packet size	200 bits
Data packet size	4000 bits
ϵ_{fs}	100 PJ/bit/m^2
ϵ_{mp}	0.0013 PJ/bit/m^4

4. The Proposed Cluster Head Selection Using Sandpiper Optimization Algorithm

This paper proposes a sandpiper optimization algorithm (SOA) to choose the right CH in IoT [34]. The sink is situated in the network's center. The sink executes the SOA for choosing the best CH. Later on, a cluster is generated on the basis of the Euclidean distance between the nodes in the network.

Sandpipers are seabirds that reside in groups called colonies. They exploit their intellect to locate and attack their prey. It has two phases, namely, the migration and attacking phase.

4.1. Migration Phase (Exploration). It is a seasonal movement of sandpipers (S) from one location to another for eating food to gain energy. It follows the properties, and it is mentioned below.

(i) The sandpipers travel in a group during the migration phase. Initially, the entire sandpiper starts with different positions to avoid a collision

(ii) In a group, the entire sandpiper moves toward the sandpiper's optimum fitness value. The optimal

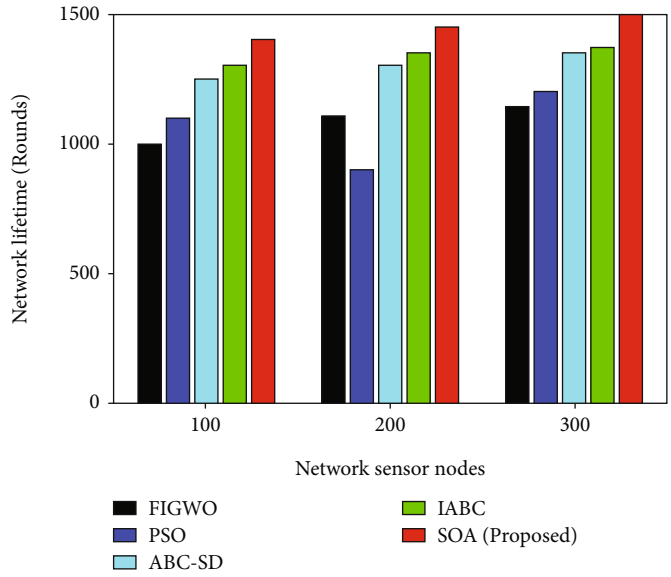

Figure 3: Network lifetime vs. network sensor nodes.

Table 2: Network lifetime vs. network sensor nodes.

Number of sensor nodes	Network lifetime (rounds)				
	FIGWO	PSO	ABC-SD	IABC	SOA
100	1000	1100	1250	1300	1400
200	1100	900	1300	1350	1450
300	1150	1200	1350	1375	1500

fitness value is the smallest in this case due to the minimization property

(iii) The sandpipers update their position based on the locations of the best sandpiper

The sandpipers need to satisfy three conditions during the migration phase.

4.1.1. Collision Avoidance. The sandpiper or search agent generates a new position without collision S_p, and it is given in the following equation:

$$S_p = S_m \times S_{cp}(t), \tag{4}$$

where S_m denotes the movement of the sandpiper, S_{cp} indicates the current position of the sandpiper, and t indicates the current iteration.

The movement of the sandpiper S_m is calculated, and it is given in the following equation:

$$S_m = S_{cf} - (t \times (S_{cf}/\text{Maximum}_{\text{iterations}})), \tag{5}$$

where S_{cf} indicates sandpiper control frequency which is decreased from 2 to 0 and t indicates the iteration which varies the values from 0 to maximum iterations.

4.1.2. Converge the Best Position of the Sandpiper. In order to converge, the sandpipers move to the direction from the current position S_{cp} to best sandpiper S_{best}, and its calculation is given in the following equation:

$$M_s = S_{BC} \times \left(S_{best}(t) - S_{cp}(t)\right), \tag{6}$$

where S_{BC} denotes the random variable which is based on the exploration.

The S_{BC} is calculated, and it is given in the following equation:

$$S_{BC} = 0.5 \times \text{rand}, \tag{7}$$

where rand is a random number that holds a value ranging between 0 and 1.

4.1.3. Updating the Position to the Best Sandpiper. Finally, the sandpiper updates its current position to the best sandpiper's position, and it is given in the following equation:

$$G_s = S_p + M_s, \tag{8}$$

where G_s indicates the gap between the sandpiper's position and the best location of the sandpiper.

4.2. Attacking Phase (Exploration). During the attacking phase, the sandpipers create the spiral behavior in the 3-dimensional plane, and its representation is given in the

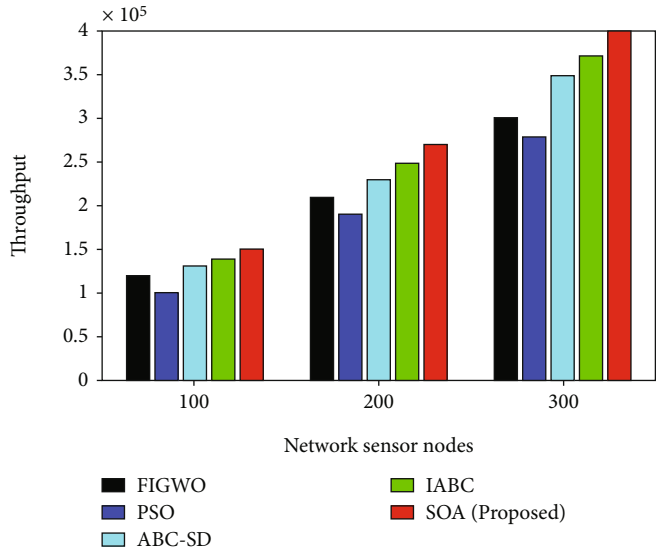

Figure 4: Throughput vs. network sensor nodes.

Table 3: Throughput vs. network sensor nodes.

Number of sensor nodes	Throughput (packets)				
	FIGWO	PSO	ABC-SD	IABC	SOA
100	120000	100000	130000	140000	150000
200	210000	190000	230000	250000	270000
300	300000	280000	350000	370000	400000

following equations:

$$X' = r \times \sin(j), \tag{9}$$

$$Y' = r \times \cos(j), \tag{10}$$

$$Z' = r \times j, \tag{11}$$

$$r = l \times e^{\mathrm{km}}, \tag{12}$$

where r indicates the radius of the spiral, j is a variable and its value between 0 and 2?, l and m are constant of the spiral value, and e is the base of the natural logarithm. Let l and m values set to be 1.

The updated position of the sandpiper $S_{p\_\mathrm{new}}(t)$ is calculated, and it is given in the following equation:

$$S_{p\_\mathrm{new}}(t) = \left(G_s \times \left(X' + Y' + Z'\right)\right) \times S_p(t). \tag{13}$$

4.3. Computing the Fitness Function. The average fitness denotes the average objective value of all the sandpipers in each iteration. The objective function is computed using the Euclidean distance. The SOA selection of the best position is based on the objective value which holds a minimum distance among various nodes in the respective iteration. The overall CH selection process is given in Algorithm 1.

4.3.1. Residual Energy (RER). The RER specifies total amount of energy available in network [35]. The following

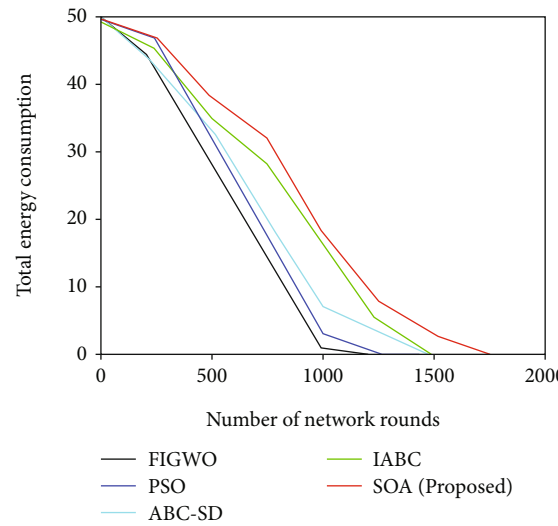

Figure 5: Total energy consumption vs. number of network rounds (network size is 100).

equation evaluates the remaining energy from spent energy and initial energy. It is given in the following equation:

$$\mathrm{RER}(n) = \frac{\mathrm{Energy}_{\mathrm{avail}}}{\mathrm{Energy}_{\mathrm{initial}}}, \tag{14}$$

where $\mathrm{Energy}_{\mathrm{avail}}$ and $\mathrm{Energy}_{\mathrm{initial}}$ are the currently available energy and initial energy of the network.

Table 4: Total energy consumption vs. number of network rounds (network size is 100).

Number of network rounds	Total energy (J)				
	FIGWO	PSO	ABC-SD	IABC	SOA
0	50	50	50	50	50
250	43	47	43	45	47
500	28	32	33	35	38
750	15	18	20	28	32
1000	1	3	7	5	8
1250	0	0	3	5	8
1500	0	0	0	0	0
1750	0	0	0	0	0
2000	0	0	0	0	0

4.3.2. Distance. The distance between the sensor node (n_i) and sink node is calculated using the Euclidean distance [36]. It is given in the following equation:

$$\mathrm{dis}(n_i, \mathrm{sink}) = \sqrt{\sum_{i=1}^{n} (\mathrm{sink} - n_i)^2}. \tag{15}$$

The current position of the sandpiper fitness function $S_{p\_\mathrm{new}}(t)_{\mathrm{fitness}}$ is calculated in the following equation:

$$S_{p\_\mathrm{new}}(t)_{\mathrm{fitness}} = 0.5 \times \left(1 - \mathrm{RER}\left(S_{p\_\mathrm{new}}(t)\right)\right) + 0.5 \times \left(1 - \mathrm{dis}\left(S_{p\_\mathrm{new}}(t)\right)\right). \tag{16}$$

4.4. Cluster Formation. The network contains "N" number of nodes which are formed into various clusters after CH selection using the Euclidean distance, and it is given in the following equation:

$$\mathrm{dist}\left(S_{\mathrm{pi}}, S_{\mathrm{pj}}\right) = \sqrt{\sum_{i=1}^{n} \left(S_{\mathrm{pj}} - S_{\mathrm{pi}}\right)^2}, \tag{17}$$

where S_{pi} and S_{pj} are two nodes in the network space.

5. Result and Discussions

The performance of proposed SOAs is evaluated in comparison to FIGWO, PSO, ABC-SD, and IABC. The MATLAB 2019a simulator is unutilized for simulation [37]. We have considered the number of nodes as 100, 200, and 300 to prove the performance of the proposed algorithm. The nodes are randomly distributed throughout the network. The simulation network area is $100 \times 100\,\mathrm{m}^2$. The overall effectiveness of the proposed SOA is assessed by means of network longevity, throughput, and overall energy usage and compared with state of art works under the same simulation. Table 1 provides the simulation setting and values.

5.1. Network Lifetime. Figure 3 shows the network lifetime with respect to the network sensor nodes. In this simulation, we have taken 100, 200, and 300 nodes. For a network size of 100, it is found that the number of nodes that are dead in FIGWO, PSO, ASC-SD, IABC, and SOA is 1000, 1100, 1250, 1300, and 1400, respectively. For a network of 200 nodes, the number of dead nodes in FIGWO, PSO, ASC-SD, IABC, and SOA is 1100, 900, 1300, 1350, and 1450, respectively. Similarly, for a network of 300 nodes, the number of dead nodes in FIGWO, PSO, ASC-SD, IABC, and SOA is 1150, 1200, 1350, 1375, and 1500, respectively. As previously stated, it is seen that the SOA enhances the lifetime in all the situations when the network size is 100, 200, and 300 nodes, respectively. It is due to the use of the sandpiper optimization algorithm, which reduces the amount of time required for convergence during the CH selection process.

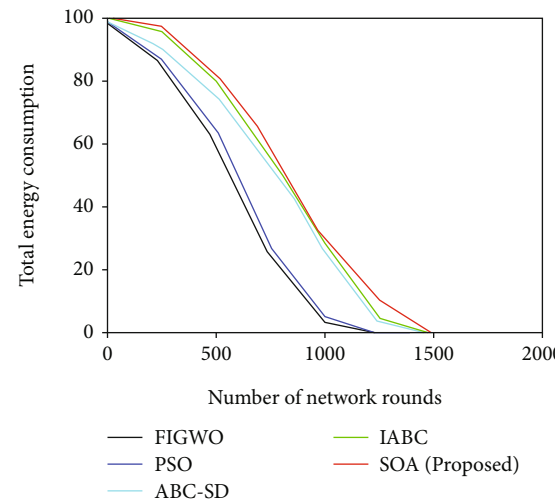

Figure 6: Total energy consumption vs. number of network rounds (network size is 200).

Table 2 shows the network lifetime with respect to the network sensor nodes. It is noticed that the SOA enhances the lifetime in all the situations when the network size is 100, 200, and 300 nodes, respectively. It is due to the use of the sandpiper optimization algorithm, which reduces the amount of time required for convergence during the CH selection process.

5.2. Throughput. Figure 4 shows the throughput with respect to the network sensor nodes. For a network size of 100, the throughput in FIGWO, PSO, ASC-SD, IABC, and SOA are

Table 5: Total energy consumption vs. number of network rounds (network size is 200).

Number of network rounds	Total energy (J)				
	FIGWO	PSO	ABC-SD	IABC	SOA
0	100	100	100	100	100
250	85	87	90	95	97
500	60	63	75	80	82
750	25	28	55	57	59
1000	3	5	25	27	29
1250	0	0	3	5	10
1500	0	0	0	0	0
1750	0	0	0	0	0
2000	0	0	0	0	0

120000, 100000, 130000, 140000, and 150000 packets, respectively. For the network size of 200, the throughput in FIGWO, PSO, ASC-SD, IABC, and SOA are 210000, 190000, 230000, 250000, and 270000 packets, respectively. For the network size of 300, the throughput in FIGWO, PSO, ASC-SD, IABC, and SOA are 300000, 280000, 350000, 370000, and 400000 packets, respectively. As previously stated, the amount of packets delivered from participants to the sink is large in SOA when compared to all other similar algorithms, including FIGWO, PSO, ASC-SD, and IABC. It is because of the proposed optimization algorithm's major consideration that it takes less time to reach convergence during the CH rotation. In addition, the proposed algorithm enhances the network's lifetime. This is the reason to increase the throughput more than all other algorithms.

Table 3 shows the throughput with respect to the network sensor nodes. As previously stated, the amount of packets delivered from participants to the sink is large in SOA when compared to all other similar algorithms, including FIGWO, PSO, ASC-SD, and IABC. It is because of the proposed optimization algorithm's major consideration that it takes less time to reach convergence during the CH rotation.

5.3. Total Energy Consumption. Figure 5 shows the overall energy use proportional to the network size. The total number of nodes is 100. For the 1000th network rounds, it is found that the overall energy consumption in FIGWO, PSO, ABC-SD, IABC, and SOA is 1 J, 3 J, 7 J, 15 J, and 18 J, respectively. The proposed SOA consumes less energy than other algorithms. This is mostly due to the consideration of the SOA algorithm, which has a shorter convergence time.

Table 4 shows the overall energy use proportional to the network size of 100 nodes. The proposed SOA consumes less energy than other algorithms. This is mostly due to the consideration of the SOA algorithm, which has a shorter convergence time.

Figure 6 shows the overall energy use proportional to the network size. The total number of nodes is 200. For the 1000th network round, it is observed that the total energy consumption in FIGWO, PSO, ABC-SD, IABC, and SOA are 3 J, 5 J, 25 J, 27 J, and 29 J, respectively. It should be emphasized that the suggested SOA consumes less energy than other algorithms. This is mostly owing to the use of the SOA algorithm, which has a faster convergence time.

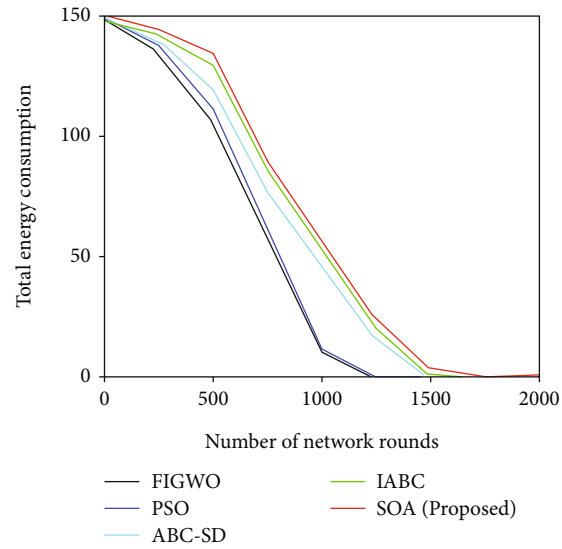

Figure 7: Total energy consumption vs. number of network rounds (network size is 300).

Table 5 shows the overall energy use proportional to the network size of 200 nodes. It should be emphasized that the suggested SOA consumes less energy than other algorithms. This is mostly owing to the use of the SOA algorithm, which has a faster convergence time.

Figure 7 shows the overall energy use proportional to the network size. The total number of nodes is 300. For the 1000th network round, it is observed that the total energy consumption in FIGWO, PSO, ABC-SD, IABC, and SOA are 10 J, 12 J, 45 J, 50 J, and 55 J, respectively. It should be emphasized that the suggested SOA consumes less energy than other algorithms. This is mostly owing to the use of the SOA algorithm, which has a faster convergence time.

Table 6 shows the overall energy use proportional to the network size of 300 nodes. It should be emphasized that the suggested SOA consumes less energy than other algorithms. This is mostly owing to the use of the SOA algorithm, which has a faster convergence time.

Table 6: Total energy consumption vs. number of network rounds (network size is 300).

Number of network rounds	Total energy (J)				
	FIGWO	PSO	ABC-SD	IABC	SOA
0	150	150	150	150	150
250	135	138	140	142	145
500	105	110	120	130	135
750	60	65	77	85	90
1000	10	12	45	50	55
1250	0	0	15	20	25
1500	0	0	0	0	3
1750	0	0	0	0	0
2000	0	0	0	0	0

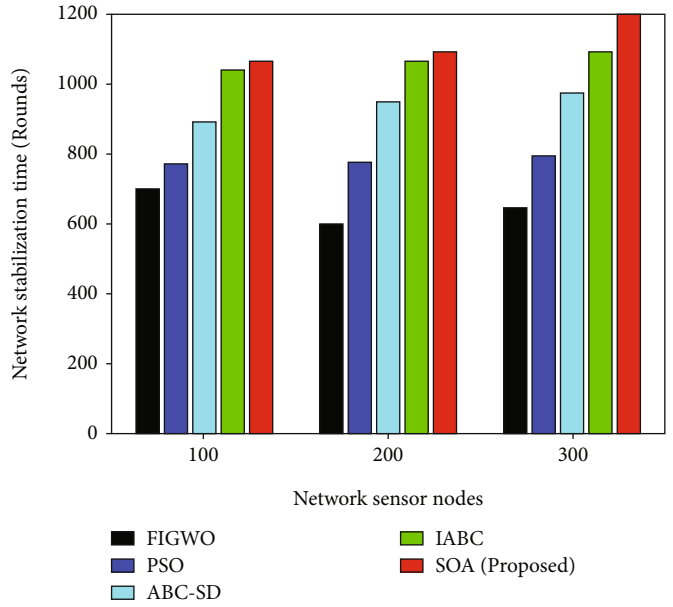

Figure 8: Network stabilization time vs. network sensor nodes.

Table 7: Network stabilization time vs. network sensor nodes.

Number of sensor nodes	Network stabilization time (rounds)				
	FIGWO	PSO	ABC-SD	IABC	SOA
100	700	775	900	1050	1075
200	600	780	950	1075	1100
300	650	800	975	1100	1200

5.4. Network Stabilization Time. Figure 8 indicates the network stabilization time with respect to network size. It is observed in Figure 8 that the proposed SOA algorithm which stabilizes the network is better than FIGWO, PSO, ABC-SD, and IABC. It is mainly due to fast convergence that consumes less energy in the network nodes. It is also noted that the proposed SOA algorithm is highly suitable for dense networks.

Table 7 indicates the network stabilization time with respect to network size. It is observed in Table 7 that the proposed SOA algorithm which stabilizes the network is better than FIGWO, PSO, ABC-SD, and IABC. For a network size of 300, the network is more stable in the 1200th round in SOA. It provides more stability and depletes energy more slowly than other existing algorithms.

6. Analysis and Discussion

The simulation results show that the proposed SOA algorithm provides superior performance than FIGWO, PSO, ABC-SD, and IABC. The simulation is conducted with different network sizes. The network sizes are varied in ranges

such as 100, 200, and 300. The sink is located at (50 m and 50 m). The placing of the sink location plays a major role in WSN and IoT networks. The sink is executed the CH selection using SOA. From the simulations, we observed that the total network lifetime and throughput are high at a network size of 300 compared to 100 and 200. It is also noticed that the proposed SOA stabilized the network at a range of 1200th round, for the network size of 300. Hence, we conclude that the proposed SOA outperforms in the dense network than other algorithms.

7. Conclusion and Future Work

Energy saving is critical in the IoT, which connects devices with limited resources. Clustering is the most effective method of extending the life of a network. As a result of the incorrect CH selection in the network nodes, the battery is depleted prematurely. To overcome this issue, this paper proposes a novel sandpiper optimization algorithm (SOA) which considers distance and residual energy parameters to form a cluster and choose the appropriate cluster head node to enhance the longevity of the network. The simulation is conducted with different network sizes, and the sink is placed at the center of the network area. The proposed SOA's accomplishments are compared to FIGWO, PSO, ABC-SD, and IABC. The proposed SOA extends the network lifespan by 3-18% and increases the throughput by 6-10%. As a result, the network's overall performance is improved.

In the future, real-time network nodes will be deployed to assess the effectiveness of SOA in comparison to similar optimization algorithms. In addition, we can also expand it for multiobjective problems or dynamic problems.

Data Availability

The dataset used for this work is randomly generated in MATLAB.

Conflicts of Interest

The authors declare that they have no conflicts of interest.

References

[1] S. Sennan, S. Ramasubbareddy, S. Balasubramaniyam, A. Nayyar, C. A. Kerrache, and M. Bilal, "MADCR: mobility aware dynamic clustering-based routing protocol in Internet of vehicles," *China Communications*, vol. 18, no. 7, pp. 69–85, 2021.

[2] A. Nauman, Y. A. Qadri, M. Amjad, Y. B. Zikria, M. K. Afzal, and S. W. Kim, "Multimedia Internet of things: a comprehensive survey," *IEEE Access*, vol. 8, pp. 8202–8250, 2020.

[3] S. Sennan, S. Ramasubbareddy, S. Balasubramaniyam, A. Nayyar, M. Abouhawwash, and N. A. Hikal, "T2FL-PSO: type-2 fuzzy logic-based particle swarm optimization algorithm used to maximize the lifetime of Internet of things," *IEEE Access*, vol. 9, pp. 63966–63979, 2021.

[4] W. A. Kassab and K. A. Darabkh, "A-Z survey of Internet of things: architectures, protocols, applications, recent advances, future directions and recommendations," *Journal of Network and Computer Applications*, vol. 163, article 102663, 2020.

[5] A. S. S. Thuluva, M. S. Somanathan, R. Somula, S. Sennan, and D. Burgos, "Secure and efficient transmission of data based on Caesar cipher algorithm for Sybil attack in IoT," *EURASIP Journal on Advances in Signal Processing*, vol. 2021, no. 1, p. 23, 2021.

[6] S. Roy, N. Mazumdar, and R. Pamula, "An optimal mobile sink sojourn location discovery approach for the energy-constrained and delay-sensitive wireless sensor network," *Journal of Ambient Intelligence and Humanized Computing*, vol. 12, no. 12, pp. 10837–10864, 2021.

[7] S. Palanisamy, S. Sankar, R. Somula, and G. G. Deverajan, "Communication trust and energy-aware routing protocol for WSN using D-S theory," *International Journal of Grid and High Performance Computing (IJGHPC)*, vol. 13, no. 4, pp. 24–36, 2021.

[8] D. Kandris, C. Nakas, D. Vomvas, and G. Koulouras, "Applications of wireless sensor networks: an up-to-date survey," *Applied System Innovation*, vol. 3, no. 1, p. 14, 2020.

[9] A. Shahraki, A. Taherkordi, Ø. Haugen, and F. Eliassen, "Clustering objectives in wireless sensor networks: a survey and research direction analysis," *Computer Networks*, vol. 180, article 107376, 2020.

[10] M. H. Kumar, V. Mohanraj, Y. Suresh, J. Senthilkumar, and G. Nagalalli, "Trust aware localized routing and class based dynamic block chain encryption scheme for improved security in WSN," *Journal of Ambient Intelligence and Humanized Computing*, vol. 12, no. 5, pp. 5287–5295, 2021.

[11] S. R. Nabavi, N. O. Eraghi, and J. A. Torkestani, "WSN routing protocol using a multiobjective greedy approach," *Wireless Communications and Mobile Computing*, vol. 2021, Article ID 6664669, 12 pages, 2021.

[12] D. K. Sah and T. Amgoth, "Renewable energy harvesting schemes in wireless sensor networks: a survey," *Information Fusion*, vol. 63, pp. 223–247, 2020.

[13] R. Priyadarshi, B. Gupta, and A. Anurag, "Deployment techniques in wireless sensor networks: a survey, classification, challenges, and future research issues," *The Journal of Supercomputing*, vol. 76, no. 9, pp. 7333–7373, 2020.

[14] G. Ravi and K. R. Kashwan, "A new routing protocol for energy efficient mobile applications for ad hoc networks," *Computers & Electrical Engineering*, vol. 48, pp. 77–85, 2015.

[15] S. El Khediri, W. Fakhet, T. Moulahi, R. Khan, A. Thaljaoui, and A. Kachouri, "Improved node localization using K-means clustering for wireless sensor networks," *Computer Science Review*, vol. 37, article 100284, 2020.

[16] M. Reddy and M. R. Babu, "Implementing self adaptiveness in whale optimization for cluster head section in Internet of things," *Cluster Computing*, vol. 22, no. S1, pp. 1361–1372, 2019.

[17] J. Amutha, S. Sharma, and S. K. Sharma, "Strategies based on various aspects of clustering in wireless sensor networks using classical, optimization and machine learning techniques: review, taxonomy, research findings, challenges and future directions," *Computer Science Review*, vol. 40, article 100376, 2021.

[18] J. Kennedy and R. Eberhart, "Particle swarm optimization," in *Proceedings of ICNN'95-international conference on neural networks (Vol. 4, pp. 1942-1948)*, Perth, WA, Australia, 1995.

[19] A. Malar, M. Kowsigan, N. Krishnamoorthy, S. Karthick, E. Prabhu, and K. Venkatachalam, "Multi constraints applied

energy efficient routing technique based on ant colony optimization used for disaster resilient location detection in mobile ad-hoc network," *Journal of Ambient Intelligence and Humanized Computing*, vol. 12, no. 3, pp. 4007–4017, 2021.

[20] A. Jari and A. Avokh, "PSO-based sink placement and load-balanced anycast routing in multi-sink WSNs considering compressive sensing theory," *Engineering Applications of Artificial Intelligence*, vol. 100, article 104164, 2021.

[21] S. Mirjalili and S. Mirjalili, "Genetic algorithm," in *Evolutionary Algorithms and Neural Networks*, pp. 43–55, Springer, Cham, 2019.

[22] E. Emary, H. M. Zawbaa, and A. E. Hassanien, "Binary grey wolf optimization approaches for feature selection," *Neurocomputing*, vol. 172, pp. 371–381, 2016.

[23] S. Mirjalili, A. H. Gandomi, S. Z. Mirjalili, S. Saremi, H. Faris, and S. M. Mirjalili, "Salp swarm algorithm: a bio-inspired optimizer for engineering design problems," *Advances in Engineering Software*, vol. 114, pp. 163–191, 2017.

[24] A. H. Gandomi and A. H. Alavi, "Krill herd: a new bio-inspired optimization algorithm," *Communications in Nonlinear Science and Numerical Simulation*, vol. 17, no. 12, pp. 4831–4845, 2012.

[25] X. S. Yang and A. H. Gandomi, "Bat algorithm: a novel approach for global engineering optimization," *Engineering Computations*, vol. 29, no. 5, pp. 464–483, 2012.

[26] Z. Wang, H. Ding, B. Li, L. Bao, and Z. Yang, "An energy efficient routing protocol based on improved artificial bee colony algorithm for wireless sensor networks," *IEEE Access*, vol. 8, pp. 133577–133596, 2020.

[27] M. Alazab, K. Lakshmanna, T. Reddy, Q. V. Pham, and P. K. R. Maddikunta, "Multi-objective cluster head selection using fitness averaged rider optimization algorithm for IoT networks in smart cities," *Sustainable Energy Technologies and Assessments*, vol. 43, article 100973, 2021.

[28] M. Bakshi, C. Chowdhury, and U. Maulik, "Energy-efficient cluster head selection algorithm for IoT using modified glowworm swarm optimization," *The Journal of Supercomputing*, vol. 77, no. 7, pp. 6457–6475, 2021.

[29] S. Sankar, S. Ramasubbareddy, F. Chen, and A. H. Gandomi, "Energy-efficient cluster-based routing protocol in Internet of things using swarm intelligence," in *2020 IEEE Symposium Series on Computational Intelligence (SSCI) (pp. 219-224)*, Canberra, ACT, Australia, 2020.

[30] Y. Zhang and Y. Wang, "A novel energy-aware bio-inspired clustering scheme for IoT communication," *Journal of Ambient Intelligence and Humanized Computing*, vol. 11, no. 10, pp. 4239–4248, 2020.

[31] P. S. Khot and U. Naik, "Particle-water wave optimization for secure routing in wireless sensor network using cluster head selection," *Wireless Personal Communications*, vol. 119, no. 3, pp. 2405–2429, 2021.

[32] M. B. Shyjith, C. P. Maheswaran, and V. K. Reshma, "Optimized and dynamic selection of cluster head using energy efficient routing protocol in WSN," *Wireless Personal Communications*, vol. 116, no. 1, pp. 577–599, 2021.

[33] S. D. Patil and P. S. Patil, "Performance evaluation of hierarchical clustering protocols in WSN using MATLAB," in *Intelligent Sustainable Systems*, pp. 65–81, Springer, Singapore, 2022.

[34] A. Kaur, S. Jain, and S. Goel, "Sandpiper optimization algorithm: a novel approach for solving real-life engineering problems," *Applied Intelligence*, vol. 50, no. 2, pp. 582–619, 2020.

[35] S. Sankar, P. Srinivasan, A. K. Luhach, R. Somula, and N. Chilamkurti, "Energy aware grid-based data aggregation scheme in routing protocol for agricultural Internet of things," *Sustainable Computing: Informatics and Systems*, vol. 28, article 100422, 2020.

[36] B. M. Sahoo, T. Amgoth, and H. M. Pandey, "Particle swarm optimization based energy efficient clustering and sink mobility in heterogeneous wireless sensor network," *Ad Hoc Networks*, vol. 106, article 102237, 2020.

[37] M. Sathyamoorthy, S. Kuppusamy, R. K. Dhanaraj, and V. Ravi, "Improved K-means based Q learning algorithm for optimal clustering and node balancing in WSN," *Wireless Personal Communications*, vol. 122, no. 3, pp. 2745–2766, 2022.

Hindawi
Journal of Sensors
Volume 2023, Article ID 8629849, 9 pages
https://doi.org/10.1155/2023/8629849

Research Article

Research on Ethical Issues and Coping Strategies of Artificial Intelligence Algorithms Recommending News with the Support of Wireless Sensing Technology

Xue Pan, Qixia Su, Lin Wei, and Lei Guo

Editorial Department of Chinese Journal of Endocrine Surgery, The First Affiliated Hospital of Chongqing Medical University, Chongqing, China

Correspondence should be addressed to Xue Pan; chongyiyiyuan@hospital.cqmu.edu.cn

Received 28 October 2022; Revised 6 March 2023; Accepted 23 March 2023; Published 20 April 2023

Academic Editor: Lei Chu

This study shows how well the wireless sensing technology may be used to forecast how people would react to AI- (artificial intelligence-) driven customization in digital news sites. We randomly picked participants to enroll in an online questionnaire. This study determines the ethical issues and coping strategies of AI-based news using sensor technology. The study proposed an improved naïve Bayes classification algorithm to forecast the acceptance of AI-driven news sites. Additionally, the technology acceptance framework characteristics continue to be crucial in determining adoption decisions. The findings demonstrate that the observed contingency has a large direct influence and an indirect effect that is moderated by improved user interaction and positivity in forecasting the acceptance of AI-driven news sites.

1. Introduction

Computer scientists, statisticians, and clinical entrepreneurs all agree that AI, and particularly machine learning, will play a crucial role in bringing about this change in healthcare. The phrase "artificial intelligence" (AI) is commonly used in the tech industry to refer to a computer's ability to reason, learn, and complete other tasks typically associated with human intelligence [1]. Adaptation, sensory comprehension, and communication are also part of this category of processes. Simply described, traditional computational algorithms are programs that, like an electrical calculator, have a single, well-defined output for a given set of inputs: "if this is the input, then this is the result." AI can learn the rules (function) by being exposed to extracting useful information from the massive amounts of digital data generated by healthcare delivery [2]. Artificial intelligence often takes the form of a hybrid system combining software and hardware components. In the realm of computer science, artificial intelligence focuses mostly on algorithms. Artificial neural networks (ANNs) are a theoretical backbone upon which to build AI programs. It is a representation of the human brain as a network of neurons linked together through weighted communication channels. Artificial intelligence employs a wide variety of methods to discover intricate nonlinear connections inside enormous data sets (analytics) [3]. Through training, machines learn to refine their algorithms and improve the reliability of their predictions (confidence).

The introduction of new technology brings with it the worry that it could become a fresh entry point for errors and security lapses. This is especially important to keep in mind because patients often interact with clinicians at extremely vulnerable points in their lives [4]. Cooperation between AI and clinicians, in which the former provides evidence-based management and the latter serves as a medical decision guide, has the potential to be highly beneficial if properly utilized (AI-health). It has the potential to improve healthcare delivery in areas such as diagnosis, medication discovery, epidemiology, individualized treatment, and organizational effectiveness. Researchers emphasize the need for a robust governance structure to safeguard human lives from all potential threats posed by AI solutions, including those arising from immoral behavior [5]. Unless the underlying

database and information technology system can limit, it may be challenging to use this type of data [6]. Nonetheless, AI in EHRs can be utilized to advance research, enhance treatment quality, and reduce waste. If properly developed and taught with sufficient data, in addition, AI can help create innovative models of healthcare delivery by studying clinical practice trends gleaned from electronic health data [7]. The function of AI in a content generation is not acknowledged. Even when an AI algorithm was utilized, the byline in news stories, for instance, seldom ever credits the algorithm. Without this notice, readers cannot infer from the text alone if an AI was utilized [8]. It might be challenging to offer acceptable and relevant news items to readers. The rationale is that the news domain has particular difficulties that set it apart from other application domains for recommender systems [9].

Future pharmaceutical research and development could benefit from the use of artificial intelligence (AI). Drug research might become less time-consuming and more cost- and data-efficient with the use of AI, which could use robots and models of genetic targets, pharmaceuticals, organs, diseases, disease progression, side effects, and therapeutic potency and safety [10]. Accelerating and improving the drug development process efficiency can be possible with the help of artificial intelligence (AI). There have been prior attempts to use AI to find treatments for the Ebola virus; however, like with any pharmacological trial, finding a promising lead molecule is no assurance of a safe and effective therapeutic [11]. The application of patient care could be greatly enhanced by implementing AI into clinical practice, but first, substantial ethical concerns must be addressed. Four primary ethical hurdles must be overcome before the medical applications of AI can reach their full potential [12]. Data privacy, security, algorithmic fairness, biases, and the ability to obtain users' informed consent before using their information are all crucial. It is not just a question of law but also of politics, whether or not AI systems can be regarded legitimate. It has been suggested that the ability to assign responsibility to a particular person or organization could be threatened by machines that operate following a set of undefined rules and learn new patterns of behavior. Concerns have been raised because of this ever-widening issue. Unfortunately, there may be no human to blame if something goes wrong when using AI. The potential for harm is unclear, and the increased reliance on robots will make it much harder to hold anyone accountable for their actions [13].

The use of modern computing techniques can obscure the reasoning behind an AIS's output, making meaningful scrutiny impossible [14]. To put it another way, the process by which an AIS produces its results is not transparent at all. Although the underlying computer science behind an AIS may be sophisticated, the implementation may be designed to be opaque to a clinical user who lacks the necessary technical training, while being intuitive to a trained expert in the subject. Emerging ML-HCAs cover a wide range of goals, potential implementations, and applications. ML-HCAs can be anything from entirely on their nonautonomous mortality projections, manual coverage and resource allocation, and artificial intelligence. Scientists should detail how these findings, together with their projections, might inform future research [15]. This information is essential for establishing the study's viability and for guiding future research. AI in healthcare must be flexible enough to deal with a constantly changing environment full of disruptions without compromising its ethical underpinnings, so that it may best serve the needs of its patients. However, a simple, crucial part of establishing the safety of any healthcare software is the capability to check the software and determine how the software might fail. In many respects, the process used to develop software is comparable to the addition of ingredients to a pharmaceutical or the incorporation of physiological mechanisms into a mechanical device [16]. Black box issues can arise with ML-HCAs since their inner workings are not always evident to evaluators, clinicians, or patients. It is incumbent upon researchers to detail how these findings, together with their projections, might inform future directions of the investigation [17]. The information is used to determine the final cost of the study and to guide similar efforts in the future.

Because of the intangibility of the digital economy and the upheaval that comes with quickly advancing technology, psychiatry is facing new ethical challenges as a result of its increasing reliance on computers. Classifying people based on large amounts of data may have far-reaching, unintended consequences outside of medicine [18]. Applications or medical websites with low-quality information all carry the risk of adverse health outcomes, including the postponement of necessary medical attention. Public and private data, as well as medical and nonmedical data, no longer have the clear distinctions they previously did in our society. Doctors may harm patients with mental illness by suggesting they employ technology without first addressing the additional ethical considerations that arise from doing so [19]. Several questions will be posed to facilitate the discussion of these ethical concerns. There is a wide gap between patients in terms of their exposure to and proficiency with digital tools, technical proficiency, Internet safety, and familiarity with the digital economy. The "digital divide" refers to the gap in Internet access that exists between people with different levels of income, education, and age, as well as the telecommunications infrastructure. Internet and smartphone use among the elderly and people having both mental and physical impairments is much lower than the general population, although access has substantially grown over the previous decade around the world [20]. Sometimes, the impoverished only have spotty, unstable access to the Internet. Differences in technological competence, online literacy, and usage patterns are now reflected in the digital divide. It is commonly considered that millennials and Gen Zers alike are fluent in all things digital. But even among people who have never known a world without computers and smartphones, there is a wide range of proficiency online. The broad adoption of digital technology like cell phones and video games can be attributed to their simplicity of use for those with no technical training. From learning the ins and outs of technology to mastering its use to accomplishing one's goals and resolving one's problems, the definition of "digital competency"

has expanded [21]. Self-assessments of technical proficiency tend to be inaccurate, and even someone who is comfortable with technology and knows how to use it effectively may be unfamiliar with the concepts behind today's interconnected digital economy.

Self-diagnosis on the Internet is becoming increasingly common, and it may have particular appeal for those who feel they have a mental illness due to stigma, a need for privacy, and a need to save money. More than 50 million people use the iTriage app each year to check their symptoms and find a doctor, and one-third of all American adults use the Internet to make their diagnoses. Online symptom checkers for mental health conditions are plentiful [22]. Online ads for direct-to-consumer (DTC) genetic and another laboratory testing may also be tailored to individual patients. In certain online mental health groups, diagnosis is a common topic of conversation. Self-diagnosis is a common practice among certain patients, and this can lead them to attempt self-treatment. Nowadays, it is possible to get just about any prescription medication from an Internet drugstore. Among the most commonly supplied types of pharmaceuticals by unregulated online pharmacies, those used to treat mental health issues are among the most problematic. Many fake pharmacy websites look exactly like those of actual pharmacies because they are professionally developed and include fake quality seals [23]. Approximately one-third of people with mental illness use some kind of dietary supplement, many of which are self-selected, acquired online, and linked to exaggeration. Few of these apps were evaluated, and those that did only saw limited brief pilot programs. Certain health-related websites engage in deceptive practices or advocate for potentially harmful actions. To give just one example, the company Lumosity was penalized for making false promises about how playing video games and using mobile apps may improve users' brainpower [24]. Some Alzheimer's disease self-tests available online lack validity and reliability and violate professional ethics guidelines. Abuse-producing substances like opioids, stimulants, and hallucinogens can all be purchased online. Some online resources openly advocate harmful activities including self-harm and eating disorders. Some people even attempt to treat themselves by constructing potentially lethal transcranial direct current stimulation devices according to online tutorials [25].

With the rise of IoT devices, emotion recognition software is commonly considered the next logical step in the development of computing technology. In this future, we will not need computers or gadgets since we will have access to AI-powered cognitive assistants that can communicate with us in our native tongues, interpret our facial expressions, voice, and written emotions and provide us with constant support will form the basis of emotion recognition in the future [26]. Users will need fewer technical abilities. There is a desire for personalized medical aides for both doctors and patients. Recently received or applied for patents allow for the inference of mood and emotion from data collected from online and mobile platforms. Algorithms based on the massive amounts of data generated by people's everyday online activities are increasingly being used by businesses and governments to profile citizens, gauge their emotional states, and anticipate their future actions. Publicly available social media data sets are being used by researchers in fields as diverse as computer science, linguistics, and psychology to make predictions about things like depression, suicide risk, psychopathy, psychological illnesses, and the severity of illness of the mind [27]. The medical profession is investigating the use of pilot studies for bipolar illness, schizophrenia, and depression that have been conducted using passive data collecting in people. Information gathered from a smartphone's sensor, including where and when the device was used, how the user moved around, how they spoke, and what they said, as well as the contents of the smartphone can all be used to inform the development of parameters which are all used in academic and medical research. The commercial profiling of consumers and the medical monitoring of patients may appear similar at first glance. However, commercial enterprises' motivation for utilizing algorithms to describe emotional or mental conditions is profit rather than patient care. In the United States, most algorithms utilized by business entities are considered trade secrets and hence cannot be independently validated. Publicly available data did not permit replication of the published results, as demonstrated by Google Flu Trends (a flu-tracking tool). However, some businesses may indicate that they employ improved versions of published algorithms, but these businesses do not have the necessary training or credentials to offer medical diagnoses or recommendations. A "propensity to seek for depression," as determined by an algorithm from a for-profit company, should not be taken as a medical fact or used against a person in the context of employment, promotion, or credit. Companies are pouring a lot of money into this field, so in the future algorithms we will be able to better understand human emotions and mental states. The market for emotion recognition and detection was predicted to grow to $22.65 billion worldwide by 2020. The paper [28] developed a multimodal content retrieval framework that uses customization and relevance feedback approaches to improve the Quality of Experience (QoE) for end users by obtaining and presenting multimedia information that is specific to their demographics and other preferences. From the article [29], efficient relevance feedback (RF) methods, in addition to personalization strategies, may improve the user experience by delivering results that are more in line with the user's preferences. The paper [30] suggested vector-space models, to which this system is similar and to which it is applicable failed to handle queries with scalar values—for example, they cannot bring up movie scenes with fewer than two actors—a problem solved in our integrated framework through the use of exact match queries and a modified relevance feedback mechanism. The paper [31] proposed an interest-driven, multimedia retrieval framework to compute the semantic and content-level similarity between media items and query descriptor vectors. The paper [32] uses quality of service (QoS) evaluation indicators such as packet loss rate, latency, jitter, and throughput. These qualities of service measurements reveal the effect on the network's

quality but do not represent the user's experience. As a result, these QoS criteria cannot account for the intangibles that contribute to the quality of life for individuals.

2. Materials and Method

The results show that better user engagement and positivity reduce the impact of observed contingency on predicting acceptance of AI-driven news sites and that the direct influence of observed contingency is considerable. Here, we present an enhanced version of the naïve Bayes classifier for gauging interest in AI-powered media outlets.

2.1. Data Analysis

2.1.1. Preprocessing Using Min-Max Normalization. To normalize a property, the values are transformed such that they all fall within a predetermined interval. About classification frameworks, normalization is a crucial step when using computational models or proximity measures. The training phase of classification using a neural network back propagation approach may go more rapidly if the input values for each measured attribute in the training set are normalized. The purpose of min-max normalization is to make the original data linear. Assume that the lowest and maximum values for attribute X are min X and $maxX$. B value of B, a_x, is mapped to a_x in the range [new- min x, new- max X] by using the following formula:

$$\ddot{B}_y = \left(B_y - \min x\right)/(\max x - \min x) * \left(new_{\max x} - new_{\min x}\right) + new_{\min x} \quad (1)$$

A data set's original values retain their correlation after min-max normalization. If a later normalization input scenario takes X outside of the starting date range, the risk of an "out-of-bounds" error rises.

2.1.2. Feature Extraction Using Principle Component Analysis (PCA). To reduce the number of variables while preserving as much information as feasible, principal component analysis (PCA) applies a series of orthogonal linear transformations to the original variables. Let M be an $n \times s$ data matrix, where n and s represent the number of factors and observations, accordingly. For simplicity, we will assume that the means of the whole Y column are 0. $U_1 = \sum_y^t = \alpha_1$ y M_y, where $\alpha_1 = (\alpha_{11}, \cdots, \alpha_1{}^s)$ and s is the definition of the first principal component. s is selected to maximize V_1'r variance, i.e.,

$$\propto_1 = \arg \max_{\propto} \propto^s \widehat{\sum} \propto \text{ subject to } \|\propto_1\| = 1, \quad (2)$$

with $\Sigma = (M^P M)/n$. All of the remaining key ingredients are defined below, in order:

$$\propto_{k+1} = \arg \max_{\propto} \propto^s \widehat{\sum} \propto \quad (3)$$

depending on

$$\|\propto\| = 1 \text{ and} \propto^s \propto_h = 0, \forall 1 \le g \le h \quad (4)$$

According to this definition, the first h k eigenvectors are the first k loading vectors.

Since SDB is formulated in terms of eigen decompositions to determine AI-driven news using sensor techniques, it is related to N's singular value decomposition. Let us pretend N stands for TRUE.

$$N = UOG^s, \quad (5)$$

where U and G are orthonormal matrices of $m \times p$ and $p \times p$ rows and columns, respectively, and E is a diagonal matrix with diagonal components $p_1, \ldots, pw$ in descending order. K is the loading matrix of the main components because the columns of K are the eigenvectors. We can see that $V_g = u_g E_g$ since $NG = UO$, U_K is the K^{th} column of U. Recognize that the RUO is a good low-rank estimate of the data matrix.

In the various geometrical understanding of SDB, straight manifolds are the best fit for information. This concept aligns with how SDB is built. Make iy the y^{th} row in X. Take the first h main components together, which equals $h_k = [h_1|\cdots|h_k]$. h_k is a $r \times g$ orthonormal matrix by definition. Each observation should be projected to the linear region covered by $\{h1, \cdots, hk\}$. The projected data are w_g N_y, $1 \le y \le n$ and the projection operator is $W_k = h_g hs$. By reducing the overall g_2 approximation error, one may determine the optimal projection.

$$\min_{A_h} \sum_{y=1}^{n} \left\| j_y - A_g A_g^s j_j \right\|^2. \quad (6)$$

Parameters in applications may be specified in a variety of length scales and measurement systems. As a consequence of parameter standardization, the marginal variance of every variable is equal to 1. Principal component analysis using this approach will provide both the raw data's correlation coefficient and the unified data's covariance matrices. Keep in mind that the eigenvalues of the covariance matrix and the correlation matrix are not always the same.

2.1.3. Prediction Using the Improved Naïve Bayes Classification Algorithm. Under the concepts of consistency and unbiasedness of an estimate, a greater classification rate may be attained by expanding the learning field (sample) size within the same data set (population) using the sensor technique. Our INBC only updates the learning field to provide the best performance using the previously evaluated data. For instance, we have a basic training data set (the first phase of data) that consists of daily meteorological observations over the last 10 years. Likewise, the study predicts the technology of acceptance of digital media news using sensor techniques. To progressively improve the initial training data set, we then split the second phase of data (a few previously validated weather records) into some predetermined

Calculate $N(C_k V_{Ai,j'})$, $N(V_{Ai,j'})$ and $P(C_k)$ from the first phase of data.
Prompt for the *StepSize*, a fixed number of data records, for evaluating the performance of AI-driven news using sensors.
Initialize $start - pos = 0$; $end - pos = 0$; $index = 1$
Do
  Set $start - pos = 0$; $end - pos + 1$
  Set $end - pos = index \times StepSize$
  Prompt for the ***NB*** Approx. (***RF*** from Eqn (2) or ***IPD*** from Eqn (3))
  For each $k = 1$ to P **do**
  Begin
    Calculate $P(C_k|V_{A,.j''}) = P(C_k)\prod_{i=1}^{n}\prod_{j''=start-pos}^{end-pos}(NB\,Approx./P(C_k))$
    Find the highest conditional probability of $A_{i\in[1,n]}$
  End
  Update $N(C_k V_{Ai,j'})$, $N(V_{Ai,j'})$and $P(C_k)$ with the second phase of data
  Set $index = index + 1$
While $end - pos < m_2$
For the rest of each $start - pos \le j'' \le m_2$
  Calculate $P(C_k|V_{A,.j''}) = P(C_k)\prod_{i=1}^{n}\prod_{j''=start-pos}^{m_2}(NB\,Approx./P(C_k))$for all k
  Find the highest conditional probability of $A_{i\in[1,n]}$
Evaluate the classification rate of all k and the overall performance.

Algorithm 1: The improved naïve Bayes classification algorithm.

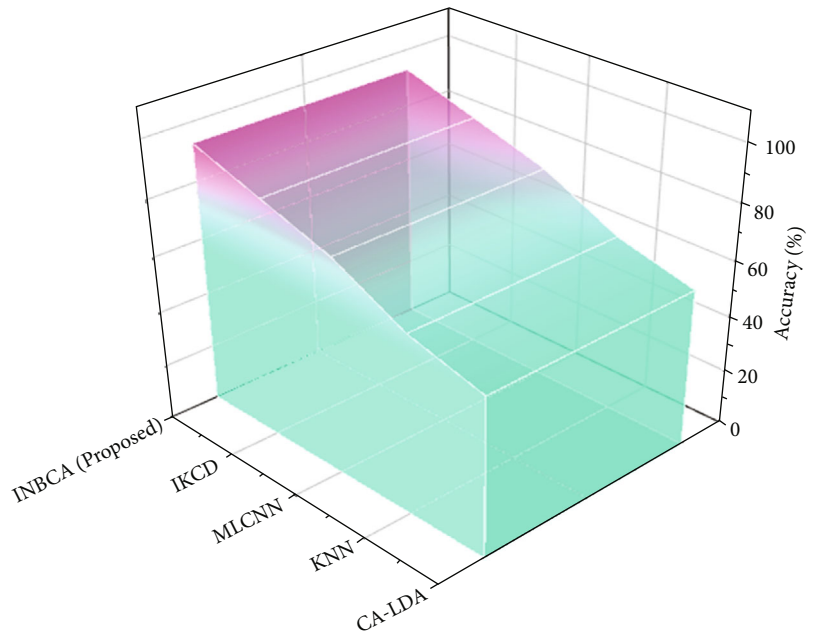

Figure 1: Accuracy.

Table 1: Accuracy.

Models	Accuracy (%)
CA-LDA	57
KNN	64
MLCNN	77
IKCD	85
INBCA (proposed)	93

data sets (step size). Such a new training model can calculate the classification rate of the third phase of data (some updated and tested). The combined effects of the second and third waves of data will be determined, and they participate in the discussion on ethical AI management. They highlight both theoretical and practical issues with AI ethical management and provide a tentative research agenda for the future. Naïve Bayes is one of the quickest and easiest machine learning techniques for forecasting a collection of data sets. It applies to classes with two categories or more. When compared to other algorithms, it is superior at

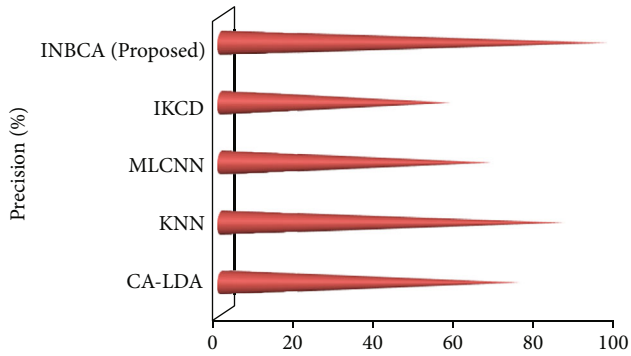

Figure 2: Precision.

Table 2: Precision.

Models	Precision (%)
CA-LDA	74
KNN	85
MLCNN	67
IKCD	57
INBCA (proposed)	96

making predictions across several classes [33]. Algorithm 1 demonstrates how our INBC approach using the sensor approach will enhance classification precision and speed.

3. Results and Discussion

The results show that better user engagement and positivity reduce the impact of observed contingency on predicting acceptance of AI-driven news sites and that the direct influence of observed contingency is considerable. With the help of sensor techniques, the influence of predicting acceptance will be derived. Here, we present an enhanced version of the naïve Bayes classifier for gauging interest in AI-powered media outlets.

A model's ability to correctly classify data may be evaluated using many different performance criteria. The article used a wide variety of measures, not only accuracy, precision, recall, and F1 score. For argument, let us say that the values of the class variables in a binary classification job may be thought of as either positive (P) or negative (N). Cases that the model correctly classified as positive (P) are called true positives (TP), whereas those classified incorrectly as negative (N) are called false negatives (FN). True negative (TN) cases are those that the model properly identifies as negative (N) cases, whereas false positive (FP) cases are those that a model incorrectly identifies as positive (P) cases.

Results for various performance metrics, including accuracy, precision, recall, and F1 score, may be given in equations (7)–(10).

$$\text{Accuracy} = \frac{(B + A)}{(B + A + D + C)}, \tag{7}$$

$$\text{Precision} = \frac{A}{A + C}, \tag{8}$$

$$\text{Recall} = \frac{A}{A + D}, \tag{9}$$

$$\text{F1 score} = 2 * \frac{\text{precision} * \text{recall}}{\text{precision} + \text{recall}}, \tag{10}$$

where A is true positive, B is true negative, C is false positive, and D is false negative.

By using the above equations, we can determine the accuracy and precision of the existing methodologies with the proposed model. Accuracy is used to evaluate a classifier based on how well its predictions match the target label. You may also express this idea by looking at the percentage of correct answers across all examinations. Equation (7) displays the accuracy. Figure 1 shows a comparison between the accuracy of the conventional and suggested approaches. When compared to the standard method, the one proposed yields better results. Accuracy for CA-LDA [34] is at 57%, KNN [35] at 64%, MLCNN [36] at 77%, IKCD [37] at 85%, and the proposed INBCA at 93%.

Accuracy is measured in many ways, but one of the most crucial is precision. As stated in equation (10), it is calculated as the proportion of properly classified instances to the total number of occurrences of predictively positive data. Table 1 represents a numerical representation of accuracy.

Figure 2 displays the results of a comparison between the precision of the conventional and the suggested approaches. Compared to the proposed technique, the precision of previous approaches like CA-LDA, KNN, MLCNN, and IKCD ranged from 74% to 85%. We obtain a 96% degree of precision in the proposed INBCA. Table 2 denotes the numerical representation of precision.

A classifier's "recall," or the percentage of instances accurately labeled "positive," is a useful metric to have. A recall is used as an indicator of performance to choose the best model. Figure 3 shows a contrast between the recall of currently used and suggested methods. The suggested technique offers more accuracy than the standard approach. CA-LDA has 53%, KNN has 85%, MLCNN has 74%, IKCD has 88%, and the proposed INBCA has 97%. Table 3 denotes the numerical representation of recall.

By averaging the accuracy and recall ratings, we get the F1 score. This calculation will help find out how many false positives and negatives there are. Figure 4 displays the F1 score difference between the conventional and proposed methods. The proposed method outperforms the state-of-the-art strategies on the F1 score. The F1 score for the traditional approaches was 55 percent for CA-LDA, 84 percent for KNN, 64 percent for MLCNN, and 73 percent for IKCD. The F1 score for the recommended INBCA is 96% as defined in Table 4.

Computational complexity is a metric for how much time and memory (resources) a certain algorithm uses when it is executed. The computational complexity difference between the proposed and standard approaches is shown in Figure 5. The suggested approach performs better in terms of computational complexity than state-of-the-art

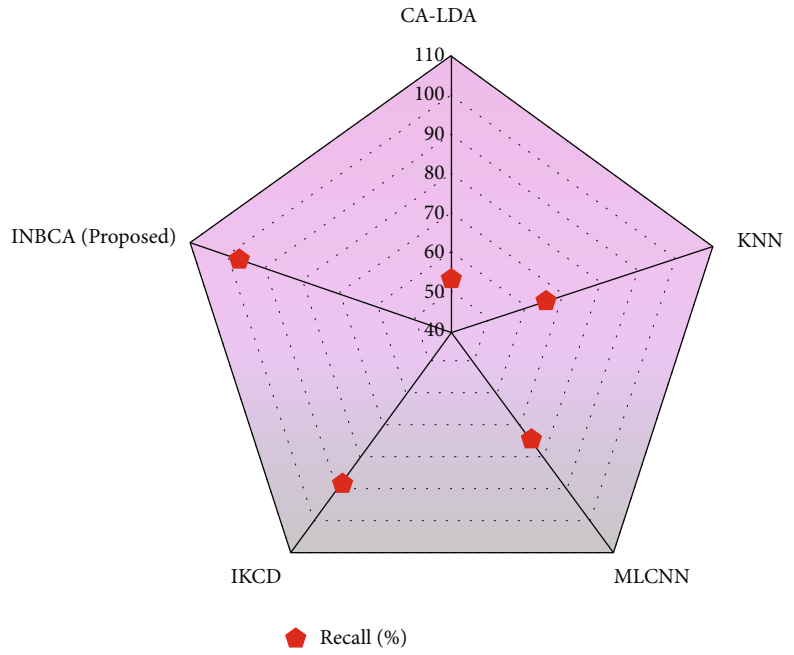

Figure 3: Recall.

Table 3: Recall.

Models	Recall (%)
CA-LDA	53
KNN	65
MLCNN	74
IKCD	88
INBCA (proposed)	97

Table 4: F1 score.

Models	F1 score (%)
CA-LDA	55
KNN	84
MLCNN	64
IKCD	73
INBCA (proposed)	96

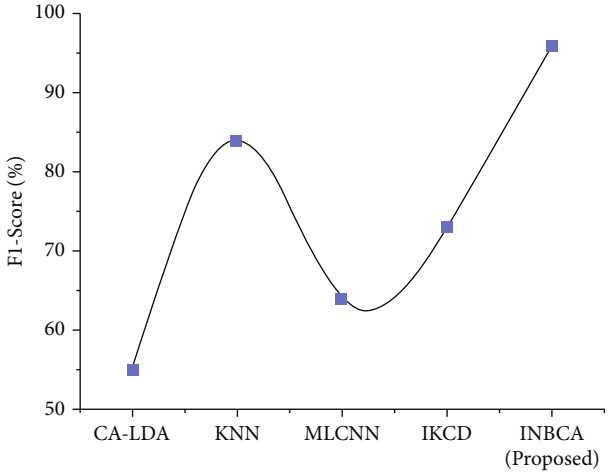

Figure 4: F1 score.

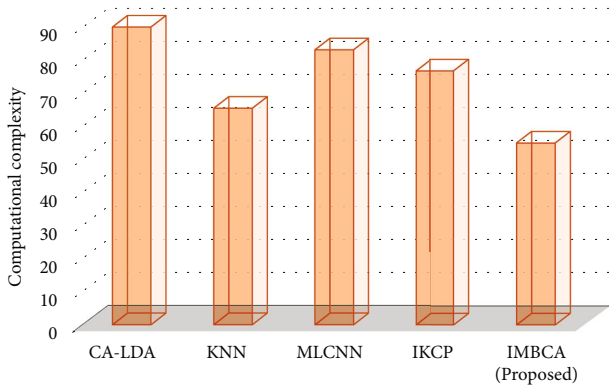

Figure 5: Computational complexity.

Table 5: Computational complexity.

Models	Computational complexity
CA-LDA	90
KNN	66
MLCNN	83
IKCP	77
INBCA (proposed)	55

methods. The standard techniques of computational complexity were CA-LDA for 90 percent, KNN for 66 percent, MLCNN for 83 percent, and IKCD for 77 percent. The suggested INBCA's computational complexity is 55%, as shown in Table 5.

From this study, it is observed that the proposed model has provided high accuracy and precision in evaluating the

acceptance behavior of individuals using sensor techniques. Effective interaction and optimism minimize the influence of observed contingency on the adoption of AI-driven news sites. This method also helps in determining the ethical challenges and coping strategies in the adoption of technology. Naïve Bayes is a simple but crucial probabilistic model. Smart machines, which are not artificial intelligence, operate only on algorithms and do not need training data. This note will utilize it as a running example. Specifically, we first address Maximum-Likelihood (ML) estimate in the situation of completely seen data, and then we analyze the Expectation Maximization (EM) technique in the case of partially observed data, where the labels for instances are absent [38].

4. Conclusion

This research demonstrates the potential utility of wireless sensing technologies for estimating readers' reactions to AI- (artificial intelligence-) driven personalization on digital news sites. We used a random selection procedure to recruit people to take part in an online survey. Using sensor technology, this research explores the ethical challenges and coping strategies presented by AI-based news and potential solutions to those challenges. This research suggested an improved version of the naïve Bayes classification approach (INBCA) to anticipate how people will react to AI-driven news websites. The results show that better user interaction and optimism reduce the effect of observed contingency on foretelling the acceptance of AI-driven news sites.

Notations

E: Diagonal matrix
N: Singular value decomposition
G: Orthonormal matrices
K: Loading vectors
g_2: Approximation error.

Data Availability

Data are available from the corresponding author upon request.

Conflicts of Interest

The authors declare that they have no conflict of interest.

Acknowledgments

The study was supported by Humanities and Social Sciences Research Project of Chongqing Municipal Commission of Education, China (Grant No. 22SKGH077).

References

[1] J. Morley and L. Floridi, "An ethically mindful approach to AI for health care," *SSRN Electronic Journal*, vol. 395, no. 10220, pp. 254-255, 2020.

[2] L. Drukker, J. A. Noble, and A. T. Papageorghiou, "Introduction to artificial intelligence in ultrasound imaging in obstetrics and gynecology," *Ultrasound in Obstetrics & Gynecology*, vol. 56, no. 4, pp. 498–505, 2020.

[3] G. Rong, A. Mendez, E. Bou Assi, B. Zhao, and M. Sawan, "Artificial intelligence in healthcare: review and prediction case studies," *Engineering*, vol. 6, no. 3, pp. 291–301, 2020.

[4] D. D. Miller and E. W. Brown, "Artificial intelligence in medical practice: the question to the answer?," *The American Journal of Medicine*, vol. 131, no. 2, pp. 129–133, 2018.

[5] H. Smith, "Clinical AI: opacity, accountability, responsibility and liability," *AI & Society*, vol. 36, pp. 535–545, 2021.

[6] M. Taddeo and L. Floridi, "How AI can be a force for good," *Science*, vol. 361, no. 6404, pp. 751-752, 2018.

[7] A. Arieno, A. Chan, and S. V. Destounis, "A review of the role of augmented intelligence in breast imaging: from automated breast density assessment to risk stratification," *American Journal of Roentgenology*, vol. 212, no. 2, pp. 259–270, 2019.

[8] C. Longoni, A. Fradkin, L. Cian, and G. Pennycook, "News from generative artificial intelligence is believed less," in *2022 ACM conference on fairness, accountability, and transparency*, pp. 97–106, Seoul, Republic of Korea, 2022.

[9] S. Raza and C. Ding, "News recommender system: a review of recent progress, challenges, and opportunities," *Artificial Intelligence Review*, vol. 55, pp. 749–800, 2022.

[10] J. De Fauw, J. R. Ledsam, B. Romera-Paredes et al., "Clinically applicable deep learning for diagnosis and referral in retinal disease," *Nature Medicine*, vol. 24, no. 9, pp. 1342–1350, 2018.

[11] G. Kunapuli, B. A. Varghese, P. Ganapathy et al., "A decision-support tool for renal mass classification," *Journal of Digital Imaging*, vol. 31, no. 6, pp. 929–939, 2018.

[12] Ó. Álvarez-Machancoses and J. L. Fernández-Martínez, "Using artificial intelligence methods to speed up drug discovery," *Expert opinion on drug discovery*, vol. 14, no. 8, pp. 769–777, 2019.

[13] D. Sharma, S. Verma, and K. Sharma, "Network topologies in wireless sensor networks: a review," *International Journal of Electronics & Communication Technology, IJECT*, vol. 4, no. 3, pp. 93–97, 2013.

[14] R. Kumar, P. Kumar, R. Tripathi, G. P. Gupta, T. R. Gadekallu, and G. Srivastava, "Sp2f: a secured privacy-preserving framework for smart agricultural unmanned aerial vehicles," *Computer Networks*, vol. 187, article 10781, 2020.

[15] A. Khan, S. Aziz, M. Bashir, and M. U. Khan, "IoT and wireless sensor network based autonomous farming robot," in *In Proceedings of the International Conference on Emerging Trends in Smart Technologies (ICETST)*, pp. 1–5, Karachi, Pakistan, 20220.

[16] C. T. Chen, C. C. Lee, and I. C. Lin, "Efficient and secure three-party mutual authentication key agreement protocol for WSNs in IoT environments," *PLoS One*, vol. 15, no. 4, article e0232277, 2020.

[17] P. Arroyo, J. Lozano, and J. Suárez, "Evolution of wireless sensor network for air quality measurements," *Journal of Electronics*, vol. 7, no. 12, p. 342, 2018.

[18] C. Wittenberg, "Cause the trend Industry 4.0 in the automated industry to new requirements on user interfaces?," in *Human-Computer Interaction: Users and Contexts: 17th International Conference, HCI International*, pp. 238–245, Los Angeles, CA, USA, 2015.

[19] M. Henze, L. Hermerschmidt, D. Kerpen, R. Häubling, B. Rumpe, and K. Wehrle, "A comprehensive approach to

privacy in the cloud-based Internet of Things," *Future generation computer systems*, vol. 56, pp. 701–718, 2016.

[20] H. Stverkova and M. Pohludka, "Business organisational structures of global companies: use of the territorial model to ensure long-term growth," *Social Science*, vol. 7, no. 6, p. 98, 2018.

[21] G. S. Rao and R. Prasad, "Impact of 5G technologies on Industry 4.0," *Wireless Personal Communications*, vol. 100, no. 1, pp. 145–159, 2018.

[22] S. Lange, J. Pohl, and T. Santarius, "Digitalization and energy consumption. Does ICT reduce energy demand?," *Ecological economics*, vol. 176, article 106760, 2020.

[23] J. M. Müller, O. Buliga, and K. I. Voigt, "Fortune favors the prepared: how SMEs approach business model innovations in Industry 4.0," *Technological Forecasting and Social Change*, vol. 132, pp. 2–17, 2018.

[24] L. D. Wocial, "Finding a voice in ethics: everyday ethical behavior in nursing," in *Nursing Ethics in Everyday Practice*, C. M. Ulrich, Ed., pp. 37–48, Sigma Theta Tau, USA, 2012.

[25] K. Langeland and V. Sørlie, "Ethical challenges in nursing emergency practice," *Journal of Clinical Nursing*, vol. 20, no. 13-14, pp. 2064–2070, 2011.

[26] C. Bartholdson, K. Lützén, K. Blomgren, and P. Pergert, "Experiences of ethical issues when caring for children with cancer," *Cancer Nursing*, vol. 38, no. 2, pp. 125–132, 2015.

[27] K. Kulju, M. Stolt, R. Suhonen, and H. Leino-Kilpi, "Ethical competence," *Nursing Ethics*, vol. 23, no. 4, pp. 401–412, 2016.

[28] V. Pouli, S. Kafetzoglou, E. E. Tsiropoulou, A. Dimitriou, and S. Papavassiliou, "Personalized multimedia content retrieval through relevance feedback techniques for enhanced user experience," in *2015 13th International Conference on Telecommunications (con TEL)*, pp. 1–8, Graz, Austria, 2015.

[29] Y. Liu, *Simple Yet Effective Pseudo Relevance Feedback with Rocchio's Technique and Text Classification [Master's Thesis]*, University of Waterloo, 2022.

[30] H. Qian, Z. Dou, Y. Zhu, Y. Ma, and J. R. Wen, "Learning implicit user profile for personalized retrieval-based chatbot," in *proceedings of the 30th ACM international conference on Information & Knowledge Management*, pp. 1467–1477, Queensland, Australia, 2021.

[31] S. Manoharan and R. Senthilkumar, "An intelligent Fuzzy rule-based personalized news recommendation using social media mining," *Computational Intelligence and Neuroscience*, vol. 2020, Article ID 3791541, 10 pages, 2020.

[32] M. Saadi, M. T. Noor, A. Imran, W. T. Toor, S. Mumtaz, and L. Wuttisittikulkij, "IoT enabled quality of experience measurement for next generation networks in smart cities," *Sustainable Cities and Society*, vol. 60, p. 102266, 2020.

[33] A. Pozzi, E. Barbierato, and D. Toti, "Cryptoblend: an AI-powered tool for aggregation and summarization of cryptocurrency news," in *Informatics*, vol. 10, no. 1p. 5, Multidisciplinary Digital Publishing Institute, 2023.

[34] C. K. Hsieh, L. Yang, H. Wei, M. Naaman, and D. Estrin, "Immersive recommendation: news and event recommendations using personal digital traces," in *In proceedings of the 25th international conference on world wide web*, pp. 51–62, Republic and Canton of Geneva, CHE, 2016.

[35] D. A. Adeniyi, Z. Wei, and Y. Yongquan, "Automated web usage data mining and recommendation system using K-nearest neighbor (KNN) classification method," *Applied Computing and Informatics*, vol. 12, no. 1, pp. 90–108, 2016.

[36] S. Manoharan, R. Senthilkumar, and S. Jayakumar, "Optimized multi-label convolutional neural network using modified genetic algorithm for popularity based personalized news recommendation system," *Concurrency and Computation: Practice and Experience*, vol. 34, no. 19, article e7033, 2022.

[37] A. F. Nayer Wanas, D. Said, N. Khodeir, and M. Fayek, "Detection and handling of different types of concept drift in news recommendation systems," *International Journal of Computer Science and Information Technologies*, vol. 11, pp. 87–106, 2019.

[38] S. Sugahara, W. Kishida, K. Kato, and M. Ueno, "Recursive autonomy identification-based learning of augmented naive Bayes classifiers," in *International Conference on Probabilistic Graphical Models*, pp. 265–276, PMLR, 2022.

Hindawi
Journal of Sensors
Volume 2023, Article ID 6383099, 7 pages
https://doi.org/10.1155/2023/6383099

Research Article

Smart E-Health System for Heart Disease Detection Using Artificial Intelligence and Internet of Things Integrated Next-Generation Sensor Networks

Muhammad Shafiq,[1] **Changqing Du**,[1] **Nasir Jamal**,[2] **Junaid Hussain Abro**,[2] **Tahir Kamal**,[3] **Salman Afsar**,[4] **and Md. Solaiman Mia**[5]

[1]*School of Information Engineering, Qujing Normal University, Yunnan, China*
[2]*School of Computer Science and Artificial Intelligence, Wuhan University of Technology, Wuhan, China*
[3]*College of Mathematics and Computer Science, Zhejiang Normal University, Jinhua, Zhejiang, China*
[4]*Department of Computer Science, University of Agriculture, Faisalabad, Pakistan*
[5]*Department of Computer Science and Engineering, Green University of Bangladesh, Bangladesh*

Correspondence should be addressed to Md. Solaiman Mia; solaiman@cse.green.edu.bd

Received 16 October 2022; Revised 9 February 2023; Accepted 5 April 2023; Published 20 April 2023

Academic Editor: Davide Palumbo

According to the World Health Organization, heart disease is the biggest cause of death worldwide. It may be possible to bring down the overall death rate of individuals if cardiovascular disease can be detected in its earlier stages. If the cardiac disease is detected at an earlier stage, there is a greater possibility that it may be successfully treated and managed under the guidance of a physician. Recent advances in areas such as the Internet of Things, cloud storage, and machine learning have given rise to renewed optimism over the capacity of technology to bring about a paradigm change on a global scale. At the bedside, the use of sensors to capture vital signs has grown increasingly commonplace in recent years. Patients are manually monitored using a monitor located at the patient's bedside; there is no automatic data processing taking place. These results, which came from an investigation of cardiovascular disease carried out across a large number of hospitals, have been used in the development of a protocol for the early, automated, and intelligent identification of heart disorders. The PASCAL data set is prepared by collecting data from different hospitals using the digital stethoscope. This data set is publicly available, and it is used by many researchers around the world in experimental work. The proposed strategy for doing research includes three steps. The first stage is known as the data collection phase, the data is collected using biosensors and IoT devices through wireless sensor networks. In the second step, all of the information pertaining to healthcare is uploaded to the cloud so that it may be analyzed. The last step in the process is training the model using data taken from already-existing medical records. Deep learning strategies are used in order to classify the sound that is produced by the heart. The deep CNN algorithm is used for sound feature extraction and classification. The PASCAL data set is essential to the functioning of the experimental environment. The deep CNN model is performing most accurately.

1. Introduction

The increasing proportion of people in their later years has made the provision of remote health monitoring an absolute need. In the field of health monitoring, recuperation, and supported living for the elderly and therapeutically tested folks, one of the most pressing challenges is maintaining consistent system administration between individuals, various pieces of medical equipment, and specialized organizations [1]. As a consequence of this, there is a need for wearable, low-control, inexpensive, and dependable medical technology that has the potential to enhance the quality of life of specific people who are afflicted with certain disorders. Additionally, it offers a potentially game-changing technical

innovation that has the capacity to realize the aforementioned benefits in human services and increase healthcare administration structures. This advancement has the potential to realize the game-changing potential of technology. Internet of Things platforms that may be worn has the potential to be utilized in the remote gathering and transmission of data on a client and the area in which they are located. After then, the data may be evaluated and kept for use at a later time, if necessary. This sort of accessibility with external devices and services will either account for early prevention (for instance, after the prediction of an impending heart attack) or it will provide speedy treatment (for example, when a client tumbles down and needs assistance). In recent years, a great number of IoT frameworks have been developed for use in IoT applications that are associated with assisted living and medical services [2].

In recent decades, cardiovascular disease has supplanted all other causes of mortality to become the leading cause of death in the United States. It is quite challenging for medical professionals to make a correct diagnosis in a timely manner [3]. Because of this, the incorporation of computer expertise into this study is essential if it is to aid healthcare practitioners in providing timely and correct diagnoses. Figure 1 shows blocked arteries.

Before these last few decades, heart disease was mostly seen as an issue that only older people faced. These days, however, it is well-acknowledged that it is one of the leading causes of mortality for individuals of all ages. It has been shown that India has a heart disease prevalence rate that is two times higher than the average for the rest of the world. In spite of the fact that heart disease is becoming more prevalent, a significant number of Indians continue to be ignorant of the symptoms that may accompany it. Even though having a history of heart disease in one's family is a significant risk factor in and of itself, the majority of heart-related disorders are caused by factors, such as high blood sugar, high cholesterol, high blood pressure, an unhealthy diet, smoking, a sedentary lifestyle, stress, and obesity. At this point in time, an individual's manner of life is the single most important factor in determining whether or not they will acquire heart disease [4].

One of the most promising technological therapies that are now developing to solve the global health equity gap is remote patient monitoring that is based on the Internet of Things (IoT) technology [5]. This specific kind of Internet of Things technology also goes by the term Internet of Medical Things (IoMT), which is an alternative moniker for IoT [6]. Throughout the whole of this dissertation, we are going to utilize the words "Internet of Things" and "Internet of Medical Things" interchangeably, despite the fact that our primary concentration will be on the medical sector. Thanks to IoMT technology, electrophysiological signals such as ECG, BP, SpO2, and glucose levels, in addition to user behaviors such as sitting, standing, and walking, may all be detected and remotely monitored in real time. This is a significant advancement. Utilizing automated decision support systems that take into consideration the data obtained from the many different monitoring indicators allows for early prognostication to be performed. This will be the beginning

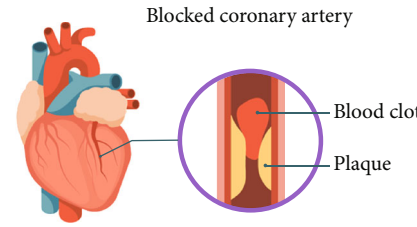

Figure 1: Blocked artery in a human heart.

of a significant shift away from the conventional practice of diagnosing and treating illnesses toward a kind of health management that is more preventive in nature and is based on prediction [7].

The use of machine learning algorithms [8] makes it possible to unearth previously undiscovered information in the form of patterns hidden within the historical records of a database. A significant challenge for data mining systems is the capacity to correctly diagnose ailments in their early stages [9]. In order to arrive at an accurate diagnosis of a patient's condition, a great number of costly tests are required to investigate a diverse spectrum of symptoms as well as possible causes. On the other hand, data mining and machine learning algorithms could make it possible to significantly cut down on the number of patients who need to be tested. Because of this, the total number of necessary tests may be cut down, which has a favorable impact not only on the amount of time it takes to make predictions but also on the accuracy of such forecasts. Even though there are various data mining algorithms that are already being used in the healthcare industry, further research into the performance evaluation of such categorization techniques is required in order to get a higher level of precision in the results [10].

This article contains a smart e-health system for heart disease detection using artificial intelligence and the Internet of Things. Biosensor enabled stethoscope collects the heart sound of a patient. A wireless sensor network is used to connect all sensors and IoT devices. IoT devices establish a connection with a centralized cloud server, where all heart sound files are accumulated. Heart sound signal is separated from other noises using the blind source separation algorithm. The PASCAL data set is used to train and test the deep convolutional neural network.

2. Literature Survey

In 2016, Yeh proposed [11] the creation of a body sensor network (BSN) by the utilization of a platform that was driven by the Internet of Things (IoT). They proposed constructing two communication ways by utilizing sophisticated cryptoprimitives in order to safeguard the privacy of data transfers and authenticate entities inside a network of smart objects. These techniques would be used to authenticate entities. Both the central processing unit (CPU) and the backend BSN server belong to this category of approaches. The authentication of entities is the goal of both of these approaches. They have demonstrated that it is possible to carry out the method in the manner that is indicated by making use of the Raspberry PI platform. They have

constructed an Internet of Things (IoT) testbed that is equipped with a number of different safety precautions. In this particular situation, the Raspberry Pi platform acts as a stand-in for a simulated LRU, which is another name for an intelligent moving object (LPU).

Heart rate sensor node analysis using embedded systems with assistance from Cogent Engineering was brought to light in 2017 by Fouad and Farouk [12]. Wellness, safety, recovery at the patient's home, assessment of the treatment's efficacy, and early sickness detection were all significant areas of focus.

Using a three-tier Internet of Things architecture and a machine learning algorithm, Kumar and Gandhi [13] developed a technique for the early identification of heart illness. This system was able to detect the disease in its earliest stages. They propose designs that are composed of three levels in order to store and handle the massive amounts of data that are created by wearable devices. This is done in order to make the data more manageable. The gathering of data is the primary objective of tier 1. The storage of massive amounts of data in the cloud is handled by tier 2 through the utilization of Apache FIBase. The development of a prediction model that is founded on logistic regression is carried out by tier 3 with the assistance of Apache Mahout. The utilization of ROC analysis ultimately results in the production of a nodal analysis of cardiac conditions.

In 2016, Park et al. [14] created a smart chair system that records and graphically portrays user posture by using a smartphone application. The goal of this system was to assist in the treatment of unequal posture. They sent data using low-power sensors such as pressure and tilt sensors, and they established connections using wireless technologies such as Bluetooth and iBeacons. Pressure and tilt sensors were two examples of these types of sensors. This Arduino implementation was done primarily with the goal of determining the various postures used by the user. This technique helps the user sit upright by recognizing their current situation and conveying that information in a manner that is simple to understand and aesthetically attractive via the use of an application on a smartphone. The graphic depicts a comparison between the user's actual posture and the ideal posture on both the left and right sides, with the amount of pressure represented by variously colored circles (red, yellow, green, and orange). This is an excellent example of how the Internet of Things technology may be put to use.

A study on the possible application of WSN technology in healthcare research to overcome challenges with patient monitoring was carried out by Alemdar and Ersoy [15]. The writers disseminated the information to a variety of subsets within the healthcare profession, such as those who deal with the chronically ill, the elderly, newborns, and youngsters whose parents are accountable for them.

Lai et al. [16] conducted an assessment of on-body sensor networks in order to compile a list of current developments and continuing challenges in a number of different disciplines. We also spoke about the many applications that the body sensor network may have. The authors hope that their in-depth study will be able to assist in fixing the problems that are still present with the existing frameworks.

In 1980, Sneha and Varshney [17] made the proposal that a framework should be developed for mobile-based patient monitoring. This framework's primary objective was to solve the issue of the high expenses associated with the underlying infrastructure of wireless sensor networks while simultaneously enhancing the communication channels that exist between patients and medical practitioners. The researchers contributed a variety of features and conceptual frameworks, such as those for power management and the design of systems. The many potential avenues of investigation served as the impetus for the research project.

Nigam et al. [18] presented a strategy to alleviate the lack of medical professionals in their paper that was published. The fundamental objective of the work that was planned was to send ECG sensor values through a remote connection. The provision of medical services was mostly limited to metropolitan regions. In addition to this, a cardiac report was compiled and forwarded to the experts for further examination.

The mobile health app was subjected to a comprehensive analysis that was supplied by Mosa et al. [19]. Following an examination of more than 2800 academic publications, a total of 88 potential applications in the medical field were discovered. These programs have been put to a wide variety of purposes, some of which include the provision of drug recommendations, health monitoring calculators, communication tools, databases of medical institutions, and tools for the diagnosis of illnesses. Additionally, the authors note the ubiquitous availability of smartphones as well as their potential usefulness as a tool for remote monitoring.

Appelboom et al. [20] conducted research not too long ago in which they collected data on the development of smart wearable biosensors as well as the clinical effectiveness of these biosensors. This review was collected by making use of a broad range of methodological domains, some of which include but are not limited to connected devices, biosensors, telemonitoring, wireless technologies, real-time home observation equipment, and so on. According to the findings of the study, the use of sensors in the healthcare industry was both beneficial and dependable. In addition, the sensors' full capabilities were not used in any way.

Neves et al. [21] investigated the use of wireless sensors in healthcare promotion because of the unique qualities that they have, such as low-cost data processing, availability, growth, and other similar attributes. The wireless sensors network was at first only available to members of the armed forces, but it was subsequently opened up to members of the civilian sector as well. According to the findings of the study, biosensors are an effective method for monitoring a broad range of diseases. In addition, some challenges connected with the adoption of WSNs in healthcare settings were investigated.

The capabilities of the wearable gadget were improved by Azariadi et al. [22] so that the researchers could have a better knowledge of the electrocardiogram data and the heartbeat. The utilization of wearable technology has shown to be extremely beneficial to the research and development of monitoring tools that are more effective for a variety of subfields within the healthcare business. The ECV and the

patient's average heart rate during the previous twenty-four hours are both taken into consideration when making a diagnosis with the use of this diagnostic tool, which was intended to aid medical professionals in the diagnosis of patients. It is now more important than ever to monitor patients remotely so that healthcare providers may serve patients who are located in a range of places while also lowering their costs.

3. Methods

This section contains a smart e-health system for heart disease detection using artificial intelligence and the Internet of Things. Biosensor enabled stethoscope collects the heart sound of a patient. A wireless sensor network is used to connect all sensors and IoT devices. IoT devices establish a connection with acentralized cloud server, where all heart sound files are accumulated. Heart sound signals are separated from other noises using the blind source separation algorithm. PASCAL data set is used to train and test the deep convolutional neural network. Figure 2 shows a smart e-health system for heart disease detection using artificial intelligence and the Internet of Things.

The continual monitoring of patients' health, as well as their fitness levels and activities, can be greatly aided by the utilization of wearable sensor technologies [16]. There is an ongoing process of conserving the data that is created by this illness in order to assist patients with a broad variety of medical therapies and to enhance the overall health of the community as a whole. This is done to help combat the effects of the illness. Reliable health data may also be utilized in the process of defining daily norms and conducting physical examinations on the individual. Many of the gadgets that are connected to the Internet of Things (IoT) are created with the purpose of monitoring a person's vital signs, such as their blood pressure, heart rate, blood sugar levels, and level of pain. These monitors, which are surgically placed within the patient's body, keep track of the subject's vital signs at all times throughout the experiment.

The phrase "wireless sensor network" (WSN) refers to a system that functions at a distance and is made up of widely dispersed, autonomous devices that employ sensors to monitor environmental or physical parameters. This kind of network is also known as a "distributed sensor network." These independent nodes, which are sometimes referred to as hubs on occasion, are part of what makes up a WSN system [15] together with switches and a conduit. Sensor systems are the means by which the data required by smart circumstances may be socially distributed. This is true regardless of whether the smart situation is in a building, a utility, a company, a house, a ship, or the automation of transportation infrastructure. We need adaptive sensor systems that are able to expand and be configured in order to battle contemporary psychological oppressors and guerrilla fighters. In these kinds of environments, installing wiring or cable is often impractical. We need a sensor network that is simple in both its installation and its ongoing maintenance. It is the intention of the illuminating paragraph to make internet-based communication between WSNs and open-source networking technologies easier to do.

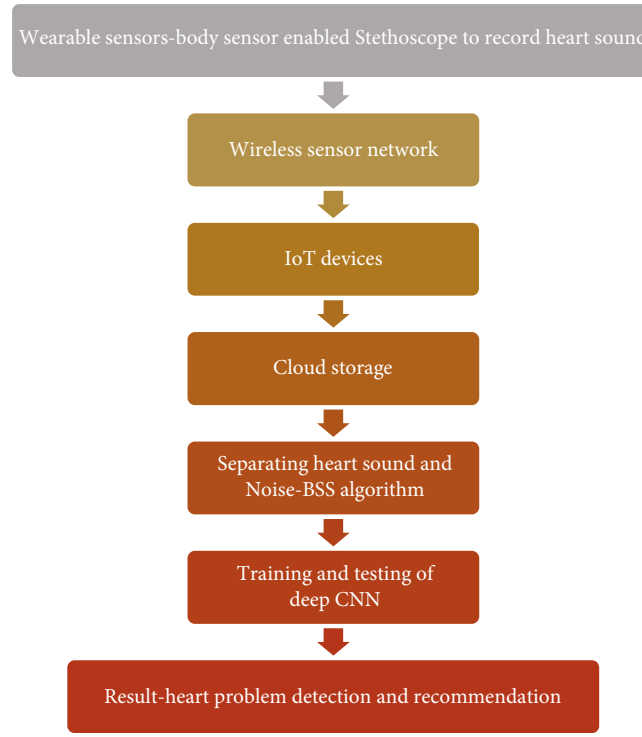

Figure 2: Smart e-health system for heart disease detection using artificial intelligence and the Internet of Things.

Since of this, cloud computing [13] is an essential enabler for e-health frameworks because it can provide the computational and storage infrastructure that is required to tackle the issue of e-health information management. As a result, caregivers have the opportunity to use this data to their benefit by redistributing it to a different cloud service. That not only relieves them of a load of maintaining and keeping the data up-to-date in a way that is both effective and cost-effective for them.

It is very challenging to reassemble a whole audio signal from a corrupted observation. Separating HSS from the ambient noise is one of the obstacles that must be overcome. Blind source separation is one of the solutions that may be applied to this issue, which is one of many possible approaches. The sensor array is part of a BSS that is considered to be the most critical. Beam creation by using the multisignal data from an array of sensors is an integral part of BSS [23]. The beam former is responsible for collecting signals from several sources in order to provide guided reaction. The signal of interest sees an improvement as a result of the interference from irrelevant sources being cut down significantly [24]. These BSS algorithms get their start from the fundamental ideas of independent component analysis (ICA), which serves as their foundation. In contrast, ICA has the ability to handle mixed signals in real time. One may be able to make inferences by making use of the pattern in the arrival time of the source that is formed by the separation matrix.

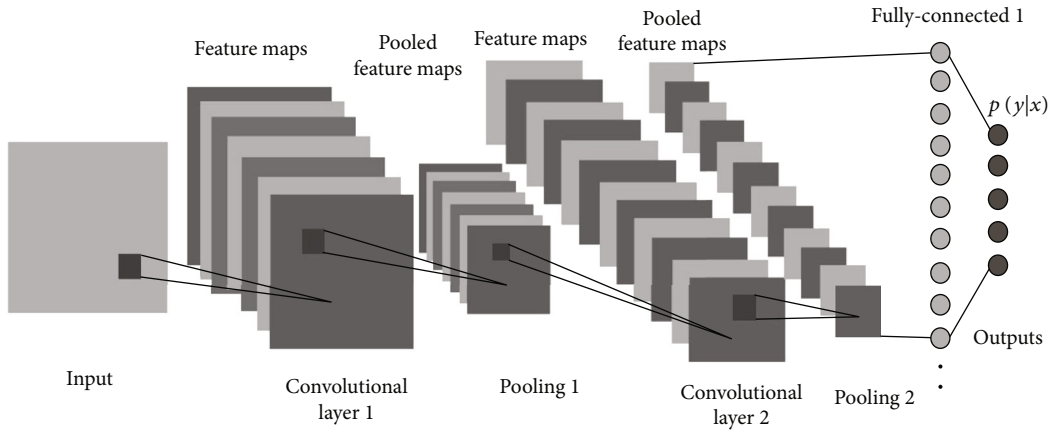

Figure 3: Architecture of deep CNN model.

The deep convolutional neural network is one of the most cutting-edge AI approaches, and it was designed specifically to solve difficult issues that arise in computer vision (Deep CNN). Deep CNN, a kind of deep learning that is represented by a feed-forward artificial neural network, has been employed in a number of articles dealing with the classification of agricultural photographs. These works may be found in the following: Important to Deep CNN are the layers known as convolutional layers, which use filters to extract properties from the photos that are sent into the network. It is possible that increasing the total quantity of training data might make deep CNN even more successful. One of the most significant benefits of using deep CNN for image classification is that it might drastically cut down on the amount of feature engineering that is required.

The deep CNN network is comprised of numerous layers, each of which is responsible for a separate convolution. An illustration of the layered architecture that may be achieved using the deep CNN approach is shown in Figure 3.

Each layer of the network creates a new representation of the training data, with the representations that are more general appearing in the outermost layers and the representations that are more particular going deeper into the network. The dimensionality of the training data is decreased by the convolutional layers, which work as feature extractors, and the pooling layers, which are responsible for the reduction in the number of dimensions. Convolutional layers are layers that take low-level inputs and turn it into higher-level properties that may be utilized for categorization. One further thing to keep in mind is that the convolutional layers are the essential component of any deep CNN system.

The process of feature engineering is what differentiates deep learning from other, more traditional types of machine learning. The pooling layer is responsible for the process of downsampling that takes place in the spatial dimension. It contributes to reducing the overall number of options available. The method known as maxpooling is implemented in the pooling layer of the recommended model. Maximum pooling performs better than average pooling in the deep CNN model that was presented. The process of removing nodes from a network is an additional layer that plays an important part in the overall structure. It is a kind of regularization that is used to reduce the effects of overfitting. The next layer, known as the dense layer, is responsible for classification. This layer gets input from the convolutional and pooling layers that came before it. Deep CNN involves a significant amount of iteration in addition to the training of several models in order to arrive at the best possible result. The basic optimization method known as gradient descent, which is often referred to as batch gradient descent, is used in gradient descent. In this approach, the gradient steps are carried out using full training data on each step. When dealing with a large training set, the gradient descent algorithm may be difficult to implement.

4. Results Analysis and Discussion

PASCAL data set [25] contains heart sound samples. It has 449 records and five classes. The classes are normal, noisy normal, extrasystole, murmur, and noisy murmur. Heart sound signals are separated from other noises using the blind source separation algorithm. PASCAL data set is used to train and test the deep convolutional neural network. 300 images are used to train the deep CNN model, and 149 images are used to test the CNN model. The results are shown in Figure 4. Different parameters are used to observe the performance of deep CNN and compare the results of deep CNN with other classification models support vector machine, ANN, and logistic regression. Framework was implemented in the Jupyter tool. It is a Python-based tool. I5 7th generation processor with 3.2 GHz with 8GB RAM was used in the experimental setup.

From Figure 4, it is clear that the accuracy of deep CNN is 98.4 percent. It is higher than the SVM, LR, and ANN algorithms. Also, the precision of deep CNN is 99 percent, which is 2.6 percent more than the precision of an ANN algorithm. Recall and the F1 score of deep CNN are also higher than other classifiers used in the experimental work.

The most essential performance measurements are the classification accuracy score, the precision score, the recall score, and the F1 score [26, 27]. It is common practice to use a confusion matrix in order to demonstrate how well the models perform on the test data. A confusion matrix is

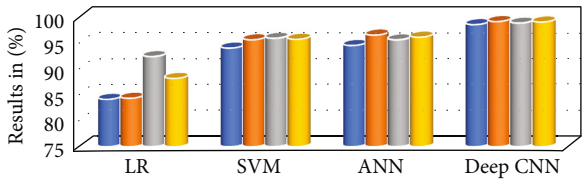

	LR	SVM	ANN	Deep CNN
Accuracy	84.1	93.9	94.4	98.4
Precision	84.3	95.5	96.4	99
Recall	92.3	95.8	95.5	98.7
F1	88.1	95.6	96	98.9

Figure 4: Performance analysis of deep CNN model on PASCAL data set.

Table 1: Confusion matrix of machine learning algorithms.

Parameter	Deep CNN	ANN	SVM	Logistic regression
TP	310	300	297	265
TN	132	124	125	113
FP	3	11	14	49
FN	4	14	13	22

a useful tool that may be used to provide a visual representation of the efficacy of various machine-learning approaches. The confusion matrix takes into account four different values: true positive (TP), false negative (FN), true negative (TN), and false positive (FP). It is shown in Table 1.

The accuracy of a classification method may be evaluated based on the percentage of a given group of test files that have been correctly assigned to their respective categories.

The total number of occurrences in which the model properly classified the data as positive is referred to as the true positive. If a number is described as true negative, it means that it has been unequivocally established as having a value that is in the negative range. To elaborate, a false positive is the occurrence of a false positive classification when the underlying data is negative. This is referred to as a false positive classification. A false positive is often referred to as a type 1 error. A false negative is a number that has been incorrectly labelled as having a negative value, regardless matter how much time it takes to arrive at that conclusion. This phenomenon also goes by the name of the type 2 error, which is also often referred to as the false negative. These parameters are what define the classification accuracy, precision, recall, and F1 score of deep convolutional neural networks and other contemporary machine learning and transfer learning methodologies.

5. Conclusion

Diseases of the heart are the leading cause of mortality on a global scale. If cardiovascular illness can be recognised in its early stages, it may be feasible to reduce the total mortality rate of people. If a heart condition is diagnosed at an earlier stage, there is a larger likelihood that it may be effectively treated and managed under the direction of a physician. This is especially true if the disease is detected earlier in its progression. Recent developments in fields like the Internet of Things, cloud storage, and machine learning have sparked a rekindled sense of optimism over the potential for technology to usher in a paradigm shift on a global scale. This article includes a cutting-edge e-health system that uses both artificial intelligence and the Internet of Things to detect heart disease in patients. The patient's heart sound is collected via a stethoscope equipped with biosensors. In order to link all of the sensors and other IoT devices, a wireless sensor network is used. Internet of Things (IoT) devices create a link with a centralized cloud server, which is where all of the heart sound recordings are gathered. Using the blind source separation technique, the heart sound signal is isolated from the surrounding background noise. In order to train and validate the deep convolutional neural network, the PASCAL data set is used. When training the deep CNN model, 300 photos are utilized, but just 149 images are used when testing the CNN model. Several distinct factors are used in order to evaluate how well deep CNN performs in comparison to other classification models and to monitor the performance of deep CNN itself. Logistic regression, support vector machine, and artificial neural networks deep CNN are doing much better than other models across all parameters.

Data Availability

Data shall be made available on request from the corresponding author.

Conflicts of Interest

All authors declare that they do not have any conflict of interest.

References

[1] Y. B. Zikria, R. Ali, M. K. Afzal, and S. W. Kim, "Next-generation Internet of Things (IoT): opportunities, challenges, and solutions," *Challenges, and Solutions Sensors.*, vol. 21, no. 4, 2021.

[2] N. Dey, A. S. Ashour, and C. Bhatt, "Internet of Things Driven Connected Healthcare," in *Internet of Things and Big Data Technologies for Next Generation Healthcare. Studies in Big Data*, C. Bhatt, N. Dey, and A. Ashour, Eds., vol. 23, Springer, Cham., 2017.

[3] S. Kumar, P. Tiwari, and M. Zymbler, "Internet of Things is a revolutionary approach for future technology enhancement: a review," *Journal of Big Data.*, vol. 6, no. 1, 2019.

[4] B. Pradhan, S. Bhattacharyya, and K. Pal, "IoT-based applications in healthcare devices," *Hindawi Journal of Healthcare Engineering*, vol. 2021, article 6632599, 18 pages, 2021.

[5] M. N. O. Sadiku, E. Kelechi, M. M. Sarhan, and G. P. Roy, "Wireless sensor networks for healthcare," *Journal of Scientific and Engineering Research*, vol. 5, no. 7, pp. 210–213, 2018.

[6] A. Rghioui, S. Sendra, J. Lloret, and A. Oumnad, "Internet of Things for measuring human activities in ambient assisted living and e-health," *Network Protocols and Algorithms*, vol. 8, no. 3, pp. 15–28, 2016.

[7] S. M. Kumar and D. Majumder, "Healthcare solution based on machine learning applications in IOT and edge computing," *International Journal of Pure and Applied Mathematics*, vol. 119, pp. 1473–1484, 2018.

[8] P. Xi, R. Goubran, and C. Shu, "Cardiac murmur classification in phonocardiograms using deep recurrent-convolutional neural networks," in *Frontiers in Pattern Recognition and Artificial Intelligence*, pp. 189–209, World Scientific, 2019.

[9] A. Raghuvanshi, U. Singh, G. Sajja et al., "Intrusion detection using machine learning for risk mitigation in IoT-enabled smart irrigation in smart farming," *Journal of Food Quality*, vol. 2022, Article ID 3955514, 8 pages, 2022.

[10] A. Tiwari, V. Dhiman, M. A. M. Iesa, H. Alsarhan, A. Mehbodniya, and M. Shabaz, "Patient behavioral analysis with amart healthcare and IoT," *Behavioural Neurology*, vol. 2021, Article ID 4028761, 9 pages, 2021.

[11] K. Yeh, "A secure IoT-based healthcare system with body sensor Networks," *Access*, vol. 4, pp. 10288–10299, 2016.

[12] H. Fouad and H. Farouk, "Heart rate sensor node analysis for designing Internet of Things telemedicine embedded system," *Cogent Engineering*, vol. 4, no. 1, p. 1306152, 2017.

[13] P. Kumar and U. Devi Gandhi, "A novel three-tier Internet of Things architecture with machine learning algorithm for early detection of heart diseases," *Computers & Electrical Engineering*, vol. 65, pp. 222–235, 2018.

[14] M. Park, Y. Song, J. Lee, and J. Paek, "Design and implementation of a smart chair system for IoT," in *2016 International Conference on Information and Communication Technology Convergence (ICTC)*, pp. 1200–1203, Jeju, Korea (South), 2016.

[15] H. Alemdar and C. Ersoy, "Wireless sensor networks for healthcare: a survey," *Computer Networks*, vol. 54, no. 15, pp. 2688–2710, 2010.

[16] X. Lai, Q. Liu, X. Wei, W. Wang, G. Zhou, and G. Han, "A survey of body sensor networks," *Sensors*, vol. 13, no. 5, pp. 5406–5447, 2013.

[17] S. Sneha and U. Varshney, "A framework for enabling patient monitoring via mobile ad hoc network," *Decision Support Systems*, vol. 55, no. 1, pp. 218–234, 2013.

[18] K. U. Nigam, A. A. Chavan, S. S. Ghatule, and V. M. Barkade, "IOT-BEAT: an intelligent nurse for the cardiac patient," in *2016 International Conference on Communication and Signal Processing (ICCSP)*, pp. 976–982, Melmaruvathur, India, 2016.

[19] A. S. M. Mosa, I. Yoo, and L. Sheets, "A systematic review of healthcare applications for smartphones," *BMC Medical Informatics and Decision Making*, vol. 12, 2012.

[20] G. Appelboom, E. Camacho, M. E. Abraham et al., "Smart wearable body sensors for patient self-assessment and monitoring," *Archives of Public Health*, vol. 72, no. 1, 2014.

[21] P. Neves, M. Stachyra, and J. Rodrigues, "Application of wireless sensor networks to healthcare promotion," *Journal of Communications Software and Systems*, vol. 4, no. 3, pp. 181–190, 2017.

[22] D. Azariadi, V. Tsoutsouras, S. Xydis, and D. Soudris, "ECG signal analysis and arrhythmia detection on IoT wearable medical devices," in *2016 5th International Conference on Modern Circuits and Systems Technologies (MOCAST)*, pp. 1–4, Thessaloniki, Greece, 2016.

[23] H. Z. Almarzouki, H. Alsulami, A. Rizwan, M. S. Basingab, H. Bukhari, and M. Shabaz, "An internet of medical things-based model for real-time monitoring and averting stroke sensors," *Journal of Healthcare Engineering*, vol. 2021, Article ID 1233166, 9 pages, 2021.

[24] A. Maccagno, A. Mastropietro, U. Mazziotta, M. Scarpiniti, Y. C. Lee, and A. Uncini, "A CNN approach for audio classification in construction sites," in *Progresses in Artificial Intelligence and Neural Systems. Smart Innovation, Systems and Technologies*, A. Esposito, M. Faundez-Zanuy, F. Morabito, and E. Pasero, Eds., vol. 184, Springer, Singapore, 2021.

[25] P. Bentley, G. Nordehn, M. Coimbra, and S. Mannor, "The PASCAL classifying heart sounds challenge 2011 results," 2011, http://www.peterjbentley.com/heartchallenge/.

[26] S. K. UmaMaheswaran, G. Prasad, B. Omarov et al., "Major challenges and future approaches in the employment of blockchain and machine learning techniques in the health and medicine," *Security and Communication Networks*, vol. 2022, Article ID 5944919, 11 pages, 2022.

[27] V. D. P. Jasti, A. S. Zamani, K. Arumugam et al., "Computational technique based on machine learning and image processing for medical image analysis of breast cancer diagnosis," *Security and Communication Networks*, vol. 2022, Article ID 1918379, 7 pages, 2022.

Hindawi
Journal of Sensors
Volume 2023, Article ID 5382375, 12 pages
https://doi.org/10.1155/2023/5382375

Research Article

Evaluation of Autism Spectrum Disorder Based on the Healthcare by Using Artificial Intelligence Strategies

Amit Sundas,[1] **Sumit Badotra**,[1,2] **Shalli Rani**,[3] **and Raymond Gyaang**[4]

[1]*Department of Computer Science and Engineering, Lovely Professional University, Phagwara, Punjab, India*
[2]*School of Computer Science and Engineering, Bennett University, Noida, UP, India*
[3]*Chitkara University Institute of Engineering and Technology, Chitkara University, Punjab, India*
[4]*Kwame Nkrumah University of Science and Technology, Ghana*

Correspondence should be addressed to Shalli Rani; shallir79@gmail.com and Raymond Gyaang; rgyaang@st.knust.edu.gh

Received 3 August 2022; Revised 23 October 2022; Accepted 24 November 2022; Published 7 March 2023

Academic Editor: Antonio Lazaro

The behaviors of children with autism spectrum disorder (ASD) are often erratic and difficult to predict. Most of the time, they are unable to communicate effectively in their own language. Instead, they communicate using hand gestures and pointing phrases. Because of this, it can be difficult for caregivers to grasp their patients' requirements, although early detection of the condition can make this much simpler. Assistive technology and the Internet of Things (IoT) can alleviate the absence of verbal and nonverbal communication in the community. The IoT-based solutions use machine Learning (ML) and deep learning (DL) algorithms to diagnose and enhance the lives of patients. A thorough review of ASD techniques in the setting of IoT devices is presented in this research. Identifying important trends in IoT-based health care research is the primary objective of this review. There is also a technical taxonomy for organizing the current articles on ASD algorithms and methodologies based on different factors such as AI, SS network, ML, and IoT. On the basis of criteria such as accuracy and sensitivity, the statistical and operational analyses of the examined ASD techniques are presented.

1. Introduction

Disabilities in social behavior and interaction are characteristics of ASD. According to Jon Baio [1], an estimated 1 in every 59 children is diagnosed with ASD. Special care and welfare facilities are needed by all impaired children more than by healthy youngsters [2]. In addition to limiting the lives of the sufferers, this long-term condition has a detrimental impact on their caretakers' quality of life (QoL). Patients can be monitored remotely using systems based on IoT devices, which have numerous beneficial characteristics. There have so been a number of healthcare applications leveraging IoT devices in recent years. GPS, heart rate, microphone, and ear clips [2] are some of the most common IoT sensors used in wearable devices like smartwatches and smartphones. Sensors and devices are used to identify autistic youngsters, rather than traditional techniques of diagnosis [3, 4].

To help protect youngsters from developing life-threatening disorders, several studies have been conducted during the last decade. However, there were no major breakthroughs. Hence, the most important components of assisting the patient are early diagnosis and improving the QoL of the patients. Autistic children are frequently misdiagnosed until they are two years old [4]. As a result, they are still unable to carry out their daily routines. Consequently, this article examines several IoT device techniques for children with ASD to evaluate and contrast novel ways of detecting the disorder or enhancing quality of life for individuals already diagnosed [4, 5]. The Internet of Things is using artificial intelligence, machine learning, SS network, and deep learning to identify and protect patients from physical and emotional problems [5]. Patients' vital signs are gathered by these systems, which then use various machine learning and deep learning algorithms to select the most appropriate responses. They may even be able to assist in the early

detection of ASD. There are risky behaviors that autistic children perform when they are irritated, which can impair their physical health. An alarm is sent to caretakers and doctors, informing them of the condition and requesting assistance. Every one of these IoT-based devices monitors the body's vital signs and records any changes depending on a variety of criteria (e.g., sensitivity, specificity, time, and accuracy) [6].

According to our knowledge, the ASD methods have not been extensively studied. In this work, methods for a Systematic Literature Review (SLR) are presented so that developing technologies such as wearable devices and mobiles can be utilized in ASD research. A technical taxonomy [6, 7] describes the classification of existing ASD approaches and algorithms employing IoT-based devices and ML/DL. Through the use of SS networks in the health sector, there will be an increase in communication and collaboration, with individuals sharing information about similar conditions and healthcare professionals sharing their knowledge of care and treatment. As a result, better health decisions can be made.

Our ASD methodologies are broken down into two main categories: ways to identifying and monitoring illness severity in children with ASD and programmed to improve the quality of life for children with ASD [6].

Among the SLR's significant contributions to ASD methods are the following:

(i) Providing an overview and analysis of ASD techniques employing IoT-based devices, ML and DL algorithms, and 28 publications

(ii) IoT-based ASD methodologies and algorithms presented in a technical taxonomy

(iii) Technical accept such as IoT, ML, AI, and SS network used in methodologies

(iv) Discussing and analyzing the technical aspects of each research study

The following is the structure of this paper: Section 2 presents a review of the literature, which is followed by Section 3, explaining the study strategy and methods. Section 4 presents a technical taxonomy for ASD methods, as well as a side-by-side comparison and summary for each research study that is based on the taxonomy that has been offered in the previous section. Following a review of the research papers, Section 5 gives an analytical commentary. Section 6 discusses unresolved difficulties and new obstacles associated with autism spectrum disorders (ASD) in detail. Finally, in Section 7, the study comes to a close with a conclusion.

2. Literature Review

Caregivers and families dealing with autistic children face one of the most challenging and difficult challenges. Systems that use the Internet of Things have attracted a lot of interest in recent years. ASD treatment and diagnosis have been the focus of several publications, but only a small number of relevant studies have been presented to study ASD in the same way.

Badotra et al. [8] addressed issues in a wide range of smart devices, sensors, and systems connected to health concerns, which are closely related to our study. Internet of Things (IoT) has emerged as a modern information technology, according to [7]. One of the most interesting uses for a growing number of wearable sensors in healthcare is to store the data collected from monitoring physiological parameters like heart rate. IoT, cloud computing, and Wireless Body Area Network (WBAN) are the primary components of this technology (WBAN). IoT-powered wireless "SS networks" rely on a machine learning technique for their effectiveness since there is a lot of data that has to be intelligently managed.

Kollias et al. [9] demonstrate that children with ASD, like those with dementia and Alzheimer's, also experience forgetfulness. As a result, individuals are more likely to encounter dangerous circumstances, such as fleeing their homes. On the other hand, this technology allows children with ASD to remain in their comfort zone. Alzimio, a solution based on IoT devices, was presented to address these problems. Using a method developed by Aisuwarya Sundas et al. [10], the exact location of patients can be displayed on the smartphones of medical professionals. When patients have departed from their comfort zone, these systems may be of great assistance.

Data mining approaches like as classification, regression, and clustering were used by Farooqi et al. [11] to diagnose ASD early. For patients and their careers, early detection of ASD is critical to providing appropriate education and support. For the most accurate diagnosis, their research found that categorization algorithms are the best.

Using data mining tools, Wong et al. [12] have studied the impact of autism treatments on proper conduct. Autistic children can be predicted and better understood using this method. On the basis of these techniques, they could distinguish between what were deemed acceptable and unacceptable behaviors.

Kaur et al. [13] analyzed 45 papers that applied supervised machine learning and classification techniques to ASD. SVM, random forest, decision trees, Least Absolute Shrinkage and Selection Operator (LASSO), Neutral Network (NN), regression, Conditional Forest (CF), Nave Bayes (NB), Elastic Net regression (ENet), Random Tree, and Flex Tree were the most utilized models. A survey of 83 publications published after the year 2000 was conducted by Koumpouros and colleagues for their study. The papers committed to intervening in the treatment of ASD with wearable technology and computer power [14].

An autistic youngster can benefit from the Robota robot toy, which was used in [15] to demonstrate the potential of the AuRoRA project. An evaluation element known as Conversation Analysis (CA) was used to study the development of three children with autism. As a result, they came to understand that the youngsters are in fact interacting with the adult robot. An autistic child's joint attention was not only defined in the study, but computer and robot therapy for ASD was also highlighted.

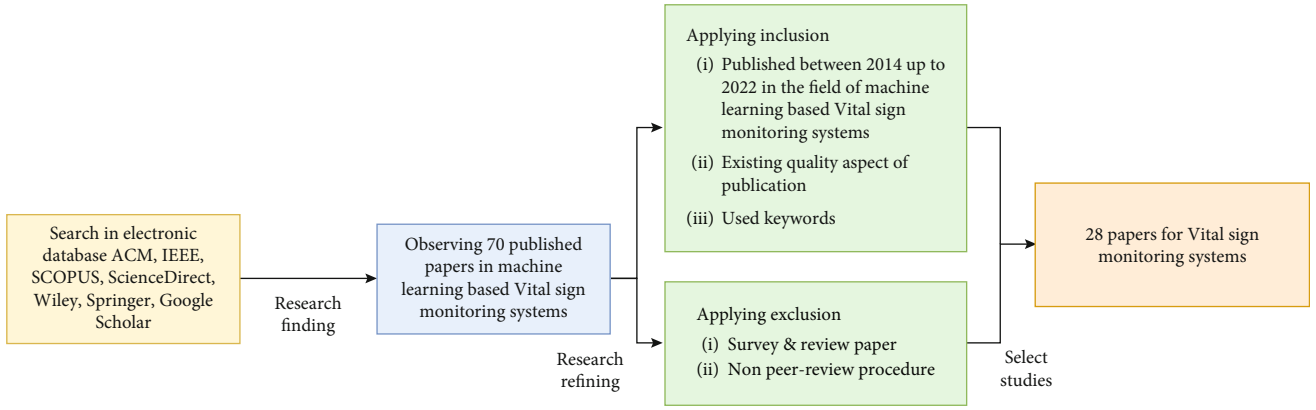

Figure 1: Methodology for doing research based on the SLR.

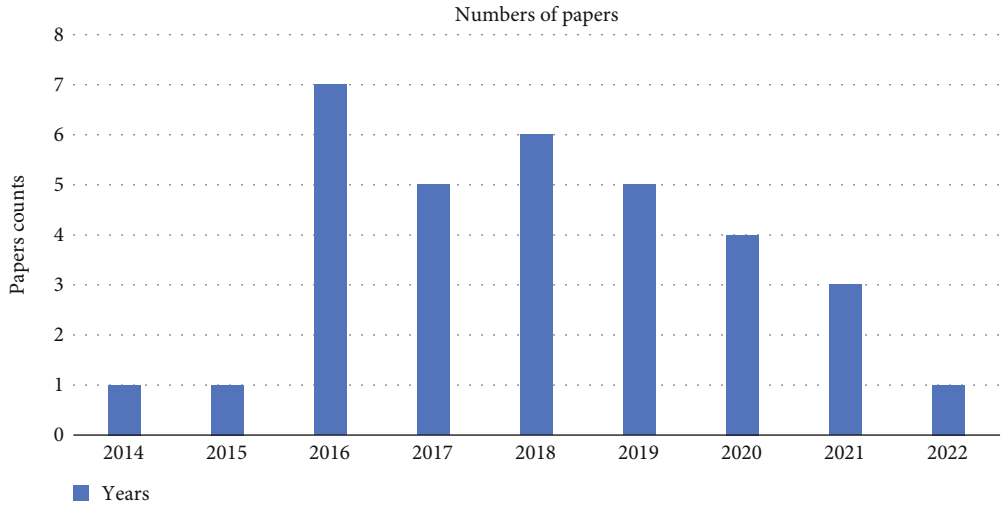

Figure 2: Annual publication analysis of ASD methods.

3. Methodology

The comprehensive literature review technique provided by current ADS approaches [16] is used in this section. The SLR is compiling pertinent papers that identify specific research issues and questions for further investigation. Three steps are depicted in Figure 1 of the methodology: gathering, refining, and analyzing.

In March of this year, we initiated our search for pertinent articles. ScienceDirect, ACM, IEEE, Springer, Google Scholar, Wiley, and SCOPUS were also significant data sources and resources. According to a variety of inclusion and exclusion criteria, over 65 publications were analyzed to determine which studies were the most pertinent to the review literature. The use of Internet of Things devices in autism spectrum disorder (ASD) research was examined in stages from 2014 to March 2020. PICO Stone [17] utilized IoT, wearable sensors, robotics therapy, smartphones, smart watches, and the Kasper robot in an effort to employ the most pertinent keywords. Survey and review papers, as well as works written in contexts other than English or by means other than peer review, are also withdrawn. In the end, 28 articles related to IoT-based products and the diagnosis and treatment of ASD (Figure 2) were retrieved. Below in Figure 2, ASD investigations employing IoT-based devices take an average of two years to come to fruition [18]. The chart shows 2 axes in which the y-axis indicates the number of papers counts and the x-axis represents years from 2014 to 2022.

The final selection of research yielded the following 28 studies as shown in Figures 1 and 2.

(i) A statistical, formal, simulation-based, and implementation-based research approach has been presented

(ii) The final version of all publications is required

(iii) It is published on the subject of ASD

For each study research, an analysis of internal and external questions was produced to link to the technical features of the SLR technique on ASD approaches. These questions were then used to conduct the study research.

(a) Which methods to autism spectrum disorder are being discussed and reviewed in this analysis?

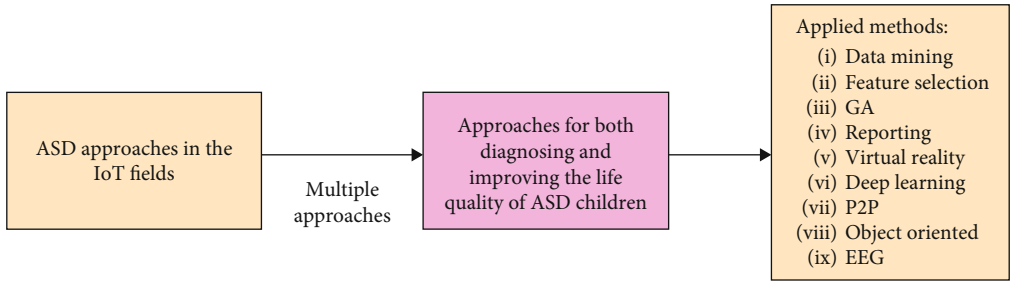

Figure 3: Presented taxonomy for the ASD approaches.

Table 1: A comparison of the approaches used for diagnosing and monitoring the degree of illness in children with autism spectrum disorder (ASD).

Ref.	Key points	Method	Characteristics of evaluation			
			Time	Specificity	Accuracy	Sensitivity
[18]	Using brain signals to focus attention on one's health using SS network	Data mining	✓	✗	✓	✗
[19]	Long-term use of wearable technologies to evaluate psychological health	Reporting	✓	✗	✓	✗
[20]	Using IoT to monitor healthcare	Feature selection	✗	✗	✓	✗
[21]	Avoid obtaining injured by autistic people who aren't at responsibility	GA	✗	✗	✓	✗
[22]	Emotional and visual indicators in a smart home	DL	✗	✗	✓	✗
[23]	Recognize the emotions of children with autism	DL	✗	✓	✓	✗
[24]	Monitoring the actions of an autistic person might be quite risky	Feature selection	✓	✗	✓	✗
[25]	Autism condition can be detected early if it is recognized using SS network	Feature select ion	✓	✓	✓	✓
[26]	Autism children's situation can be properly appreciated with virtual reality therapy	Virtual reality	✓	✗	✗	✗
[27]	A reliable strategy for the early detection of autistic spectrum disorders in youngsters	Feature selection	✓	✓	✓	✓
[28]	A framework for detecting autism in children using SS network	Data mining	✗	✓	✓	✓
[29]	ML-based ASD detection	Feature selection	✓	✗	✗	✗

(b) What techniques and processes are used in the treatment of autism spectrum disorder?

(c) What are the ASD performance metrics?

(d) Find out which scientific journals or conferences published based on ASD?

(e) ASD techniques use which platforms and sensors?

4. ASD Approaches

Autism is an incurable condition that requires the sufferer to deal with it for the rest of their lives. If you can foresee immediately that the therapeutic procedures should be used, you can act swiftly to implement them. In this part, there is a lot of attention paid to ASD research. The publications need to be studied more thoroughly in order to improve ASD treatment approaches. According to Figure 3, our study methodologies included two elements in the following subsections: ways for diagnosing and assessing the severity of ASD for children and programmed for enhancing the quality of life of children with ASD. Following studies used a variety of ways to achieve these objectives, including data mining, feature selection, genetic algorithms, reporting on DL, virtual reality, object-oriented, EEG (electroencephalography), and peer-to peer (P2P).

4.1. Children with ASD May Be Diagnosed and Their Condition Severity Measured Using a Variety of Different Methods. Forecasting and monitoring are two of ASD's thorniest problems. The educational and health assistance sectors are impacted by the impact of autism's unique way of seeing the world. With IoT services, the sickness is anticipated in 2- or 3-year-old children in mild and severe ranges; however the approach has been hastened.

The individuals will benefit from this enhancement in the quality of educational and health services. Table 1 shows the fundamental concept, implemented technique, platforms and sensors, and the evaluation elements that were examined.

Wearable sensors that scan brainwaves have been proposed by Sundhara Kumar and Bairavi [18] as a framework for autonomous monitoring of health issues. Caregivers of autistic persons received regular updates on the progress of their loved ones. When a patient's health is in jeopardy, a health description is communicated to their careers and physicians via sensors that monitor brain activity. Predicting the illness is more accurate with brain data.

Yang et al. [19] presented wearable technology based on social sensing, privacy audio feature merging, environment sensing, and behavior tracking. To evaluate voice quality and information without storing unprocessed audio data, the wellbeing monitoring platform developed privacy audio wellbeing capabilities. In their case study, they utilized Android smartphones and servers to create an application that explains the long-term relationship between physical and psychological data. It may also be evaluated on actual humans in clinical trials. Krishna and Sampath [20] have also presented an IoT system for monitoring important patient metrics and health situations. This information is transmitted to the cloud server via a smartphone or other device. Using cloud computing and the collected metrics, such as heart rate, oxygen saturation percentage, and body temperature, we can determine the health status of a user. A programmed laptop or smartphone can be used to display the data from the user's mobile phone.

A Service-Oriented Architecture (SOA) for persons with an autistic condition was developed by Eshetu et al. [21]. In the proposed wearable sensors, autistic persons and their environment may be monitored for their physiological state. Using readily accessible and inexpensive devices such as smartphones, cameras, and other wireless items, Mano et al. [22] developed an Internet of Things therapeutic system for the home use of handicapped patients and the elderly. For the treatment of patients, they made use of image processing and embedded computers and aided in the development of a health-conscious household. Accuracy and cognitive theory emphasize were outlined by the authors. For Parkinson's sufferers as well as children with ASD, this therapy may be able to enhance facial expression. Some of the behaviors and reactions of autistic children, such as voice pitch, communication without words, and complex techniques, have been reported by Lavanya et al. [23].

An IoT system that uses a wristwatch to identify autistic children's stereotyped behaviors was introduced by Amiri et al. [24]. For children with autism, weeping, flapping of the hands, and painting are frequent behaviors. The accelerometer in the wristwatch is designed to recognize these three common reactions. Sensors are used to collect data, which is subsequently sent to the cloud for processing. Parents, clinicians, and caregivers will benefit from this technology since the process changes decision trees and improves their correctness. When it comes to early detection, Moradi et al. [25] used a smart toy automobile. In the toy car, the SVM algorithm was used to tell between healthy children and autistic youngsters. So far, this method has the highest level of accuracy, sensitivity, and specificity, based on the results of their experimentation. An autistic child's emotional, attentional, and social ties can be reinforced in a therapy-based virtual world that has several levels. Attracting attention with color lights and loud noises first, the atmosphere focuses on boosting social ties and engagement by allowing people to touch each other, as well as throw a ball at each other. When it comes to choosing a decision, this is it! Autistic children's terror, frustration, and eagerness may all be predicted with virtual reality therapy [26].

Using linear or nonlinear EEG variable selection, Abdolzadegan et al. [27] developed a robust technique for early identification of children with ASD using EEG data description and analysis. MI, SVM, GA, and K-nearest neighbor were all important factors in the feature selection process (KNN). In terms of KNN and SVM, they came out on top. Deep neural network and hybrid classifications were not supported by the suggested technique.

Data analysis and machine learning techniques were used by Shankar et al. [28] to create a paradigm for diagnosing autism in babies. Their structure also made extensive use of SVM-based training of data models and of data analysis in general. It was able to attain an accuracy of 89% but will need to be improved using DL and biomedical imaging in order to be more efficient. Praveena et al. [29] used ML algorithms to diagnose ASD early enough to provide the most effective treatment for the condition. They used the UCI dataset to test their own method. The technique can be used in conjunction with other diagnostic tools for autism spectrum disorder, such as EEG and MRI scans. For SVM and DL algorithms, in particular, an intelligence detective needs to be constructed.

4.2. Children with ASD May Be Diagnosed and Their Condition Severity Measured Using a Variety of Different Methods. ASD is a serious problem that has to be addressed. Few studies have looked at some significant factors related to the quality of life for children with autism spectrum disorder. Table 2 gives more information on these studies.

An IoT system was described by Alam et al. [30]. ASD symptoms and indicators are gathered by ubiquitous sensor nodes in the Belief Rule Base (BRB) in order to categorize different autistic kid kinds. They monitored their heart rate, social contact, and other activities with a variety of devices. Rule weight and patient believe level are the system's criteria. Sensors and IoT systems can, however, be used to increase their accuracy. For children with autism, Rahman and Bhuiyan [31] developed an individual need platform that assessed physiological signals and utilized data gathered and converged from applications. The wearable system's design featured an array of sensors, multiple integrated wearable sensors, and medical servers to detect the health state of autistic children. Sensors and other embedded devices are used in the multimodal intelligent mode to enhance patients' day-to-day activities. Wearable features that are comfortable for laboratory usage cannot be employed in the workplace or for everyday activities. A wearable gadget developed by Shi et al. [32] is also being used in classrooms to study the interaction and behavior of children with ASD. Obsessive-compulsive disorder (ASD) sufferers can improve their social skills with the use of technology. Using this strategy, teachers receive the best feedback and responses, which improves classroom involvement.

A fuzzy assistive approach developed by Sumi et al. [33] decreases the amount of dependence on the user. In order to restore order, the system gathers data from numerous sensors and transmits it to the aiding personnel. If a child is damaged or hurt, helpers will be alerted instantly thanks to wearing sensors. Using the ASD's facial expressions and

Table 2: Approaches for increasing quality of life for children with autism spectrum disorder (ASD).

Ref.	Key points	Method	Characteristics of evaluation			
			Time	Specificity	Accuracy	Sensitivity
[30]	Autism spectrum disorder assessment in children using SS network	Data mining	✓	✗	✓	✗
[31]	IoT sensors detect autism-related special needs in youngsters	Data mining	✓	✗	✗	✗
[32]	Providing instructors of autistic children with the greatest possible feedback	Data mining	✓	✗	✓	✗
[33]	Removing the autistic learner from reliance on others' help and support	Data mining	✓	✗	✓	✗
[34]	ASD's ability to recognize and express emotion	Data mining	✗	✗	✓	✗
[35]	Acknowledging the necessity of ASD via PECS	Data mining	✓	✗	✗	✗
[36]	Using robots to train autistic children and enhance their talents using SS network	Genetic algorithm	✓	✗	✓	✗
[37]	The recommended technological treatment for ADD/ADHD in parents using SS network	Reporting	✓	✗	✓	✗
[38]	Investigating the ways in which intelligent items assist autistic individuals	Feature selection	✓	✗	✗	✗
[39]	Intelligent technology has enabled autistic children to perform previously inaccessible tasks	Object- oriented	✗	✗	✓	✗
[40]	In order to improve the autistic patient's heuristic detection issue,	P2P	✓	✗	✗	✓
[41]	Students' social and communication skills will be improved thanks to the robot Kasper to detect ASD	P2P	✓	✗	✗	✗
[42]	To assess the effectiveness of human and robot-based treatment for children with autism spectrum disorder (ASD)	Reporting	✗	✗	✗	✗
[43]	To develop an IoT-based assistive device for people with autism spectrum disorder (ASD)	Reporting	✓	✗	✓	✓

body movements, Tang [34] has developed an IoT-based approach for understanding emotions. It is a difficult challenge for neurotypical people, thus they evaluated various sensors to add emotion labels to emotion API and system training prediction emotion. For those with ASD, an image exchange communication system developed by Tang and Winoto [35] has been shown to assist them in expressing themselves as well as aiding their families, caretakers, and teachers in using the system. As a result of data gathered by sensing instruments, autistic people's descriptions are automatically sent to their aides if social communication is in a poor state. However, the sensors now in use do not provide adequate coverage for all of the potentially lethal scenarios.

The effects of geofencing the safe zone and activity identification in illnesses including Alzheimer's autism, and dementia were also demonstrated by Kollias et al. [9], who created a smartphone app. IoT-based software, Azimo, should be able to run on a variety of various devices. The authors developed an Android app by analyzing activity detection algorithms and enhancing accuracy and efficiency with the least amount of delay. An instructional platform was developed by Liu et al. [36]. The researchers created a robot that can mimic ASD and vice versa. As a teacher, coach, etc., the robot is requested to mimic the autistic child's activities in order to better understand them. Improves social communication and imitation abilities in autistic children, as well as behavior analysis and feedback to caregivers, using motor learning techniques. However, by engaging in more complicated dialogues, it is possible to increase DL and neural language processing.

The energy route and life balance of IoT devices were highlighted as a solution by Einarson et al. [37]. The prototype systems are impacted by the IoT's common and underlying structure. Based on the detection of the stress, they propose to improve the participation activities of the targeted end-users and link the gadgets. Using IoT, Badotra and Panda [38] have developed a smart object-oriented gadget that has a direct influence on enhancing the quality of life of autistic persons They used platforms and intelligent objects to categorize the various kinds of autism. There are three main kinds of beneficial technologies and objects: social interaction enhancers, learning supporters, and behavior deterrents. This categorization aids in the eradication of the particular requirements of each and every autistic and impaired person [44].

An IoT and P2P-based method to improve the quality of life (QoL) of autistic children has been reported by Sula et al. [39]. Gadgets and technology like cellphones, laptops, and touch screen tablets thrill children with autism. Children are forced to consider the consequences of their actions, feelings, and desires as a result of the introduction of smart gadgets into their lives. Autistic children's focus and quality of life are considered to improve with the development of abilities such as mathematics, language, and socialization. For students diagnosed with ASD, Badotra and Panda [40] provided an environment. IoT and P2P with diverse visual systems, such as photos, realistic drawings, objects, and written phrases, are all part of their strategy. There were a few variations in the study offered in order to improve and expand on their earlier work. For example, they analyzed the pros and downsides of several arithmetic aids for autistic pupils.

Karakosta et al. [41] used the Kaspar robot to treat seven kids with ASD at an elementary school in Greece. Unprompted imitation, patients' interpersonal and communication skills, prompted speech, and attention were studied to see if employing Kaspar had any effect on them. Patients' teachers were astonished to find that their treatment had a good effect on their speaking and communication abilities. Eye gazing, attentiveness, imitation, and gesture recognition prompted and unprompted were some of the characteristics they used to assess their performance [45, 46]. A group of 23 autistic youngsters were divided into two groups: one for human teachers and one for robots. They then compared the development and identification of novel gestural gestures using these two serving techniques. In the end, the input obtained by the two teams was identical. To put it another way, the structure of a child's lesson can have a substantial influence on the gestural learning of children with autism spectrum disorder (ASD).

Regarding hypersensitive individuals with autism spectrum disorder, Khullar et al. [43] have proposed an IoT companion that can recognize and control the patient's environment. Sensory information is detected and retrieved by electrical sensors in their suggested method. 93percent of respondents of caregivers agree with the technique, but VR, ML, and DL algorithms can make it smarter. [42] provides a robot-based engagement method for kindergarten students with autism to strengthen their narrative abilities. NAO was used to facilitate communication and gestures amongst patients who spoke Chinese [47–49]. According to the researchers' findings, children are better able than physicians to conduct constructive conversations with robots. However, the study's results did not show a significant improvement in the participants' motions [50, 51].

5. Discussion

Technical and comparative analyses of current ASD methods are presented here. Some technical and statistical replies to the problems posed in Section 1 were as follows.

5.1. Which Methods to ASD Are Being Discussed and Reviewed in This Analysis? Figure 4 shows the proportion of current ASD treatment options. It is clear that the majority of publications focus on enhancing the quality of life for children with autism spectrum disorders. There are 16 studies using this method for the diagnosis of autistic condition. On the other hand, a total of 12 publications examined all possible methods for diagnosing and measuring illness severity. Autism is a lifelong illness with no known treatment, so finding ways to improve the quality of life for those who are affected by it is a compelling reason to continue research in this area.

Additionally, parents or caregivers identify autism and its severity at the earliest age of 3 and provide treatment remedies. Early detection of autism has numerous advantages, though [52, 53].

5.2. What Techniques and Processes Are Used in the Treatment of Autism Spectrum Disorders? According to Figure 5, data mining approaches are the most popular

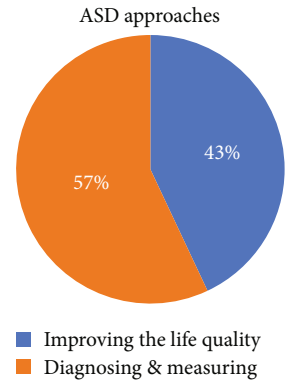

Figure 4: A variety of ASD treatment methods in the published literature.

which is further described as in 2 axes in which the y -axis indicates the number of papers counts and the x -axis represents different approaches used in ASD. Pattern-recognition algorithms are the primary way of extracting useful information from big datasets. Data mining and the healthcare sector have produced effective early identification methods and other health service technologies regarding clinical and diagnostic data. Also, the mining algorithms include characterization, generalization, clustering, classification, evolution, association, data visualization, pattern matching, and metarule-guided extraction. This study found that data mining technologies are most commonly utilized to improve the quality of life for children with autism spectrum disorders (ASD). It can, however, only be used with wearable sensors and smart devices that collect information. It is important to point out that such technology lacks sufficient intelligence approaches. Since it is a controlled setting, it is utilized instead of being used in the actual world.

In this study, the second and third most popular techniques of feature selection and reporting are discussed. It is possible to minimize dimensionality by picking a subset of the features input variables using feature selection technique such as GA or other approaches. Papers that used robots to improve patients' quality of life were the source of the reporting methodologies. It is used to compare the impressions of human and machine treatment. Since they have enough speed, but still require additional development, they are a viable option.

In addition, recent publications have featured GA, DL, and P2P approaches that provide a variety of services for individuals with ASD by utilizing AI. The approaches are fast enough, but the precision is not high enough to be useful for parallel computation done with IoT devices [54].

5.3. What Are the ASD Performance Metrics? The research papers have been reviewed based on various quality characteristics such as sensitivity, accuracy, reaction and specificity time in the ASD approaches, as depicted in Figure 6. According to our findings, the reaction speed and efficiency were the most important attribute aspects in Internet of Things-based autism spectrum disorder detection devices and systems. In general, we discussed four procedures and

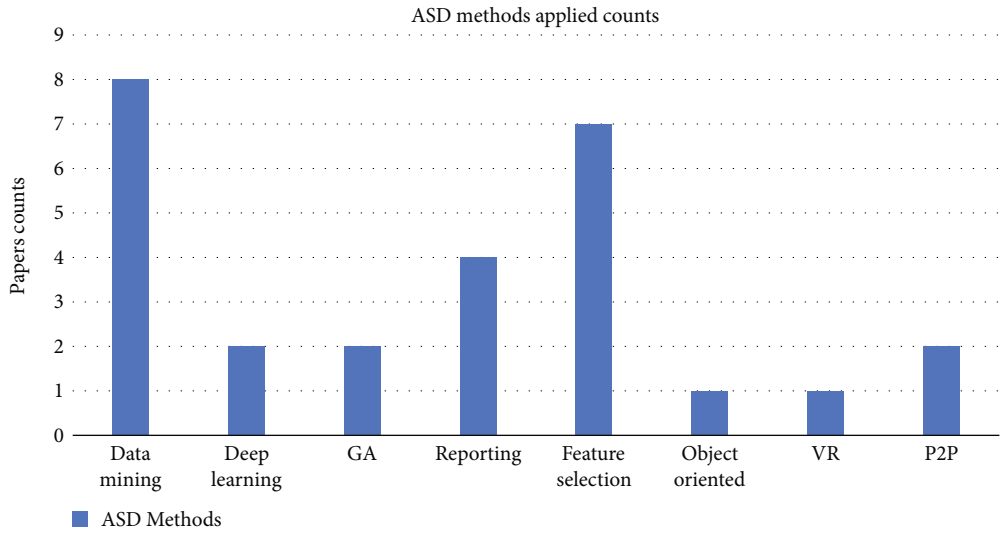

Figure 5: The proportion of procedures employed in ASD approaches that have been published in the literature.

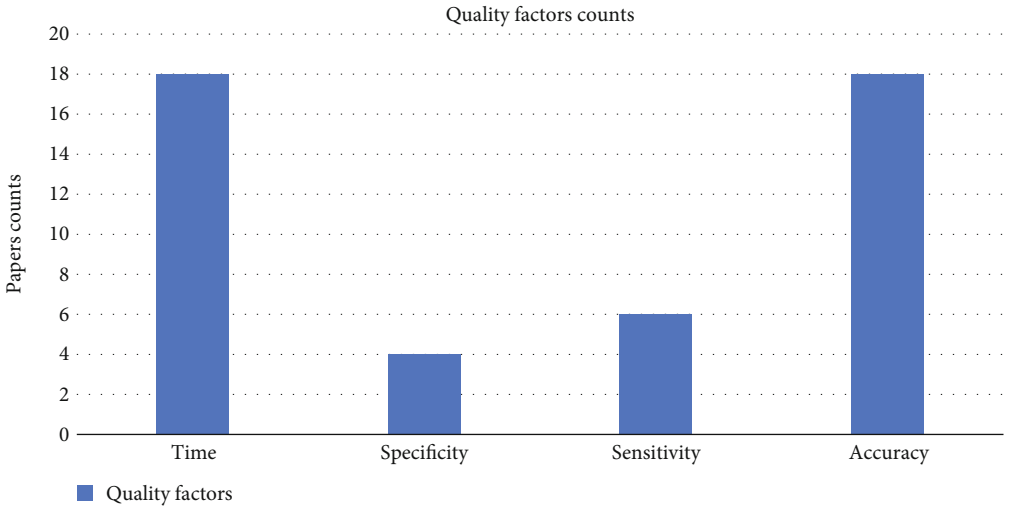

Figure 6: Quality elements in ASD approaches are compared and contrasted.

fundamental factors in the x-axis; however, other essential aspects, such as CCR, reliability, and processing speed, might be examined as well with respect to their counts in the y-axis.

5.4. Find Out Which Scientific Journals or Conferences Are Published Based on ASD. As per Figure 7 and the application of SLR techniques on the Asperger syndrome investigations, IEEE has published 11 articles out of a total of 28 research work that were selected. As a result, IEEE has the maximum number of publications that have been evaluated. The chart shows 2 axes in which the y-axis indicates the number of publishers papers counts and the y-axis represents different publisher names.

5.5. ASD Techniques Use Which Platforms and Sensors? Figure 8 illustrates how several research projects use a range of platforms and sensors to put ASD concepts into practice. Smart belts, heart rate variability (HRV), and pulse oximetry are just a few of the current technologies and sensors that go under the umbrella term "wearable sensors." The pie chart shows different platforms and sensor comparison in ASD methods.

6. Open Issues

This research indicates that creating IoT-based strategies for children with ASD faces several unresolved concerns and different experiences. The following are some of the concerns that have not been fully addressed so far:

(i) Object-oriented segmentation strategy aid reduces the particular demands of children with autism in the diagnosis and measurement of illness severity for those with ASD

(ii) Using various automatons to improve the quality of life for children with autism spectrum disorder is

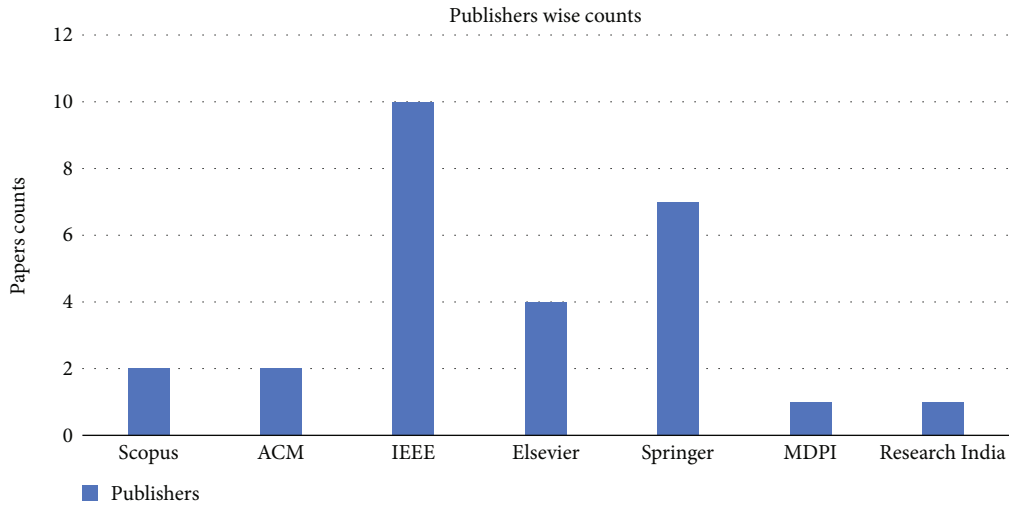

Figure 7: Some ASD articles are already being published by some publications.

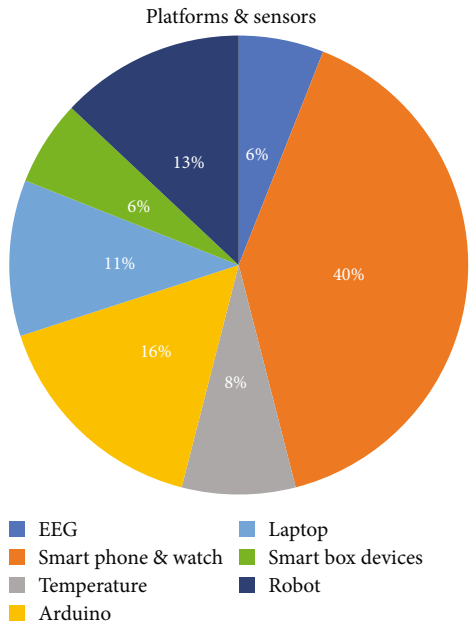

Figure 8: Sensor and platform comparison in ASD methods.

one of the most unanswered questions in the approach towards this end. It is a method for learning autistic children how to imitate gestures and simultaneously speak

(iii) To anticipate and assess autistic behavior, wearable gadgets are employed in all classifications of techniques (EMG, pulse oximeters, GSR, and GPS). Sensors may be integrated into any gadget or worn as a separate outfit

(iv) DL is a significant unanswered issue in the field of autism spectrum disorder diagnosis, and it may be used to a range of approaches, including multiside databases and brain imaging

Additionally, the ASD that integrates Internet of Things-based devices raises a variety of challenges, including the following:

(i) Integrity: the integrity of all information must be preserved during the transmission process between devices and arrive at its final destination intact and secure

(ii) Availability: availability ensures that the approved portion has access to all IoT-based healthcare services, including global, local, and cloud-based services, when required due to different attacks

(iii) Self-healing: it is vital for IoT-based networks to have self-healing capabilities because of the risk of medical equipment failing. Additional devices for interaction should therefore be able to provide a minimal level of security

7. Conclusion

Patients with ASD benefit greatly from the adoption of IoT devices with SS network consist. One of the most difficult aspects of treating autism in children is finding the correct IoT solutions. Sensors, platforms, and methodologies in ASD can have a significant influence on the children, and this is often the case. There were 28 articles included in this review that looked at various methods to ASD published between 2014 and 2020. In both 2016 and 2018, the number of articles published was close to the previous year's total. The most papers are published in the IEEE journal, with a percentage of 51%. Selected 28 studies were divided into two groups: those that focused on diagnosing patients and those that supported efforts to enhance the QoL of such patients. Nearly 43% of respondents thought of studies examining new methods for diagnosing and assessing the severity of ASD in children, while 57% thought about ways to enhance the quality of life for such youngsters. Additionally, all of the selected methodologies were evaluated in

terms of accuracy, sensitivity, specificity, and time, among other variables. There has been a comparative examination of ASD and IoT-based devices based on the case studies offered. Most research studies are aimed at enhancing the QoL of autistic children, according to the findings. New ASD techniques and gadgets for autistic persons will benefit from research into IoT-based variations on traditional ASD approaches such as AL, ML, and SS network.

To keep classic ASD techniques safe, IoT-based devices are becoming more and more common. Also, several studies have shown that children with ASD prefer robots over people for assistance. NAO's eye contact attention is steadier than in a traditional classroom for youngsters with ASD [47]. In addition, IoT solutions cut caregiving and support expenses and are simple to use, in contrast to traditional methods of protecting patients.

Emotions, on the other hand, can have an impact on the effectiveness of human-based therapy in ways that sensors and robots cannot. Robotic behavior should resemble that of humans in order to prepare for the unpredictability of our reality. In order to accomplish the goal, robots or other technologies that interact with people will need to incorporate emotional and cognitive computing. These are some of the limitations of this review: When searching for research, we used the terms "autism spectrum disorder," "internet of things," and "autism in the internet of things" (non-English speakers).

Journals, chapter books, and thesis were not included in this investigation. Research on IoT-based ASD methods has been addressed and published in different languages (we think).

Data Availability

Data is not supported by this research.

Conflicts of Interest

The authors do not have any conflict of interest with anyone.

References

[1] M. Masum, I. M. Nur, M. J. H. Faruk, M. I. Adnan, and H. Shahriar, *A Comparative Study of Machine Learning-Based Autism Spectrum Disorder Detection with Feature Importance Analysis*, COMPSAC 2022: Computer Software and Applications Conference, 2022.

[2] A. Rehman, T. Saba, M. Kashif, S. M. Fati, S. A. Bahaj, and H. Choudhary, "A revisit of Internet of Things technologies for monitoring and control strategies in smart agriculture," *Agronomy*, vol. 12, no. 1, p. 127, 2022.

[3] S. Badotra and S. N. Panda, "A review on software-defined networking enabled IoT cloud computing," *IIUM Engineering Journal*, vol. 20, no. 2, pp. 105–126, 2019.

[4] A. Sundas and S. Panda, "IoT and WSN based smart surveillance system for patients with closed-loop alarm," *International Journal of Scientific & Technology Research*, vol. 8, pp. 508–511, 2019.

[5] C. J. Raman, "An IoT-based system for supporting children with autism spectrum disorder," in *2021 Innovations in Power and Advanced Computing Technologies (I-PACT)*, pp. 1–5, Kuala Lumpur, Malaysia, November 2021.

[6] M. Hosseinzadeh, J. Koohpayehzadeh, A. O. Bali et al., "A review on diagnostic autism spectrum disorder approaches based on the Internet of Things and machine learning," *The Journal of Supercomputing*, vol. 77, no. 3, pp. 2590–2608, 2021.

[7] S. Badotra and A. Sundas, "A systematic review on security of E-commerce systems," *International Journal of Applied Science and Engineering*, vol. 18, no. 2, pp. 1–19, 2021.

[8] S. Badotra, D. Nagpal, S. N. Panda, S. Tanwar, and S. Bajaj, "IoT-enabled healthcare network with SDN," in *2020 8th International Conference on Reliability, Infocom Technologies and Optimization (Trends and Future Directions)(ICRITO)*, pp. 38–42, Noida, India, June 2020.

[9] K. F. Kollias, C. K. Syriopoulou-Delli, P. Sarigiannidis, and G. F. Fragulis, "The contribution of machine learning and eye-tracking technology in autism spectrum disorder research: a review study," in *2021 10th International Conference on Modern Circuits and Systems Technologies (MOCAST)*, pp. 1–4, Thessaloniki, Greece, July 2021.

[10] A. Sundas, S. Badotra, Y. Alotaibi, S. Alghamdi, and O. I. Khalaf, "Modified Bat algorithm for optimal VM's in cloud computing," *Computers, Materials & Continua*, vol. 72, no. 2, pp. 2877–2894, 2022.

[11] N. Farooqi, F. Bukhari, and W. Iqbal, "Predictive analysis of autism spectrum disorder (ASD) using machine learning," in *2021 International Conference on Frontiers of Information Technology (FIT)*, pp. 305–310, Islamabad, Pakistan, December 2021.

[12] C. M. V. Wong, R. Y. Y. Chan, Y. N. Yum, and K. Wang, "Internet of Things (IoT)-enhanced applied behavior analysis (ABA) for special education needs," *Sensors*, vol. 21, no. 19, p. 6693, 2021.

[13] N. Kaur, A. Kaur, N. Dhiman, A. Sharma, and R. Rana, "A systematic analysis of detection of autism spectrum disorder: IOT perspective," *International Journal of Innovative Science and Modern Engineering (IJISME)*, vol. 6, no. 6, pp. 10–13, 2020.

[14] S. Dedgaonkar, R. K. Sachdeva-Bedi, K. Kothari, R. Loya, and S. Godbole, "Role of iot and ml for autistic people," *International Journal of Future Generation Communication and Networking*, vol. 13, no. 3s, pp. 773–781, 2020.

[15] M. J. Afzal, S. Tayyaba, M. W. Ashraf, F. Javaid, and V. E. Balas, "A case study: impact of Internet of Things devices and pharma on the improvements of a child in autism," in *Emergence of Pharmaceutical Industry Growth with Industrial IoT Approach*, pp. 49–83, Academic Press, 2020.

[16] L. Gundaboina, S. Badotra, T. K. Bhatia et al., "Mining cryptocurrency-based security using renewable energy as source," *Security & Communication Networks*, vol. 2022, article 4808703, 13 pages, 2022.

[17] V. Deepak, S. J. J. Thangaraj, and M. R. Khanna, "An improved early detection method of autism spectrum anarchy using Euclidean method," in *2020 Fourth International Conference on I-SMAC (IoT in Social, Mobile, Analytics and Cloud) (I-SMAC)*, pp. 1173–1178, Palladam, India, October 2020.

[18] K. B. Sundhara Kumar and K. Bairavi, "IoT based health monitoring system for autistic patients," *Proceedings of the 3rd International Symposium on Big Data and Cloud Computing Challenges (ISBCC – 16')*, V. Vijayakumar and V. Neelanarayanan, Eds., , Springer, Cham, 2016.

[19] S. Yang, B. Gao, L. Jiang et al., "IoT structured long-term wearable social sensing for mental wellbeing," *IEEE Internet of Things Journal*, vol. 6, no. 2, pp. 3652–3662, 2018.

[20] C. Krishna and N. Sampath, "Healthcare monitoring system based on IoT," in *2017 2nd International Conference on Computational Systems and Information Technology for Sustainable Solution (CSITSS)*, Bengaluru, India, 2017.

[21] Y. Eshetu, P. Bhuyan, and A. Behura, "A service-oriented IoT system to support individuals with ASD," in *2018 International Conference on Communication, Computing and Internet of Things (IC3IoT)*, Chennai, India, 2018.

[22] L. Y. Mano, B. S. Faiçal, L. H. V. Nakamura et al., "Exploiting IoT technologies for enhancing Health Smart Homes through patient identification and emotion recognition," *Computer Communications*, vol. 89-90, pp. 178–190, 2016.

[23] K. Lavanya, S. M. Anitha, J. Joveka, R. Priyatharshni, and S. Mahipal, "Emotion recognition of autism children using IoT," *International Journal of Applied Engineering Research*, vol. 14, no. 6, 2019.

[24] A. M. Amiri, N. Peltier, C. Goldberg et al., "WearSense: detecting autism stereotypic behaviors through smartwatches," *Healthcare*, vol. 5, no. 1, p. 11, 2017.

[25] H. Moradi, S. E. Amiri, R. Ghanavi, B. N. Aarabi, and H. R. Pouretemad, "Autism screening using an intelligent toy car," in *ubiquitous computing and ambient intelligence*, pp. 817–827, Springer, Cham, 2017.

[26] T. Manju, S. Padmavathi, and D. Tamilselvi, "A rehabilitation therapy for autism spectrum disorder using virtual reality," in *Smart Secure Systems—IoT and Analytics Perspective*, pp. 328–336, Springer, Singapore, 2018.

[27] D. Abdolzadegan, M. H. Moattar, and M. Ghoshuni, "A robust method for early diagnosis of autism spectrum disorder from EEG signals based on feature selection and DBSCAN method," *Biocybernetics and Biomedical Engineering*, vol. 40, no. 1, pp. 482–493, 2020.

[28] V. G. Shankar, D. S. Sisodia, and P. Chandrakar, "DataAutism: an early detection framework of autism in infants using data science," in *Data Management, Analytics and Innovation*, pp. 167–178, Springer, New York, 2020.

[29] T. L. Praveena and N. M. Lakshmi, "Detection of autism spectrum disorder effectively using modified regression algorithm," in *Emerging Research in Data Engineering Systems and Computer Communications*, pp. 163–175, Springer, New York, 2020.

[30] M. E. Alam, M. S. Kaiser, M. S. Hossain, and K. Andersson, "An IoT-belief rule base smart system to assess autism," in *2018 4th international conference on electrical engineering and information & communication technology (iCEEiCT)*, Dhaka, Bangladesh, 2018.

[31] M. A. Rahman and M. Bhuiyan, "IOT enabled sensor in multimodal intelligent applications for children with special needs," in *2015 Internet Technologies and Applications (ITA)*, Wrexham, UK, 2015.

[32] Y. Shi, S. Das, S. Douglas, and S. Biswas, "An experimental wearable IoT for data-driven management of autism," in *2017 9th International Conference on Communication Systems and Networks (COMSNETS)*, Bengaluru, India, 2017.

[33] A. I. Sumi, M. F. Zohora, M. Mahjabeen, T. J. Faria, M. Mahmud, and M. S. Kaiser, "fASSERT: a fuzzy assistive system for children with autism using Internet of Things," in *Brain Informatics. BI 2018. Lecture Notes in Computer Science*, vol. 11309, Springer, Cham, 2018.

[34] T. Y. Tang, "Helping neuro-typical individuals to "Read" the emotion of children with autism spectrum disorder," in *Proceedings of the 15th international conference on interaction design and children-IDC'16*, pp. 666–671, Manchester United Kingdom, 2016.

[35] T. Y. Tang and P. Winoto, "An interactive picture exchange communication system (PECS) embedded with augmented aids enabled by IoT and sensing technologies for Chinese individuals with autism," in *Proceedings of the 2018 ACM international joint conference and 2018 international symposium on pervasive and ubiquitous computing and wearable computers-UbiComp'18*, pp. 299–302, Singapore Singapore, 2018.

[36] X. Liu, X. Zhou, C. Liu et al., "An interactive training system of motor learning by imitation and speech instructions for children with autism," in *2016 9th International Conference on Human System Interactions (HSI)*, Portsmouth, July 2016.

[37] D. Einarson, P. Sommarlund, and F. Segelström, "IoT-support systems for parents with ADHD and autism," in *2016 International Conference on Computation System and Information Technology for Sustainable Solutions (CSITSS)*, Bengaluru, India, October 2016.

[38] S. Badotra and S. N. Panda, "SNORT based early DDoS detection system using Opendaylight and open networking operating system in software defined networking," *Cluster Computing*, vol. 24, no. 1, pp. 501–513, 2021.

[39] A. Sula, E. Spaho, K. Matsuo, L. Barolli, F. Xhafa, and R. Miho, *An IoT-Based Framework for Supporting Children with Autism Spectrum Disorder. Information Technology Convergence*, Springer, New York, 2013.

[40] S. Badotra and S. N. Panda, "Evaluation and comparison of OpenDayLight and open networking operating system in software-defined networking," *Cluster Computing*, vol. 23, no. 2, pp. 1281–1291, 2020.

[41] E. Karakosta, K. Dautenhahn, D. S. Syrdal, L. J. Wood, and B. Robins, "Using the humanoid robot Kaspar in a Greek school environment to support children with autism spectrum condition," *Paladyn, Journal of Behavioral Robotics*, vol. 10, no. 1, pp. 298–317, 2019.

[42] W. C. So, M. K. Y. Wong, W. Y. Lam et al., "Who is a better teacher for children with autism? Comparison of learning outcomes between robot-based and human-based interventions in gestural production and recognition," *Research in Developmental Disabilities*, vol. 86, pp. 62–75, 2019.

[43] V. Khullar, H. P. Singh, and M. Bala, "IoT based assistive companion for hypersensitive individuals (ACHI) with autism spectrum disorder," *Asian Journal of Psychiatry*, vol. 46, pp. 92–102, 2019.

[44] M. Masum, I. Nur, M. H. Faruk, M. Adnan, and H. Shahriar, *A Comparative Study of Machine Learning-Based Autism Spectrum Disorder Detection with Feature Importance Analysis*, COMPSAC 2022: Computer Software and Applications Conference, 2022.

[45] A. Patel, *Caregiver Satisfaction of Telehealth Initiatives for Developmental Surveillance and Evaluation in Pediatric Autism Spectrum Disorder*, The Eleanor Mann School of Nursing Undergraduate Honors Theses, 2022, https://scholarworks.uark.edu/nursuht/166.

[46] M. Jodra and V. Rodellar, "What Can Technology Do for Autistic Spectrum Disorder People?," in *International Work-Conference on the Interplay between Natural and Artificial Computation*, pp. 301–309, Springer, Cham, 2022.

[47] M. Masud, G. S. Gaba, K. Choudhary, R. Alroobaea, and M. S. Hossain, "A robust and lightweight secure access scheme for cloud based E-healthcare services," *Peer-to-Peer Networking and Applications*, vol. 14, no. 5, pp. 3043–3057, 2021.

[48] M. S. Farooq, A. Arooj, R. Alroobaea et al., "Untangling computer-aided diagnostic system for screening diabetic retinopathy based on deep learning techniques," *Sensors*, vol. 22, no. 5, p. 1803, 2022.

[49] T. Ahsan, F. Z. Khan, Z. Iqbal et al., "IoT devices, user authentication, and data management in a secure, validated manner through the blockchain system," *Wireless Communications and Mobile Computing*, vol. 2022, Article ID 8570064, 13 pages, 2022.

[50] S. S. Joudar, A. S. Albahri, and R. A. Hamid, "Triage and priority-based healthcare diagnosis using artificial intelligence for autism spectrum disorder and gene contribution: a systematic review," *Computers in Biology and Medicine*, vol. 146, p. 105553, 2022.

[51] P. Moridian, N. Ghassemi, M. Jafari et al., "Automatic autism spectrum disorder detection using artificial intelligence methods with MRI neuroimaging: a review," 2022, https://arxiv.org/abs/2206.11233.

[52] C. Iwendi, S. U. Rehman, A. R. Javed, S. Khan, and G. Srivastava, "Sustainable security for the Internet of Things using artificial intelligence architectures," *ACM Transactions on Internet Technology*, vol. 21, no. 3, pp. 1–22, 2021.

[53] A. Shabbir, M. Shabbir, A. R. Javed, M. Rizwan, C. Iwendi, and C. Chakraborty, "Exploratory data analysis, classification, comparative analysis, case severity detection, and Internet of Things in COVID-19 telemonitoring for smart hospitals," *Journal of Experimental & Theoretical Artificial Intelligence*, vol. 8, pp. 1–28, 2022.

[54] R. Abid, C. Iwendi, A. R. Javed et al., "An optimised homomorphic CRT-RSA algorithm for secure and efficient communication," *Personal and Ubiquitous Computing*, vol. 1, pp. 1–14, 2021.

Hindawi
Journal of Sensors
Volume 2022, Article ID 6099330, 12 pages
https://doi.org/10.1155/2022/6099330

Research Article

Intelligent Water Drops Algorithm-Based Aggregation in Heterogeneous Wireless Sensor Network

S. Nonita[1], **Pardayev Abdunabi Xalikovich**[2], **C. Ramesh Kumar**[3], **Manik Rakhra**[4], **Issah Abubakari Samori**[5], **Yuselino Maquera Maquera**[6] and **José Luis Arias Gonzáles**[7]

[1]*Department of Information Technology, Indira Gandhi Delhi Technical University for Women Delhi, India*
[2]*Department of Scientific Research, Innovation and Training of Scientific and Pedagogical Personnel, Tashkent Institute of Finance, Tashkent, Uzbekistan*
[3]*School of Computing Science and Engineering, Galgotias University, Greater Noida, Uttar Pradesh, India*
[4]*Department of Computer Science and Engineering, Lovely Professional University, Phagwara, Punjab 144411, India*
[5]*School of Engineering Sciences, University of Ghana, Ghana*
[6]*Universidad Nacional del Altiplano Puno, Puno, Peru*
[7]*Pontificia Universidad Católica del Peru, Peru*

Correspondence should be addressed to Issah Abubakari Samori; iasamori@st.ug.edu.gh

Received 25 July 2022; Revised 22 August 2022; Accepted 3 September 2022; Published 28 September 2022

Academic Editor: Linesh Raja

This paper provides a novel implementation of the intelligent water drops (IWD) method for resolving data aggregation issues in heterogeneous wireless sensor networks (WSN). When the aggregating node is utilized to transmit the data to the base station, the research attempts to show that the traffic situations of WSN may be modified appropriately by parameter tuning and algorithm modification. IWD is used to generate an optimum data aggregation tree in WSN as one of its applications. IWD assumes that all nodes in the environment are identical, resulting in identical parameter updates for all nodes. In practical scenarios, however, diverse nodes with variable beginning energy, communication range, and sensing range characteristics are deployed. In order to replicate the influence of heterogeneity in the environment, improved IID (IIWD) is offered as an enhancement to the original IID. The suggested enhancement is appropriate for scenarios in which the aggregation node is utilized to transmit data to the base station in heterogeneous configurations. In terms of residual energy, dead nodes, payload, and network lifespan, a series of simulation results demonstrates that the proposed IIWD significantly improves the accuracy and effectiveness of the IWD method in comparison.

1. Introduction

The study of nature to model the solution of practical problems with a computer is gaining great popularity as a result of its multiple applications for tackling optimization-related issues. There are several explorable algorithms, and intelligent water drops (IWD) is one of these nature-inspired algorithms that has recently been implemented. IWD algorithm takes into account the dynamics followed by water droplets in order to route their pathways to the lake or ocean through rivers. The algorithm employs the process occurring between river water droplets and riverbed dirt. The IWD method, proposed by Hosseini [1], has been successfully used to tackle several optimization-related issues and provides benefits such as an active feedback mechanism and a high degree of resilience [2]. IWDs are formed from natural water droplets and collaborate to discover the greatest solution to any given problem. The IWD method can be used to solve problems involving maximization or minimization [3, 4]. The treatments are as follows: The IWD algorithm builds objects in stages. As a

result, IWD is a population-based beneficial algorithm. In the IWD algorithm, two basic ways are used to build IWDs: dirt and velocity are attributes. Both of these characteristics may change throughout the course of a lifetime [5, 6]. The International Women's Day an IWD flows from a source to a destination. The IWD begins its trip with 0 initial velocity dirt. During its voyage, it goes through the environment from which it originated. It accelerates and some dirt is eliminated [7, 8]. The method employs several iterations in which water droplets attempt to uncover the optimum path from source to destination on a bed of environment particles. In order to do this, the node(s) create control packets that go to the destination. These packets, known as IWDs, have two primary characteristics: velocity and dirt. The environment consists mostly of the dirt of the environment bed. The environmental movement of IWD is governed by the following principles:

(i) The velocity of IWD decreases near a high soil bed and vice versa

(ii) High-velocity IWD accumulates more soil than a low-velocity IWD

(iii) The soil in the environment is eroded more by a high-velocity IWD than a low-velocity IWD

Further, IWD has been used to create optimal aggregation tree and has also been proven to achieve the energy efficiency in homogeneous WSN, given the lack of critical attention paid to heterogeneity [9]. Furthermore, there are several applications of WSN, where the deployed nodes possess different characteristics with regard to communication range, sensing range, battery, and sensing services. It is possible to refer to a wireless sensor network as dynamic if it is able to handle the following two atomic operations: node-move-in and node-move-out, which, respectively, refer to nodes leaving an existing network and nodes entering into an existing network. The primary IWD algorithm has proved to be efficient in discovering the optimal path in the sensor network. However, it does not incorporate the effect of heterogeneity in the network, which is introduced due to distinctive characteristics of the nodes.

The heterogeneity of the node's features offers applications with flexibility and improves network operations within predetermined cost restrictions. For instance, if a network is installed with fewer high-energy nodes, the network may survive for a longer period of time, but the sensing range will be constrained. In contrast, deploying a network with a greater number of low-energy nodes would reduce the network's lifespan while increasing its sensing range. However, a mixture of nodes with varying energy levels may achieve a perfect balance between network longevity and sensing range [10, 11]. Experimentation on energy-based heterogeneous node deployment demonstrates a substantial increase in sensing performance. In addition, the cost analysis of hybrid sensor networks verifies these networks' cost effectiveness [10].

In this paper, we suggest using the IWD technique to construct an efficient data aggregation tree in heterogeneous WSN. Heterogeneity in WSN is determined by the initial energy of the network's nodes. Thus, the words low nodes and high nodes are used to categorize nodes based on energy. Low nodes indicate low-energy sensor nodes, while high nodes indicate high-energy sensor nodes.

2. Problem Statement

The WSN is modelled as a join of two graphs: $G = G1 + G2$, where G_1 is (V_n, E_n) and $V_n = V_l \bigcup V_h$. Here, V_n represents all the sensing nodes, and V_l represents the low nodes and V_h represents the high nodes. Also, $E_n \bigcup e_{ij}$, where e_{ij} is the edge connecting the node i to node j, which is based on the premise that if the distance between the node and the neighboring node is less than the predefined communication range R of the node i. However, G_2 is (V_a, E_a), where V_a represents the set of aggregation nodes and E_a represents the edges connecting the aggregation nodes to the base station (BS).

The problem can be stated as to find a subset $G_{\text{opt}} \subset G_1$, where $G_{\text{opt}} = (V_{\text{opt}}, E_{\text{opt}})$, where $V_{\text{opt}} \subset V_n$,where V_{opt} are the optimal number of low-energy and high-energy sensing nodes and $E_{\text{opt}} \subset E_n$, minimizing the hop count from the sensing nodes to the aggregation nodes. The problem can be solved as a constrained optimization problem, having the nonlinear programming form as Minimize $f(X)$, where $X = \{x_1, x_2, x_3 \cdots .. x_n\}$ subject to R, where R is the cost function subject to the following constraint:

$$R = \sum h_{lh} + h_{ha}. \tag{1}$$

Here, h_{hs} denotes the hop count from low-energy nodes to high-energy nodes and h_{sa} represents the hop count from high energy nodes to the aggregation nodes.

Assumption: All the aggregation nodes, V_a, are connected directly to the BS.

3. Related Work

This section depicts the key features of the current routing protocols in WSN. Because WSNs differ from other networks such as MANETs (mobile ad hoc networks) and mobile networks, routing is particularly complex. The main task of WSN is sensing, collecting, and delivering the information for further processing. Many methods have been developed in this area [12, 13]. Furthermore, according to a complex network theory, predicting connection quality in wireless sensor networks is akin to predicting link quality in social networks. The routing problem of a network determines the quickest route (also known as the optimum path) between the transmitter and the destination [14, 15]. Signal strength changes a lot on mobile and ad hoc networks, causing a lot of route failures and lowering performance. Several ideas have been proposed to estimate the signal strength-based link availability projection for best routing [16, 17]. This link information may be utilized to calculate the connection breakdown time and, as a result, either repair the existing route or locate a new one for the packets. The reduction of packet losses and end-to-end latency improves performance [18, 19]. Because of specific WSN characteristics, the routing algorithms in WSN vary from conventional networks in numerous ways.

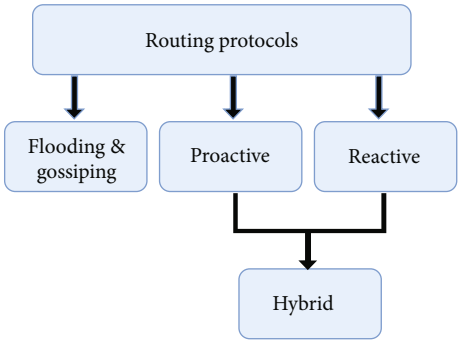

Figure 1: Taxonomy of routing protocols in WSNs.

WSN sensor nodes are energy restricted and cannot be recharged owing to their special application requirements. Furthermore, the major uses of WSN are to detect data, analyzes it, and then broadcast it to the BS. As a result, routing towards the BS is a critical job, and multiple algorithms have been presented [20], aimed at distinct circumstances or situations owing to their unique characteristics. In terms of infrastructure building and maintenance approach, the routing algorithms in WSN may be divided into three broad classes:

Flooding and gossiping [21] do not need to retain topological information in advance and build routing paths after network setup or the commencement of network activity. The flooding-based routing algorithm transmits the observed data to all adjacent nodes and continues this process until the data reaches the base station. In contrast, routing systems based on gossiping randomly choose a limited number of neighbors and relay messages to them until the BS is reached. In contrast to the flooding technique, the gossiping approach reduces the quantity of data packets transferred across the network but creates the data packet implosion problem, which incurs additional expenses for WSN. Independent of network activities, proactive routing algorithms design and maintain the routing architecture continually. BS establishes and transmits the path to all sensor nodes to all network nodes. During network operations, the sensor nodes retain this information and use it to route data packets over these channels. In MANET, the proactive DSDV [22] protocol is used, but for WSN, a variety of tree-based methods [23] are offered (e.g., one-phase pull diffusion [24]). The intelligent interaction of wireless sensor networks (WSN) and mobile ad hoc networks (MANET) with the Internet of Things increases its user appeal and commercial viability [25, 26]. By merging wireless sensor and mobile networks with the Internet of Things, it is possible to develop new MANET-IoT devices and IT-based networks. This technology facilitates user mobility while decreasing network implementation expenses [27, 28]. One of the fundamental principles of Internet of Things systems is the networking of intelligent objects and their compliance with communications technology. Wireless networks (wireless sensor networks (WSN), whose characteristics include sensing, data collecting, heterogeneous connectivity, and data processing, play a major role in the Internet of Things (IoT) system [29, 30]. Paths are continuously maintained during network operations, although at a great cost of resources. Several evolutions of the classical methods, such as BVR [31], VRR [32], and S4 [33], are provided, providing enhancements to the classical approaches in terms of reduced resource utilization, a quality required for realistically scaled WSN.

Reactive routing algorithms generate routing pathways as necessary. The architecture for routing is constructed by the sensing nodes that must convey data to the base station, not previously. In MANETs, the most used reactive routing method is AODV [34], whereas in WSN push diffusion [35], in FRA [36] and LRDE [37] are the most prevalent. These techniques save resources during times of inactivity but incur the cost of identifying pathways for each originating node.

The following significant category of routing algorithms contains hybrid algorithms, which integrate both reactive and proactive network behaviors based on network circumstances. Several hybrid routing techniques for MANETs now exist. Zone routing protocol (ZRP) [38] is the first hybrid method utilized in MANETs. The ZRP protocol splits the network into zones, and inside these zones, routes are decided proactively, while outside of these zones, routes are established reactively. ZRP has a lower routing overhead benefit. However, zones are determined statically in ZRP. Therefore, the SHARP protocol [39] presented an enhancement based on the dynamic generation of zones. The zones are only generated around nodes that generate a considerable amount of incoming data, which decreases routing overhead along with jitter and loss rate. However, in the context of WSN, the routing strategy that incorporates a hybrid adaptive solution has not yet been extensively deployed. In addition, MANET routing techniques are inapplicable to WSN owing to its fundamental properties.

Figure 1 [40] depicts a thorough overview of routing methods in WSN based on node heterogeneity. Significant benefits of adopting energy-based node heterogeneity in WSN include increased throughput and decreased latency. However, heterogeneity reduces the hop count among the sensor nodes and the sink; hence, the delivery rate in heterogeneous WSN is greater than homogeneous WSN.

Broadly, there are three primary types of heterogeneity, namely, energy, computational, and link heterogeneity. Energy heterogeneity focuses on nodes' diverse battery power. Higher-end nodes get more energy. Few nodes have higher computing capacity than others in computational heterogeneity. Complex data processing and memory-intensive processes need powerful nodes. Connection heterogeneity focused on link bandwidth between nodes. Long-distance nodes are provided a high-bandwidth transmission connection to ensure reliable data transfer. Most WSNs employ energy heterogeneity since it uses the least resources. Computational and connection heterogeneities hinder WSN without energy heterogeneity. Figure 2 illustrate the types of heterogeneity.

Energy heterogeneity is split into three types based on node power levels: two-level, three-level, and multilevel. Two-level defines regular and advanced nodes. Normal, advanced, and super nodes are specified in three-level networks. Multilevel randomizes energy distribution in nodes. Recent routing techniques have been developed to improve WSN performance [41, 42]. Cluster-based and tree-based routing protocols are the main types.

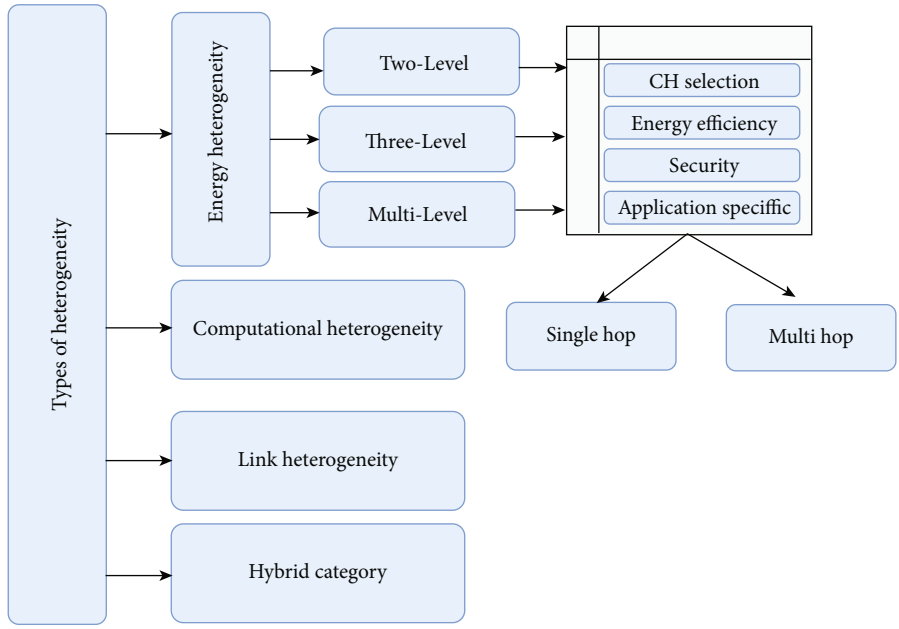

Figure 2: Types of heterogeneity in WSN.

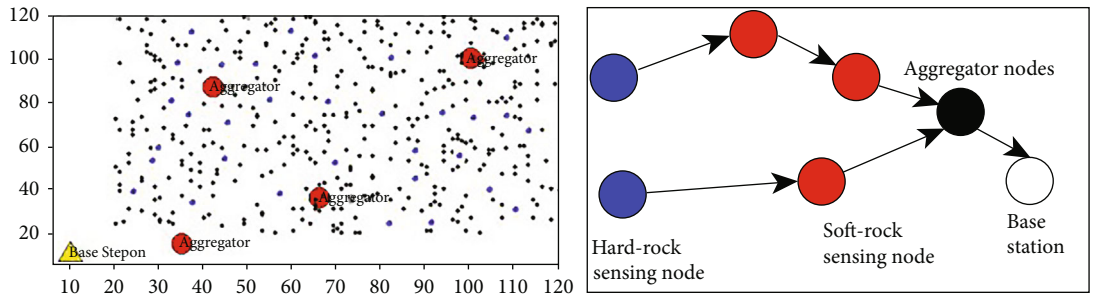

Figure 3: Data aggregation tree in heterogeneous WSN.

Table 1

Type of packet	Source ID	Next hop ID	IWD soil	IWD velocity

Table 2: Simulation parameters.

Parameters	Values	Description
N	300	Total number of nodes
S	5 – 30	Total number of source nodes
R	10-12 m	Communication energy
E_{init}	0.5 J	Initial energy of each node

LEACH is a clustering routing technique that forms clusters and elects cluster leaders to communicate with the BS [43–45]. LEACH does not consider residual energy while choosing a cluster head [20, 46, 47]; hence, it performs poorly in diverse environments [48]. As a result, stable election protocol (SEP), a clustering routing protocol, was devised. Cluster heads are chosen using a weighted probability [49]. SEP's two-level heterogeneous network performed well. Multilevel heterogeneous WSNs could not use the routing protocol properly. This led to the DEEC algorithm for multilevel heterogeneous networks [50]. In DEEC, cluster heads were chosen based on the average network energy and sensor node energy. Other clustering-based routing protocols include EDFCM [51], an enhancement of DEEC, REP [52], and EEPCA [53].

The second type of routing protocols is tree-based, wherein nodes are organized as trees and root node does the data aggregation and further transmitting it to the BS. Tree-based techniques suit aggregation needs [54] like forest fire, industrial, event, health, and other monitoring systems.

Data aggregation in tree-based protocols is optimized for energy efficiency. Finding an optimum aggregation tree is NP-hard [55], similar to Steiner tree, weighted set cover issue [56]. DD [57] identifies the quickest routing channels to transport data packets throughout the network and opportunistically

Table 3: IIWD parameters.

Parameters	Values	Description
Initsoil	1000	Initial soil of edge
Initvel	200	Initial velocity of an IWD
a_v, b_v, c_v	1,0.01,1	Velocity updating parameters
a_s, b_s, c_s	1,0.01,1	Soil updating parameters
ρ_n	0.9	Local soil updating parameter

aggregates them. However, DD is not considered efficient since the aggregation nodes are chosen randomly and may be distant from the source nodes. GIT is an approximation approach suggested to build an energy-efficient route in an ideal aggregation tree [58]. Krishnamacharya et al. [59] also demonstrated the advantages of data aggregation.

Liao et al. [60] devised ant colony optimization (ACO) method, which simulates ant foraging behavior. These ants drop pheromone to designate a trail for the colony to follow. The ant colony method is used by Schurgers et al. [61] to aggregate data. Wu et al. [62] improved the chance of locating aggregation nodes in WSN exploiting ACO by widening search area surrounding routing pathways. These works outperform standard approaches in energy conservation.

4. System Model

The system model used here takes into account the random distribution of stationary sensor nodes in a monitoring region. Here, there are three distinct kinds and configurations of nodes: sensor nodes, aggregator nodes, and the base station (BS). The sensing node collects data and transmits it at regular intervals to the aggregation node. However, sensing nodes are designed to be of two types: low nodes (representing low-energy sensing nodes) and high nodes (representing high-energy sensing nodes). Figure 3 depicts the aggregation tree for data. The aggregator node aggregates data and transmits it to the BS. The BS should be installed outside of the network, and it should transfer the processed data to the control center.

The heterogeneous WSN thus categorizes nodes as low nodes (), high nodes (), and aggregator nodes (). The upper nodes contain tenfold more energy than the low nodes. The communication model used in this study is the first-order radio model, whereas the sensing model previously applied was the deterministic sensing model [63]. This model implies that each node participates in the sensing process. The detected data is compared to aThreshold, whose value is predetermined. If the detected data exceeds the defined threshold, the data is sent to the next node. Consequently, sensing coverage is the total of the sensing coverage of all network nodes. However, the difference lies in predefined communication and sensing ranges. Subsequently, the communication and the sensing range of 'N_h,' 'N_l,' and 'N_a' are abbreviated as 'R_{ch},' 'R_{sh}'; 'R_{cl},' 'R_{sl}'; and 'R_{ca},' 'R_{sa}' respectively. In addition, the ranges are defined in incremental order as '$R_{ca} > R_{ch} > R_{cl}$' and '$R_{sa} > R_{sh} > R_{sl}$.'

5. Preliminaries

The primary IWD algorithm is based on the evidence that water drops always find the shortest route towards lake or ocean. Despite encountering obstacles and constraints, water drops always find an optimal path trailing twists and turns. Correspondingly, the environment is also affected as the water drops move from one place to another. In the same way, the environment also tries to alter the nature of the water drops. In a way, both water drops and environment have a tendency to influence each other. The environment here refers to the soil bed of the river. When the drops move fast, they tend to remove more soil from the soil beds than when they are slow. Drops that are trying to find an optimal path are called intelligent water drops (IWD). The three essential parameters that define the path taken by the water drops are velocity ($\text{Velocity}^{\text{IWD}}$), Soil ($\text{Soil}^{\text{IWD}}$), and Soil of the river bed $\text{Soil}^{\text{Edge}}$. These parameters change as the data packet moves from source node to destination. The change of the velocity is updated by a parameter $\Delta\text{Vel}^{\text{IWD}}$, which is calculated as follows:

$$\Delta\text{Vel}^{\text{IWD}}(t) = \frac{a_v}{b_v + c_v[soil(i,j)]^2}, \tag{2}$$

where a_v, b_v, and c_v are constants that are application dependent. $\text{soil}(i, j)$ is the soil on the bed of edge between node i and node j. During the initialization phase, each edge is assigned an equal amount of this parameter. The velocity can be evaluated as

$$\text{Vel}^{\text{IWD}}_{(t+1)} = \text{vel}^{\text{IWD}}_{t} + \Delta\text{Vel}^{\text{IWD}}_{(t+1)}. \tag{3}$$

The decrease in the soil of an edge is calculated as

$$\Delta\text{soil}(i,j) = \frac{a_s}{b_s + c_s[\text{time}(i,j)]^2}, \tag{4}$$

where a_s, b_s, and c_s are the application dependent constants, which specify the relationship between the weight of the edges and the time that a data packet takes to move from a node i to j. The time taken is given by

$$\text{time}(i,j) = \frac{\text{HUD}(i,j)}{\text{Vel(IWD)}}, \tag{5}$$

where $\text{HUD}(i, j)$ is the heuristic function defined for an application for calculating the hop counts on the path.

$$\text{HUD}(i,j) = \sum_{k \in R_j} h_{sj} + h_{jd}, \tag{6}$$

where R_j represents the routing nodes in the neighborhood of node j, and h_{kj} and h_{jd} represents the hop count from source node s to node j and from node j to destination node d or the BS, respectively.

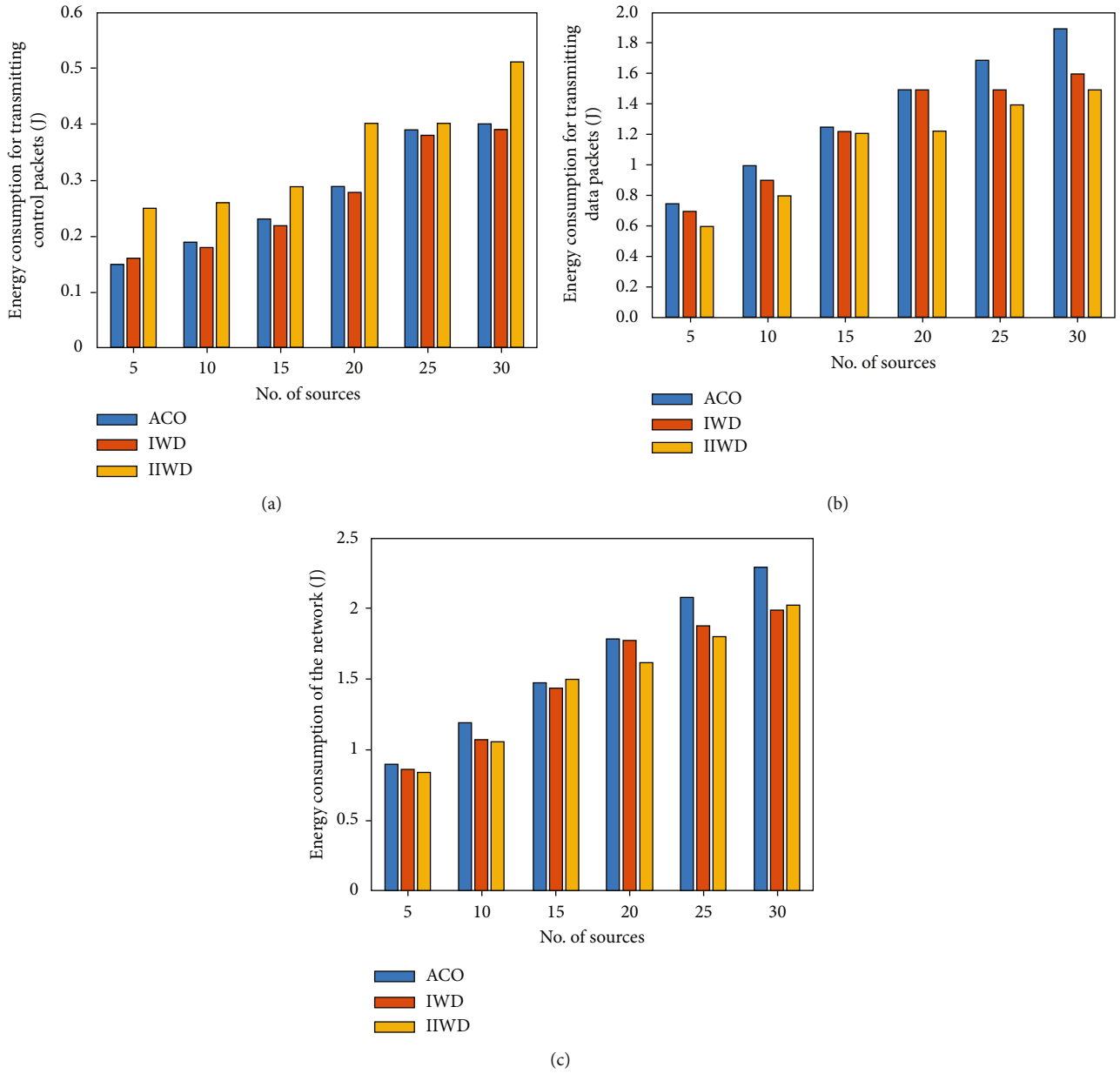

Figure 4: (a) Energy Consumption for transmitting control packets (Joule). (b) Energy consumption for transmitting data packets (Joule). (c) Energy consumption of the network (Joule).

6. IWD Algorithm for Heterogeneous Network

In homogeneous environments, the IWD method may be used to produce an optimum data aggregation tree solution. Sensing nodes with data produce IWD to search for pathways linking to the base station or the closest aggregator node. These IWDs produce an aggregate tree by generating pathways using the approach described in Section 2. Here, it is proposed that the low node will locate a way to the high node, which will then transfer the data to the base station or aggregator nodes. Since a result, the energy consumption of low nodes will be decreased, as they will be required to find a way to the closest high nodes. Nonetheless, there are instances in which the route constructed by this IWD lacks a connection point and hence cannot discover other nodes visited by other IWDs. In such a case, the chance of constructing an ideal tree will be diminished. To update the soil in this situation, the IWD packet is transmitted to the neighbors of all modes. When a high node receives an IWD packet, it broadcasts an updated soil packet to its neighbors. Each neighboring node u updates the soil(u, v) based on the information received. The packet format of IWD is as shown in Table 1.

In the table, type of packet determines whether it is a data packet or a control packet. Source ID is the ID of the source node generating the IWD. Next hop ID is the next neighboring node. IWD soil and IWD velocity are the updated parameters of IWD on the path for a particular IWD. However, there

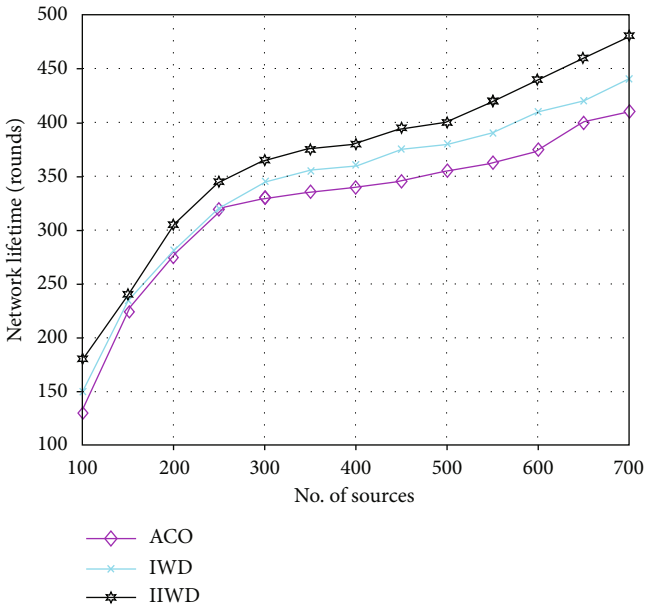

Figure 5: Network lifetime of IIWD vs. IWD.

exists a condition when an IWD cannot find any nodes that are visited by other nodes.

The algorithm for the heterogeneous network proceed as follows. Initially, all the aggregation nodes store the identity of the BS and broadcast their ID(s) to the network. Each sensing node stores the aggregation ID along with the information of next hop neighbors and the soil value of all the paths. Initially, all the paths are assigned equal values. Later, these values are updated as the IWD traverses on that edge. The edge connecting the node to the BS is assigned a lesser value of soil so that the additional gain in the velocity can be achieved. Additionally, lower soil value of an edge represents lesser number of hop counts, thus attracting more IWDs on this path. Because of this proposed modification, the probability of IWD to reach an aggregation node is higher, when a high node receives a soil update packet, an update message to all the neighboring nodes is sent and hence, following this approach, IWD reaches the aggregation nodes faster. In a way, high node increases the velocity of the IWD. Thus, the velocity parameters of the neighboring nodes of the high nodes are evaluated from the following:

$$\mathrm{vel}^{\mathrm{IWD}} = \mathrm{InitVel} + \frac{a_v}{b_v + c_v[\mathrm{soil}(k,j)]^2}. \tag{7}$$

Additionally, the soil of the edge between the high node and the aggregation node is updated as follows:

$$\Delta\mathrm{soil}(k,j) = \frac{a_s}{b_s + c_s\left(\mathrm{HUD}(a,i)/\mathrm{vel}^{\mathrm{IWD}}\right)}. \tag{8}$$

Here, equation is defined from the node i to the aggregation node, representing the hop counts from the node i to the aggregation node a.

$$\Delta\mathrm{soil}(k,j) = (1-\rho_n)\mathrm{soil}(a,i) - \rho_n\left(1 + hd_k - hd_j\right)\Delta\mathrm{soil}(a,i), \tag{9}$$

where ρ_n is the local soil updating factor for the path connecting to the aggregation node. By updating these values repeatedly, the probability of IWD to reach the aggregation nodes becomes higher, and hence, the IWD reaches the aggregation node faster, reducing the delay. By enhancing the probability of all the neighboring nodes, the soil of the path is declined notably, thus making IWD reach faster to the destination. The algorithm starts with the initialization of static parameters a_s, b_s, c_s, and a_v, b_v, c_v, and then follows the steps mentioned below, going through several iterations:

The sensing node generates a control packet named IWD with initial values of velocity and soil viz. Initvel and Initsoil.

(1) A neighboring node is selected randomly by calculating the probability values, which is inversely proportional to the soil of the edges. The probability value which is inversely proportional to the soil of the edge is calculated as

$$P_{\mathrm{IWD}}(i,j) = \frac{\mathrm{soil}(i,j)}{\sum_{k \notin vc(\mathrm{IWD})}\mathrm{soil}(i,k)}, \tag{10}$$

where $vc(\mathrm{IWD})$ is the subset of the nodes, which IWD should not visit in order to satisfy the application constraints

(2) If the next hop node is a high node, therefore, the velocity is updated from Equation (7); otherwise, it is updated from Equation (2)

(3) Similarly, the soil of the edge for high node is updated from Equation (8); otherwise, it is updated from Equation (4)

(4) The process continues till the state of complete termination is reached, which is when the IWD either reaches an aggregation node or a BS

This IWD algorithm described above can build a data aggregation tree with a minimum number of hop count in heterogeneous setup. Once an aggregation node is found, the steps mentioned above updates the amount of soil in its neighborhood and hence increases the likelihood of selecting the best aggregation. Thereby, enhancing the chances of IWD moving through this aggregation node whenever it reaches its neighborhood in the next round.

6.1. Assumptions

(1) IWDs will try to find paths to the nearest aggregation nodes instead of BS

(2) All the aggregation nodes are connected to the BS directly, i.e., using single-hop

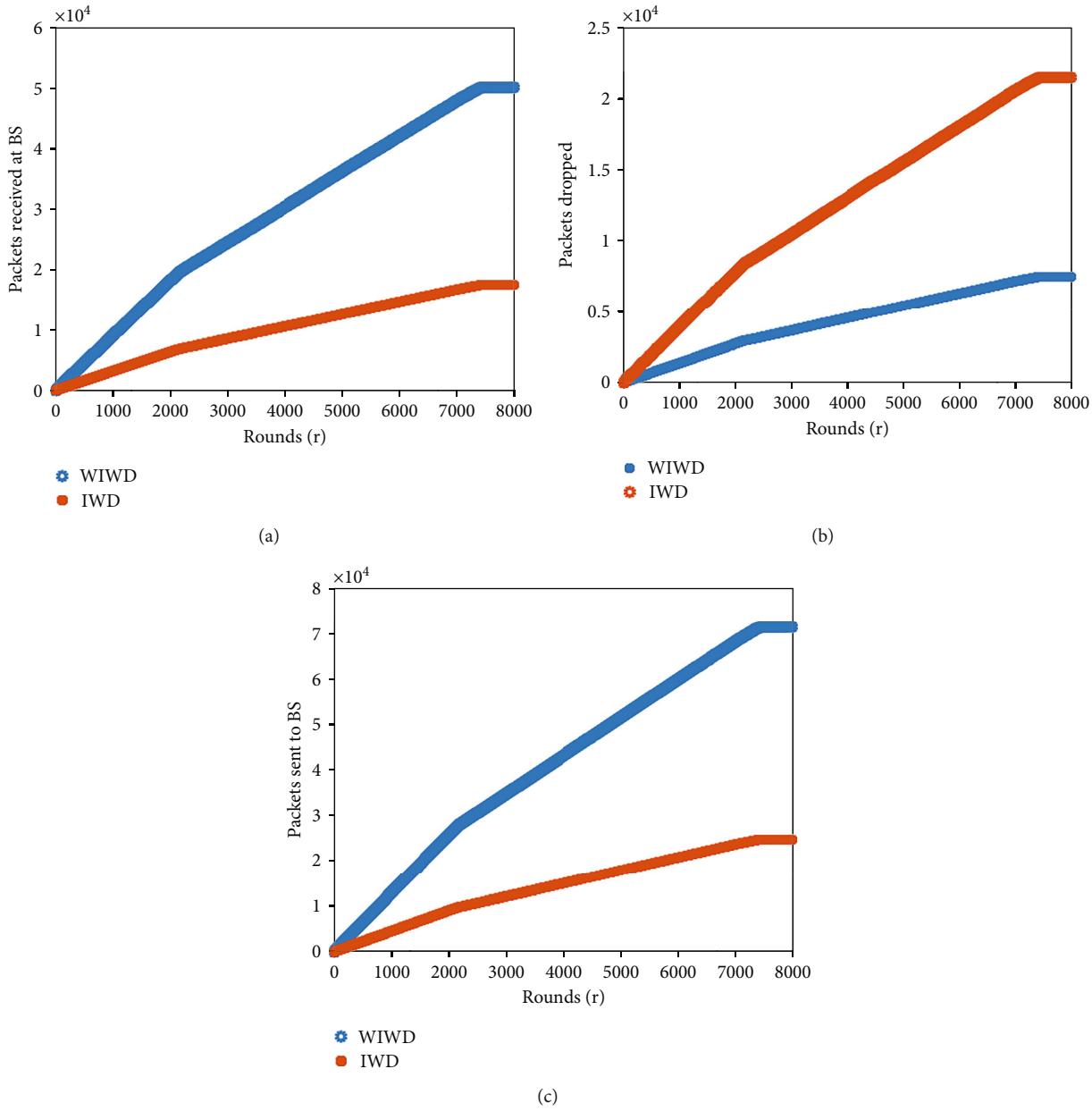

Figure 6: (a) Packets received at BS of WIWD vs. IWD. (b) Packets dropped of WIWD vs. IWD. (c) Packets sent to BS of WIWD vs. IWD.

(3) Each node maintains an information table containing the details of neighbors and the soil

(4) Sensor nodes are deployed uniformly in the field of square dimension

(5) Sensor nodes and BS are stationary

(6) The heterogenous nature of WSN is defined in terms of node energy

(7) BS is supposed to be equipped with a battery source and hence it is not energy limiting like the other deployed nodes

7. Results and Discussions

C++-based simulator is used to mimic the state-of-the-art ant colony optimization (ACO), IWD and the proposed IIWD. This simulator models' actual events like as collisions, carrier sensing, latency, network lifespan, and backoff. For aggregator nodes, the proposed requirements are consistent with iPAQ motes since they compute quicker, use less power, and have a greater sensing and communication range [64, 65], while the proposed specifications for sensing nodes are consistent with MICA2 sensor nodes [66, 67]. The performance of a 100-node network randomly spread across a $100 \times 100\,m^2$ region with single sink is evaluated. The total number of aggregation nodes picked for a specific simulation cycle ranges from 5 to 30. The data packet is of 250

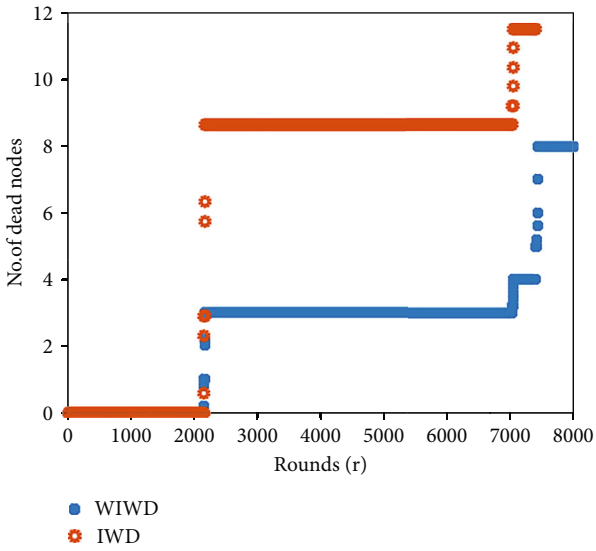

Figure 7: No. of dead nodes of WIWD vs. IWD.

bytes and the control packet is of 8 bytes, with transmission frequencies of 100 Hz and 10 Hz, respectively. Every time the configuration is executed, 30 random deployments are taken into account and the mean of the results is calculated. When simulation starts, random nodes are distributed throughout the network with sink node at the center position. Once positioned, nodes exchange messages to begin routing. Table 2 displays simulation parameters.

Parameters for the proposed IIWD algorithm are presented in Table 3. The values are taken according to the parameters provided in [9]. The evaluation metrics are as follows: total energy consumption (J) and network lifetime (rounds, which are discussed in the subsequent section.

7.1. Total Energy Consumption: Analysis. Total energy consumption is the sum of the energy spent transmitting control packets, sending data packets, and the network's total energy consumption. The total energy consumption is the sum of the energy used by all network nodes in a particular round. Various simulations are run with a variety of source node counts. The fundamental IWD, the ACO, and the proposed IIWD algorithm are compared. As shown in Figure 4, the average energy consumption for sending control packets is slightly higher than that of ACO and IWD (a). This may be a result of the increased number of control packets transmitted to refresh the edge soil. As demonstrated in Figure 2, the average energy consumption for transmitting data packets through IIWD is slightly less than that of IWD and ACO Figure 4(b). This is because the number of hops necessary for data transmission has dropped. In addition, it can be determined from Figure 4(c) that IIWD's overall energy usage is less than that of IWD and ACO since its routing function provides greater aggregation options. Consequently, the network's total energy consumption is dramatically reduced.

7.2. Network Lifetime. A comparison is made between the performance of IIWD and ACO and IWD in terms of network lifespan calculated as the time until the first node runs out of energy as shown in Figure 5. The notion of updating the velocity of all IWDs along the designated path expedites the delivery of packets to aggregation nodes, hence extending their lifespan. IIWD has showed the greatest improvement in network lifespan. This improvement is due to the algorithm's suggested method, which minimizes the total number of data packets transmitted in the network, consequently reducing energy consumption of the nodes. As all aggregation nodes are directly linked to the BS, the resulting routing pathways are shorter. The results illustrate the efficacy of the proposed strategy for extending network life.

7.3. Payload. Payload is determined by comparing the actual number of data packets delivered at the base station as shown in Figure 6(a) vis-à-vis number of packets supplied by the source nodes. Typically, payload consists of the actual data transported over a network for an application. The primary concern addressed in this paper is that the payload varies based on the aggregation process used. The effectiveness of aggregation in WIWD in a heterogeneous environment is determined using payload parameter. Figure 6(b) depicts the number of data packets received at the base station for varying numbers of rounds. In the WIWD method, payload, or the total amount of packets delivered over the network, is around 70 percent fewer than in the IWD algorithm. The fewer data packets sent may be ascribed to the aggregating procedure. Figure 6(c) provide details of packets sent to BS Instead of being routed immediately to the base station, the data packets are passed to the aggregation node, which aggregates them before sending them to the base station. Thus, the total number of rounds remains the same despite a modest reduction in the amount of data packets transferred to the base station.

7.4. Number of Alive Nodes. The proposed WIWD algorithm shows significant improvement in the number of alive nodes with respect to the total number of nodes. Since the nodes create paths to the aggregation nodes and send data packets up to these aggregation nodes, the nodes tend to stay longer and subsequently improve this performance metric vis-a-vis IWD. Here, the same logic implies that the incorporation of high-end nodes and the concept of waterfall in the network enhance the number of alive nodes in the network. Remarkably, the number of alive nodes in the WIWD increases by almost 40% Figure 7.

8. Conclusion

The suggested optimization model seeks to crystallize the different aspects that affect the sensor network's heterogeneity. The study draws on prior understanding of efficient routing algorithms for homogenous networks. In the context of this study, aggregator nodes insert new packet entries with regard to time and pop depending on the freshness factor defined by packet length for each node. Incorporating heterogeneity into a network may increase the total energy consumption and network longevity, according to the findings of this study. This method has been seen to save both the

residual energy of the nodes and the average energy of the network. This is evident from the results of the studies conducted to determine the performance of the IIWD. The technique outperforms prior algorithms due to the fact that the route selection performed by its routing function offers superior aggregation alternatives. The threshold of the nodes' remaining energy is used to determine which aggregation node is chosen. The findings demonstrate that the network's longevity has also been greatly enhanced.

9. Future Scope

The issue which leaves room for further investigation is that of time synchronization. There lies great scope for future research while exploring strategies for weak and strong time synchronization that may be experimented on, to further streamline the aggregation process with the BS.

Data Availability

Data available from the corresponding author upon request.

Conflicts of Interest

There authors declare that they have no conflict of interest.

References

[1] H. S. Hosseini, "Problem solving by intelligent water drops," in *2007 IEEE Congress on Evolutionary Computation*, pp. 3226–3231, Singapore, 2007.

[2] A. B. Dariane and S. Sarani, "Application of intelligent water drops algorithm in reservoir operation," *Water Resources Management*, vol. 27, no. 14, pp. 4827–4843, 2013.

[3] V. Singh, G. Sharma, R. C. Poonia, N. K. Trivedi, and L. Raja, "Source redundancy management and host intrusion detection in wireless sensor networks," *Recent Advances in Computer Science and Communications*, vol. 14, no. 1, pp. 43–47, 2021.

[4] H. Shah-Hosseini, "Intelligent water drops algorithm: A new optimization method for solving the multiple knapsack problem," *International Journal of Intelligent Computing and Cybernetics*, vol. 1, no. 2, pp. 193–212, 2008.

[5] R. K. Garg, J. Bhola, and S. K. Soni, "Healthcare monitoring of mountaineers by low power wireless sensor networks," *Informatics in Medicine Unlocked*, vol. 27, article 100775, 2021.

[6] S. Gupta, R. C. Poonia, V. Singh, and L. Raja, "Tier application in multi-cloud databases to improve security and service availability," in *Handbook of Research on Cloud Computing and Big Data Applications in IoT*, pp. 82–93, IGI Global, 2019.

[7] R. A. Rahman, S. Masrom, N. B. Zakaria, and S. Halid, "Auditor choice prediction model using corporate governance and ownership attributes: machine learning approach," *International Journal of Emerging Technology and Advanced Engineering*, vol. 11, no. 7, pp. 87–94, 2021.

[8] A. Singh, "Existence of coincidence and fixed point theorems for non-linear hybrid map on generalized space," *Journal of Informatics and Mathematical Sciences*, vol. 5, no. 1, pp. 21–28, 2013.

[9] H. Shah-Hosseini, "The intelligent water drops algorithm: a nature-inspired swarm-based optimization algorithm," *International Journal of Bio-Inspired Computation*, vol. 1, no. 1/2, pp. 71–79, 2009.

[10] H. Shah-Hosseini, "An approach to continuous optimization by the intelligent water drops algorithm," *Procedia-Social and Behavioral Sciences*, vol. 32, pp. 224–229, 2012.

[11] S. Salmanpour, H. Omranpour, and H. Motameni, "An intelligent water drops algorithm for solving robot path planning problem," in *2013 IEEE 14th International Symposium on Computational Intelligence and Informatics (CINTI)*, pp. 333–338, Budapest, Hungary, 2013.

[12] I. F. Akyildiz, S. Weilian, Y. Sankarasubramaniam, and E. Cayirci, "A survey on sensor networks," *IEEE Communications Magazine*, vol. 40, no. 8, pp. 102–114, 2002.

[13] J. Yick, B. Mukherjee, and D. Ghosal, "Wireless sensor network survey," *Computer Networks*, vol. 52, no. 12, pp. 2292–2330, 2008.

[14] A. S. Arora, L. Raja, and B. Bahl, "Data centric security approach: a way to achieve security & privacy in cloud computing," in *Proceedings of 3rd International Conference on Internet of Things and Connected Technologies (ICIoTCT)*, pp. 26-27, Jaipur, 2018.

[15] M. S. Avhankar, D. J. A. Pawar, S. Majalekar, and S. Kedari, "Mobile Ad Hoc Network Routing Protocols Using OPNET Simulator," *International Journal on Recent and Innovation Trends in Computing and Communication*, vol. 10, no. 1, pp. 1–7, 2022.

[16] M. B. Monir, A. A. Mohamed, and J. Bhola, "Energy aware routing for wireless sensor networks," *International Journal of Communication Networks and Information Security (IJCNIS)*, vol. 14, no. 1, p. 12, 2022.

[17] J. M. Sahayaraj, N. C. S. Kumar, P. Mukunthan, N. Tamilarasan, and S. Jaya Pratha, "IEEHR: improved energy efficient honeycomb based routing in MANET for improving network performance and longevity," *International Journal on Recent and Innovation Trends in Computing and Communication*, vol. 10, no. 7, pp. 85–93, 2022.

[18] B. Boyapati and J. Kumar, "Parasitic Element Based Frequency Reconfigurable Antenna with Dual Wideband Characteristics for Wireless Applications," *In International Journal on Recent and Innovation Trends in Computing and Communication*, vol. 10, no. 6, pp. 10–23, 2022.

[19] M. A. Haq, "A review on deep learning techniques for IoT data," *Electronics*, vol. 11, no. 1604, pp. 1–23, 2022.

[20] W. R. Heinzelman, A. Chandrakasan, and H. Balakrishnan, "Energy-efficient communication protocol for wireless microsensor networks," in *Proceedings of the IEEE Hawaii international conference on system sciences*, p. 110, Maui, HI, USA, 2000.

[21] S. Hedetniemi and A. Liestman, "A survey of gossiping and broadcasting in communication networks," *Networks*, vol. 18, no. 4, pp. 319–349, 1988.

[22] C. Perkins and P. Bhagwat, "Highly dynamic destination-sequenced distance-vector routing (DSDV) for mobile computers," in *ACM Conference on Communications Architectures, Protocols and Applications (SIGCOMM'94)*, pp. 234–244, London, UK, 1994.

[23] S. R. Drishya, S. R. Devi, and V. Vaidehi, "A Stable Clustering Scheme with Node Prediction in MANET," *International Journal of Communication Networks and Information Security*, vol. 13, no. 1, pp. 33–41, 2021.

[24] D. Yang, M. Ji, Y. Lv, F. Zhao, Q. Geng, and J. Bhola, "Research on zoning, optimization, stability, and nonlinear control of

wireless network in power grid communication," *Journal of Interconnection Networks*, 2022.

[25] T. Alhussain, "An energy-e?cient scheme for IoT networks," *International Journal of Communication Networks and Information Security*, vol. 13, pp. 199–205, 2021.

[26] D. Bhargava, B. Prasanalakshmi, T. Vaiyapuri, H. Alsulami, S. H. Serbaya, and A. W. Rahmani, "CUCKOO-ANN based novel energy-efficient optimization technique for IoT sensor node modelling," *Wireless Communications and Mobile Computing*, vol. 2022, Article ID 8660245, 9 pages, 2022.

[27] G. S. Sriram, "Challenges of cloud compute load balancing algorithms," *International Research Journal of Modernization in Engineering Technology and Science*, vol. 4, no. 1, pp. 1186–1190, 2022.

[28] S. L. Bangare, G. Pradeepini, and S. T. Patil, "Implementation for brain tumor detection and three dimensional visualization model development for reconstruction," *ARPN Journal of Engineering and Applied Sciences (ARPN JEAS)*, vol. 13, no. 2, pp. 467–473, 2018.

[29] S. Debnath, P. Satya, and B. C. Saha, "Pathotype characterization of Xanthomonas oryzae pv oryzae isolates of West Bengal and evaluation of resistance genes of bacterial blight of rice (Oryza sativa L.)," *Journal of Crop and Weed*, vol. 9, no. 1, pp. 198–200, 2013.

[30] P. H. Levine, K. Ajmera, B. O'Neill, V. Venkatesh, P. Garcia-Gonzalez, and H. J. Hoffman, "Demographic factors related to young age at diagnosis of chronic myeloid leukemia in India," *Clinical Epidemiology and Global Health*, vol. 4, no. 4, pp. 188–192, 2016.

[31] J. Heidemann, F. Silva, and D. Estrin, "Matching data dissemination algorithms to application requirements," in *1st International Conference on Embedded Networked Sensor Systems (SenSys'03)*, pp. 218–229, Los Angeles, CA, USA, 2003.

[32] R. Fonseca, S. Ratnasamy, D. Culler, S. Shenker, and I. Stoica, "Beacon vector routing: scalable point-to- point routing in wireless sensornets," in *USENIX 2nd Symposium on Networked Systems Design and Implementation (NSDI'05)*, Boston, MA, USA, 2005.

[33] M. Caesar, M. Castro, E. B. Nightingale, and A. Rowstron, "Virtual ring routing: network routing inspired by DHTs," in *ACM Annual Conference of the Special Interest Group on Data Communication (SIGCOMM'06)*, Pisa, Italy, 2006.

[34] Y. Mao, F. Wang, L. Qiu, S. S. Lam, and J. M. Smith, "S4: small state and small stretch routing protocol for large wireless sensor networks," in *USENIX 4th Symposium on Networked Systems Design and Implementation (NSDI'07)*, Cambridge, MA, USA, 2007.

[35] L. Gundaboina, S. Badotra, and S. Tanwar, "Reducing resource and energy consumption in cryptocurrency mining by using both proof-of-stake algorithm and renewable energy," in *2022 International Mobile and Embedded Technology Conference (MECON)*, pp. 605–610, Noida, India, 2022.

[36] E. Nakamura, H. Ramos, L. Villas, H. Oliveira, A. Aquino, and A. Loureiro, "A reactive role assignment for data routing in event-based wireless sensor networks," *Computer Networks*, vol. 53, no. 12, pp. 1980–1996, 2009.

[37] D.-H. Chae, K.-H. Han, K.-S. Lim, S.-Y. Ahn, and S.-S. An, "A localized route discovery for on-demand routing protocols in event-driven wireless sensor networks," *IEICE Transactions on Communications*, vol. E89-B, no. 10, p. 2828, 2006.

[38] Z. Haas and M. Pearlman, "The performance of query control schemes for zone routing protocol," in *ACM Conference on Applications, Technologies, Architectures and Protocols for Computer Communication (SIGCOMM'98)*, pp. 167–177, Vancouver, BC, Canada, 1998.

[39] R. L. Graham, L. Levi, D. Burredy et al., "Scalable Hierarchical Aggregation and Reduction Protocol (SHARP)TM Streaming-Aggregation Hardware Design and Evaluation," *High Performance Computing*, vol. 22, no. 2, pp. 41–59, 2020.

[40] K. Lin, J. J. P. C. Rodrigues, H. Ge, N. Xiong, and X. Liang, "Energy efficiency QoS assurance routing in wireless multimedia sensor networks," *IEEE Systems Journal*, vol. 5, no. 4, pp. 495–505, 2011.

[41] S. Tyagi and N. Kumar, "A systematic review on clustering and routing techniques based upon LEACH protocol for wireless sensor networks," *Journal of Network and Computer Applications*, vol. 36, no. 2, pp. 623–645, 2013.

[42] R. Paliwal and I. Khan, "Design and Analysis of Soft Computing Based Improved Routing Protocol in WSN for Energy Efficiency and Lifetime Enhancement," *International Journal on Recent and Innovation Trends in Computing and Communication*, vol. 10, no. 3, pp. 12–24, 2022.

[43] J. Yu, Y. Qi, G. Wang, and G. Xin, "A cluster-based routing protocol for wireless sensor networks with nonuniform node distribution," *AEU-International Journal of Electronics and Communications66*, vol. 66, no. 1, pp. 54–61, 2012.

[44] D. Kumar, T. C. Aseri, and R. B. Patel, "Multi-hop communication routing (MCR) protocol for heterogeneous wireless sensor networks," *Communications Convergence*, vol. 1, no. 2, pp. 130–145, 2011.

[45] S.-S. Wang and Z.-P. Chen, "LCM: a link-aware clustering mechanism for energy-efficient routing in wireless sensor networks," *IEEE Sensors Journal*, vol. 13, no. 2, pp. 728–736, 2013.

[46] A. H. Abdulaal, A. F. M. S. Shah, and A. K. Pathan, "NM-LEACH: A novel modified LEACH protocol to improve performance in WSN," *International Journal of Communication Networks and Information Security*, vol. 14, no. 1, pp. 1–10, 2022.

[47] J. Bhola, S. Soni, and G. K. Cheema, "Genetic algorithm based optimized leach protocol for energy efficient wireless sensor networks," *Journal of Ambient Intelligence and Humanized Computing*, vol. 11, pp. 1281–1288, 2020.

[48] G. Smaragdakis, A. Bestavros, and S. E. P. Ibrahim Matta, *A stable election protocol for clustered heterogeneous wireless sensor networks*, Boston University Computer Science Department, 2004.

[49] L. Qing, Q. Zhu, and M. Wang, "Design of a distributed energy-efficient clustering algorithm for heterogeneous wireless sensor networks," *Computer Communications*, vol. 29, no. 12, pp. 2230–2237, 2006.

[50] H. Zhou, W. Yuanming, H. Yanqi, and G. Xie, "A novel stable selection and reliable transmission protocol for clustered heterogeneous wireless sensor networks," *Computer Communications*, vol. 33, no. 15, pp. 1843–1849, 2010.

[51] N. Sharma and A. K. Sharma, "Cost analysis of hybrid adaptive routing protocol for heterogeneous wireless sensor network," *Sādhanā*, vol. 41, no. 3, pp. 283–288, 2016.

[52] J. Peng, T. Liu, H. Li, and B. Guo, "Energy-efficient prediction clustering algorithm for multilevel heterogeneous wireless sensor networks," *International Journal of Distributed Sensor Networks*, vol. 9, no. 2, Article ID 678214, 2013.

[53] G. Han, X. Jiang, A. Qian, J. J.. Rodrigues, and L. Cheng, "A comparative study of routing protocols of heterogeneous wireless sensor networks," *Scientific World Journal*.

[54] J. N. Al-Karaki, R. Ul-Mustafa, and A. E. Kamal, "Data aggregation in wireless sensor networks-exact and approximate algorithms," in *2004 Workshop on High Performance Switching and Routing, 2004. HPSR*, pp. 241–245, Phoenix, AZ, USA, 2004.

[55] C. Intanagonwiwat, R. Govindan, D. Estrin, J. Heidemann, and F. Silva, "Directed diffusion for wireless sensor networking," *IEEE/ACM Transactions on Networking (ToN)*, vol. 11, no. 1, pp. 2–16, 2003.

[56] C. Intanagonwiwat, D. Estrin, R. Govindan, and J. Heidemann, "Impact of network density on data aggregation in wireless sensor networks," in *Proceedings 22nd international conference on distributed computing systems*, Vienna, Austria, 2002.

[57] M. Dorigo and L. M. Gambardella, "Ant colony system: a cooperative learning approach to the traveling salesman problem," *IEEE Transactions on Evolutionary Computation*, vol. 1, no. 1, pp. 53–66, 1997.

[58] R. Misra and C. Mandal, "Ant-aggregation: ant colony algorithm for optimal data aggregation in wireless sensor networks," in *2006 IFIP International Conference on Wireless and Optical Communications Networks*, Bangalore, India, 2006.

[59] L. Krishnamachari, D. Estrin, and S. Wicker, "The impact of data aggregation in wireless sensor networks," in *Proceedings 22nd international conference on distributed computing systems workshops*, Vienna, Austria, 2002.

[60] W.-H. Liao, Y. Kao, and C.-M. Fan, "Data aggregation in wireless sensor networks using ant colony algorithm," *Journal of Network and Computer Applications*, vol. 31, no. 4, pp. 387–401, 2008.

[61] C. Schurgers, V. Tsiatsis, S. Ganeriwal, and M. Srivastava, "Optimizing sensor networks in the energy-latency-density design space," *IEEE transactions on mobile computing*, vol. 1, no. 1, pp. 70–80, 2002.

[62] J. Wu and S. Yang, "Coverage issue in sensor networks with adjustable ranges," in *Workshops on Mobile and Wireless Networking/High Performance Scientific, Engineering Computing/Network Design and Architecture/Optical Networks Control and Management/Ad Hoc and Sensor Networks/Compil*, Montreal, QC, Canada, 2004.

[63] A. Hossain, S. Chakrabarti, and P. K. Biswas, "Impact of sensing model on wireless sensor network coverage," *IET Wireless Sensor Systems*, vol. 2, no. 3, pp. 272–281, 2012.

[64] V. Tsiatsis, R. Kumar, and M. B. Srivastava, "Computation Hierarchy for In-Network Processing," *Mobile Networks and Applications*, vol. 2022, Article ID 8555489, pp. 505–518, 2005.

[65] R. Kumar, V. Tsiatsis, and M. B. Srivastava, "Computation hierarchy for in-network processing," in *Proceedings of the 2nd ACM international conference on Wireless sensor networks and applications*, San Diego, CA, USA, 2003.

[66] C. Li, Z. Sun, H. Wang, and H. Song, "A novel energy-efficient k-coverage algorithm based on probability driven mechanism of wireless sensor networks," *International Journal of Distributed Sensor Networks*, vol. 12, no. 4, Article ID 7474926, 2016.

[67] V. Kumar, S. B. Dhok, R. Tripathi, and S. Tiwari, "Cluster size optimisation with tunable Elfes sensing model for single and multi-hop wireless sensor networks," *International Journal of Electronics*, vol. 104, no. 2, pp. 312–327, 2017.

Hindawi
Journal of Sensors
Volume 2022, Article ID 6732150, 11 pages
https://doi.org/10.1155/2022/6732150

Research Article

Automatic Detection of Atrial Fibrillation from ECG Signal Using Hybrid Deep Learning Techniques

Saroj Kumar Pandey,[1] **Gaurav Kumar**,[1] **Shubham Shukla**,[2] **Ankit Kumar**,[1] **Kamred Udham Singh**,[3] **and Shambhu Mahato**[4]

[1]*Department of Computer Engineering & Applications, GLA University, Mathura 281406, India*
[2]*KIET Group of Institutions, Ghaziabad 201001, India*
[3]*Department of Computer Science and Information Engineering, National Cheng Kung University, 701 Tainan, Taiwan*
[4]*Department of Education, Janajyoti Multiple Campus, Lalbandi, Sarlahi, Nepal*

Correspondence should be addressed to Shambhu Mahato; shambhu.mahato@jjmc.edu.np

Received 13 July 2022; Revised 23 August 2022; Accepted 6 September 2022; Published 22 September 2022

Academic Editor: Aijun Yin

In cardiac rhythm disorders, atrial fibrillation (AF) is among the most deadly. So, ECG signals play a crucial role in preventing CVD by promptly detecting atrial fibrillation in a patient. Unfortunately, locating trustworthy automatic AF in clinical settings remains difficult. Today, deep learning is a potent tool for complex data analysis since it requires little pre and postprocessing. As a result, several machine learning and deep learning approaches have recently been applied to ECG data to diagnose AF automatically. This study analyses electrocardiogram (ECG) data from the PhysioNet/Computing in Cardiology (CinC) Challenge 2017 to differentiate between atrial fibrillation (AF) and three other rhythms: normal, other, and too noisy for assessment. The ECG data, including AF rhythm, was classified using a novel model based on a combination of traditional machine learning techniques and deep neural networks. To categorize AF rhythms from ECG data, this hybrid model combined a convolutional neural network (Residual Network (ResNet)) with a Bidirectional Long Short Term Memory (BLSTM) network and a Radial Basis Function (RBF) neural network. Both the F1-score and the accuracy of the final hybrid model are relatively high, coming in at 0.80% and 0.85%, respectively.

1. Introduction

A common arrhythmia known as atrial fibrillation (AF) has been linked to serious heart-related diseases such stroke and heart failure [1, 2]. It increases the risk of cardiovascular disappointment and, as a result, significantly impacts depression and mortality [3, 4]. Furthermore, AF affects many people worldwide, and the risk increases with age [5]. The capacity of Artificial Intelligence (AI) and AI techniques to enhance the early detection of cardiovascular diseases with little effort in ECG testing is still mostly unknown. The 2017 Physionet/Computing in Cardiology competition discourages mainstream academics from proposing solutions for programmed AF detection from brief single-lead ECG data [1]. The test is presented as a traditional machine learning issue, with a marked preparation set and suggestions evaluated against a cloaked test set of records. Regardless of whether the primary assessment for the final placement is the precision of the proposed model, various distinct features should be evaluated for the prior appropriation of each proposition in clinical practice. Because it perfectly captures the electrical movement of the cardiac activity [1] ECG determination can provide competent AF detection in clinical practice [3]. Because symptoms occur in episodes, it is challenging to examine AF during normal in-office visits [2]. Recent techniques consider the high fatality rate and inadequacy in detecting AF [6]. ECG signal examinations for AF localization are conducted in the time or recurrence area. The current AF recurrence is commonly assessed over a sign with deleted QRS complex and T peak edifice [7, 8]. This study aims to provide a characterization model and evaluate its ability to separate brief single-lead ECG signals

classified as AF, Normal (N), noisy, and Other Rhythms (O) using the 2017 PhysioNet/Computing in Cardiology Challenge database [9].

The most common symptomatic tool for identifying cardiac arrhythmias is the ECG. AF is the most prevalent cardiac musicality problem characterized by disorganized chamber compression [4]. The prevalence of AF increases with each succeeding decade of age, from 0.5% at 50-59 years to approximately 9% at 80-90 years [10]. It is estimated that 2.3 million adults in the United States suffer from AF, which is expected to rise to 5.6 million by 2050 as the population ages [11]. AF is considered a substantial cause of death and misery as it increases the risk of heart failure and stroke.

For this reason, an assortment of programmed calculations managing the surface of ECG signals has been proposed in recent years. Many misuse the two changes incited by the arrhythmia on the ECG. From one perspective, AF is portrayed by a quick atrial movement, whose rate can change between 240 and 540 actuation/min [12]. Since everyone shells the atrioventricular (AV) hub, a quick and sporadic ventricular reaction can be seen on the ECG. Unmistakably, this conduct diverges from the ordinary example of the R-R interim arrangement amid typical sinus mood (NSR). However, during NSR, the homogeneous P-wave associated with atrial depolarization is replaced by a series of low-fullness fibrillatory waves with varied morphology (f-waves) [12, 13]. AF is underanalyzed and ordinarily distinguished after a patient presents serious complications such as stroke or heart failure.

Drugs can ease side effects and help forestall genuine difficulties, for example, stroke. Electrophysiological medical procedures and radiofrequency removal have effectively restored an ordinary mood [14]. Late progress in versatile innovation (arrange and computational power network) makes it conceivable to grow minimal effort, broadly accessible, and exact medicinal gadgets. These gadgets can be utilized to address the lack of medicinal services assets in the creating scene and lower the expense of social insurance in developed countries. AF finders consider preliminary screening and recognizable proof of AF contrasted with manual strategies. Most current calculations are found in ventricular reaction and atrial movement investigations. Garcia et al. [15, 16] describe AF, including pulse variability, wavelet entropy, and P-wave recognition. However, current AF identification strategies in clinical settings are restricted [17]. In past examinations, an order was performed just to clean information. Be that as it may, clamor is unavoidable in nonstop observing settings because of lead separation, breath, or movement.

Furthermore, such a setup distinguishes AF signals from common indications [17]. Since AF is regularly misdiagnosed as other arrhythmia types, the characterization of AF against an elective cadence would help make the finder more robust. AF is a brilliant possibility for which the effect of such all-around designed versatile innovation would be high. In any case, despite the availability of low-effort therapeutic equipment, the ability to legitimately process information over the phone, and the availability of vast databases of biosignals, almost nothing has been done to make insightful calculations that could naturally translate this therapeutic information. The Physionet/Computing in Cardiology Challenge 2017 [18] subject addresses this theme. It energizes analysts worldwide to create methods for arranging AF from a short single-lead electrocardiogram (ECG) recording acquired utilizing a cell phone.

Much work has gone into ECG categorization, and more is being done in the process. In [19], Garcia et al. propose a new strategy that takes advantage of ventricular and atrial activity variability, as shown on the surface electrocardiogram (ECG). First, the time series generated from RR intervals and fibrillatory wave morphology derived from TQ intervals are developed. The Coefficient of Sample Entropy is then used to measure their regularity (COSEn). The gathered data is at long last consolidated through a multiclass Support Vector Machine way to deal with perceiving among short episodes of AF, Normal Sinus Rhythm (NSR), and Other Rhythms (OR).

Rajpurkar et al. [20] propose using the ResNet model to categorize the ECG data into four different groups. Rajpurkar et al. also incorporate a number of other advanced features, such as statistical modeling of atrial activity, study of heart rate variability in both the frequency and temporal domains, spectral power analysis, and so on. They devised a hierarchical classification model by employing oversampling techniques across categories to determine if an electrocardiogram signal is normal, noisy, exhibiting atrial fibrillation (AF), or displaying an alternative rhythm. Maknickas V and Maknickas A [21] suggest using a LSTM network for the classification of ECG data. This network leverages directly learnt patterns from precomputed QRS complex characteristics. The procedure for extracting information from each pulse of ECG data is outlined in reference [22].

Jiménez-Serrano et al. [9] devised a method for automatically extracting 72 ventricular activity parameters from 8528 ECG recordings that were submitted to the 2017 PhysioNet/Computing in Cardiology Challenge. Following that, a grid search was performed using a set of Feed Forward Neural Network (FFNN) training parameters to carry out a Feature Selection (FS) and training/validation method [3]. The authors use templates that are responsive to a certain heart rate variability, waveform, and AdaBoost classifier. The classification of multiparametric atrial fibrillation is described in [23]. This classification is based on HRV analysis, noise detection, the discovery of atrial activity by the presence of a P-wave in the average beat and f-waves during TQ intervals, and beat morphology analysis following robust synthesis of an average beat and delineation of P, QRS, and T waves. [23] is cited as an example. A linear discriminant classifier was used to categorize the ECG data, which was then separated into four categories. Furthermore, Ojha et al. [24] constructed a deep autoencoder-based SVM classifier to categorize the ECG signal into five categories using the arrhythmia database and previously published research, with better results. This resulted in a more accurate classification of the ECG signal.

This classification task is performed using various pattern recognition algorithms. Therefore, this research work aims to develop a new model based on deep learning

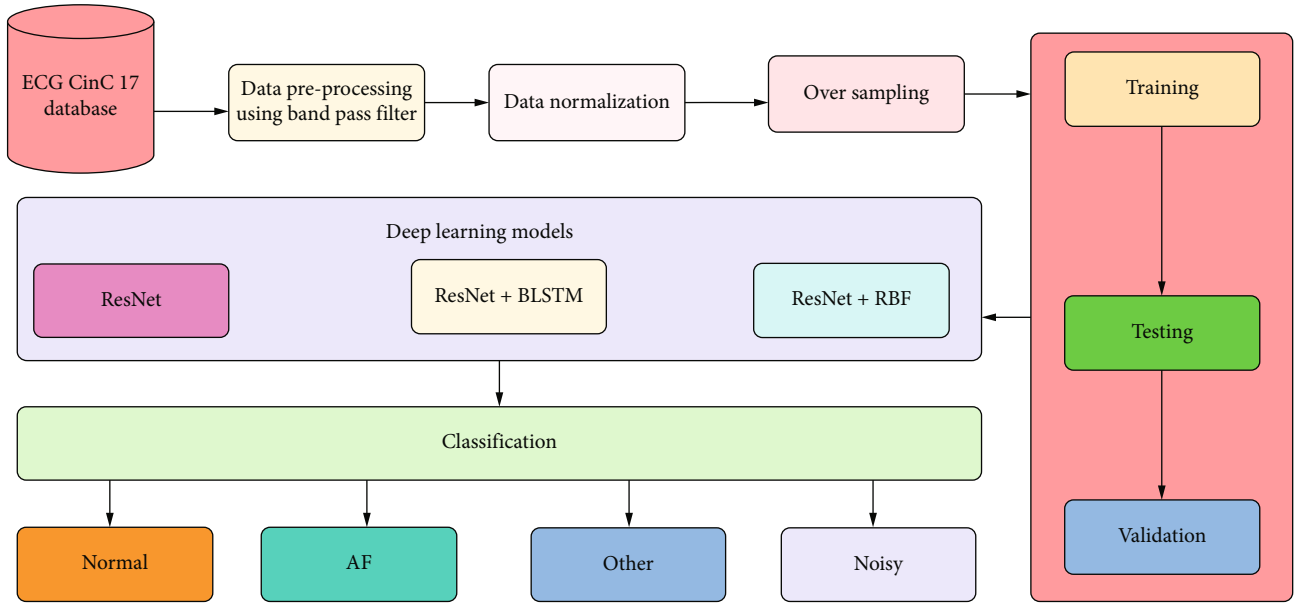

Figure 1: Workflow for classification of short ECG signals into four classes.

techniques for the early diagnosis of arrhythmias from ECG signals. That is, it focuses on arrhythmia and ECG signal processing and classification models to propose new models that can help the cardiologist for the early diagnosis of arrhythmia.

The significant contributions of this paper are the following:

(i) this paper's data set is taken from a PhysioNet challenge (Computing in Cardiology Challenge) 2017

(ii) firstly, we performed a data preprocessing task using bandpass Butterworth filters to remove the noise from the ECG signals

(iii) after that, the Z-Score normalization is performed on the amplitude values of the filtered ECG signals

(iv) the dataset used in this paper is highly imbalanced. Therefore, we have used SMOTE (Synthetic Minority Sampling Technique) technique to balance the dataset, and then the dataset is divided into testing and training datasets for modeling

(v) we have trained three different combinations of deep learning models for the training of the dataset, namely, ResNet, a mixture of BLSTM and ResNet, and a combination of ResNet with RBF techniques for the detection of atrial fibrillation heartbeats in the ECG signals

(vi) then, validation is performed on test datasets that classify ECG signals into four classes: normal, AF, noisy, and others

(vii) finally, this study introduces a new hybrid model based on deep learning techniques that classify ECG signals into four classes: normal, AF, noisy, and others. These models also enhance the effectiveness and efficiency of the heartbeat classification compared to other machine learning and deep learning models using the same ECG signal challenge dataset

Table 1: Distribution of recordings with different rhythms.

Rhythm	No. of recordings
N	5,050
A	738
O	2,456
~	284

The rest of the paper is structured as follows: the methodology and materials are described in Section 2. Section 3 presents the outcome results and a discussion of the proposed methods. Finally, Section 4 states the conclusion of this paper.

2. Materials and Methods

Deep learning techniques are most commonly used in healthcare nowadays. Two deep learning methods have been proposed in this study, which are Convolutional Neural Networks (CNN) and LSTM. Parameter sharing, translation invariance, and sparse connectivity make CNN training computationally efficient and well-liked in computer vision [25, 26]. The downside of CNNs is that they rely on grid-like structures to function (e.g., images or fixed segment windows).They are shown in Figure 1.

One recent finding that has helped with the training and improved accuracy of deeper CNNs is the Residual Network (ResNet) [27]. By utilizing shortcut identity connections similar to a feedforward LSTM (a subtype of RNNs) [18, 28], ResNet makes feature mappings from lower layers accessible at higher stages.

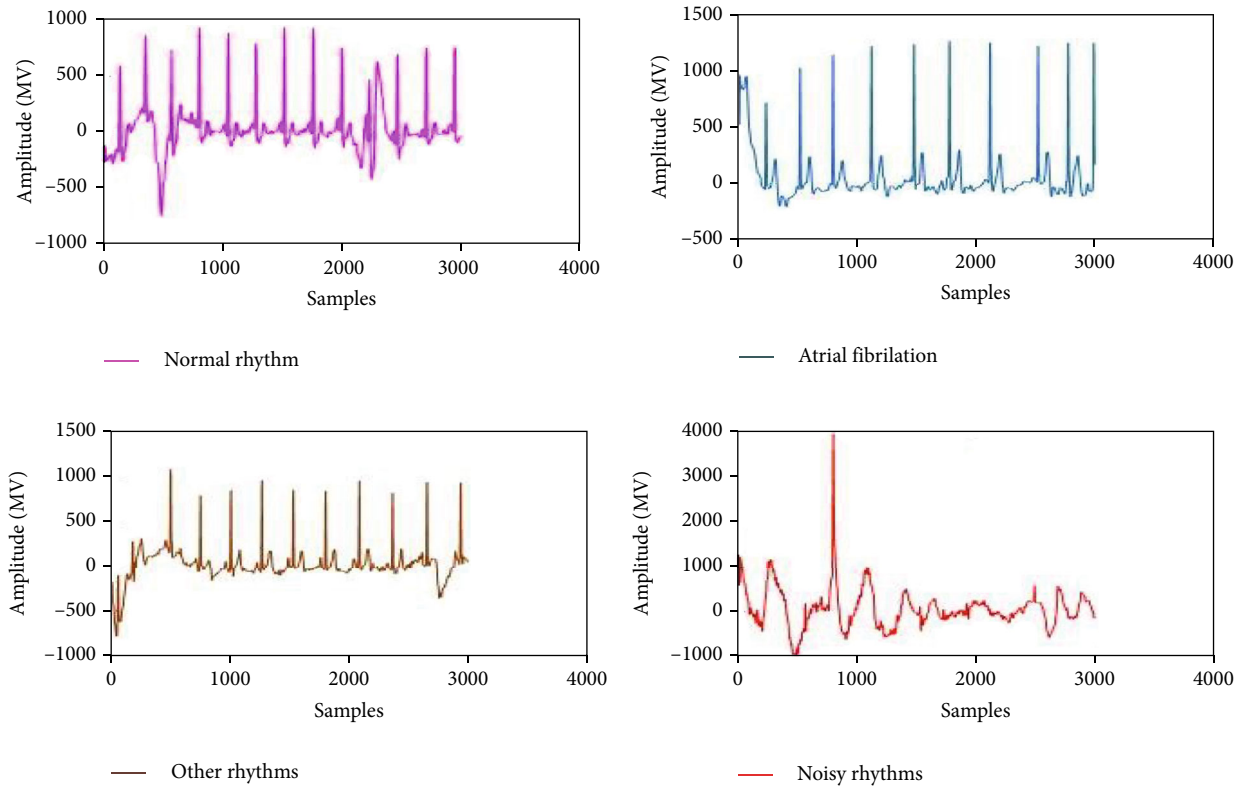

Figure 2: ECG signals for each category: (i) normal, (ii) atrial fibrillation, (iii) other, (iv) noisy rhythms.

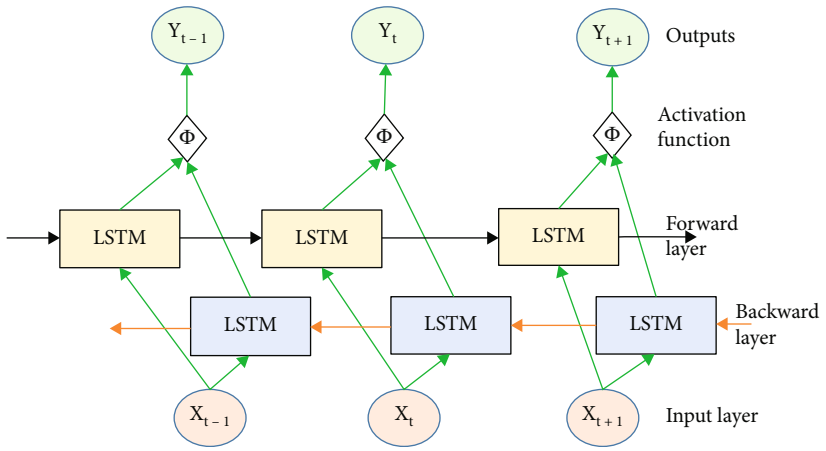

Figure 3: Bidirectional LSTM architecture.

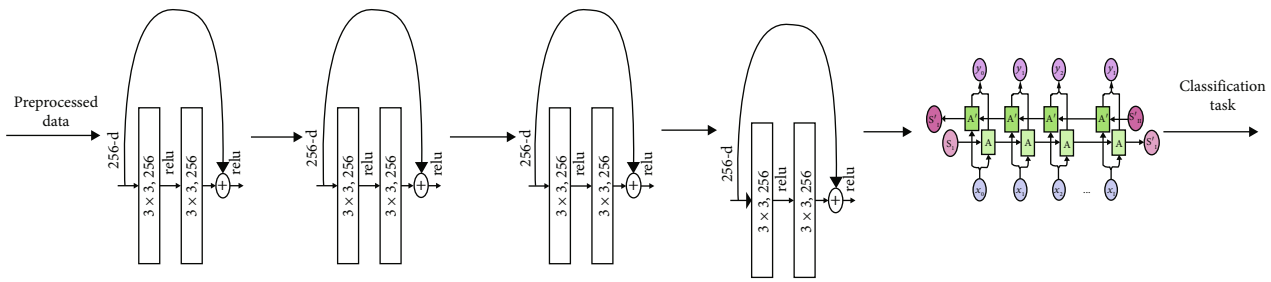

Figure 4: Hybrid architecture ResNet and bidirectional LSTM.

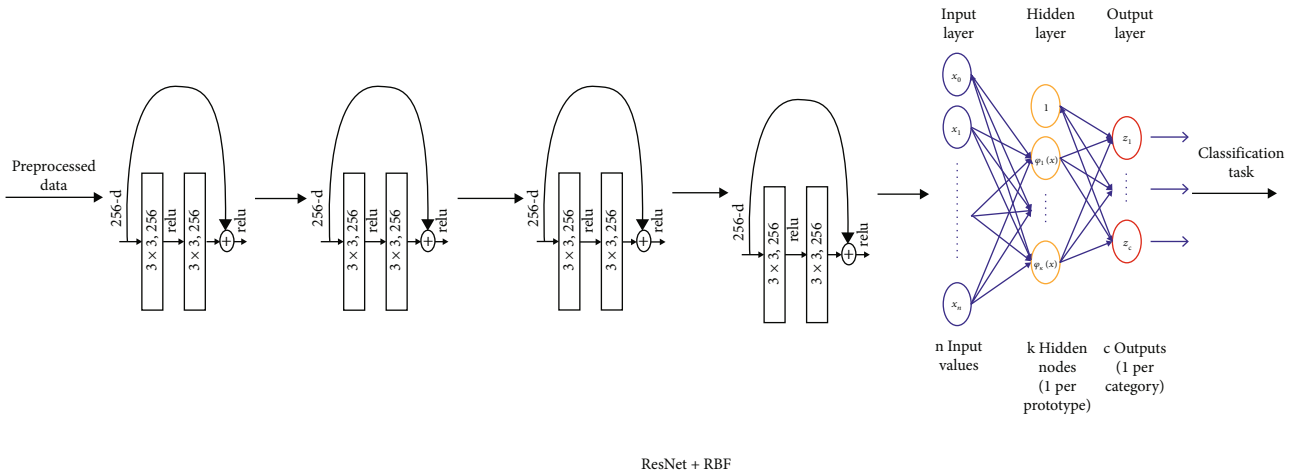

Figure 5: Architecture of ResNet and radial basis function (RBF).

2.1. Dataset Collection. ECG readings were taken during the challenge using the AliveCor gadget and made public. The Physionet Challenge server was used for training with an open database of 8528 single-lead ECGs and accompanying annotations and testing using a closed database of 3658 ECG recordings (dataset). Normal Sinus Rhythm (N), Atrial Fibrillation (A), Other Rhythms (O), and Noisy Recordings were the four categories of ECGs found in the database. These range from 9 to 61 seconds in length and are single-lead 300 Hz ECG recordings. The information repository is offered as a downloadable zip file. Table 1 and Figure 2 show the sum of heartbeats for various categories.

2.2. Signal Preprocessing and Normalization. Each ECG segment was preprocessed using 10th-order bandpass Butterworth filters [29]. These filters had a cut-off frequency of either 5 Hz or 45 Hz (narrowband) or 1 Hz or 100 Hz (wideband). The frequency response of the Butterworth filter is perfectly flat (i.e., has no ripples) in the passband and goes to zero in the stopband. The filter has the flattest magnitude curve possible. For this analysis, we have chosen to segment the ECG data into 20-second samples, each representing a single heartbeat.

Given that there is a 300 Hz sampling rate.

Consequently, each training segment is 20 seconds in length, matching the requirements of the CinC 2017 database. Before segmenting an ECG recording, the recording is normalized to have a mean value of zero and a standard deviation of one. This is because the ECG was already bandpass filtered [22] by the recording device, so there was no need for any additional filters. Then, using the Z-score normalization technique, the amplitude values are transformed into the range of 0-1 to make them more comparable.

$$Z - score = \frac{X - mean}{SD}, \tag{1}$$

where X represents each sample of heartbeats, and the mean is calculated by taking the mean of the 20 second ECG signal values. Here SD represents the standard deviation.

Table 2: ResNet model accuracy and F1 score variation across five-fold cross-validation.

Validation number	No. of epochs	Accuracy (%)	F1 score (%)
1	5	66.39	75.61
	10	69.62	
	15	76.60	
	20	81.23	
2	5	60.70	77.87
	10	68.04	
	15	75.60	
	20	81.17	
3	5	62.64	80.23
	10	69.43	
	15	77.81	
	20	82.80	
4	5	68.21	83.54
	10	72.42	
	15	78.03	
	20	83.11	
5	5	64.52	85.67
	10	77.77	
	15	82.84	
	20	84.40	
Overall F1 score (%)		80.58	

2.3. Oversampling. Predictive accuracy is commonly used to evaluate the performance of deep learning algorithms. Although, this is not acceptable when the data is unbalanced, and the costs of different errors vary significantly. The present work uses Synthetic Minority Oversampling Technique (SMOTE) [30]. It is based on an oversampling strategy where the minority class is over inspected by making "manufactured" models instead of overtesting for replacements. SMOTE method generates new synthesized sample data

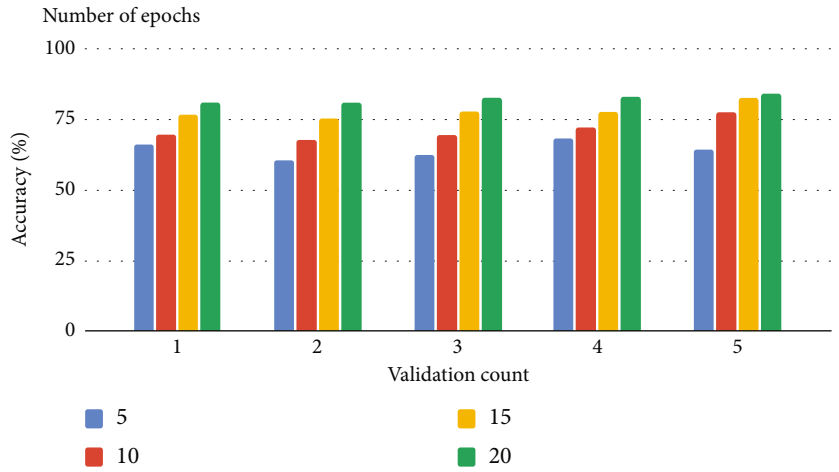

Figure 6: Variation of ResNet model accuracy.

for minority classes without duplicity. It calculates the k-nearest neighbors for each minority class observation. Then, the synthetic data samples are created using one or more k-nearest neighbors, depending on the degree of oversampling required.

2.4. Proposed Deep Learning Model. In the present work, we take two different approaches. One is similar to [20], in which the ResNet model is used to classify the ECG recordings into four classes, and the other approach uses more than one model, including the ResNet model. This ResNet model has 36 layers, combining a convolutional layer, max-pooling layer, and fully connected layer. This approach uses the Bidirectional Long Short Term Memory (BLSTM) and Radial Basis Function (RBF) model. It is an intuitive hybrid approach to gain an insight into how different combinations of neural network models can be combined to form a singular hybrid model that can perform the classification task with improved efficiency.

2.4.1. Bidirectional LSTM (BLSTM). Bidirectional LSTMs enhance the model performance on grouping characterization tasks by augmenting traditional LSTM [31, 32]. BLSTM trains two LSTMs rather than one with info succession. The first is based on the information sequence, while the second is based on a duplicate of the information sequence turned around [33]. It includes copying the intermittent main layer in the system such that there are presently two layers adjacent to each other, giving the information grouping as a contribution to the top layer and a switched duplicate of the second information arrangement (https://machinelearningmastery.com/develop-bidirectional-lstm-sequence-classification-python-keras/). The associations between LSTM units enable the data to push through a circle over the nearby time steps that makes an inside the condition of criticism, allowing the system to comprehend the idea of time and discover the transient elements inside the introduced data. LSTM units can recall or overlook data by keeping up a memory state. The most critical data is kept and back-engineered, while the less critical data is ignored and discarded [34]. The architecture of the BLSTM network is shown in Figure 3.

Table 3: Performance of hybrid model (ResNet and bidirectional LSTM) using five-fold cross-validation.

Validation number	Epochs	Accuracy (%)	F1 score (%)
1	5	59.14	71.73
	10	66.79	
	15	72.33	
	20	79.26	
2	5	62.44	77.97
	10	69.36	
	15	73.57	
	20	80.02	
3	5	61.47	79.85
	10	70.61	
	15	76.27	
	20	81.11	
4	5	64.56	84.93
	10	71.24	
	15	78.69	
	20	82.33	
5	5	61.29	85.94
	10	69.55	
	15	76.34	
	20	82.87	
Overall F1 score (%)		80.08	

$$
\begin{aligned}
h_{t_f} &= H_f(W_x x_t + W_{hh} h_{t-1} + b_h),\\
h_{t_b} &= H_b(W_x x_t + W_{hh} h_{t+1} + b_h),\\
y_t &= W_y h_{t_f} + W_h h_{t_b} + b_y).
\end{aligned}
\tag{2}
$$

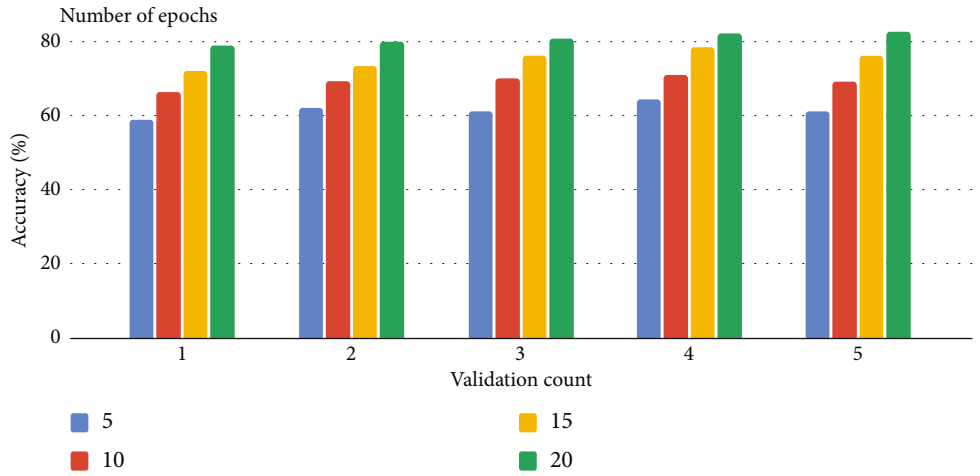

Figure 7: Variation of accuracy with number of epochs for hybrid model (ResNet + BLSTM).

2.4.2. Hybrid Architecture. General classification applied directly to LSTM does not produce specific results. Therefore, it is an excellent strategy to use a hybrid model combining a ResNet (CNN) with LSTM to have more accurate results [35, 36]. The ResNet (CNN) LSTM model utilizes ResNet layers for learning features to join the LSTM layer to help accurate prediction. Both ResNet (CNN) and LSTM performed reasonably well on ECG signals. Besides, profound learning models do not require any extraction of handmade highlights, and they are generally simple to implement [34]. Henceforth, this paper uses the blend of these two calculations to determine arrhythmias. The bidirectional LSTM bolsters the yield of ResNet engineering to order the information into four classes, viz. AF, Normal, Noisy, and others. Figure 4 shows the hybrid structure of the ResNet and BLSTM model.

Another variant includes feeding the output of the ResNet model into an RBF [37, 38]. RBF neural network then has the task of classifying the incoming data from the ResNet model into the four classes discussed above, as shown in Figure 5.

3. Results and Discussion

The above models are trained and tested using the publicly available free cloud notebook (http://colab.research.google.com). The Google Collab environment provides a free GPU limit of up to 11GB and a memory of 358.27 GB, with a CPU frequency of 2.3 GHz on the Tesla T4 system with a memory clock rate of 1.59 GHz. The dataset is directly downloaded from the PhysioNet website to avoid the overhead of uploading data from a local machine. Thus, the above hardware setup provides an efficient way to train and test the deep learning neural network without any interference from the local devices. The learning rate used by the model is 0.001, and the Adam optimizer is used, which is present in the Keras library. Cross-validation is a resampling method for evaluating AI models with a limited information sample. A five-fold cross-validation strategy is utilized in this paper. The given methodology includes only one parameter, k, which refers to the number of meetings in which a specific information test is included. This methodology is generally called k-fold cross-validation. The whole dataset is first divided into k equal parts in this strategy. Then K-1 parts are used for training the classification models, and the last K^{th} part is used for testing the trained models. Therefore, in this fashion, the model is trained K^{th} time on the different parts of the dataset, and every time, we test the model on a

Table 4: Performance of ResNet and RBF models using five-fold cross-validation.

Validation number	Epochs	Accuracy (%)	F1 score (%)
1	5	63.11	73.93
	10	68.24	
	15	73.67	
	20	79.51	
2	5	62.04	78.36
	10	71.28	
	15	77.34	
	20	80.67	
3	5	63.86	79.98
	10	70.27	
	15	78.37	
	20	81.61	
4	5	61.99	82.80
	10	69.33	
	15	76.38	
	20	82.63	
5	5	64.79	85.96
	10	72.58	
	15	80.67	
	20	84.56	
Overall F1 score (%)		80.20	

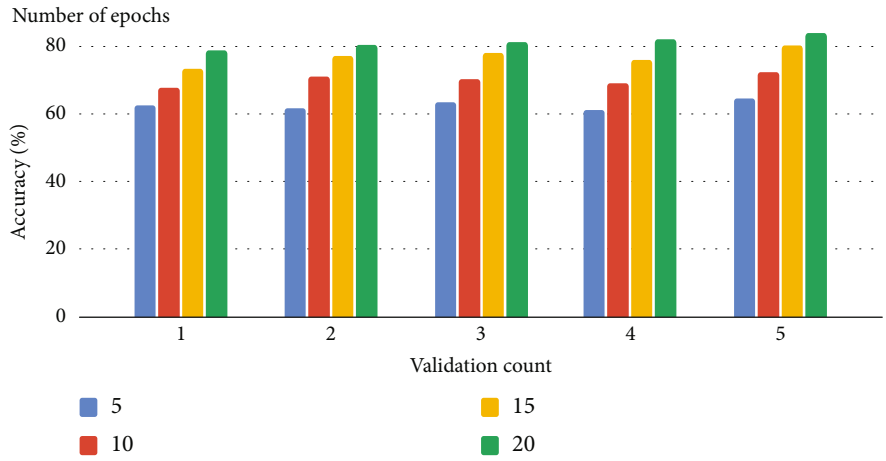

Figure 8: Variation of accuracy with number of epochs for the hybrid of ResNet and RBF model.

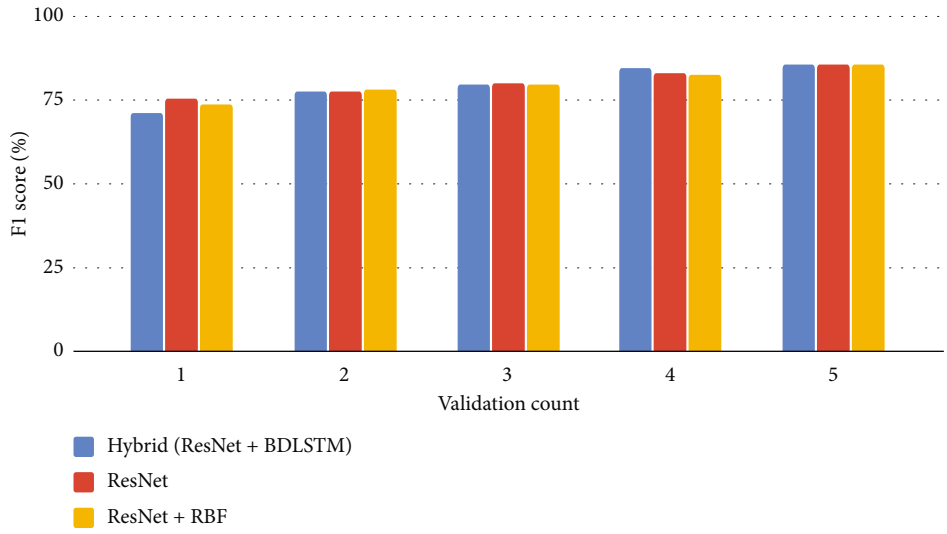

Figure 9: Comparison of F1 scores for different models using five-fold cross-validation.

new K^{th} part of the dataset that the model does not see during the training period.

The following table describes our experiment results, and different models are trained and tested using a five-fold cross-validation strategy. The training and test datasets are split into 80-20 for all models used in this paper. Accuracy and F1 score are used to evaluate the performance of the models. F1 is a metric that combines precision and recall to assess a model's correctness.

$$\begin{aligned} Accuracy &= \frac{True\ positive + True\ negative}{Total\ number\ of\ instances}, \\ F1 &= 2 \times \frac{Precision \times recall}{Precision + recall}. \end{aligned} \tag{3}$$

Table 2 presents the results for five-fold cross-validation on the ResNet-36 model and plots the variation of validation accuracy on validation runs and the computed F1 score, achieving an overall F1 score of 80.58%.

Figure 6 plots the variation of validation accuracy with the ResNet 36 model for different epochs like 5, 10, 15, and 20. It can be inferred that the maximum validation accuracy achieved is 84.40% for epoch number 20 with cross-validation number 5. Validation accuracy has been growing linearly over the number of epochs.

Table 3 presents the accuracy and computed F1 score using five-fold cross-validation for the hybrid model of ResNet and bidirectional LSTM. The overall computed F1 score is 80.08%, with different F1 scores across five-fold cross-validation as 71.73, 77.97, 79.85, 84.93, and 85.94%, respectively.Figure 7 shows how the number of epochs affects the validation accuracy for various cross-validation methods. It achieved the highest validation accuracy of 82.87% and increased with an increase in epochs.

Table 4 shows the variation in F1 score and validation accuracy for ResNet and RBF networks using five-fold cross-validation. It has achieved an overall F1 score of 80.20%. Figures 8 and 9 show the accuracy variation and F1 score of the different epochs achieving the highest validation accuracy of 84.56%.

Table 5: Performance comparison of the proposed model with the existing works.

	S. No.	Year	Author	Methodology	F1 score (%)
A	1	2017	Manuel et al. [10]	Multiclass SVM	73
B	2	2017	Rajpurkar et al. [11]	The deep CNN model has 34 layers that map ECG signal samples into arrhythmia heartbeat classes.	79.9
C	3	2017	Coppola et al. [12]	Hierarchical classification model	78.55
D	4	2017	Neha et al. [13]	A LSTM network, which learns patterns directly from precomputed QRS complex features that classify ECG signals	78
E	5	2017	Schwab et al. [14]	Ensemble RNN with the LSTM attention model	79
F	6	2017	Andreotti et al. [15]	ResNet CNN	79
G	7	2017	Jiménez-Serrano et al. [16]	Feedforward neural network (FFNN)	77
H*	8	2022	*(present work)	CNN-ResNet model	80.58
				Hybrid-ResNet and LSTM (bidirectional)	80.08
				ResNet and RBF	80.20

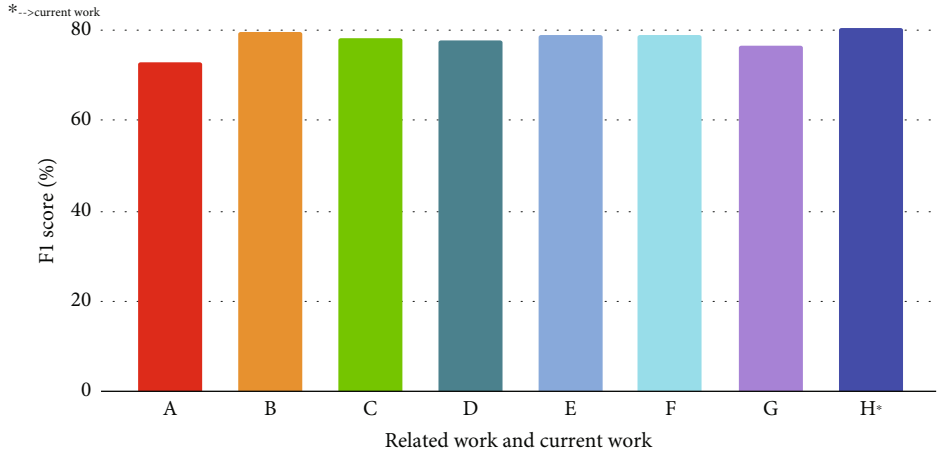

Figure 10: Comparison with related works.

In the present work, we have classified the short ECG recordings into four classes using deep learning neural networks such as ResNet, hybrid model (ResNet and bidirectional LSTM), and ResNet + RBF neural network. We have compared the results across different models and concluded that the presented models achieved a significant outcome compared to related works discussed in [29]. The model used in [29] is limited to expanding the model up to only a specific value due to computational leverage, but our present work does not consider that factor. Our results have improved significantly. However, the limitation of distorted and noisy signals presents a setback that leads to having a bottom hand in overall accuracy and computes the F1 score.

The work demonstrated by Garcia et al. [19] used a multiclass SVM approach for classification and achieved an F1 score of 73%. In comparison, Rajpurkar et al. [20] used the approach of ResNet (34 layers) that converts the sequence of ECG samples into a sequence of rhythm classes. They achieved an overall F1 score of 79.9%. On the other hand, Coppola et al. [1] used a hierarchical classification model for ECG classification into different rhythm classes with an F1 score of 78.55%. Maknickas V and Maknickas A [21] used the LSTM network to learn patterns directly from precomputed QRS complex features that classify ECG signals and achieved an F1 score of 78%. Schwab et al. [22] used ensemble RNN with the LSTM attention model and achieved an F1 score of 79%. Andreotti et al. [29] used a ResNet model and achieved an accuracy of 79%. Jiménez-Serrano et al. [9] used a Feedforward Neural Network (FFNN) with an F1 score of 77%. Our present work has two different approaches, one is similar to the [20, 29] with a ResNet model, and the other is a variation of a hybrid model of ResNet with BLSTM and ResNet with RBF achieving an F1 score of 80.58%, 80.08%, and 80.20%, respectively. Table 5 and Figure 10 describe the performance comparisons of the proposed model with the existing works.

4. Conclusion

Overall, many studies have been done on ECG rhythm classification, and the present work adds another variation of the ResNet model and two new hybrid architectures involving BLSTM and RBF networks. The results shown are promising and can be increased in various ways with the accessibility of more publicly accessible and open data, which has been a continuous obstacle to the current study. New biomedical

technologies allow researchers to deal with an unprecedented amount of precise data. However, given the nature of this work and different deep neural networks, we can rest assured that there is a broad scope of improvement that can be done in this field. Many researchers are constantly working on this problem domain, and many R&D institutes have taken interest in it. Thus, it led us to assume that this domain is going to flourish and outshine shortly.

Although we tried our best to incorporate a maximum of models in this domain, given the limited time and computational resources, a vast plethora of techniques and models like Multilayer Perceptron (MLP), etc., can be applied to the given problem domain. As the work involves a lot of computational and physical data resources, with the advent of new and better technologies, we can try to reduce the complexity to infer results in more optimized time.

Data Availability

Data will be made available on demand.

Conflicts of Interest

The authors declare no conflicts of interest.

References

[1] E. E. Coppola, P. K. Gyawali, N. Vanjara, D. Giaime, and L. Wang, "Atrial fibrillation classification from a short single lead ECG recording using hierarchical classifier," *Computing in Cardiology*, vol. 44, 2017.

[2] D. T. Linker, "Accurate, automated detection of atrial fibrillation in ambulatory recordings," *Cardiovascular Engineering and Technology*, vol. 7, no. 2, pp. 182–189, 2016.

[3] M. Da Silva-Filarder and F. Marzbanrad, "Combining template-based and feature-based classification to detect atrial fibrillation from a short single lead ECG recording," *Computing in Cardiology*, vol. 44, 2017.

[4] T. M. Munger, L. Q. Wu, and W. K. Shen, "Atrial fibrillation," *The Journal of Biomedical Research*, vol. 28, no. 1, 2014.

[5] European Heart Rhythm Association, "Guidelines for the management of atrial fibrillation: the task force for the management of atrial fibrillation of the European Society of Cardiology (ESC)," *European Heart Journal*, vol. 31, no. 19, 2010.

[6] M. Rienstra, S. A. Lubitz, S. Mahida et al., "Symptoms and functional status of patients with atrial fibrillation: state of the art and future research opportunities," *Circulation*, vol. 125, no. 23, pp. 2933–2943, 2012.

[7] I. I. Jekova, T. V. Stoyanov, and I. A. Dotsinsky, "Arrhythmia classification via time and frequency domain analyses of ventricular and atrial contractions," *Computing in Cardiology*, vol. 44, 2017.

[8] N. Sasaki, Y. Okumura, I. Watanabe et al., "Frequency analysis of atrial fibrillation from the specific ECG leads V7-V9: A lower DF in lead V9 is a marker of potential atrial remodeling," *Journal of Cardiology*, vol. 66, no. 5, pp. 388–394, 2015.

[9] S. Jiménez-Serrano, J. Yagüe-Mayans, E. Simarro-Mondéjar, C. J. Calvo, F. Castells, and J. Millet, "Atrial fibrillation detection using feedforward neural networks and automatically extracted signal features," *Computing in Cardiology*, vol. 44, 2017.

[10] National Collaborating Centre for Chronic Conditions (Great Britain), *Atrial Fibrillation: National Clinical Guideline for Management in Primary and Secondary Care*, Royal College of Physicians, 2006.

[11] A. S. Go, E. M. Hylek, K. A. Phillips et al., "Prevalence of diagnosed atrial fibrillation in adults: national implications for rhythm management and stroke prevention: the anticoagulation and risk factors in atrial fibrillation (ATRIA) study," *Journal of the American Medical Association*, vol. 285, no. 18, pp. 2370–2375, 2001.

[12] P. Kirchhof, S. Benussi, D. Kotecha et al., "2016 ESC guidelines for the management of atrial fibrillation developed in collaboration with EACTS," *European Heart Journal*, vol. 37, no. 38, pp. 2893–2962, 2016.

[13] H. Neha, K. Sardana, R. Kanwade, and S. Tewary, "Arrhythmia detection and classification using ECG and PPG techniques: a review," *Physical and Engineering Sciences in Medicine*, vol. 44, no. 4, pp. 1027–1048, 2021.

[14] H. Calkins, K. H. Kuck, R. Cappato et al., "2012 HRS/EHRA/ECAS expert consensus statement on catheter and surgical ablation of atrial fibrillation: recommendations for patient selection, procedural techniques, patient management and follow-up, definitions, endpoints, and research trial design," *Journal of Interventional Cardiac Electrophysiology*, vol. 33, no. 2, pp. 171–257, 2012.

[15] M. García, J. Ródenas, R. Alcaraz, and J. J. Rieta, "Application of the relative wavelet energy to heart rate independent detection of atrial fibrillation," *Computer Methods and Programs in Biomedicine*, vol. 131, pp. 157–168, 2016.

[16] S. Mian Qaisar and A. Subasi, "Cloud-based ECG monitoring using event-driven ECG acquisition and machine learning techniques," *Physical and Engineering Sciences in Medicine*, vol. 43, no. 2, 2020.

[17] C. Huang, S. Ye, H. Chen, D. Li, F. He, and Y. Tu, "A novel method for detection of the transition between atrial fibrillation and sinus rhythm," *IEEE Transactions on Biomedical Engineering*, vol. 58, no. 4, 2011.

[18] G. D. Clifford, C. Liu, B. Moody et al., "AF classification from a short single lead ECG recording: the PhysioNet/computing in cardiology challenge 2017," *Cardiology*, vol. 44, 2017.

[19] M. García, J. Ródenas, R. Alcaraz, and J. J. Rieta, "Atrial fibrillation screening through combined timing features of short single-lead electrocardiograms," *Computing in Cardiology*, vol. 44, 2017.

[20] P. Rajpurkar, A. Y. Hannun, M. Haghpanahi, C. Bourn, and A. Y. Ng, "Cardiologist-level arrhythmia detection with convolutional neural networks," 2017, https://arxiv.org/abs/1707.01836.

[21] V. Maknickas and A. Maknickas, "Atrial fibrillation classification using qrs complex features and lstm," in *2017 Computing in Cardiology (CinC)*, Rennes, France, 2017.

[22] P. Schwab, G. C. Scebba, J. Zhang, M. Delai, and W. Karlen, "Beat by beat: classifying cardiac arrhythmias with recurrent neural networks," *Computing in Cardiology*, vol. 44, 2017.

[23] I. Christov, V. Krasteva, I. Simova, T. Neycheva, and R. Schmid, "Multi-parametric analysis for atrial fibrillation classification in ECG," *Computing in Cardiology*, vol. 44, 2017.

[24] M. K. Ojha, S. Wadhwani, A. K. Wadhwani, and A. Shukla, "Automatic detection of arrhythmias from an ECG signal using an auto-encoder and SVM classifier," *Physical and Engineering Sciences in Medicine*, vol. 45, pp. 665–674, 2022.

[25] I. Goodfellow, Y. Bengio, and A. Courville, *Deep Learning An MIT Press Book*, vol. 29, MIT Press, 2016.

[26] A. Mangal, H. Garg, and C. Bhatnagar, "Image co-saliency detection using CLAHE and modified Resnet-50 convolution neural network," ResearchSquare, 2022.

[27] K. He, X. Zhang, S. Ren, and J. Sun, "Deep residual learning for image recognition," in *Proceedings of the IEEE conference on computer vision and pattern recognition*, pp. 770–778, Las Vegas, NV, USA, 2016.

[28] S. Hochreiter and J. Schmidhuber, "Long short-term memory," *Neural Computation*, vol. 9, no. 8, pp. 1735–1780, 1997.

[29] F. Andreotti, O. Carr, M. A. F. Pimentel, A. Mahdi, and M. De Vos, "Comparing feature-based classifiers and convolutional neural networks to detect arrhythmia from short segments of ECG," *Computing in Cardiology*, vol. 44, 2017.

[30] S. K. Pandey and R. R. Janghel, "Automatic detection of arrhythmia from imbalanced ECG database using CNN model with SMOTE," *Physical and Engineering Sciences in Medicine*, vol. 42, no. 4, pp. 1129–1139, 2019.

[31] Z. Ding, R. Xia, J. Yu, X. Li, and J. Yang, "Densely connected bidirectional LSTM with applications to sentence classification," *Lecture Notes in Computer Science (including subseries Lecture Notes in Artificial Intelligence and Lecture Notes in Bioinformatics)*, vol. 11109, 2018.

[32] S. K. Pandey and R. R. Janghel, "Automated detection of arrhythmia from electrocardiogram signal based on new convolutional encoded features with bidirectional long short-term memory network classifier," *Physical and Engineering Sciences in Medicine*, vol. 44, no. 1, 2021.

[33] Z. Huang, B. Research, W. Xu, and K. Y. Baidu, "Bidirectional LSTM-CRF nodels for sequence tagging," 2015, https://arxiv.org/abs/1508.01991.

[34] S. L. Oh, E. Y. K. Ng, R. San Tan, and U. R. Acharya, "Automated diagnosis of arrhythmia using combination of CNN and LSTM techniques with variable length heart beats," *Computers in Biology and Medicine*, vol. 102, pp. 278–287, 2018.

[35] Y. Fan, X. Lu, D. Li, and Y. Liu, "Video-based emotion recognition using CNN-RNN and C3D hybrid networks," in *Proceedings of the 18th ACM international conference on multimodal interaction*, New York, 2016.

[36] R. Mishra, A. S. Jalal, M. Kumar, and S. Jalal, "A deep learning approach for the early diagnosis of Parkinson's disease using brain MRI scans," *International Journal of Applied Pattern Recognition*, vol. 7, no. 1, pp. 64–77, 2022.

[37] A. Ebrahimzadeh and A. Khazaee, "An efficient technique for classification of electrocardiogram signals," *Advances in Electrical and Computer Engineering*, vol. 9, no. 3, 2009.

[38] V. Tiwari and C. Bhatnagar, "Automatic caption generation via attention based deep neural network model," in *2021 9th International Conference on Reliability, Infocom Technologies and Optimization (Trends and Future Directions)(ICRITO)*, Noida, India, 2021.

Hindawi
Journal of Sensors
Volume 2022, Article ID 6871085, 12 pages
https://doi.org/10.1155/2022/6871085

Research Article

A Novel AI-Based Approach for Better Segmentation of the Fungal and Bacterial Leaf Diseases of Rice Plant

Yogesh Kumar Rathore,[1] **Rekh Ram Janghel**,[1] **Saroj Kumar Pandey**,[2] **Ankit Kumar**,[2] **Kamred Udham Singh**,[3] **and Mohd Asif Shah**[4]

[1]*Department of Information Technology, National Institute of Technology, Raipur, India*
[2]*Department of Computer Engineering and Applications, GLA University, Mathura, India*
[3]*Department of Computer Science and Information Engineering, National Cheng Kung University, 701 Tainan, Taiwan*
[4]*Kebri Dehar University, Ethiopia*

Correspondence should be addressed to Mohd Asif Shah; drmohdasifshah@kdu.edu.et

Received 5 July 2022; Revised 23 July 2022; Accepted 4 August 2022; Published 21 September 2022

Academic Editor: Pankaj Dadheech

Rice is the most consumed food for more than half the world. All over the world, approximately 15% of the rice get wasted because of leaf diseases. A computer-aided system needs a clear segmented lesion to detect such diseases, but blurriness, bad contrast, and dust particles on leaves are the challenge in proper segmentation and, further, for better feature extraction. In this work, first, SegNet deep learning model was trained to separate the weed from the images captured from the field; then, in the next step, a novel automated segmentation technique named RPK-means proposed combining random path (RP) and K-means clustering to separate lesion spots from the leaf images. The work of the model is multifold. First, the SegNet model is trained for weed separation; then, two clusters of the image are generated by *K*-means clustering to find out pixel coordinates lying on the lesion spot and healthy part of the leaves. Thereafter, to separate the lesion part from the background, automatic segmentation is performed by the novel random path *K*-means (RPK-means) method using coordinate positions obtained at the last stage. Fungal and bacterial diseases like brown spot, rice blast, sheath blight, leaf scaled, and bacterial blight have been collected from the field to perform the experiments. Experimental result shows that the performance of the deep learning classifier increased by approximately 2-6% while applying to RPK-means preprocessed images, rather than the traditional *K*-means segmentation technique.

1. Introduction

Agriculture is the backbone of the economy of any country, and rice is among the most cultivated plants in all over the world. But farmer losses his 37% rice every year because of bad weather conditions and weed and leaf diseases in which 5 to 10% losses in rice occur due to rates, whereas bacterial and fungal disease causes approximately 15% of loss. Diseases that occur in leaves completely destroy the leaves, due to which the fruit does not grow in the plant. To detect these diseases with the help of computer, clear pictures of leaves are required, but when a farmer takes a picture of infected leaves from the field, there may be some more leaves visible in background. To separate these background leaves, we always need an automated system which can segment the region of interest accurately which may lead to better feature extraction in future. Recently, color-based segmentation techniques are used in many research to segment the disease portion from a leaf of crop, most of such approaches first convert the RGB inputs into gray color then segmented by thresholding technique [1]. Weed separation from the crop is another most challenging task because images directly taken from the field contain three classes of rice, weed, and background thereafter; also, we need ground truth image dataset, to evaluate the quality of segmentation [2]. So, segmentation of plant disease is a multifold approach, i.e., separation of weed, separation of background, and finally preparation of ground truth dataset for evaluation. Many

research has been done recently to focus on proper segmentation of boundaries of the object rather than concentrating on central pixels. Also, the use of supervised machine learning algorithms [3] like support vector machine, decision tree, and neural network models and many unsupervised learning approaches like *K*-means clustering and fuzzy means clustering [4] has been proposed for better segmentation. All these techniques provide better segmentation of leaf diseases but need more data and time for training. In the same manner, some authors proposed the use of deep learning model in their research for segmentations, which uses pooling layer to reduce the feature by reducing background information, but at the same time, some part of the region of interest also reduces. To overcome this issue, some authors presented the use of SegNet model [5]; in the SegNet, before performing the max pooling operation, it keeps the record of index of each pixel so that it can be used later for upsampling.

Segmentation of images for the extraction of the accurate region of interest (ROI) plays a crucial role that drastically reduces the data size to be analysed as well as performs better for feature extraction. Hence, it is desirable to extract only ROI for effectively analysing the required problem. Fuzzy logic and *K*-means clustering-based techniques have been used by many researchers to segment the ROI from plant images [6]. Due to irregular texture, presence of dust particles on the leaf, the effect of sunlight, presence of shadow, and presence of bacterial and fungal diseases make the boundary of leaves irregular and thus leads to inaccurate segmentation while using traditional image processing approaches [7]. In the real-time images, there may be lots of leaves in the background which need to separate for better segmentation of lesion portion and has a major challenge in this area.

For the excessive green index (EXG), vegetative index (VEG), and color index of vegetative extraction (CIVE), the idea was based on that in RGB images of plant, and green channel information is more useful for segmentation and can be treated as foreground object [8]. The color-based segmentation suffers from oversegmentation due overlapping leaves and similar background. Other techniques like mean shift segmentation [9], *K*-means segmentation [10], and random walk segmentation [11] are used by many authors to detect region of interest from plant leaves. But clustering and mean shift techniques have limitations in finding accurate boundary of lesions and suffer from oversegmentation or undersegmentation, whereas random walk method needed more human intervention to select the coordinates of foreground and background pixels. Deep learning models, like SegNet [5] and UNet [12], became more popular these days to segment lesions from plant leaves as these models are artificial intelligence-based models, and their prediction is more near to a human being unlike other conventional image processing-based models [13]. Similarly, feature extraction uses conventional image processing techniques limited to texture features [14], color features [15], local features, and global features [16], but as the plant disease has versatile nature, so some additional features like angle of pixel shifting after disease, change in shape of leaf, time to time change in color of leaf needed to predict the disease in early stage. So deep learning models have been used in many researches to extract minute features of the input image. In most of the research, we found that signet model outperforms the fully connected neural network model because it extracts the low features using encoders and converts them to high-resolution features using decoders [17, 18].

Automated *K*-means clustering method [10] and some authors have also used soft computing techniques to get the threshold value for segmentation [19]. Most of these techniques mainly faced the problem of under- and oversegmentation. So, for the betterment of segmentation result, various researchers proposed the fusion of two or more techniques. Fusion of color space transformation and clustering applied on leaves of crops and vegetables [20] faced the problem of low accuracy in classification. In another work [21], a fusion of super pixel segmentation with *K*-means clustering got better accuracy, but study is limited to 2 types of disease only. Another study said that the combination of color features and region-based segmentation shows better results over other traditional methods [22]. Segmentation of images for the extraction of the accurate region of interest (ROI) plays a crucial role that drastically reduces the data size to be analysed as well as performs better for feature extraction. Hence, it is desirable to extract only ROI for effectively analysing the required problem. Segmentation is an approach that can be used to extract ROI, and it is always a challenging task for extracting ROI. Fuzzy logic and *K*-means clustering-based techniques have been used by many researchers to segment the ROI from plant images [23]. Due to irregular texture, presence of dust particles on the leaf, the effect of sunlight, presence of shadow, and presence of bacterial and fungal diseases make the boundary of leaves irregular and thus lead to inaccurate segmentation while using traditional image processing approaches [24]. Background also plays very important role in the segmentation, because taking images of leaves from a farmer's land may have many leaves in the background and generate the irregular shape.

Various automated systems have been proposed using image segmentation techniques to extract the lesion part from the rice leaf, as hue part separation, then mapping with base image after RGB to HIS color space conversion [25], and *K*-means clustering method to highlight the diseased portion in the leaf of rice plant [26]. Recently, deep learning methods have been applied in various fields for image enhancement [27] and local feature extraction [28] and to implement ensemble learning [29]. Now, it is also been applied in agriculture to identify leaf disease and to separate the diseased portion from the plant images [30] and video frames [31] which are more accurate but have an overhead of maintaining a large amount of data to process.

On increasing epochs further, the problem of the overfitting has been encountered and the performance of the system starts decreasing because our model tries to reach zero error and started to get trained from the noisy data. Through the literature, we observed that segmentation of leaf disease is the biggest challenge due to dust particles present on the

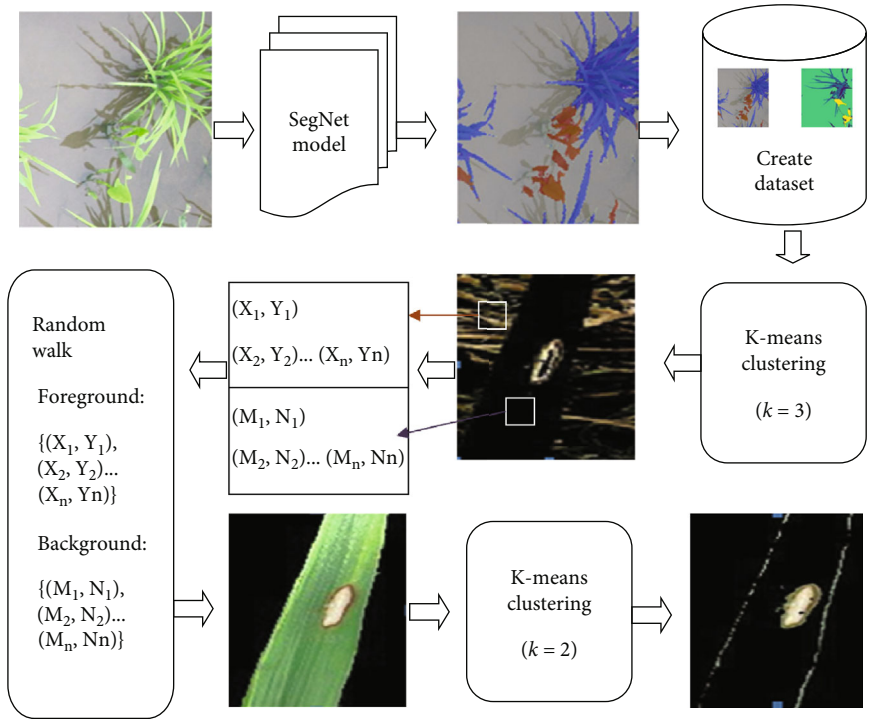

Figure 1: AI-based multilevel segmentation process.

leaf, the angle of the camera, and due to similar background information. So, it is a very tough task to detect the diseased part using conventional image processing methods.

The motivation behind this work is to resolve the problem of misclassification by training a deep neural network model to separate the weed from the crop. Another motivation was to develop an automated system to increase the productivity of crops by early detection of leaf disease, which needs better segmentation followed by feature extraction.

1.1. Main Contributions

(i) Here, we have focused to develop a novel "multilevel deep segmentation model (MDSM)" to reduce the effect of multiple objects available in background by applying SegNet at first stage and novel RPK-means segmentation algorithm to overcome the problem of over- and undersegmentation without any human intervention

(ii) A new "RPK-means" algorithm is proposed, which is a combination of K-means clustering (K-means) and random path algorithm; later on, the findings of the model are compared with other similar models

(iii) A new algorithm named "ground truth algorithm" is proposed to create ground truth image to analyse the performance of any segmentation technique

2. Materials and Methods

2.1. Database. We have recorded videos from farmer's land of Chhattisgarh state of India. The recording is done by using Nikon COOLPIX 20.1 megapixels, 3.0 LCD camera, having 5x zooming facility to capture the desired space from distance. We have captured the video at day time between 8 AM to 2 PM, so that we could get sufficient light from the environment for better video quality. Each video is recorded for 10 to 30 seconds for a particular disease. Video to frame conversion is performed by 2019a version MATLAB of software; to perform semantic segmentation, we installed deep learning toolbox and embedded toolbox computer vision used for further processing. Finally, dataset of 1500 images is prepared for further process. The image dataset contains 6 classes of leaves, rice blast (RB) 250 image frames, leaf scaled (LS) 300 image frames, sheath blight (SL) 200 image frames, brown spot (BS) 250 image frames, healthy leaves (HL) 250 image frames, and bacterial leaf blight (BLB) 250 image frames shown in Figure 1.

Here, (X_i, Y_i) represents the coordinates of the background, and (M_i, N_i) represents the pixels on the leaf. At the upper part, $k = 3$ choose to generate 3 clusters of foreground, background, and lesion part of the leaf, whereas at the lower part, $k = 2$ choose to generate only two clusters of diseased portion and normal portion.

2.2. Weed Separation. SegNet model [17, 32] is used in many ways for segmentation; the model contains encoder layer to compress the features, decoder layer to decompress the features, and a classifier layer to classify the particular segment in the image. In this model, we have kept similar architecture for encoder and decoder layer to make sure that the size of input and output images must be same; after decoding process, output is fed to classifier to produce the probability that a particular pixel belongs to ROI (region of

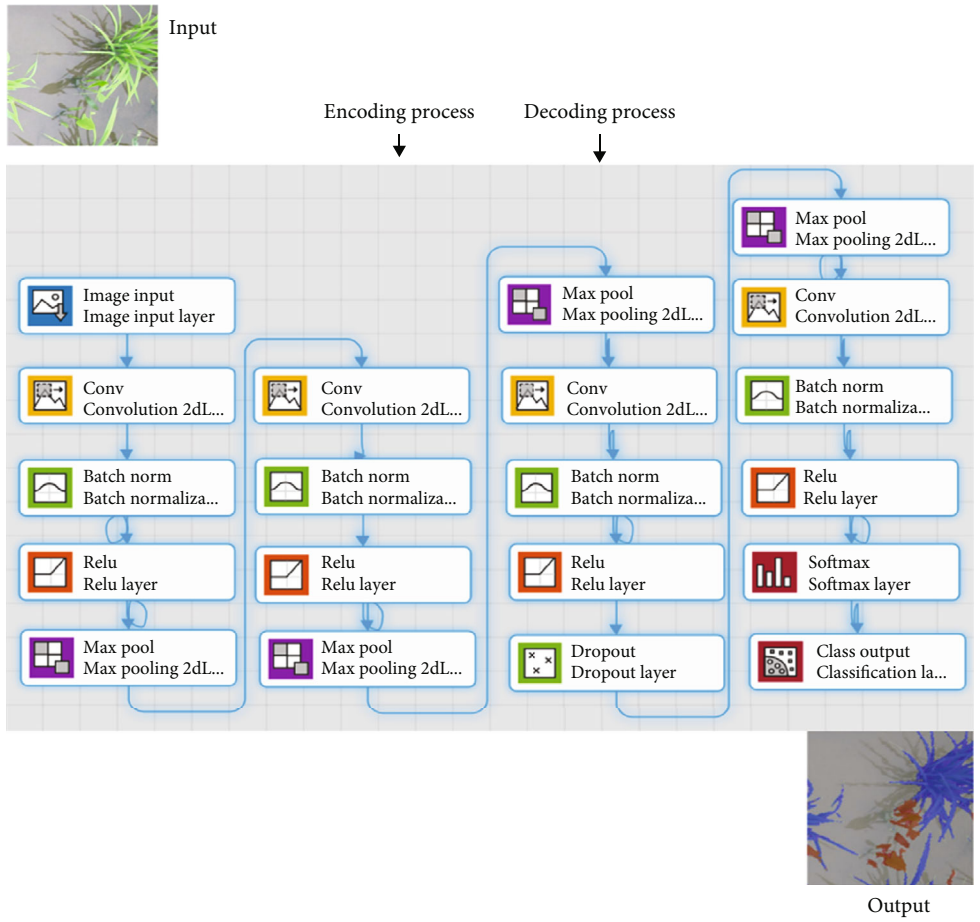

Figure 2: Layered architecture of SegNet model.

Step 1. Initialize K=n // n = no f clusters, taking n=3 initially
Step 2. Select C_i for each K_i, // C_i is a center for each cluster K_i, say (x0, y0)
Step 3. Calculate distance D using the below equation, for each pixel (xi, yi) form C_i, such that $C_i \in K_i$

$$D = \sqrt{(xi - x0)^2 + (yi - y0)^2}$$

Step 4. Merge all the (xi, yi) to cluster where $D = Dmin$ (Where, $Dmin$ is the minimum distance)
Step 5. Store (xi, yi) of each C_i for further operation.
Step 6. A_i=Area (C_i), // {i=1, 2,…n} A_1, A_2…..A_n represents the area of cluster C_1, C_2,..C_n
Step 7. Sort (Ascending (A_i)) // {A_1, A_2,.A_n}
Step 8. Select C_1 and C_2 such that, C_1, C_2 $\in$ A_n, A_{n-1}, Respectively,
For random walk we assumed that user provided coordinate positions (xi, yi) of cluster C_1 and (xj, yj) of cluster C_2 (Stored in step 5) as seed pixels to connect the path of foreground and background object
Step 9. If intensity of pixel (xi, yi) is represented by Inti , Intensity of (xj, yj) is represented by Intj, and distance between theses intensities denoted by Di, j then we can calculate the weight Wi, j of edge connecting theses two vertices as:

$$Di, j = Inti - Intj$$

$$Wi, j = e^{-\beta.(Di,j)^2}$$

Step 10. Finally, pixels with similar weights Wi, j can be connect to generate random path for foreground and background objects

Algorithm 1: RPK-means algorithm.

interest) or belongs to background class. The design of the encoder and decoder consists of a convolutional layer of window size 3 × 3 to produce the feature map, a batch normalization layer to reduce the cost of calculation, and rectified linear unit (ReLU) layer to filter out the negative values in each section. In addition, max pooling layer of size 2 × 2 window is used with encoders to perform downsampling of data. The architecture of working model is shown in Figure 2.

We have trained the SegNet model with the labeled data having 3 classes, i.e., rice seedling, weed, and background.

To create Ground truth image dataset, we applied following steps:
1. Read Image Img(x, y)
2. For i = 1 to 100
Manually select pixels Img(x, y)and Img(p, q)such that,
if
$I(x, y) = \pm 10\, I(p, q.)$
Where intensity of Img(x, y) is I(x, y), and intensity of Img(p, q)is I(p, q) and (x,y)and (p,q)are randomly selected pixel coordinates on image Img. Here we are taking a random value ±10 because intensity having nearby gray values has similar color, so they can be part of foreground or background.
Store coordinates (x, y) and (p, q) in dataset d1
else
Store coordinates (x, y) and (p, q) in dataset d2
end
end
Here, d1 and d2 are two datasets contains the coordinates of the pixels found in foreground and background of the output of k-means clustering.
3. Remove entries from **d2 if any**$(\mathbf{x}, \mathbf{y})$ or $(\mathbf{p}, \mathbf{q}) \in$ **d1**
4. Now coordinates of dataset d1 and dataset d2 may use as coordinates of foreground objects and coordinates of background object.
5. Exit

Algorithm 2: Ground truth algorithm.

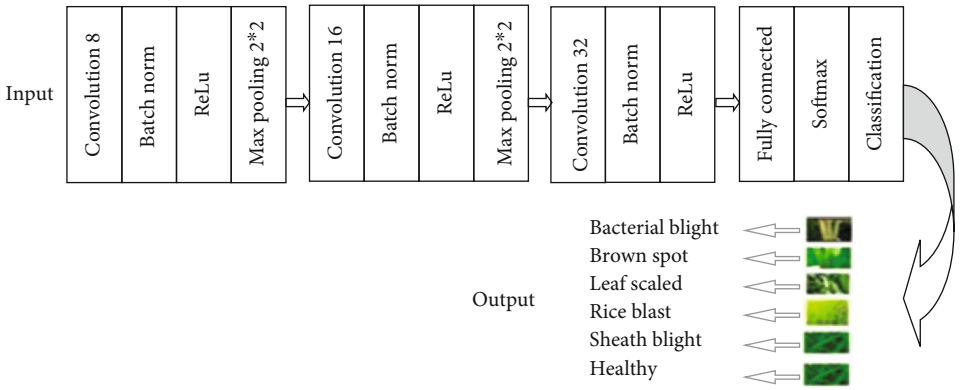

Figure 3: Proposed 15-layer CNN architecture for classification.

Table 1: Calculation of trainable parameters for each convolution layer.

S. no.	Input layer	Filter size	No. of filters in current layer	No. of filters in previous layer	No. of parameters
1	Input (227,227,3)	—	—	—	—
2	Convolution 8	$(3 * 3 * 3)$	8	3	$[(3 * 3 * 3) * 3 + 1] * 8 = 416$
3	Convolution 16	$(3 * 3 * 3)$	16	8	$[(3 * 3 * 3) * 8 + 1] * 16 = 3472$
4	Convolution 32	$(3 * 3 * 3)$	32	16	$[(3 * 3 * 3) * 16 + 1] * 32 = 13856$

The model shows significant output in terms of separation of weed form rice seedlings. Testing has been performed on our dataset and output image of SegNet model stored in another dataset for further processing. We used 2,000 images taken from different agriculture land to train the SegNet and U-Net models. The model is trained to label each pixel of the particular class, so that we can get perfect boundary box with label after segmentation.

2.3. Lesion Segmentation. The segmentation of real-time input images is a big challenge, as real-time images contain multiple overlapping leaves in the background. First, we need to perform background subtraction to separate infected leaves; at the same time, we need to extract the region of interest from the infected leaves as well. When we apply *K*-means clustering to segment the image into 2 clusters of foreground and background, we observed that it cannot separate the background completely, as some pixels in the background contain similar information as foreground pixels. At the same time, the random path method for segmentation removes the background portion very effectively but cannot segment the diseased portion on a leaf. Also, is

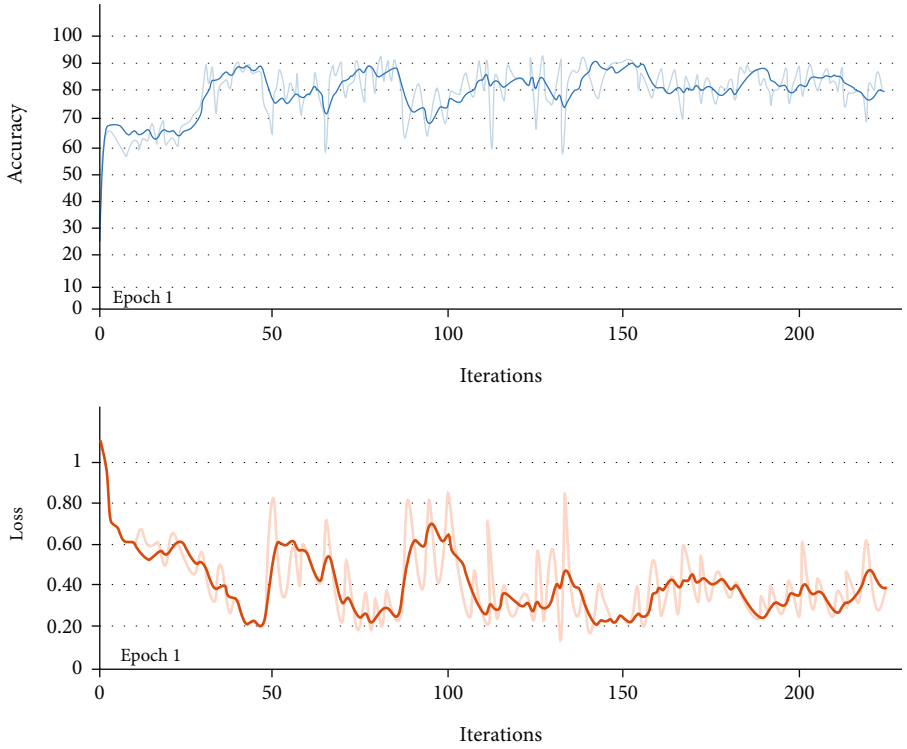

Figure 4: Accuracy and loss function graph while training of SegNet model.

has one major limitation of need of human intervention to provide coordinates of the foreground and background pixels. The proposed RPK-means algorithm is a fusion of these two algorithms which is able to not only segment the lesion properly but also needs no human intervention. We have selected images randomly from dataset to perform next level segmentation. This technique will also be able to reduce the problem of over- and undersegmentation as it selects the seed pixel more accurately because after K-means clustering foreground and background pixels, coordinates are stored in datasets d1 and d2 given by the equations in Algorithm 2. Thereafter, it is supplied to random path method to generate the final segmented image.

The task of lesion separation is performed by applying RPK-means algorithm explained below.

Segmented image obtained after Algorithm 1 needs to be checked for its accuracy, so a dataset of ground truth image has been made by using the ground truth algorithm (explained below); in this algorithm, we have randomly selected 100 pixels from image to create a dataset of coordinates of pixels whose intensities are similar. The same process is applied for background also. Later on, we can use these coordinate positions to match with the coordinates of the foreground and background image obtained with different segmentation algorithms.

2.4. Classification Based on Deep Learning Model. We have created a deep learning model for feature extraction and classification; we used all the convolution filters of $3 \times 3 \times 3$ with stride [1] and "same" padding; at first stage, the number

Table 2: Comparing accuracy by varying training parameter.

Epoch	Iteration	Execution elapsed (hh:mm:ss)	Accuracy	Loss
1	1	00 : 00 : 01	38.42%	0.7711
	20	00 : 00 : 15	49.03%	0.7142
	100	00 : 01:21	73.26%	0.5856
	200	00 : 02 : 44	77.66%	0.5009
	220	00 : 02 : 44	77.66%	0.5009
5	1	00 : 02 : 56	78.26%	0.5002
	20	00 : 28 : 17	91.12%	0.2163
	100	00 : 29 : 26	91.42%	0.2106
	200	00 : 31 : 04	91.75%	0.2039
	220	00 : 31 : 25	91.83%	0.2026
10	1	01 : 10 : 47	91.89%	0.2013
	20	01 : 11 : 02	91.96%	0.2001
	100	01 : 13 : 19	92.02%	0.1987
	200	01 : 14 : 35	92.07%	0.1976
	220	01 : 15 : 45	92.07%	0.1976

Table 3: Comparison of accuracy of segmentation on using SegNet and U-Net models.

S. no.	Model applied	Accuracy (in %)
1	SegNet	92.07
2	U-Net	87.51

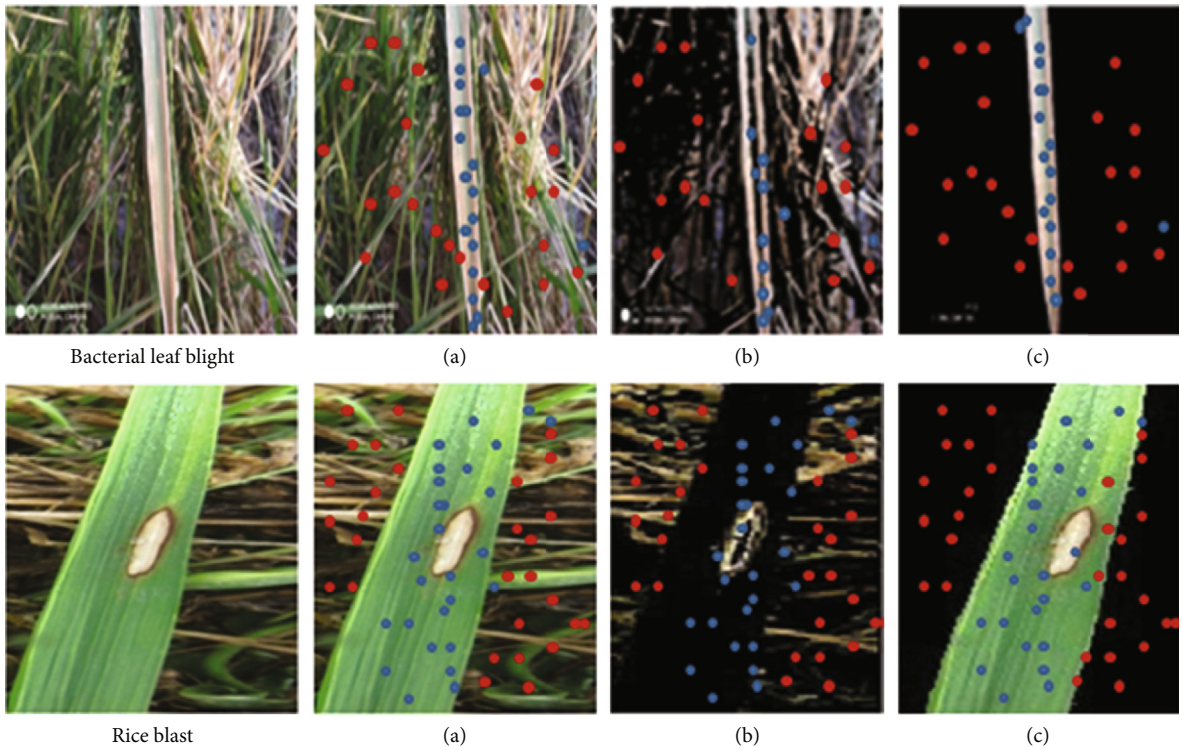

FIGURE 5: Foreground and background pixel prediction based on K-means and RPK-means techniques. (a) Ground truth image. (b) Segmentation using K-means clustering. (c) Segmentation using RPK-means clustering.

of such filters is 8; then, at second stage, it is 16, and at third stage, it is 32. For feature reduction, max pooling used 2×2 filter size with stride [2] and "same" padding. Fully connected layer has 6 neurons to classify 5 possible diseases along with healthy leaves, and at the end, softmax layer is used to classify bacterial blight, brown spot, leaf scaled, rice blast, and sheath blight. The arrangement of layers changed many times to analyse the effect on classification accuracy; finally, after the experiments, the model shown in Figure 3 has been selected for further processing.

Here, we created the handmade lightweight model to classify the disease; the model has 15 layers (including the input layer) and is capable of classifying the diseases with remarkable accuracy. Other similar models like VGG-16, VGG-19, ResNet-50, and GoogleNet may produce similar accuracy of the classification but will need more time as they have more layers in their architecture.

We have trained the model with 416, 3472, and 13856 training parameters at the 1st, 2nd, and 3rd levels of convolution layer, respectively. Calculation of number of training parameters at each convolution layer is tabulated in Table 1.

3. Result and Discussion

In this section, the result and their analysis work are performed to check the system validation.

3.1. Performance Analysis of SegNet Model Used for Weed Separation. SegNet model has been used to segment the rice seedlings from the weeds; we have trained the SegNet model (architecture shown in Figure 2) for 10 epochs of 224 iterations each. The training accuracy and loss graph are shown in Figure 3. To compare the performance of the model, the same dataset is also trained for standard U-Net model [5], which is a similar model as SegNet with small changes in encoder and decoder layers.

We consider parameters no of epoch, execution time, batch accuracy, and learning rate during our experiments. We got the best results at learning rate 0.0010, number of epochs 10 with 224 iterations each, on increasing more iterations, accuracy graph get saturated after this limit, and further increase of epoch leads in problem of memory overflow and oversegmentation.

The graphical representation of output is shown in Figure 4, and the results obtained after varying parameters are tabulated in Table 2. We observed the best accuracy of 92.07% after 13th epoch; thereafter, the accuracy gets saturated.

U-Net is another widely used architecture for image segmentation which has a series of convolution layers without padding to perform downsampling. There is one max pooling layer applied between the two sets of convolution filters to extract better features; the whole process is known as the encoding of data. The decoder process regenerates the original shape of the image by applying upsampling using upconvolution. The highest accuracy of standard U-Net model was observed as 87.5% with the same number of epoch as SegNet as shown in Table 3.

3.2. Performance Analysis of K-Means and RPK-Means Models Used for Segmentation. To analyse the performance of the segmentation, we have created ground truth image

Table 4: Analysis of pixels matching with background and foreground pixels comparing with ground truth image.

Type of disease	*K*-means clustering		RPK-means clustering		Accuracy	
	No. of pixels matched in foreground	No. of pixels matched in background	No. of pixels matched in foreground	No. of pixels matched in background	*K*-means	RPK-means
Bacterial leaf blight	28	61	31	62	89	93
Sheath blight	26	58	28	60	84	88
Rice blast	32	64	33	65	96	98
Leaf scaled	29	59	30	59	88	89
Brown spot	28	55	30	62	83	92
Healthy leaves	34	65	34	65	99	99

Table 5: Accuracy comparison of *K*-means and RPK-means segmentation.

Type of disease	K-means clustering		RPK-means clustering	
	Pixels matched with foreground (in %)	Pixels matched with background (in %)	Pixels matched with foreground (in %)	Pixels matched with background (in %)
Bacterial leaf blight	80.000	93.800	88.500	95.402
Sheath blight	74.300	89.201	80.000	92.301
Rice blast	91.400	98.500	94.312	98.512
Leaf scaled	82.802	90.100	85.701	90.102
Brown spot	80.210	84.600	85.701	95.401
Healthy leaves	97.102	98.460	97.101	98.460

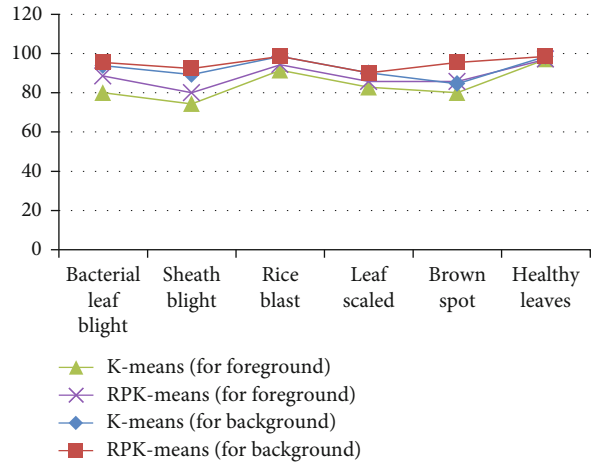

Figure 6: Accuracy comparison of different classifiers

dataset by selecting total 100 pixels, 65 from background, and 35 from diseased portion of image (using Algorithm 2 described in Section 3.2). The performance of *K*-means and RPK-means algorithm is shown in Figure 5, where blue pixels represent the pixels recognized as pixel at diseased portion and red pixels represents the pixels detected as background of the image.

The quality of the segmentation is analysed by comparing coordinate position of blue color pixels and red color pixels with the ground truth image such that

$$\text{Accuracy of segmentation } (A) = \frac{\sum_{i=1}^{n} \text{No. of foreground pixels (blue color)} \mathcal{E}\, d1 + \sum_{j=1}^{m} \text{no.of foreground pixels (blue color)} \mathcal{E}\, d2}{\text{no.of pixels in } (d1 + d2)} \cdots, \tag{1}$$

Table 6: Training-testing ratio (90-10) and learning rate 0.001.

Layers	Epochs	Accuracy		Execution time	
		K-means	RPK-means	*K*-means	RPK-means
11	15	90.01%	90.02%	9 minutes, 20 seconds	9 minutes, 42 seconds
11	20	91.94%	92.30%	12 minutes,55 seconds	13 minutes,10 seconds
11	25	93.60%	94.34%	16 minutes,10 seconds	16 minutes, 50 seconds
11	30	94.58%	95.24%	19 minutes, 15 seconds	20 minutes,05 seconds
15	15	92.50%	93.20%	9 minutes, 20 seconds	9 minutes, 45 seconds
15	20	93.54%	94.25%	12 minutes, 55 seconds	13 minutes, 34 seconds
15	25	95.42%	96.88%	16 minutes, 10 seconds	16 minutes, 52 seconds
15	30	94.80%	95.35%	19 minutes, 15 seconds	19 minutes, 58 seconds

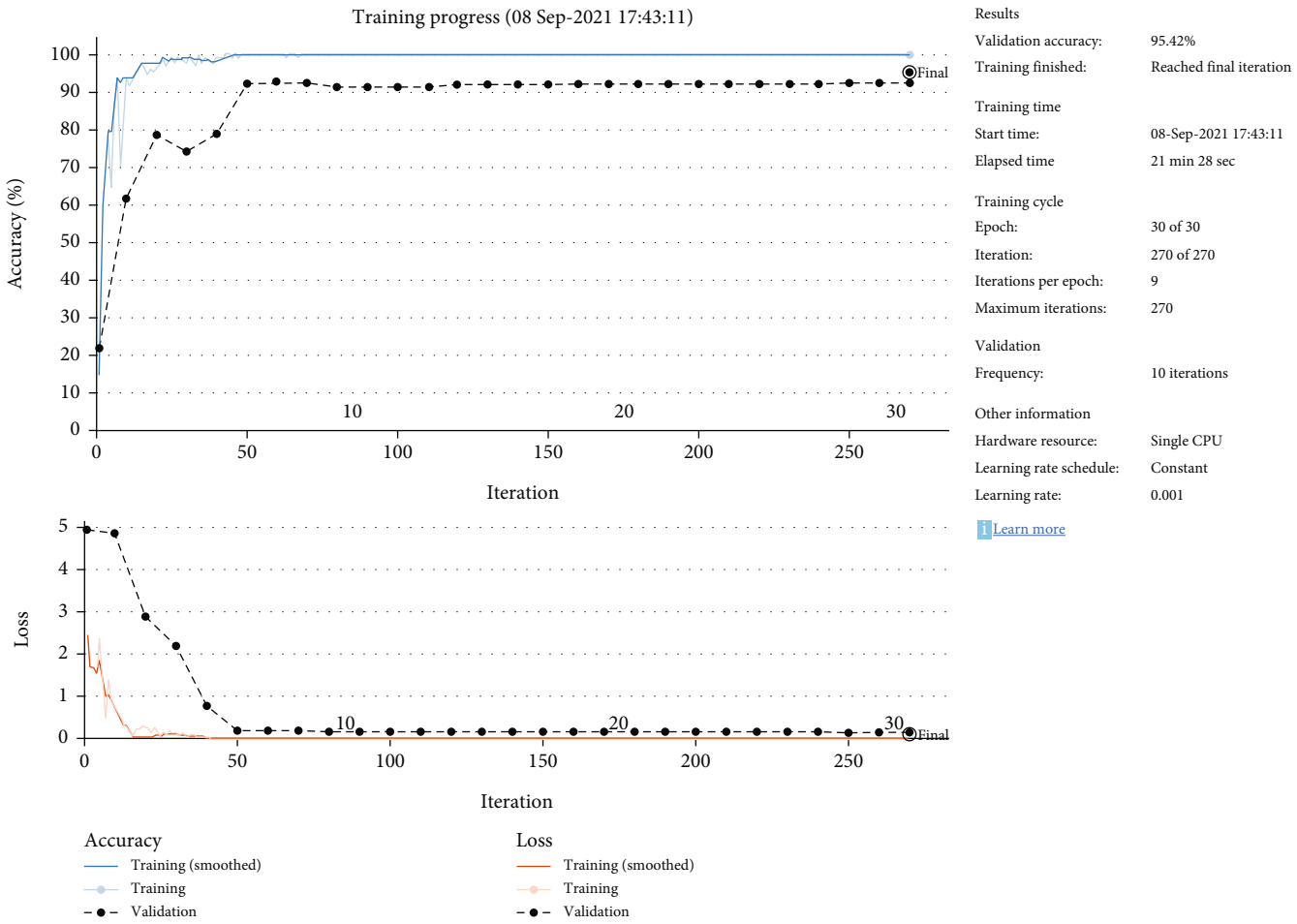

Figure 7: Best accuracy obtained by the HCNN model on *K*-means clustering processed image.

where m and n are the number of blue color and red color pixels in segmented image, respectively, and $d1$ and $d2$ are the datasets of pixels created using the equations in Algorithm 2.

Form Tables 4 and 5, we observed that segmentation accuracy of RPK-means algorithm is 2%-6% more than the traditional *K*-means clustering. That is because of in case of centroid in outliers makes their own cluster instead of get avoided. RPK-means clustering resolves this problem by selecting automated centroid based on similarity of pixel intensities. Yue et al. [32] proposed similar SegNet method for segmentation of plant disease, but their accuracy is limited up to 79.12%. Also, misclassification error of our model is relatively lower than the model proposed by Liao et al. [1].

The accuracy achieved by different classifiers is presented in Figure 6. Here, we observed that RPK-means algorithm is able to identify the background of the diseased leaf with accuracy in the range of 80% to 97% and also able to detect the lesion portion with accuracy more than 90% to 98.5%, as shown in Figure 6. At the same time for

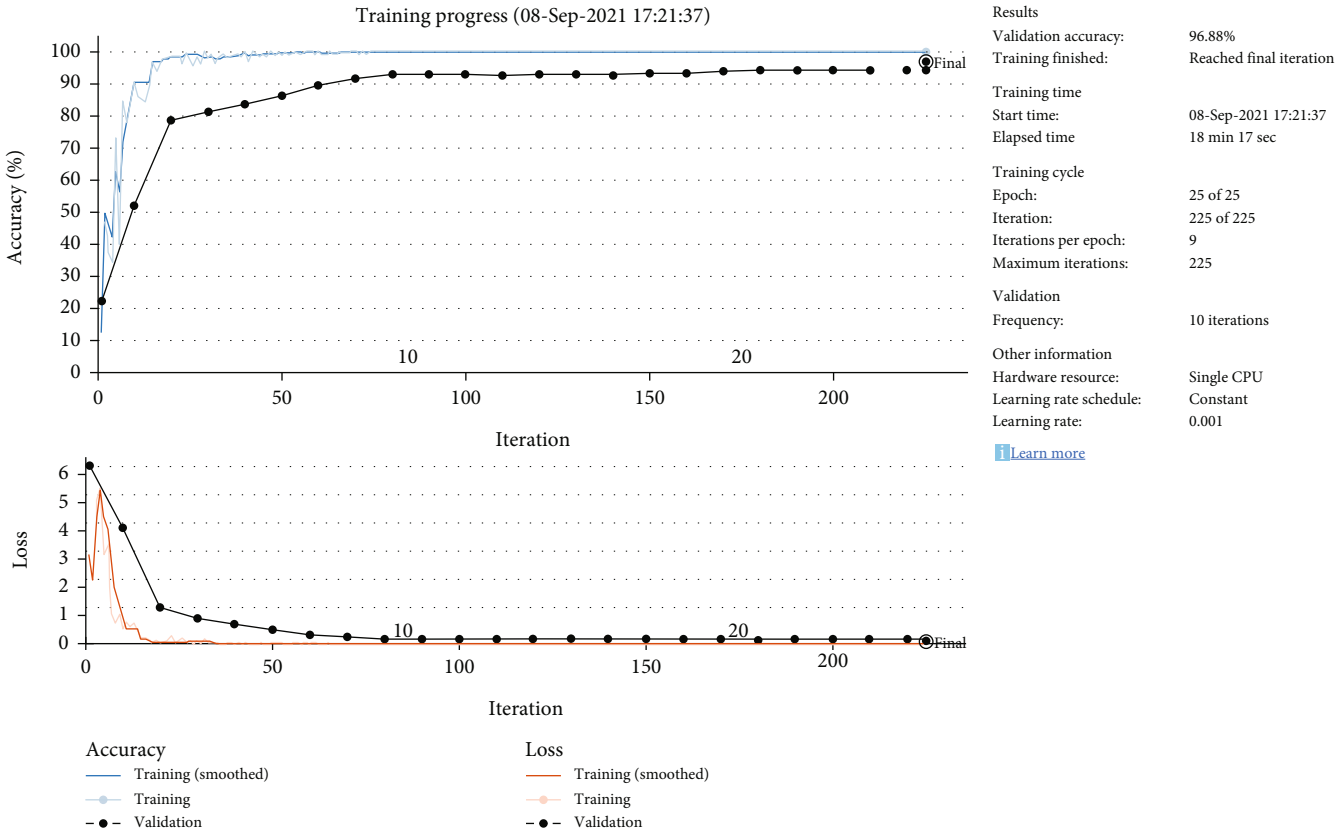

Figure 8: Best accuracy obtained by HCNN model on applying RPK-means clustering output.

convention *K*-means clustering, the ability for background separation ranges from 84% to 97%, and for lesion portion detection, its range is 89%-98.5%.

3.3. Performance Analysis of CNN Models. To analyse the effect of segmentation on classification, we have created different CNN models starting from 11 layers. First, training and validation (90-10 ratio) are performed on 11 layers model for 15,20,25 and 30 epochs; the validation accuracy of 90.1%, 91.94%, 93.6%, and 94.58% is obtained, respectively, as shown in above graph. Furthermore, if we increase the number of epochs, then we found the problem of overfitting. To build this 11-layer model, after input layer, we used two sets of convolutions, batch normalization, ReLU, and max pooling layer along with fully connected, softmax, and classification layers at the end. Further, 8 convolution filters are used at first layer to extract the outer features and number of filters doubled in subsequent layers to extract deeper features. Sampling is performed after each convolution layer to reduce the features.

In order to increase the accuracy of classification, the number of layers increased to 15, by adding one more set of convolutions, batch normalization, ReLU, and max pooling layers in the above 11-layer model. On this new model, experiments are performed by varying the epochs from 15, 20, 25 and observed the accuracy of 92.5%, 93.54%, and 96.88%, respectively; on increasing epochs further, the problem of overfitting has been encountered and performance of system starts decreasing as increasing the number of epochs of our model tries to reach towards zero error and started get trained from the noisy data.

From Table 6, we observed that classification accuracy of the handmade CNN (HCNN) outperforms well the RPK-means clustering and increases the accuracy to 1-2% rather than with *K*-means clustering. At the same time, as RPK-means clustering has an additional step of random path selection; it needs slightly more time than the traditional *K*-means clustering. The experiment performs on fixed learning of 0.001 for different epochs ranging from 15 to 30. We used slow learning to achieve more training accuracy and to avoid the problem of overfitting.

In Figures 7 and 8, upper half shows the increase in training accuracy (blue color line) after each iteration and validation accuracy (black color line) following the boundary of the training curve. The lower half of the Figure 7 shows the decrease in training loss (red color line) and validation loss merging with training loss after 225 iterations. From Figures 7 and 8, we observed that accuracy of HCNN model is slightly better when being applied on output obtained from RPK-means algorithm, the highest accuracy obtained by classifier is 95.42% for *K*-means processed image, and it increases by 1-2% while being processed on RPK-means processed images.

4. Conclusions

To solve the problem of misleading treatments that arise due to the wrong identification of disease that further leads to

huge losses in crop production, a novel RPK-means clustering has been proposed along with SegNet segmentation at preprocessing. Through extensive experiments, it has been observed that the proposed approach obtains a decent performance in terms of standard evaluation measures and is proficient to solve the current problem of crop disease which can also be opted to make a better vegetable disease identification system. To analyse the effect of segmentation techniques, we used a handmade CNN model (HCNN) quantitatively; accuracy of the model is 96.88%, for RPK-means preprocessed images; and it is 95.42% for K-means processed image. While compiling models used for weed separation, SegNet model outperforms the UNet model by leading about 3-4% better accuracy. Further, it has been assured that the proposed approach outperforms the recent state-of-the-art techniques in the presented domain. In future directions, the behavior of the approach will be experimented with and undergone through evolutionary techniques.

Data Availability

The data used to support the findings of this study are available from the corresponding author upon request.

Conflicts of Interest

The authors declares that they have no known competing financial or personal relationships that could be viewed as influencing the work reported in this paper.

References

[1] J. Liao, Y. Wang, J. Yin, L. Liu, S. Zhang, and D. Zhu, "Segmentation of rice seedlings using the YCrCb color space and an improved Otsu method," *Agronomy*, vol. 8, no. 11, p. 269, 2018.

[2] X. Ma, X. Deng, L. Qi et al., "Fully convolutional network for rice seedling and weed image segmentation at the seedling stage in paddy fields," *PLoS One*, vol. 14, no. 4, article e0215676, 2019.

[3] J. Adams, Y. Qiu, Y. Xu, and J. C. Schnable, "Plant segmentation by supervised machine learning methods," *The Plant Phenome Journal*, vol. 3, no. 1, article e20001, 2020.

[4] P. Zhang and L. Xu, "Unsupervised segmentation of greenhouse plant images based on statistical method," *Scientific Reports*, vol. 8, no. 1, pp. 1–13, 2018.

[5] M. Agarwal, S. K. Gupta, and K. K. Biswas, "A compressed and accelerated SegNet for plant leaf disease segmentation: a differential evolution based approach," in *Pacific-Asia Conference on knowledge discovery and data mining*, vol. 12714 of Lecture Notes in Computer Science, , pp. 272–284, Springer, Cham, 2021.

[6] Y. K. Rathore and R. R. Janghel, "Major challenges on using machine learning and deep learning techniques to detect leaf diseases in Asian countries," *Plant Cell Biotechnology and Molecular Biology*, vol. 22, no. 33-34, pp. 232–244, 2021.

[7] M. Sibiya and M. Sumbwanyambe, "An algorithm for severity estimation of plant leaf diseases by the use of colour threshold image segmentation and fuzzy logic inference: a proposed algorithm to update a "Leaf Doctor" application," *AgriEngineering*, vol. 1, no. 2, pp. 205–219, 2019.

[8] A. Khan, T. Ilyas, M. Umraiz, Z. I. Mannan, and H. Kim, "Ced-net: crops and weeds segmentation for smart farming using a small cascaded encoder-decoder architecture," *Electronics*, vol. 9, no. 10, p. 1602, 2020.

[9] L. Zheng, J. Zhang, and Q. Wang, "Mean-shift-based color segmentation of images containing green vegetation," *Computers and Electronics in Agriculture*, vol. 65, no. 1, pp. 93–98, 2009.

[10] K. Tian, J. Li, J. Zeng, A. Evans, and L. Zhang, "Segmentation of tomato leaf images based on adaptive clustering number of K-means algorithm," *Computers and Electronics in Agriculture*, vol. 165, article 104962, 2019.

[11] J. Hu, Z. Chen, R. Zhang, M. Yang, and S. Zhang, "Robust random walk for leaf segmentation," *IET Image Processing*, vol. 14, no. 6, pp. 1180–1186, 2020.

[12] S. Chen, K. Zhang, Y. Zhao et al., "An approach for rice bacterial leaf streak disease segmentation and disease severity estimation," *Agriculture*, vol. 11, no. 5, p. 420, 2021.

[13] G. Sun, X. Jia, and T. Geng, "Plant diseases recognition based on image processing technology," *Journal of Electrical and Computer Engineering*, vol. 2018, Article ID 6070129, 7 pages, 2018.

[14] C. Yang, "Plant leaf recognition by integrating shape and texture features," *Pattern Recognition*, vol. 112, article 107809, 2021.

[15] A. Caglayan, O. Guclu, and A. B. Can, "A plant recognition approach using shape and color features in leaf images," in *International Conference on Image Analysis and Processing*, A. Petrosino, Ed., vol. 8157 of Lecture Notes in Computer Science, pp. 161–170, Springer, Berlin, Heidelberg, 2013.

[16] F. Y. Lin, C. H. Zheng, X. F. Wang, and Q. K. Man, "Multiple classification of plant leaves based on gabor transform and lbp operator," in *International Conference on Intelligent Computing*, D. S. Huang, D. C. Wunsch, D. S. Levine, and K. H. Jo, Eds., vol. 15 of Communications in Computer and Information Science, pp. 432–439, Springer, Berlin, Heidelberg, 2008.

[17] K. Garg, S. Bhugra, and B. Lall, "Automatic quantification of plant disease from field image data using deep learning," in *Proceedings of the IEEE/CVF Winter Conference on Applications of Computer Vision (WACV)*, pp. 1965–1972, Nashville, TN, USA, 2021.

[18] S. Kolhar and J. Jagtap, "Convolutional neural network based encoder-decoder architectures for semantic segmentation of plants," *Ecological Informatics*, vol. 64, article 101373, 2021.

[19] V. Singh, "Sunflower leaf diseases detection using image segmentation based on particle swarm optimization," *Artificial Intelligence in Agriculture*, vol. 3, pp. 62–68, 2019.

[20] D. Al Bashish, M. Braik, and S. Bani-Ahmad, "Detection and classification of leaf diseases using K-means-based segmentation and neural-networks-based classification," *Information Technology Journal*, vol. 10, no. 2, pp. 267–275, 2011.

[21] S. Zhang, H. Wang, W. Huang, and Z. You, "Plant diseased leaf segmentation and recognition by fusion of superpixel, K-means and PHOG," *Optik*, vol. 157, pp. 866–872, 2018.

[22] J. Ma, K. Du, L. Zhang, F. Zheng, J. Chu, and Z. Sun, "A segmentation method for greenhouse vegetable foliar disease spots images using color information and region growing," *Computers and Electronics in Agriculture*, vol. 142, pp. 110–117, 2017.

[23] A. Kumar, K. U. Singh, M. K. Singh, A. K. S. Kushwaha, A. Kumar, and S. Mahato, "Design and Fabrication of Solar Dryer System for Food Preservation of Vegetables or Fruit," *Journal of Food Quality*, vol. 2022, Article ID 6564933, 2022.

[24] S. K. Pandey and R. R. Janghel, "Classification of electrocardiogram signal using an ensemble of deep learning models," *Data Technologies and Applications*, vol. 55, no. 3, pp. 446–460, 2021.

[25] S. Ramesh and D. Vydeki, "Recognition and classification of paddy leaf diseases using optimized deep neural network with Jaya algorithm," *Information Processing in Agriculture*, vol. 7, no. 2, pp. 249–260, 2020.

[26] S. Maity, S. Sarkar, A. Vinaba Tapadar et al., "Fault area detection in leaf diseases using k-means clustering," in *2018 2nd International Conference on Trends in Electronics and Informatics (ICOEI)*, pp. 1538–1542, Tirunelveli, India, 2018.

[27] S. C. Agrawal and A. S. Jalal, "A comprehensive review on analysis and implementation of recent image dehazing methods," in *Archives of Computational Methods in Engineering*, pp. 1–52, Springer, 2022.

[28] R. K. Tripathi and A. S. Jalal, "Novel local feature extraction for age invariant face recognition," *Expert Systems with Applications*, vol. 175, article 114786, 2021.

[29] R. Pradhan and D. K. Sharma, "An ensemble deep learning classifier for sentiment analysis on code-mix Hindi–English data," in *Soft Computing*, pp. 1–18, Springer, 2022.

[30] Y. Guo, J. Zhang, C. Yin et al., "Plant disease identification based on deep learning algorithm in smart farming," *Discrete Dynamics in Nature and Society*, vol. 2020, Article ID 2479172, 11 pages, 2020.

[31] D. Li, R. Wang, C. Xie et al., "A recognition method for rice plant diseases and pests video detection based on deep convolutional neural network," *Sensors*, vol. 20, no. 3, p. 578, 2020.

[32] Y. Yue, X. Li, H. Zhao, and H. Wang, "Image segmentation method of crop diseases based on improved SegNet neural network," in *2020 IEEE International Conference on Mechatronics and Automation (ICMA)*, pp. 1986–1991, Beijing, China, 2020.